(2)

Final Report

AEOSR-TR- 91 0232

Experimental Verification of an Innovative Performance-Validation Methodology for Large Space Systems

For
Department of the Air Force
Air Force Office of Scientific Research (AFSC)
Bolling Air Force Base, DC 20332-6448

Attention:
Program Manager
Directorate of Aerospace Sciences

January 1991

HARRIS

HARRIS CORPORATION GOVERNMENT AEROSPACE SYSTEMS DIVISION
P.O. BOX 94000, MELBOURNE, FLORIDA 32902 (407) 727-5115

Final Report

Experimental Verification of an Innovative Performance-Validation Methodology for Large Space Systems

For
Department of the Air Force
Air Force Office of Scientific Research (AFSC)
Bolling Air Force Base, DC 20332-6448

Attention:
Program Manager
Directorate of Aerospace Sciences

January 1991

Per telecon with Karen Callaghan
(AFOSR) doc. is complete as is.
7-3-91 JK

A-1

UNCLASSIFIED
SECURITY CLASSIFICATION OF THIS PAGE

REPORT DOCUMENTATION PAGE

1a. REPORT SECURITY CLASSIFICATION	1b. RESTRICTIVE MARKINGS
2a. SECURITY CLASSIFICATION AUTHORITY	3. DISTRIBUTION / AVAILABILITY OF REPORT Approved for public release; distribution unlimited
2b. DECLASSIFICATION / DOWNGRADING SCHEDULE	
4. PERFORMING ORGANIZATION REPORT NUMBER(S)	5. MONITORING ORGANIZATION REPORT NUMBER(S)
6a. NAME OF PERFORMING ORGANIZATION Harris Corporation 6b. OFFICE SYMBOL (*If applicable*)	7a. NAME OF MONITORING ORGANIZATION AFOSR/NA
6c. ADDRESS (*City, State, and ZIP Code*) MS 22/4842 Melbourne, FL 32902	7b. ADDRESS (*City, State, and ZIP Code*) Bldg. 410 Bolling AFB DC 20332-6448
8a. NAME OF FUNDING / SPONSORING ORGANIZATION AFOSR 8b. OFFICE SYMBOL (*If applicable*) NA	9. PROCUREMENT INSTRUMENT IDENTIFICATION NUMBER F49620-87-C-0108
8c. ADDRESS (*City, State, and ZIP Code*) AFOSR/NA Bldg 410 Bolling AFB, DC 20332-6448	10. SOURCE OF FUNDING NUMBERS PROGRAM ELEMENT NO: 63221C PROJECT NO.: 1200 TASK NO.: K1 WORK UNIT ACCESSION NO:
11. TITLE (*Include Security Classification*) Validation Methodology for Large Space Structures (U)	
12. PERSONAL AUTHOR(S) Dr. David C. Hyland	
13a. TYPE OF REPORT Final	13b. TIME COVERED FROM 8/15/87 TO 2/14/91
14. DATE OF REPORT (*Year, Month, Day*) 1991, February 9	15. PAGE COUNT
16. SUPPLEMENTARY NOTATION	

17. COSATI CODES			18. SUBJECT TERMS (*Continue on reverse if necessary and identify by block number*)
FIELD	GROUP	SUB-GROUP	
22	02		
12	01		

19. ABSTRACT (*Continue on reverse if necessary and identify by block number*)

A technology gap exists in verifying performance of large space systems. To fill that gap the proposed program seeks to develop and validate an efficient pre-flight performance verification methodology. The approach involves selective component testing along with analysis of subsystem interactions. The methodology exploits MEOP (Maximum Entropy/Optimal Projection) Control-System Design and Majorant Robustness Analysis. The approach is formulated for several representative large space systems and experimentally verified on a 3-meter diameter multi-hex panel ground-based active control testbed.

20. DISTRIBUTION / AVAILABILITY OF ABSTRACT ☒ UNCLASSIFIED/UNLIMITED ☒ SAME AS RPT ☐ DTIC USERS	21. ABSTRACT SECURITY CLASSIFICATION (U)
22a. NAME OF RESPONSIBLE INDIVIDUAL Lt. Col. George Haritos	22b. TELEPHONE (*Include Area Code*) (202) 767-4987 22c. OFFICE SYMBOL NA

DD FORM 1473, 84 MAR 83 APR edition may be used until exhausted
All other editions are obsolete

SECURITY CLASSIFICATION OF THIS PAGE
UNCLASSIFIED

Table of Contents

Figures

Experimental Verification of an Innovative Performance Validation Methodology for Large Space Systems (EVM)

Annual Report No. 3

Contract: F49260-87-C-0108
Principal Investigator: Dr. D. C. Hyland

1. Technical Background

The size of SDI space systems poses significant new challenges to traditional pre-launch performance validation. Because of the inability to test large lightweight structures in an ambient environment, there exists a technology gap in verifying performance of large space systems. What is needed to fill that gap is a systematic methodology for planning a combined analysis and testing qualification program that will result in maximum preflight performance prediction accuracy at minimal cost. This program aims to fill that technology gap by developing and validating an efficient preflight performance-validation methodology for large space systems.

The approach involves selective component testing along with analysis of subsystem uncertainties and interactions. The methodology exploits MEOP (Maximum Entropy/Optimal Projection) control system design and Majorant Robustness Analysis. The innovative design and analysis methods also incorporate the breakthrough discoveries of Bernstein and Haddad which allow optimal H_∞ design with constraints on controller complexity. In the application of MEOP/Majorant techniques, a large space structure is modeled as a collection of interacting subsystems with both subsystem and interaction uncertainties. Majorant Robustness Analysis identifies subsystem components and subsystem interaction which contribute critically to prediction uncertainty. Selective hardware testing thus efficiently reduces model uncertainty for refining MEOP control-system designs. Using this rationale, we experimentally test the methodology using the Harris multi-hex prototype (MHPE) ground based active controller testbed.

The MHPE testbed being utilized in this study was developed and fabricated on the Harris Precision Structures and Controls IR&D Program. Fabrication of the apparatus was completed in June 1988 and test activities have been underway since then.

For completeness, we give a brief overview of the MHPE apparatus as it existed before March 1990. After March 1990, we executed significant hardware upgrades to the MHPE. Thus the following description provides the basic background for the discussion of recent upgrades given in Section 3.

The MHPE was designed to emulate the dynamics of a seven segment primary mirror and focuses on the primary mirror *dephasing problem*. The dephasing problem refers to the degradation of pointing accuracy and beam quality due to the relative motion of mirror segments.

Figure 1 shows a photograph of the apparatus as of May 1988 and before March 1990 and Figure 2 shows a blow-up drawing indicating the separate components. The basic structure consists of 42 surrogate mirror facets mounted on a seven-panel truss array. The hexagonal box truss array is in turn mounted on a six-member support truss supported by a circular base plate. Air bag isolators support the static weight, and electrodynamic shakers are used to provide base plate disturbances emulating aft-spacecraft disturbances.

As indicated in Figure 2, the MHPE is equipped with six Linear Precision Actuators (LPACT's) to provide actuation for vibration control. Figure 3 shows a diagram of the LPACT and lists its

significant properties. Developed two years ago on Harris IR&D and subsequently patented, the LPACT possesses unique features (such as an internal force control loop) which endow it with exceptionally flat frequency response over a very large frequency range (5 Hz to at least 5 KHz).

Figure 4 indicates the controller/processor architecture implemented on the MHPE. The large grey-outlined block encloses either hardware or analog electronics components. As indicated, there are two types of control loops, namely, a set of purely decentralized loops implemented with analog electronics in parallel with a centralized controller implemented with the MCX-5 computer. The MCX-5 is used for both on-line vibration control and for data acquisition.

In order to address the dephasing problem, the control objective for the MHPE apparatus is to suppress the relative motion of the hexagonal panels due to vibration induced by the broadband disturbances. In the past, the mirror surface error was not measured directly by optical means but was constructed using eighteen accelerometers mounted at various points within the hexagonal panels. Basically, the outputs of the eighteen accelerometers were processed by the MCX-5 to provide a real-time estimate of the array dephasing (rms surface error). Recent experiments, however, employ direct optical measurements using the Optical Position Measurement System (OPMS) upgrade described in Section 3.

The more recent MHPE upgrades are described briefly in Section 3 and full details of the current MHPE apparatus are given in the "Facility Description and User's Guide" reproduced in Appendix A. The present program activities have resulted in a significant number of publications. These are listed in Appendix B and selected papers are reproduced in Appendix C.

2. Objectives/Program Tasks

The objectives of this study are attained by the accomplishment of the following general tasks:

1. Characterize subsystem uncertainties (using MHPE as benchmark).

2. Develop test sequence plan and perform initial check of majorant analysis on MHPE.

3. Identify and test critical components.

4. Perform full-up verification using MHPE tests.

The task flow is illustrated in Figure 6. The task schedule with a more detailed indication of the tasks is given in Figure 7. As shown, Task 1 involves initial (pre-testing) modelling, control design and a priori characterization of uncertainties. Task 2 follows up with planning of subsystem/component test activities and comparison of test results with a priori analysis. Task 3 undertakes the testing of subsystems/components in order to reduce overall uncertainty. Refined subsystem/component models are then used to obtain a higher-performance control design. This leads to a second full-up MHPE controls test as part of Task 4.

3. Progress To-Date

All tasks have now been completed, including the full-up testing phase of Task 4. March 1990 marks a dividing point in the past year's activities since, at that time, the MHPE apparatus was relocated *and* the hardware was significantly upgraded as part of the Harris IR&D program. Accordingly, we first describe activities between August 1989 and April 1990, including

for completeness a recapitulation of progress reported in the Second Annual Report for the period August 1988 to August 1989.

Next, we review the new MHPE configuration completed as of April 1990 and report research progress since that time up until the present.

Progress during the period August 1988 through March 1990

As indicated in Figure 7, activities in this period alternated between system identification and hardware upgrades and vibration and control testing. The first stage of our study involved a priori modelling and initial control design studies. This was followed, shortly after MHPE fabrication was completed, by initial open- and closed-loop tests using a simple rate feedback control law. The purposes of the initial tests were to establish open-loop dynamics data and provide end-to-end checkout of the electronics. The initial test data showed substantial disparities with the predictions of the pre-test model. To refine the model, sensitivity and majorant analysis were used to ascertain the most important potential sources of error. Subsequently, the relevant subsystems and structural components were subjected to simple static or vibration tests to determine the values of the uncertain physical parameters. The refined parameter values were then used to construct a refined model and the MHPE apparatus was fully reassembled and subjected to vibration testing. Good agreement was observed for all modes up to 200 Hz.

As Figure 7 shows, while component testing and model refinement were proceeding, control design studies were also underway. Tradeoffs between centralized and decentralized control architectures were performed. While the high order LQG dynamic compensator design was found to be nonrobust, the decentralized designs exhibited good nominal performance and excellent robustness. In particular, a decentralized digital compensator combined with independent rate feedback loops was designed utilizing the decentralized control design extension of MEOP developed in a previous study for AFOSR.

The above decentralized design was chosen for implementation and testing after the MHPE was reassembled and open-loop tested. Figures 8 and 9 show examples of test results. The pseudo-rate measurement output of one of the LPACT accelerometers is indicated in Figure 8. In this test the shaker disturbances were initiated shortly before t=0. There follows a period of open-loop vibration during which all control loops were off. Then at t=5 sec., the control loops were turned on, resulting in the vibration suppression evident in the Figures. For the same test, Figure 9 shows the MHPE dephasing (as synthesized from the eighteen accelerometer outputs). The control system evidently accomplishes substantial vibration suppression. The open loop rms dephasing of 75 μm is reduced by a factor of nine in the closed loop.

The above control results are a significant achievement. However, the nine to one attenuation fell short of the nominal system prediction, although the test results were within the bounds predicted by majorant analysis. Although much of this is due to residual uncertainties, a portion of the performance degradation is attributable to phase shifts due to dynamics in the LPACT casing-mounted accelerometer. The QA700 accelerometer has a dynamic resonance near 600Hz. which ultimately limits the gain that can be achieved in the rate feedback loops. Thus, as indicated in Figure 7, we decided to eliminate the problem entirely by developing the new "hybrid" accelerometer. This accelerometer design, developed conceptually in an earlier IR&D study, was fabricated and tested. Test results show extremely flat frequency response from D.C. up to 10 KHz. With their ultra-high bandwidth, the new hybrid accelerometers should result in improved control performance.

The above discussion covers events up to the end of December 1988. Until this time, the MHPE test facility was housed in Building 21 in the Palm Bay facilities of Harris Corporation. Beginning in December construction work for the remodelling of Building 21 was initiated, necessitating the relocation of the entire test facility to temporary quarters in Building 7 (see Figure 8). After the relocation, six additional hybrid accelerometers were fabricated and installed on the six LPACT's, replacing the QA700 accelerometers. However, before we could carry out further closed-loop tests, another difficulty was noticed. Disturbances imparted to the MHPE structure during the relocation process snapped the bonds between many of the mechanical flexures and the surface facets. It was decided to make a virtue of necessity by removing all surface facets and then testing the analog portion of the previous control design on this new altered structure. Such tests demonstrate robustness under gross system modifications. The test results showed that the previous control design was still stable and still provided substantial vibration suppression over a very broad frequency band. Incidentally, these test results were displayed in more than ten live demonstrations for DOD and SDIO visitors. Further live demonstrations can be made available upon request.

During the period February 1989 through April 1990, the MHPE apparatus was maintained as it was in Building 21 except for the gradual assembly of the Optical Position Measurement Subsystem (OPMS).

The OPMS is a hardware upgrade performed for the MHPE on Harris IR&D. Previously, accelerometer data had been used to characterize structural response with an equivalent surface error measurement resolution of approximately 600 nanometers. The intent of the OPMS was to provide independent optical measurement of the surface shape errors at a level consistent with large optics by providing a resolution of approximately 3 nanometers. In Harris FY 89 (July 1, 1988 through June 30, 1989), the OPMS design was devised and a basic operating capability was fabricated and installed. The goal of IR&D activities for Harris FY 90 was to replicate the existing design to extend the measurement capability.

The general configuration used is shown in Figure 10. The principle of measurement is optical, heterodyne interferometry. An optics bench is mounted underneath the MHPE facets to be measured. The optics look up to corner cubes mounted on the three corners of each facet to be measured (refer to Figure 11). Changes in the heights of the corners are monitored and converted into center of mass height changes and rotations about the horizonal axes.

The items composing the OPMS can be seen in Fig. 12. The optics and local electronics were purchased from a single sensor vendor (ZYGO). The optical bench and support structure are built from readily available components. The PC interface cards are standard units that are easily obtained from industry vendors, as are the software development aids. Only the software resident in the PC is to be custom developed. It coordinates the data acquisition and processing with the events occurring in the MCX minicomputer.

As indicated in Fig. 11, the FY'89 IR&D program implemented the basic capability to measure one surface facet. The FY'90 plan was to replicate the existing design to measure a total of four facets yielding a representative sample of the MHPE surface errors. The full OPMS with a twelve channel measurement capability was completed and integrated within the new MHPE facility (described below) in April 1990.

MHPE Upgrades and Progress during the Period April 1990 through September 1990

In March 1990, facilities requirements for another program required the relocation of the MHPE

facility from Building 7 to its now permanent location within a $30' \times 40'$ lab space in a high-bay area of Bldg. 19 of the Harris Palm Bay facilities. This relocation was effected on March 30, 1990. Since relocation would cause suspension of testing activities anyway, we decided to avail ourselves of the opportunity to execute substantial hardware upgrades (supported by Harris IR&D) to the MHPE just prior to and immediately following the relocation. These upgrades substantially extended the technical scope of the experimental apparatus and rendered it significantly more traceable to systems of current interest.

The first set of upgrades modifies the MHPE into a Cassagrain beam-expander configuration. A Graphite-Epoxy tripod tower for support of a surrogate secondary mirror was fabricated and integrated to the seven-panel hex array. This occurred just prior to the March relocation and is illustrated in Fig. 13 (which shows the configuration within Building 7). Secondly, the joint fittings connecting the center and outer panels were modified to cant the outer panels upward - thus giving the hex. array a parabolic shape consistent with a primary mirror reaction structure for a Cassagrain telescope. With these modifications, the MHPE fully emulates the dynamics of a deployable large aperture Cassagrain beam expander system.

A second set of modification extended the technical scope of the MHPE to address the control of Line-of-Sight (LOS) jitter as well as Primary Mirror dephasing. An optical LOS scoring system was implemented consisting of a laser source and optics bench (mounted below the hex array) a faceted secondary mirror mounted at the top of the tripod structure and six mirror flats mounted on the hex array to simulate subaperature of a Primary Mirror. the scoring operates by directing the laser beam up through the central hole of the center panel onto the secondary mirror, where the beam is split into six beams directed to the "Primary Mirror" mirror flats. The mirror flats are aligned so that, without vibrational disturbances, the six beams are reflected onto a single spot on the ceiling of the high bay. The description or splitting of this spot into six spots and their relative motion provide a direct optical indication of both primary mirror segment misalignments and overall LOS jitter due to vibration. Finally, to provide the means to actively control the secondary mirror support tower vibrations contributing to LOS error, three additional LPACTS were fabricated and mounted on the secondary mirror platform at the top of the tripod.

Figure 14 shows the current MHPE configuration within the Building 19 lab with all the above upgrades completed. Design and test activities were then resumed on this configuration. Activities after April 1990 consisted of (1) the reconstitution and testing of the earlier decentralized control design and (2) dynamic modeling and system identification of the new MHPE structure preparatory to the final design and testing of a centralized MIMO controller design.

First, the decentralized control involving the six array-mounted LPACTs was reconstituted, appropriately modified for the upgraded MHPE and tested. Dephasing suppression with broad-band disturbances is essentially that shown in Figs. 8 and 9. In addition, because the hybrid accelerometers are now being used, the controller gives high attenuation of even the very high frequency modes. This is illustrated for a 411 Hz mode by the test data shown in Fig. 15.

It was also demonstrated experimentally that the decentralized control design provides a high degree of fault tolerance. That is, if any of the actuators and sensors fail, the remaining actuator/sensor pairs will provide reduced but stable vibration attenuation performance, Fig. 16 (obtained from OPMS output) displays this fault tolerance by showing that stability is maintained and performance degrades gracefully as the Pacts are turned off one-by-one.

A similar decentralized control design was implemented for the three secondary tower Pacts. The performance of the entire nine LPACT design has been shown via live demonstrations to many

Harris visitors since May 1990, including AF and NASA guests in June.

The final step in this program was the execution and testing of an advanced MEOP control design. Preparatory to this, we employed the system modelling and identification tools and methodology evolved earlier in this program to obtain a detailed finite-element structural model and closed-loop system model of the upgraded MHPE configuration. Fig. 17 compares analytical versus experimental data for a typical actuator/sensor loop. Such comparisons indicate excellent gain and phase agreement to support the advanced MEOP control design effort. These models are further described in the MHPE User's Guide given in Appendix A. The advanced MEOP controller achieved noticeable performance improvement as shown in Fig. 18.

The final experimental tests were videotaped and are included as an addendum to this report.

4. Research Progress Forecast

Additional work could involve the development of an advanced CAD package for developing MEOP designs. This ability would significantly aid in designing high performance control laws.

Future would could also involve the development of advanced finite element model refinement methods. These methods could greatly enhance the ability to correlate a nominal finite element model with experimental data.

MULTI-HEX PROTOTYPE EXPERIMENT (MHPE) EMULATES THE DYNAMICS OF A SEVEN SEGMENT PRIMARY MIRROR

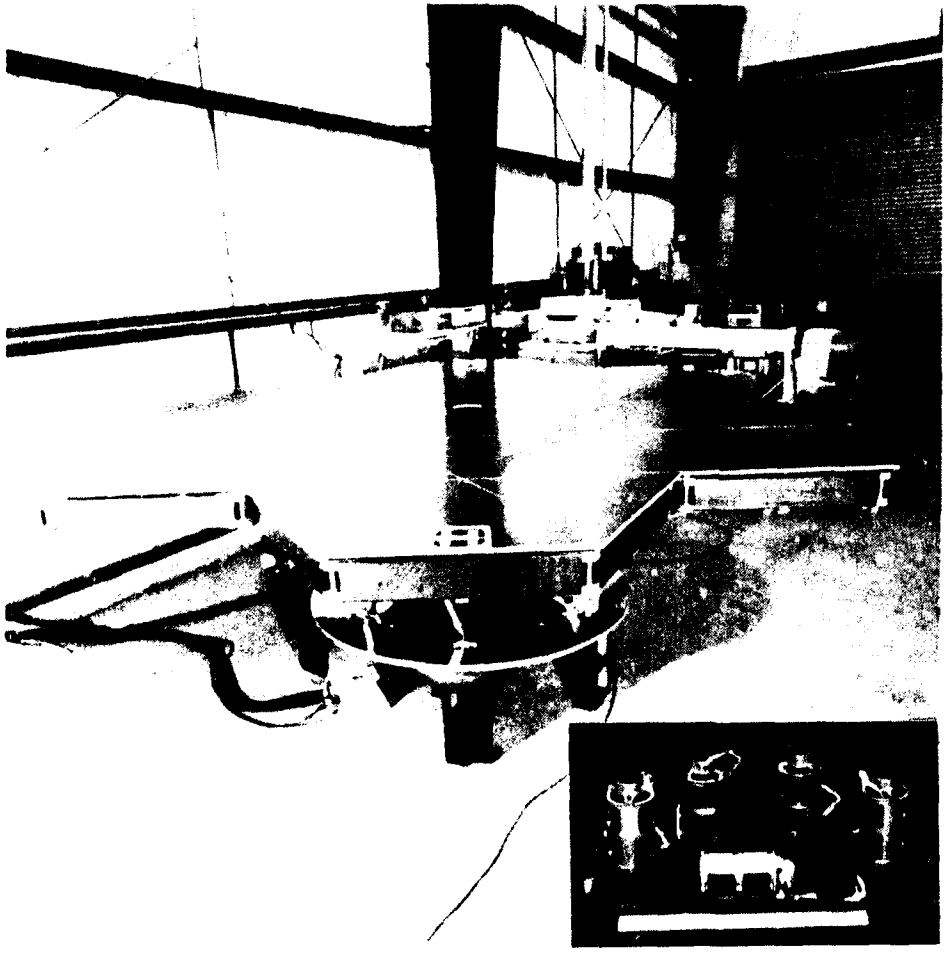

- 42 SURROGATE MIRROR FACETS ON A SEVEN HEX-PANEL GRAPHITE-EPOXY TRUSS ARRAY
- LOWEST STRUCTURAL MODE AT 26 HZ
- SHAKERS ACTING ON BASE-PLATE EMULATE (A/I ATTENUATED) AFT SPACECRAFT DISTURBANCES
- SIX LINEAR PRECISION ACTUATORS (LPACT'S) MOUNTED INSIDE THE OUTER HEX PANELS
- TEST ACTIVITIES FOCUS ON DEPHASING CONTROL USING ACE-LIKE DECENTRALIZED CONTROL ARCHITECTURE

Figure 1.

MULTI-HEX PROTOTYPE EXPERIMENT (MHPE)
STRUCTURAL CONFIGURATION

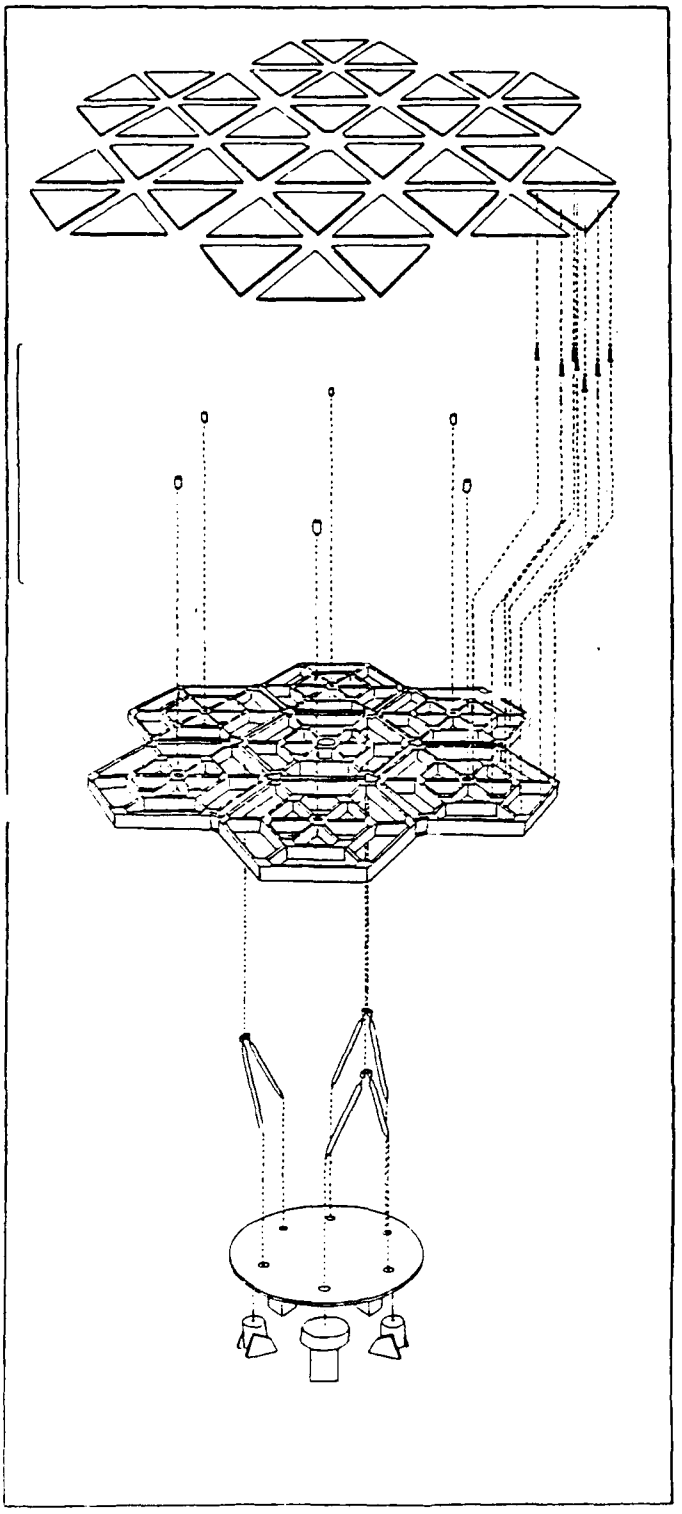

Figure 2.

LPACT ACTUATOR / SENSOR DAMPING UNIT PROVIDES RELIABLE, HIGH BANDWIDTH ACTUATION

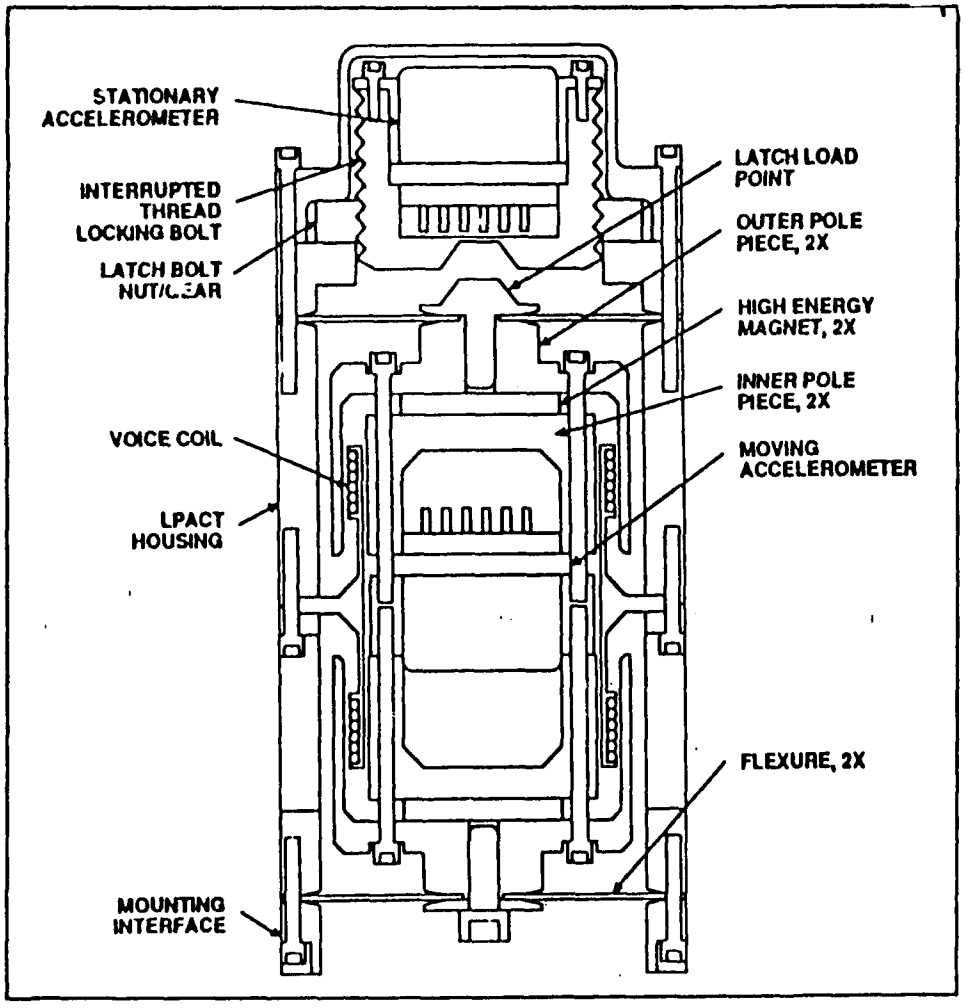

- PROOF MASS / VOICE COIL DESIGN
- GRAPHITE-EPOXY FLEXURES OBVIATE BEARING STICTION PROBLEMS
- ULTRA-HIGH-BANDWIDTH CASING-MOUNTED ACCELEROMETER MEASURES STRUCTURAL MOTION
- PROOF-MASS MOUNTED ACCELEROMETER CLOSES INTERNAL CONTROL LOOP RESULTING IN RELIABLY SHAPED FREQUENCY RESPONSE
- LAUNCH LOAD PROTECTION PROVIDED BY REDUNDANT DRIVE LOCK-DOWN

Figure 3.

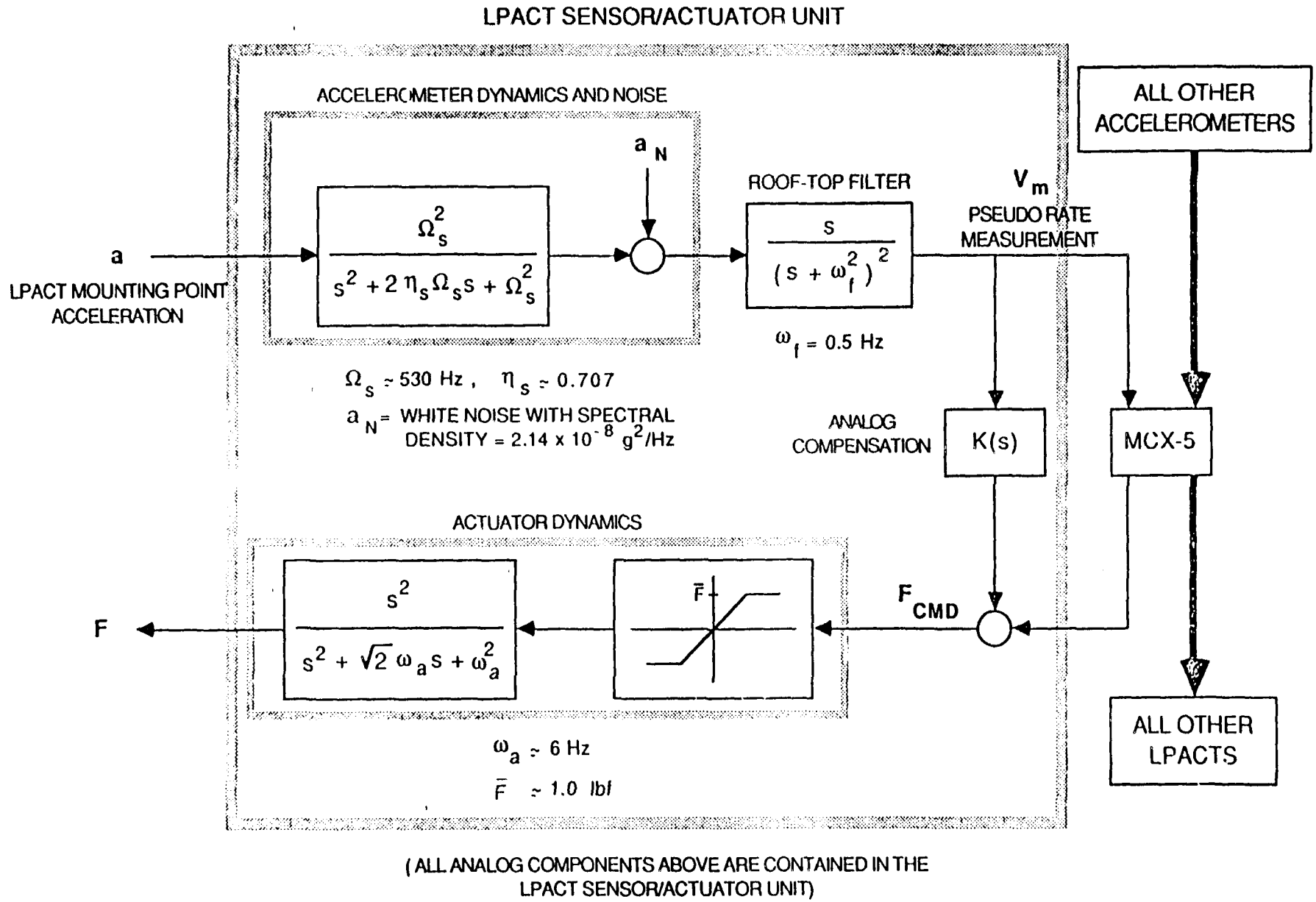
LPACT SENSOR/ACTUATOR UNIT
ACCELEROMETER DYNAMICS AND NOISE
a N
a
LPACT MOUNTING POINT ACCELERATION
$\frac{\Omega_s^2}{s^2 + 2\eta_s\Omega_s s + \Omega_s^2}$
$\Omega_s \simeq 530$ Hz , $\eta_s \simeq 0.707$
a_N = WHITE NOISE WITH SPECTRAL DENSITY = 2.14×10^{-8} g^2/Hz
ROOF-TOP FILTER
$\frac{s}{(s + \omega_f^2)^2}$
$\omega_f = 0.5$ Hz
V_m
PSEUDO RATE MEASUREMENT
ALL OTHER ACCELEROMETERS
ANALOG COMPENSATION
K(s)
MCX-5
ACTUATOR DYNAMICS
F
$\frac{s^2}{s^2 + \sqrt{2}\,\omega_a s + \omega_a^2}$
$\bar{F}$
F_{CMD}
$\omega_a \simeq 6$ Hz
$\bar{F} \simeq 1.0$ lbf
ALL OTHER LPACTS
(ALL ANALOG COMPONENTS ABOVE ARE CONTAINED IN THE LPACT SENSOR/ACTUATOR UNIT)

Figure 4.

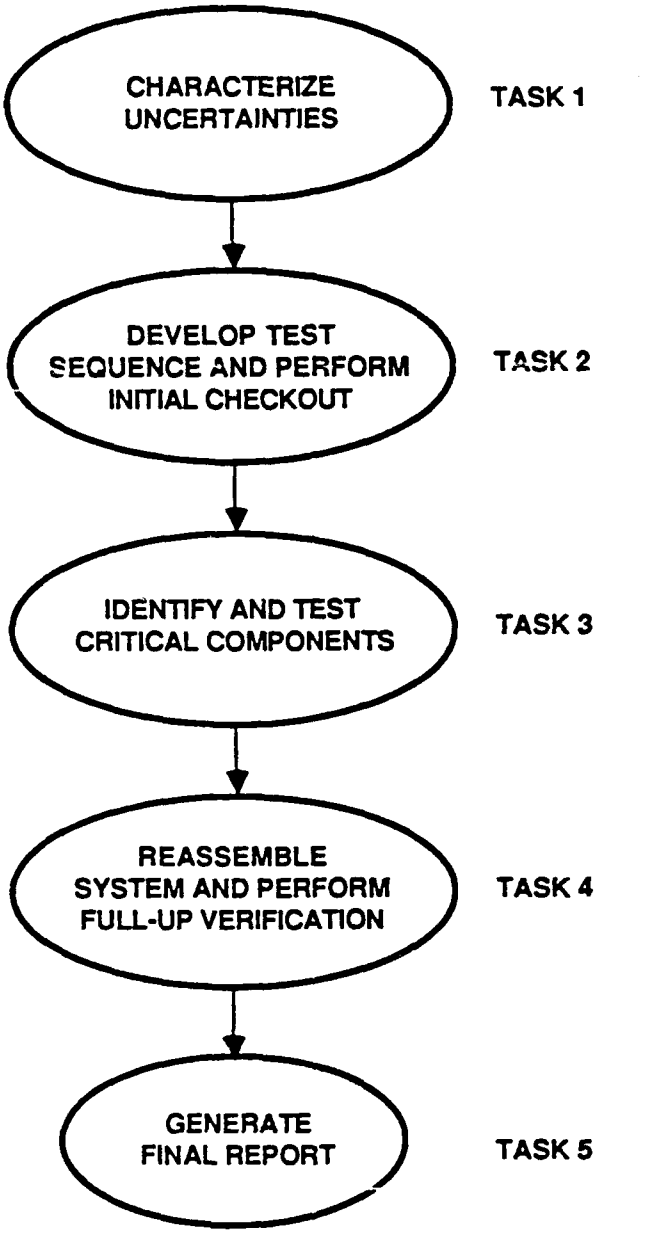

Figure 5. The Task Flow Involves Methodology Formulation for Representative Systems Followed by Methodology Validation for the Multi-Hex Testbed

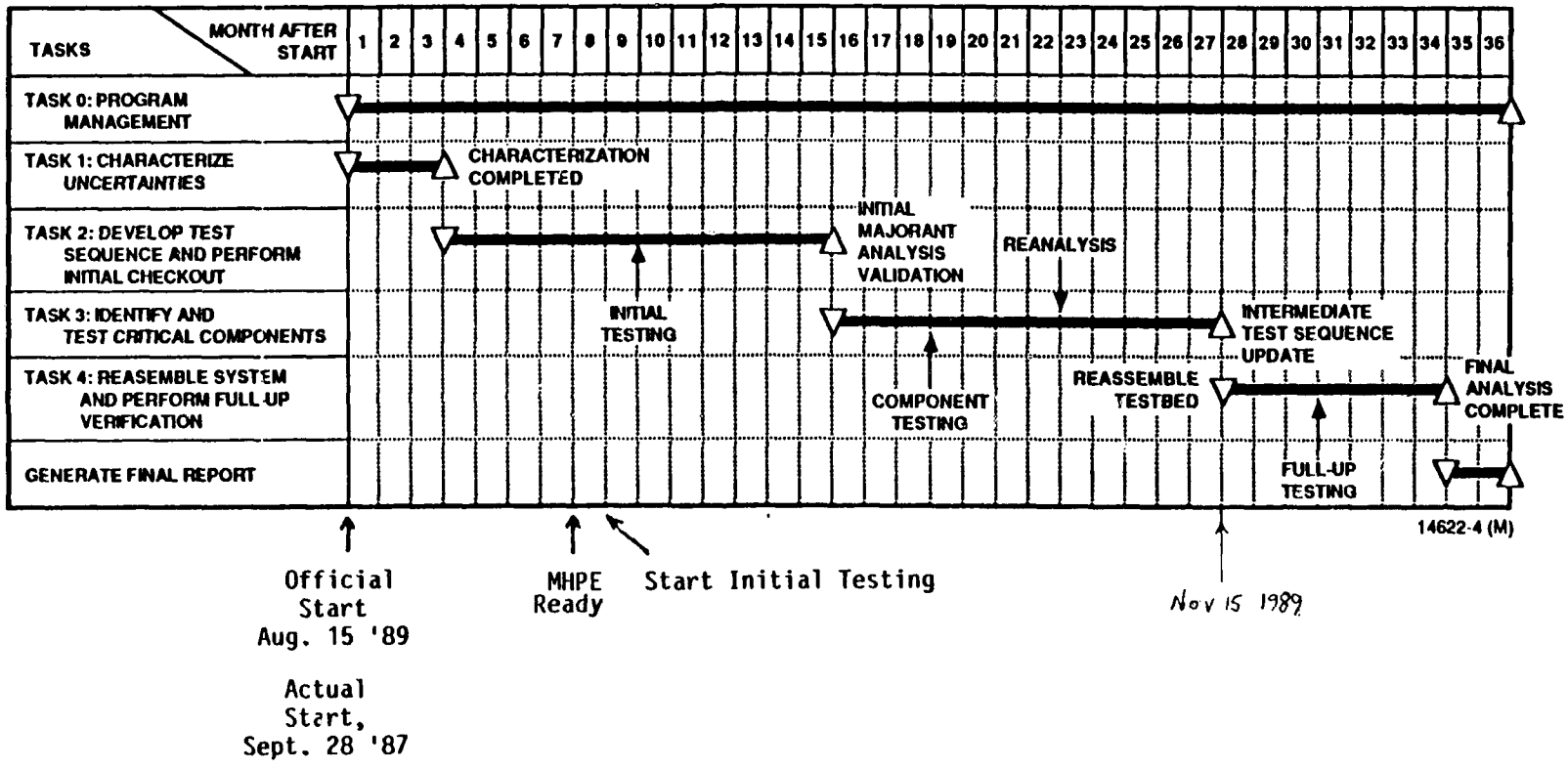

Figure 6. Task Schedule

Model Correlation / Syst ID and Vibration & Control Testing Activities

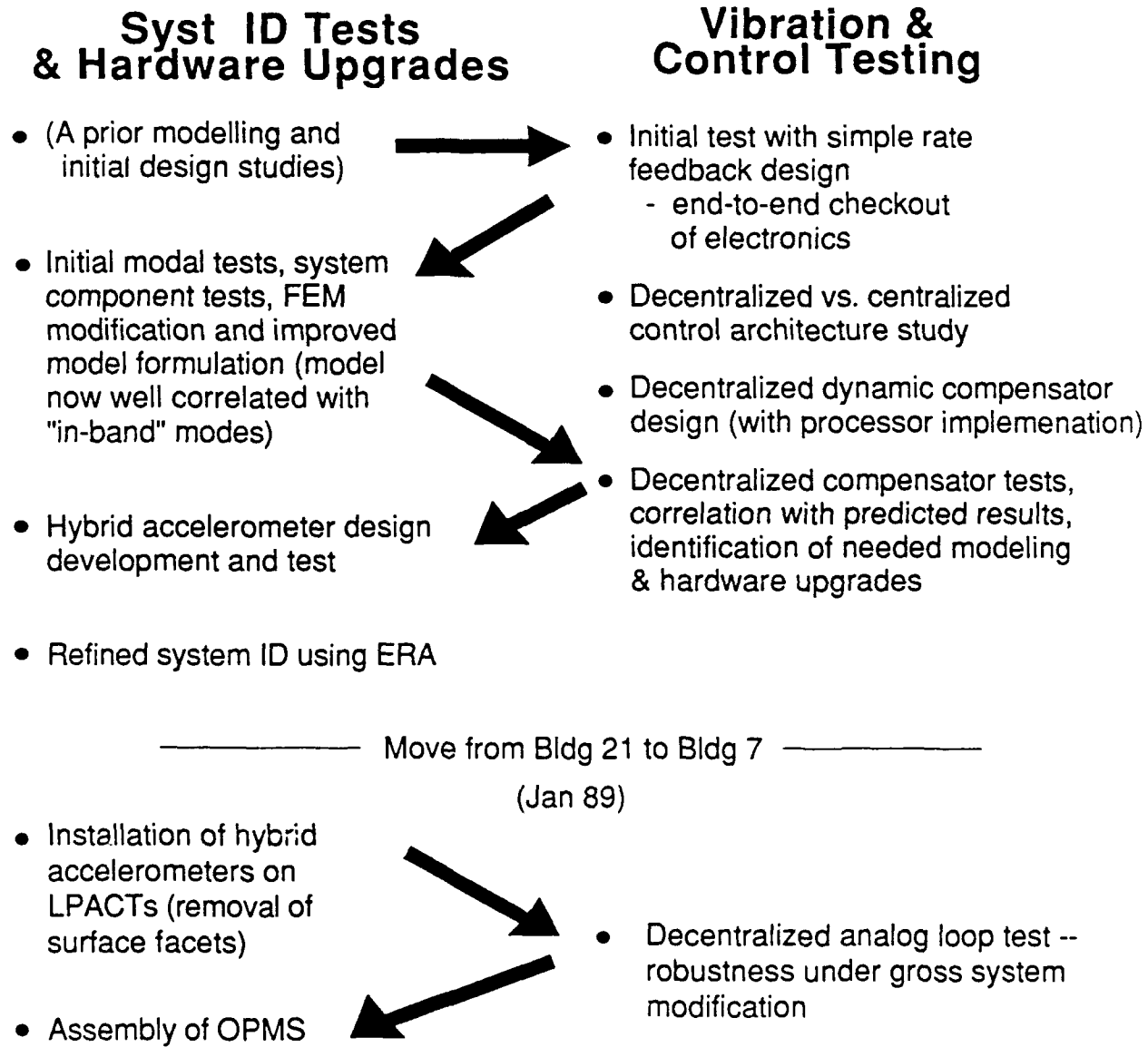

Figure 7.

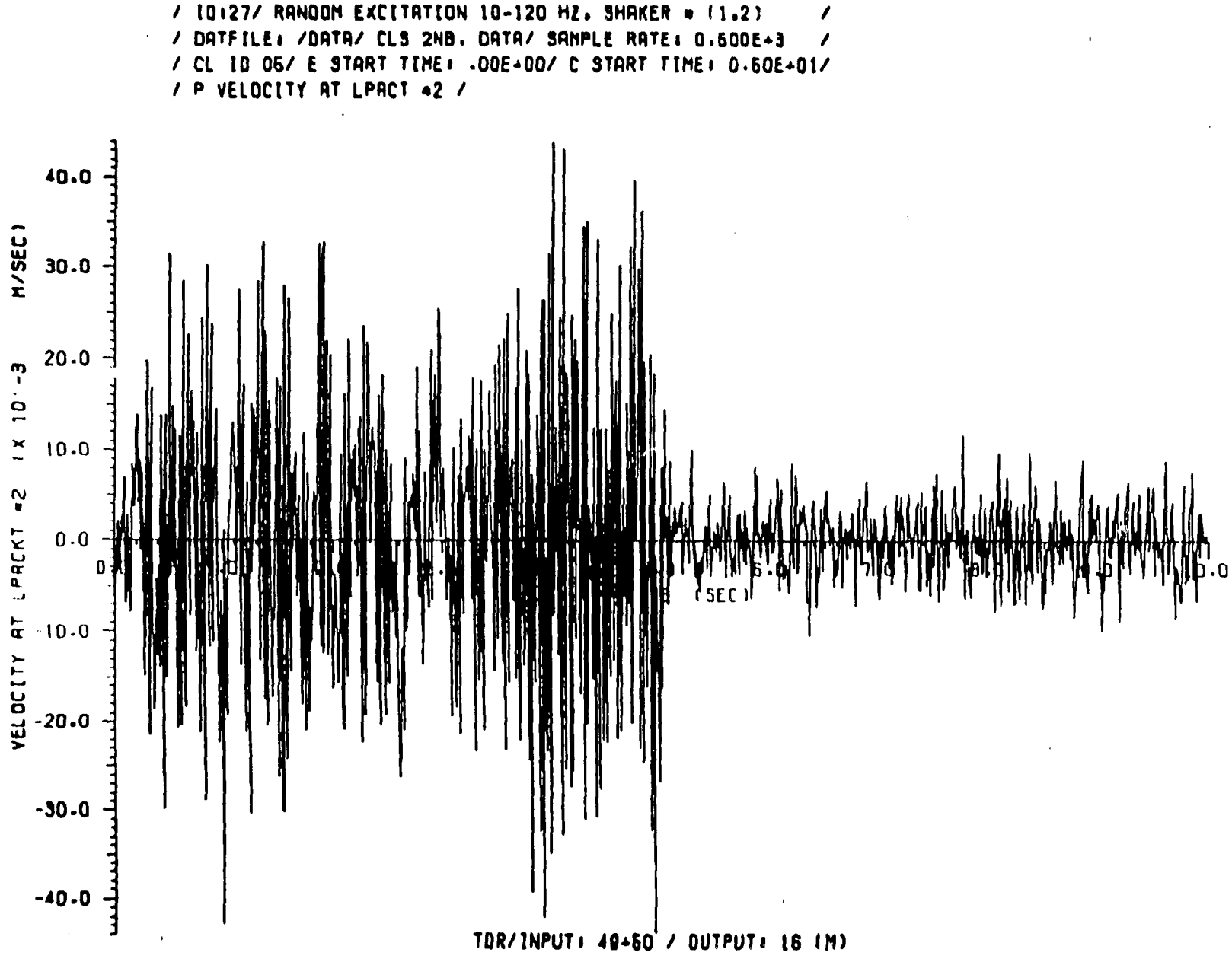
/ 10:27/ RANDOM EXCITATION 10-120 HZ. SHAKER # (1,2) /
/ DATFILE: /DATA/ CLS 2NB. DATA/ SAMPLE RATE: 0.500E+3 /
/ CL 10 05/ E START TIME: .00E+00/ C START TIME: 0.50E+01/
/ P VELOCITY AT LPACT #2 /
VELOCITY AT LPACKT #2 (X 10**-3 M/SEC)
40.0
30.0
20.0
10.0
0.0
-10.0
-20.0
-30.0
-40.0
0
(SEC)
TDR/INPUT: 40+50 / OUTPUT: 16 (M)

Figure 8.

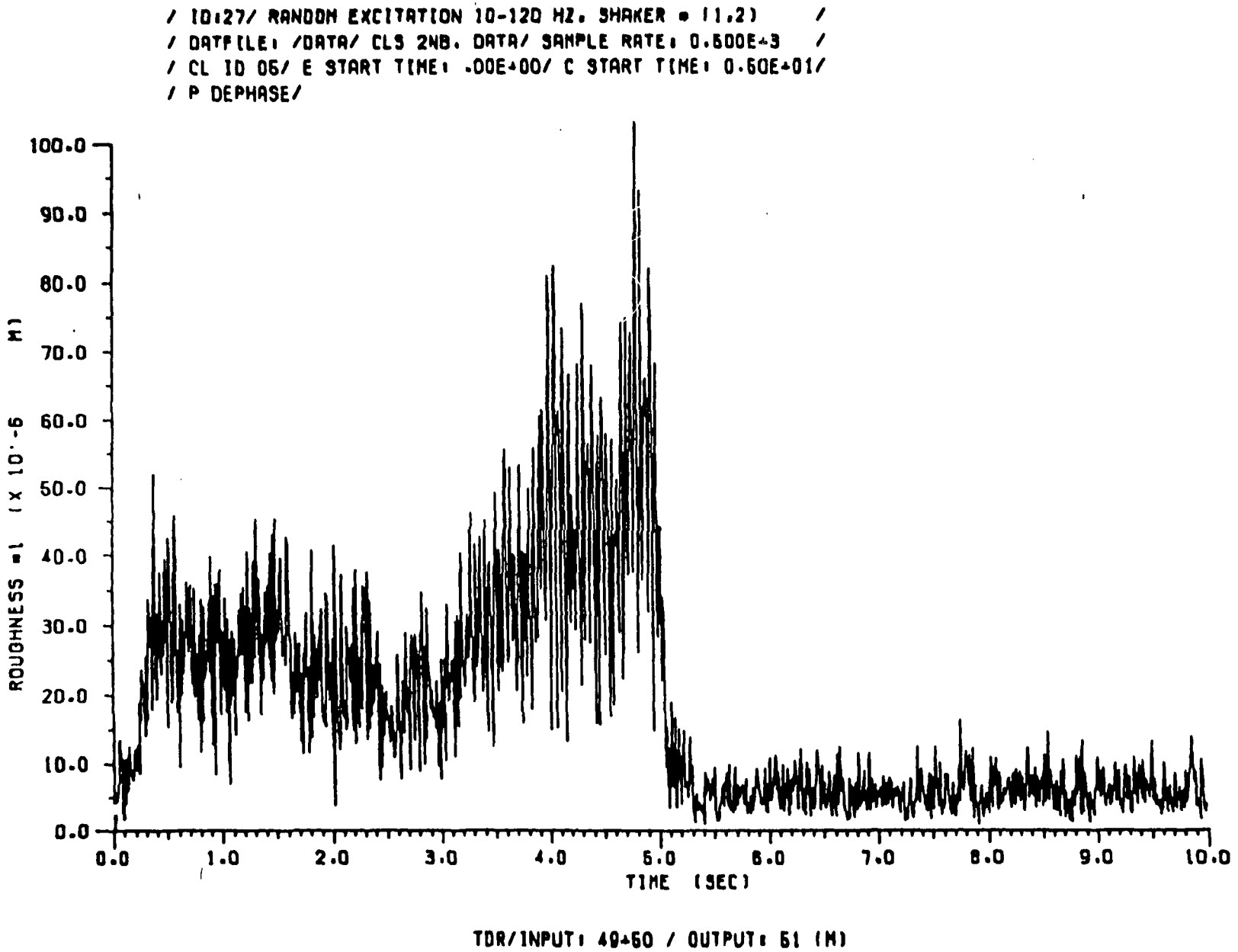
/ ID:27/ RANDOM EXCITATION 10-120 HZ. SHAKER = (1,2) /
/ DATFILE: /DATA/ CLS 2NB. DATA/ SAMPLE RATE: 0.500E-3 /
/ CL ID 05/ E START TIME: .00E+00/ C START TIME: 0.50E+01/
/ P DEPHASE/
ROUGHNESS =1 (X 10**-6 M)
100.0
90.0
80.0
70.0
60.0
50.0
40.0
30.0
20.0
10.0
0.0
0.0
1.0
2.0
3.0
4.0
5.0
6.0
7.0
8.0
9.0
10.0
TIME (SEC)
TDR/INPUT: 40+50 / OUTPUT: 51 (M)

Figure 9.

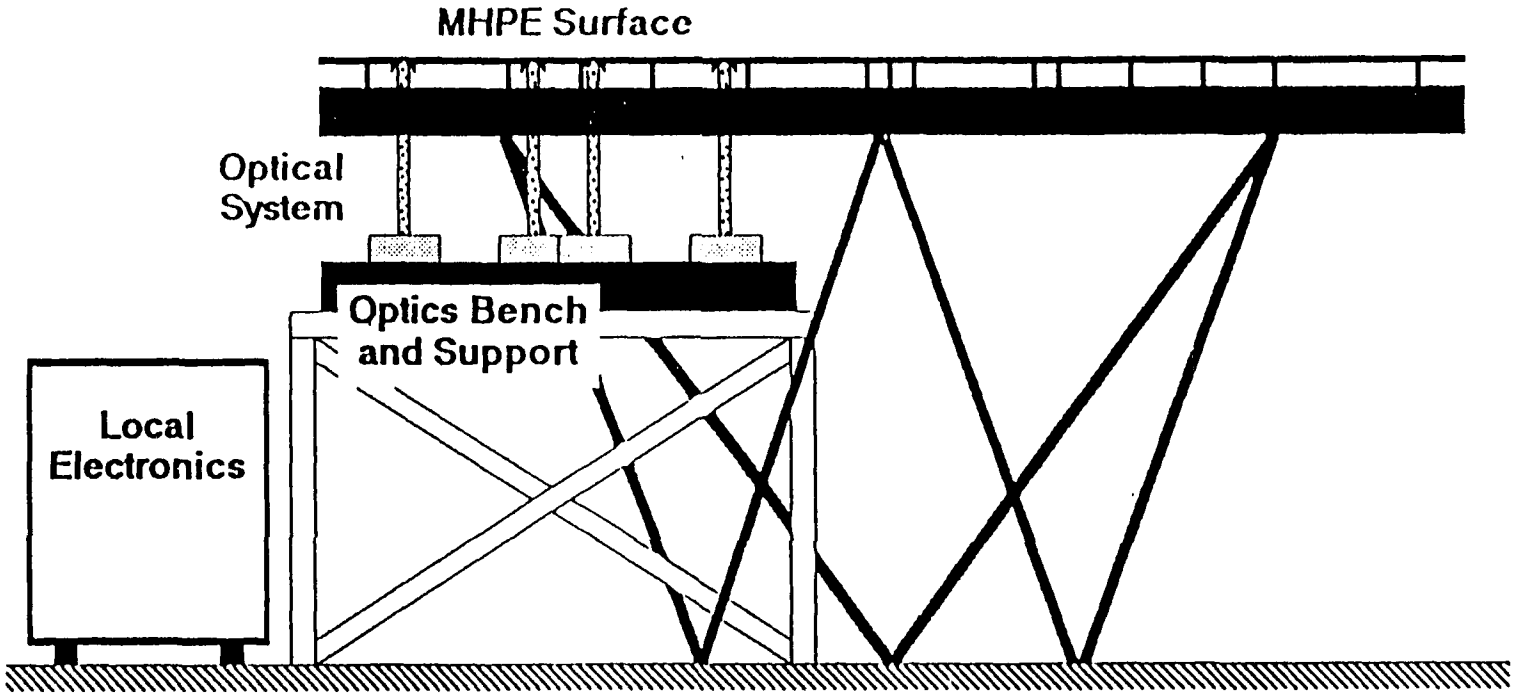

MHPE OPTICAL MEASUREMENTS PROVIDE ESSENTIAL SCORING CAPABILITIES

Figure 10.

INTERIM CONCEPT MEASURES ONE FACET OF AN ADJACENT PAIR

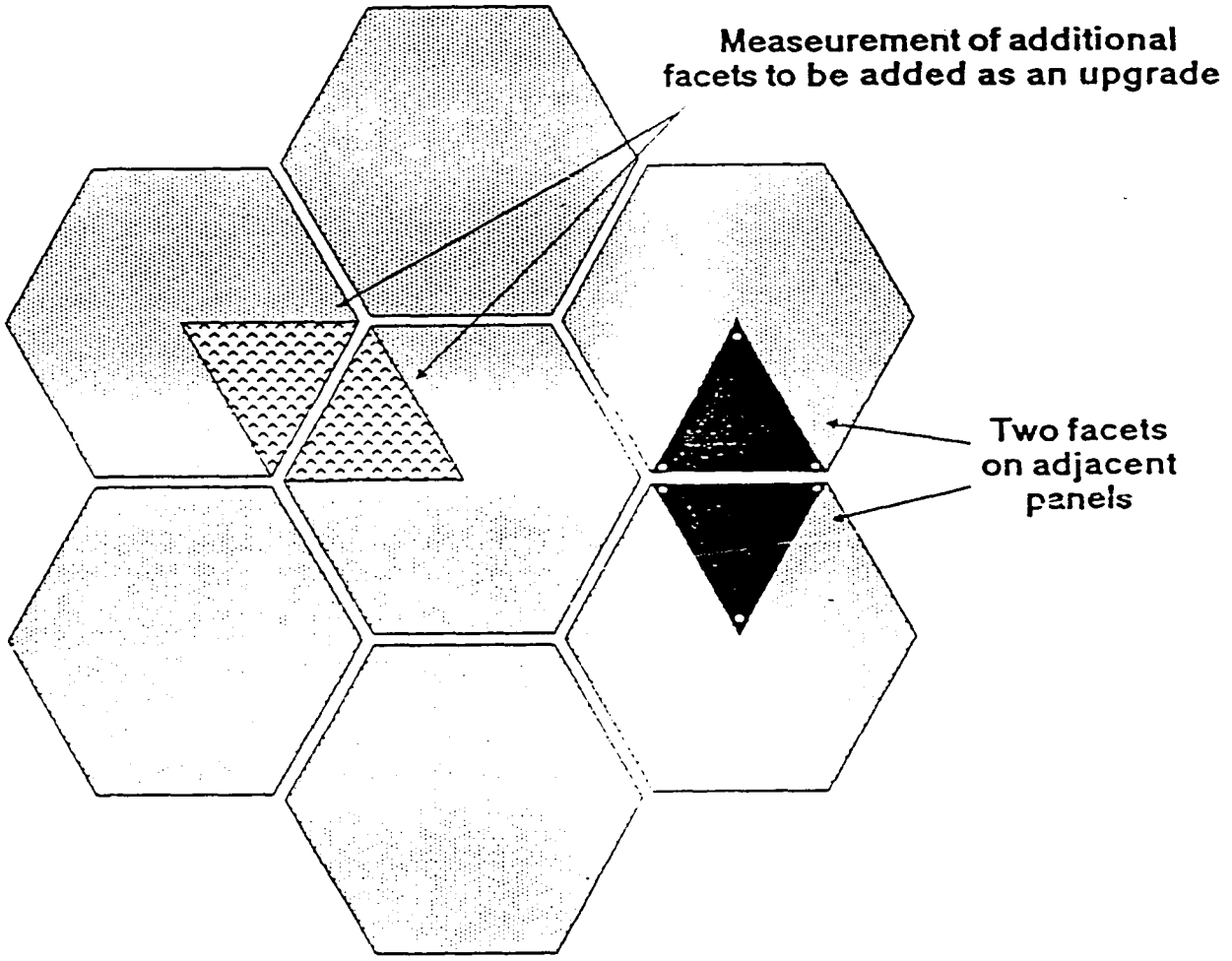

- Typical performance is adequate for scoring
- Configuration addresses rigid body motion of separate panels as well as inter – panel motion
- Initial configuration measures one facet of one pair only, easy upgrade to two facets

Figure 11.

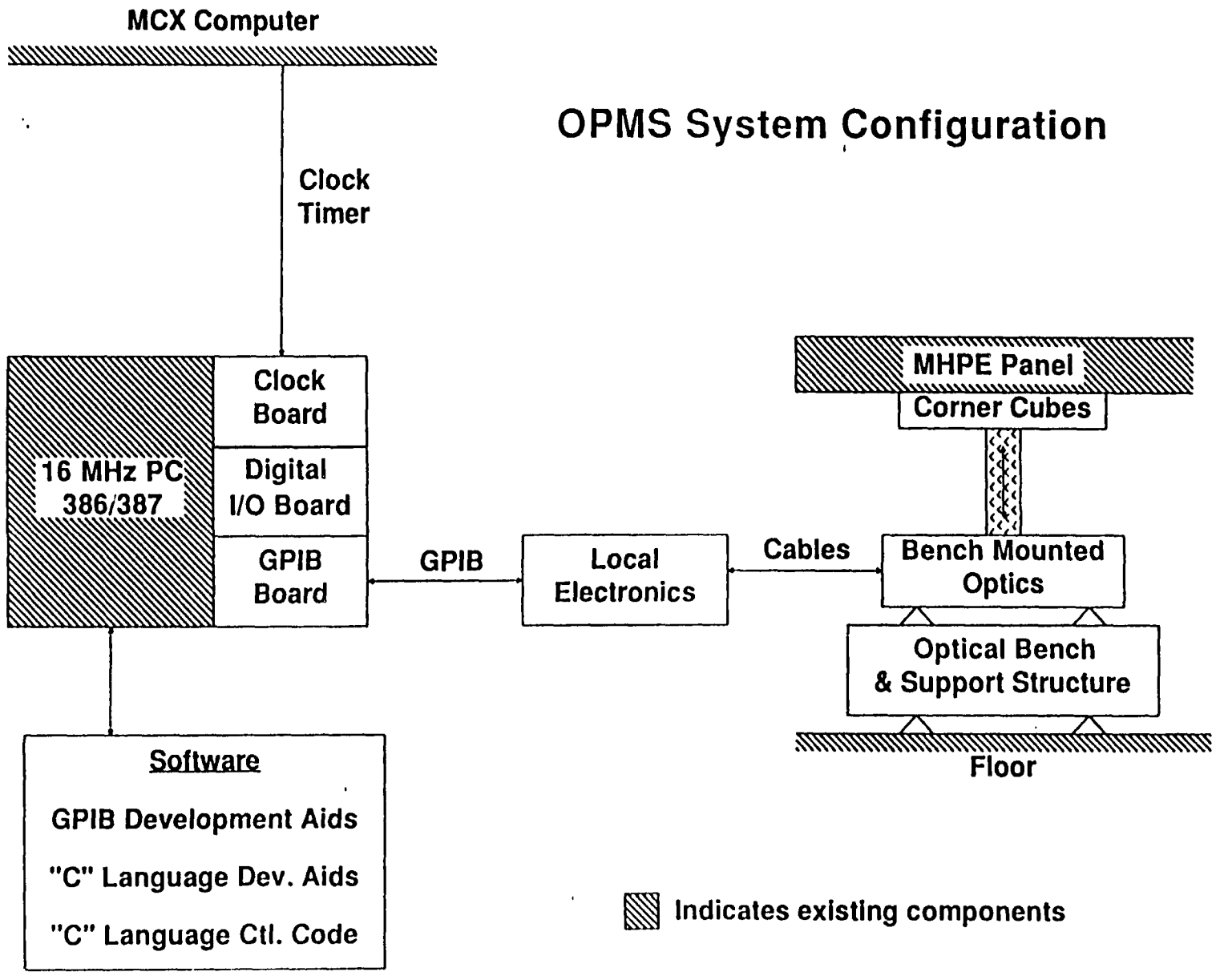
MCX Computer
OPMS System Configuration
Clock
Timer
Clock
Board
16 MHz PC
386/387
Digital
I/O Board
GPIB
Board
GPIB
Local
Electronics
Cables
MHPE Panel
Corner Cubes
Bench Mounted
Optics
Optical Bench
& Support Structure
Floor
Software
GPIB Development Aids
"C" Language Dev. Aids
"C" Language Ctl. Code
Indicates existing components

Figure 12.

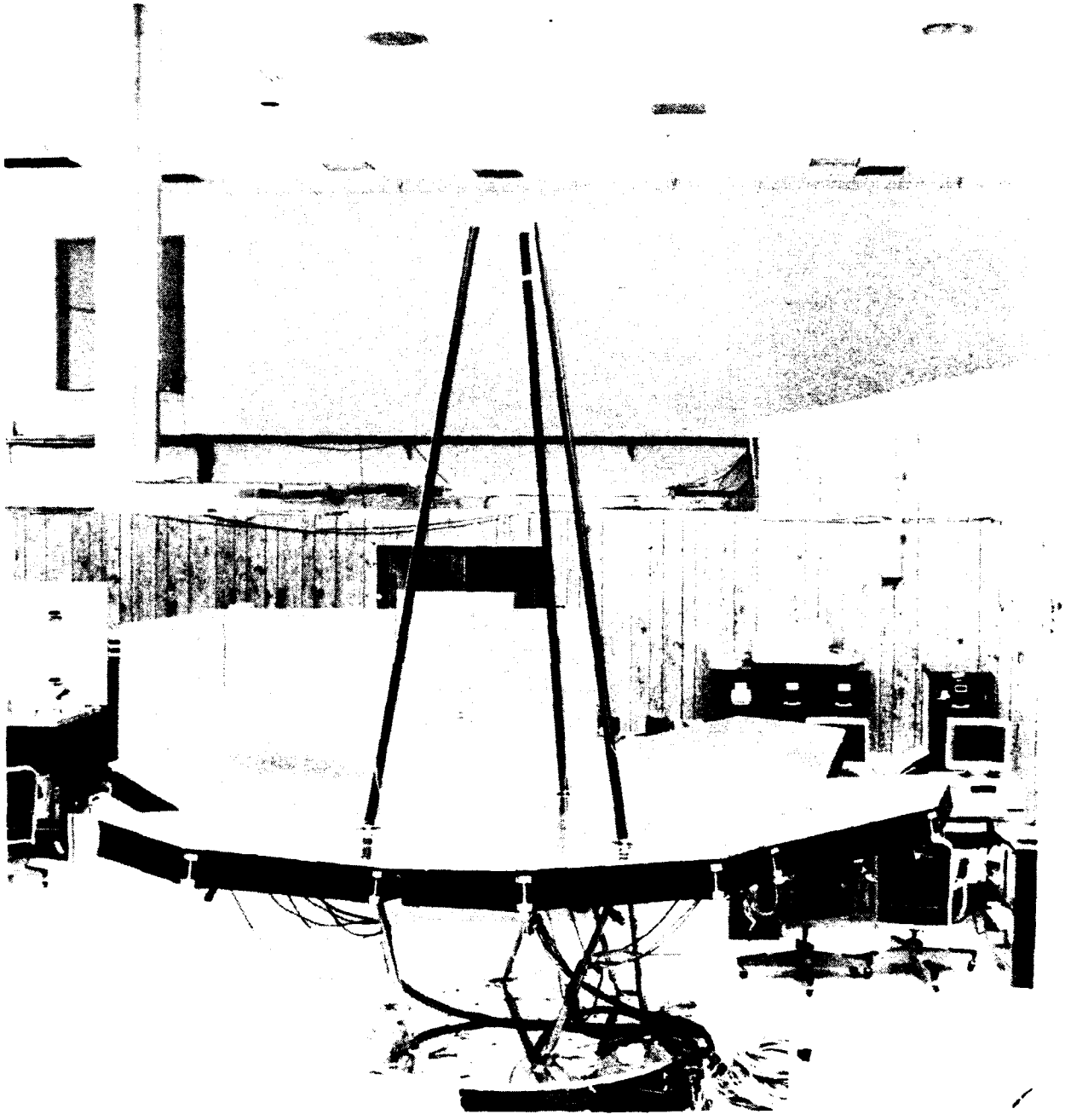

Fig. 13. The Multi-Hex Prototype Experiment with secondary mirror tripod support tower (as intially installed within the Bldg. 7 facility).

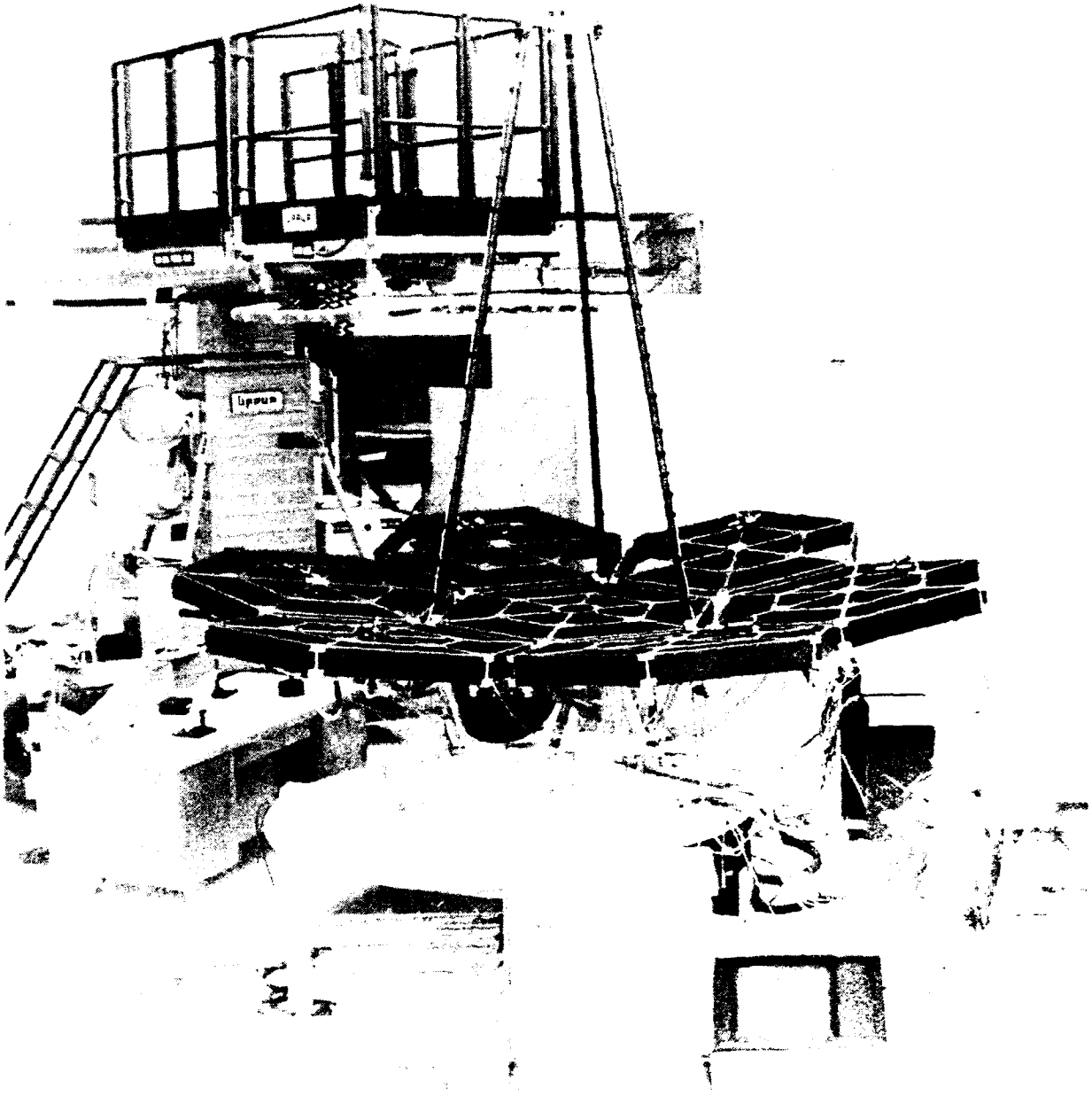

Fig. 14. Final MHPE configuration within the Bldg. 19 lab (All hardware upgrades completed)

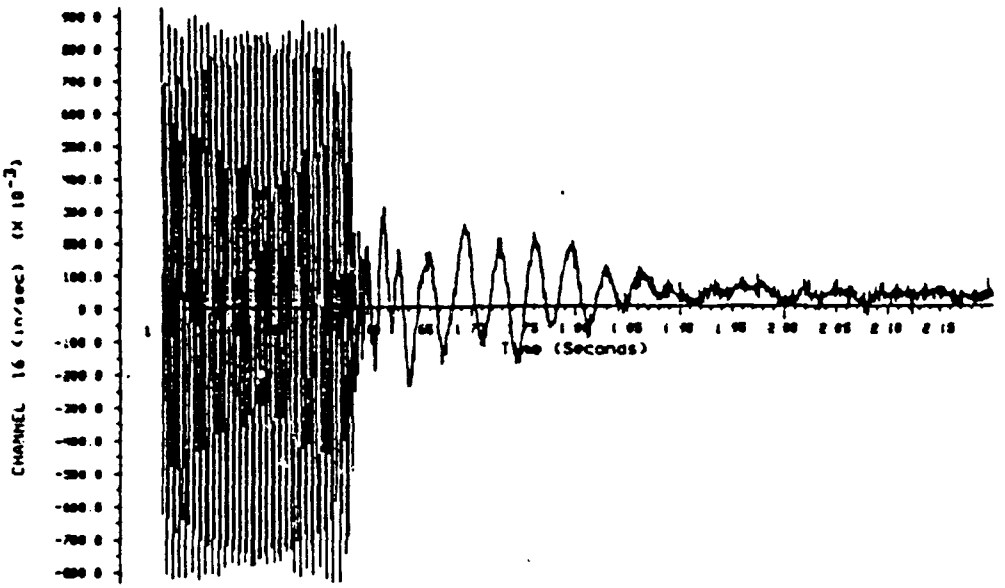

Fig. 15. Performance of the MHPE controller for a 411 Hz disturbance. (The controller was turned on after 1.58 secs.) This illustrates strong attenuation of a high frequency mode.

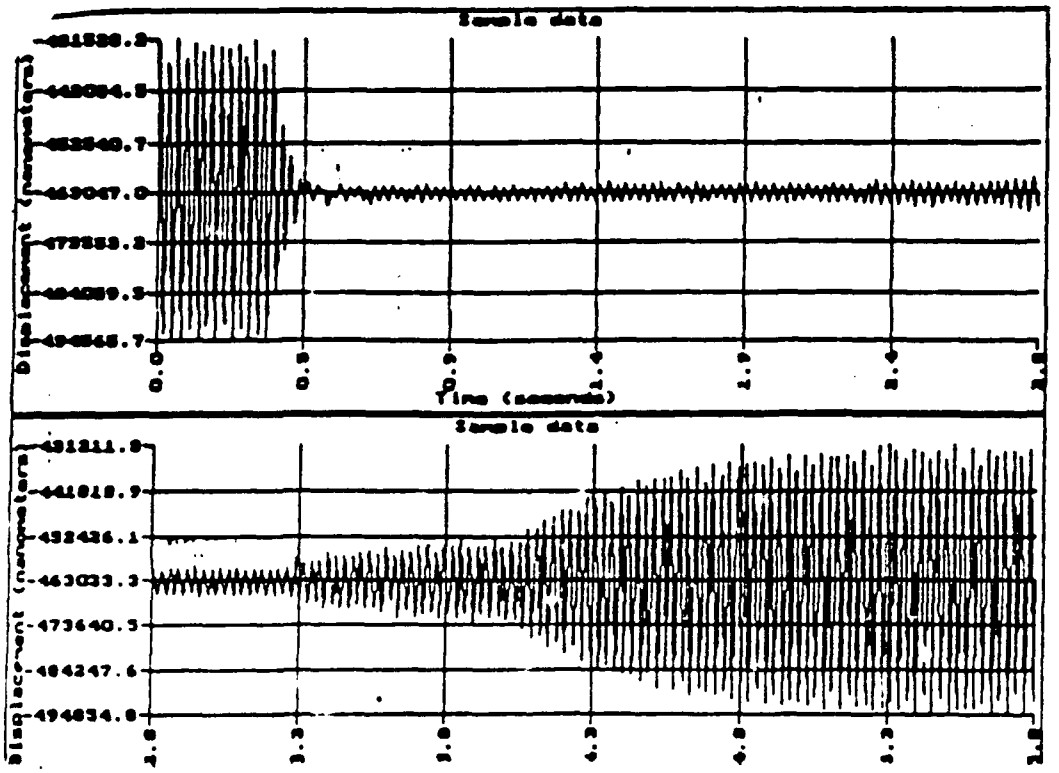

Fig. 16. Performance of a hybrid controller for the MHPE as the LPACTs are turned off one at a time. (The controller was turned on after .4 sec.) This illustrates controller fault-tolerance.

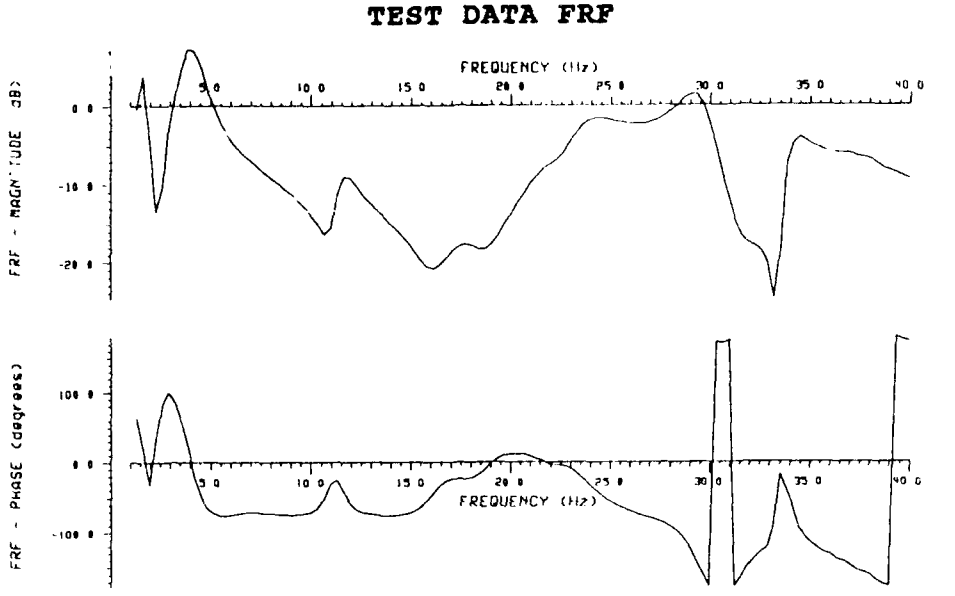

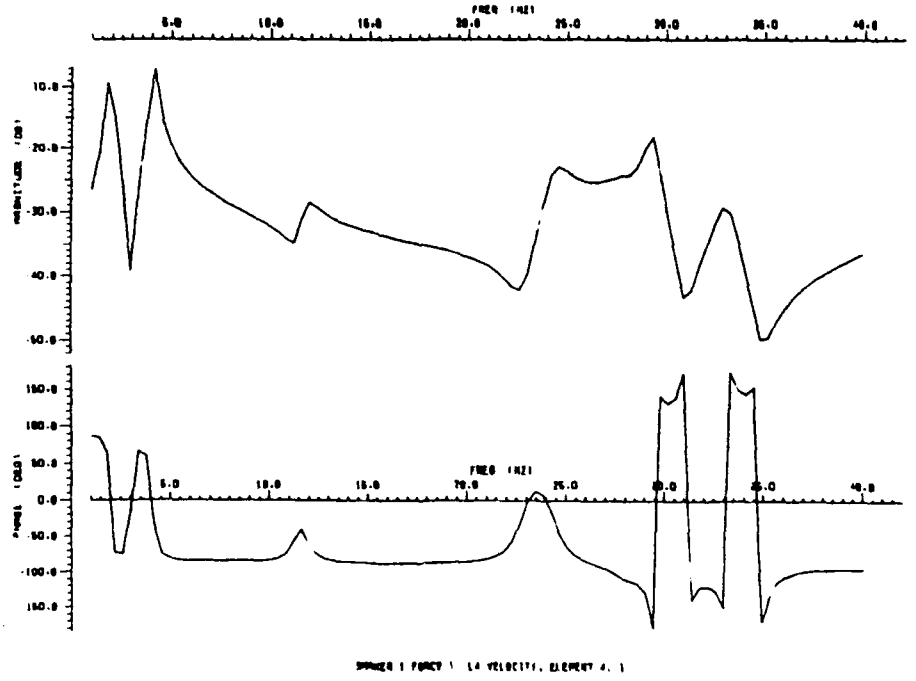

Fig. 17. Analytical and measured frequency response function from LPACT - to accelerometer - illustrating the modelling accuracy achieved with the modelling/identification methodology evolved within this study.

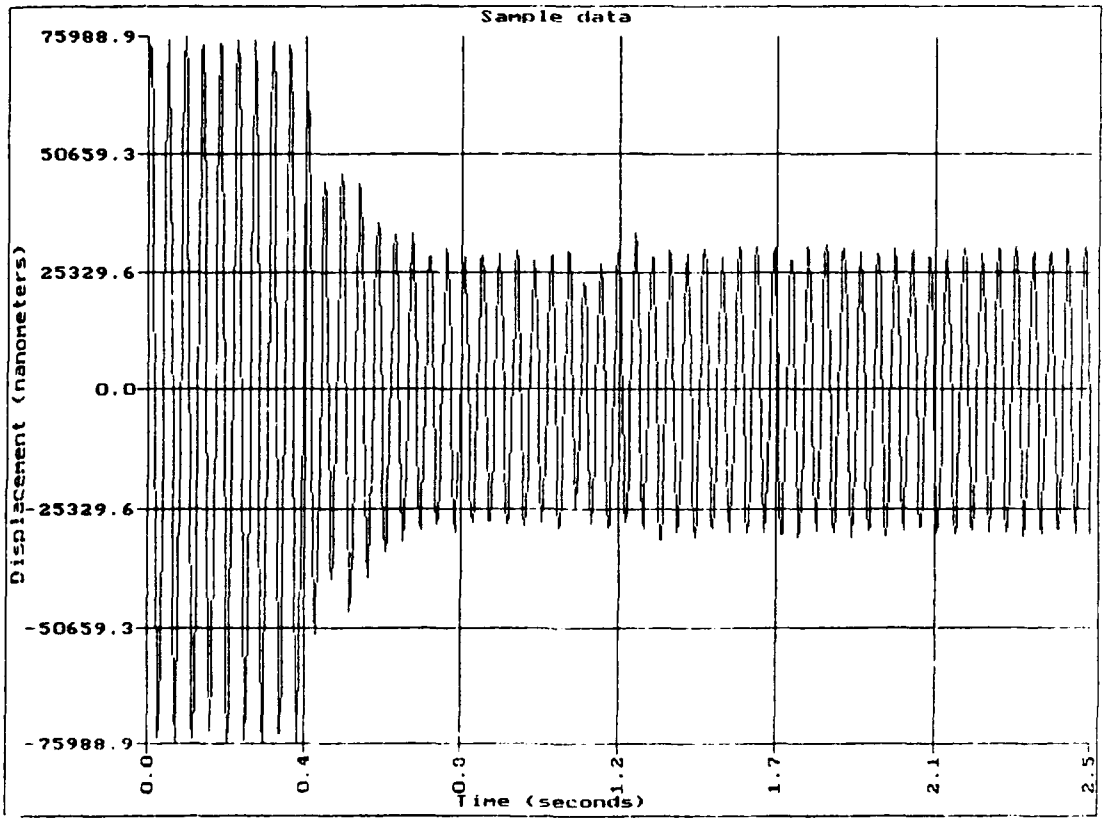

Fig. 16. Performance of the Advanced MEOP Controller for a 21.6 Hz disturbance. (The controller was turned on at .4 sec.)

Appendix A

The Multi-Hex Prototype Exeriment – Facility Description and User's Guide

The Multi-Hex Prototype Experiment: Facility Description and User's Guide

Harris Corporation
Government Aerospace Systems Division
MS 22/4842
Melbourne, FL 32902
(407) 727-5164

(January 1991)

Contact Personnel:

Douglas J. Phillips

David C. Hyland

Version 1

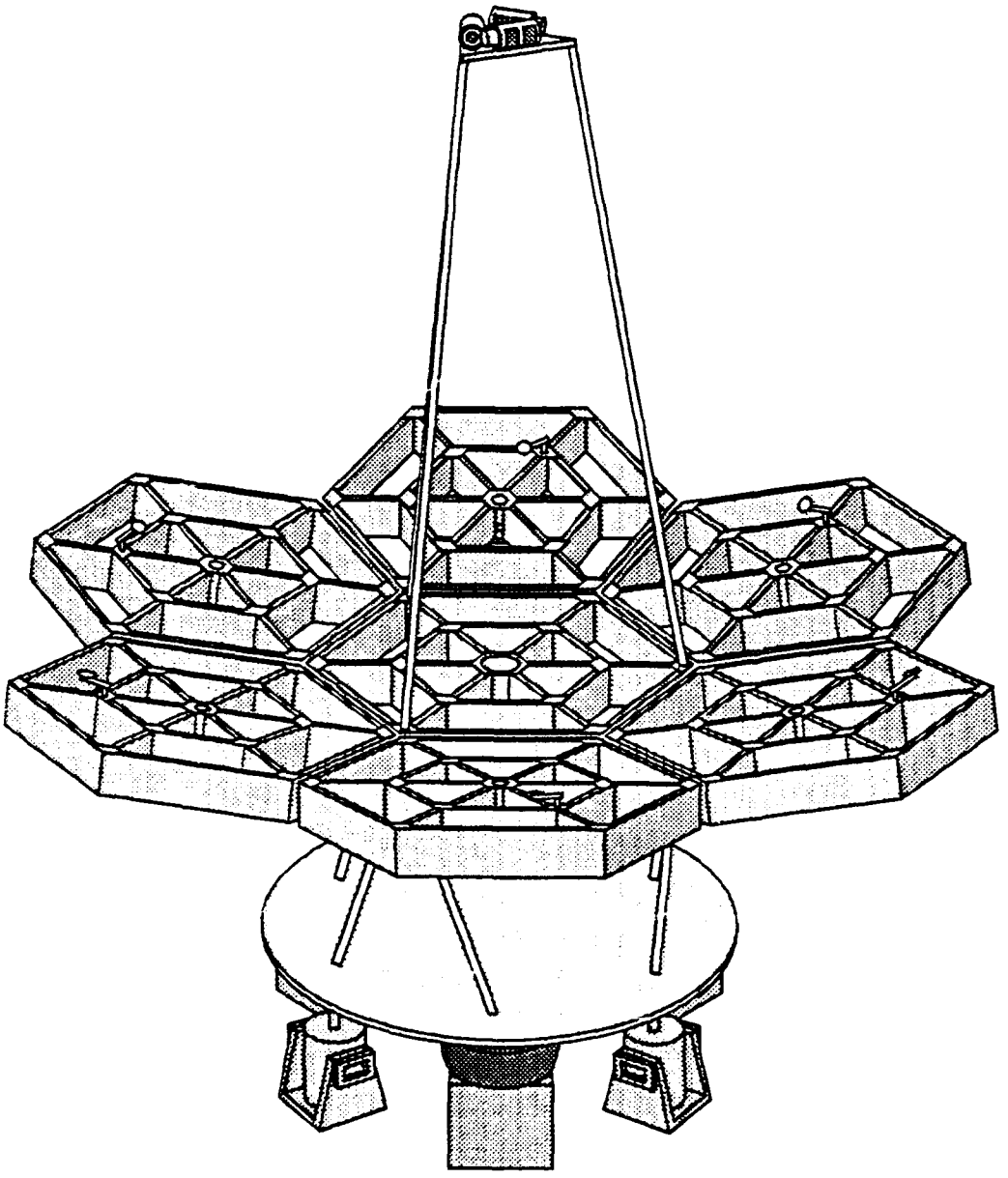

THE MULTI-HEX PROTOTYPE

Table of Contents

Tables

Figures

1. Introduction

It is expected that many future space missions involving flexible structures will require active vibration control to satisfy mission objectives. Hence, it is important for active control of flexible structures to be practically demonstrated in ground-based experiments. These experiments can be used to test existing theories and technologies and provide practical directions for future research. The Multi-Hex Prototype Experiment (MHPE) described in this report is an experiment designed to help meet these objectives. The MHPE was developed at Harris Corporation and is actually the third in a series of experiments designed and implemented at Harris to demonstrate active structural control technology.

The first experimental apparatus was the Double Pendulum testbed, shown in Figure 1.1. The Pendulum was designed to emulate low frequency, high amplitude dynamics which are associated with large truss structures and was used to test the capabilites of the Linear DC Motor (LDCM), the proof mass actuator shown in Figure 1.2. The second experiment involved the Plate testbed, shown in Figure 1.3. The Plate was used to investigate control of a structure with a wide band of closely spaced modes.

The MHPE testbed, shown in Figure 1.4, was developed using the experience gained in the previous experiments. The MHPE was designed to emulate the generic properties of large space structure concepts pertaining to high frequency RF or optical applications. The next section gives the evolution of the MHPE apparatus and discusses its major hardware components.

2. Description of the MHPE

The MHPE, as shown in Table 2.1, contains six major subsystems: the secondary tower, the seven hexagonal-panel structure, the vibration platform, the actuators and sensors, the support electronics and the support computer. The actuators and sensors are described in some detail in Section 3 while the supportelectronics and computer are detailed further in Section 4. In this section, we will primarily focus on the structural components and the vibration platform.

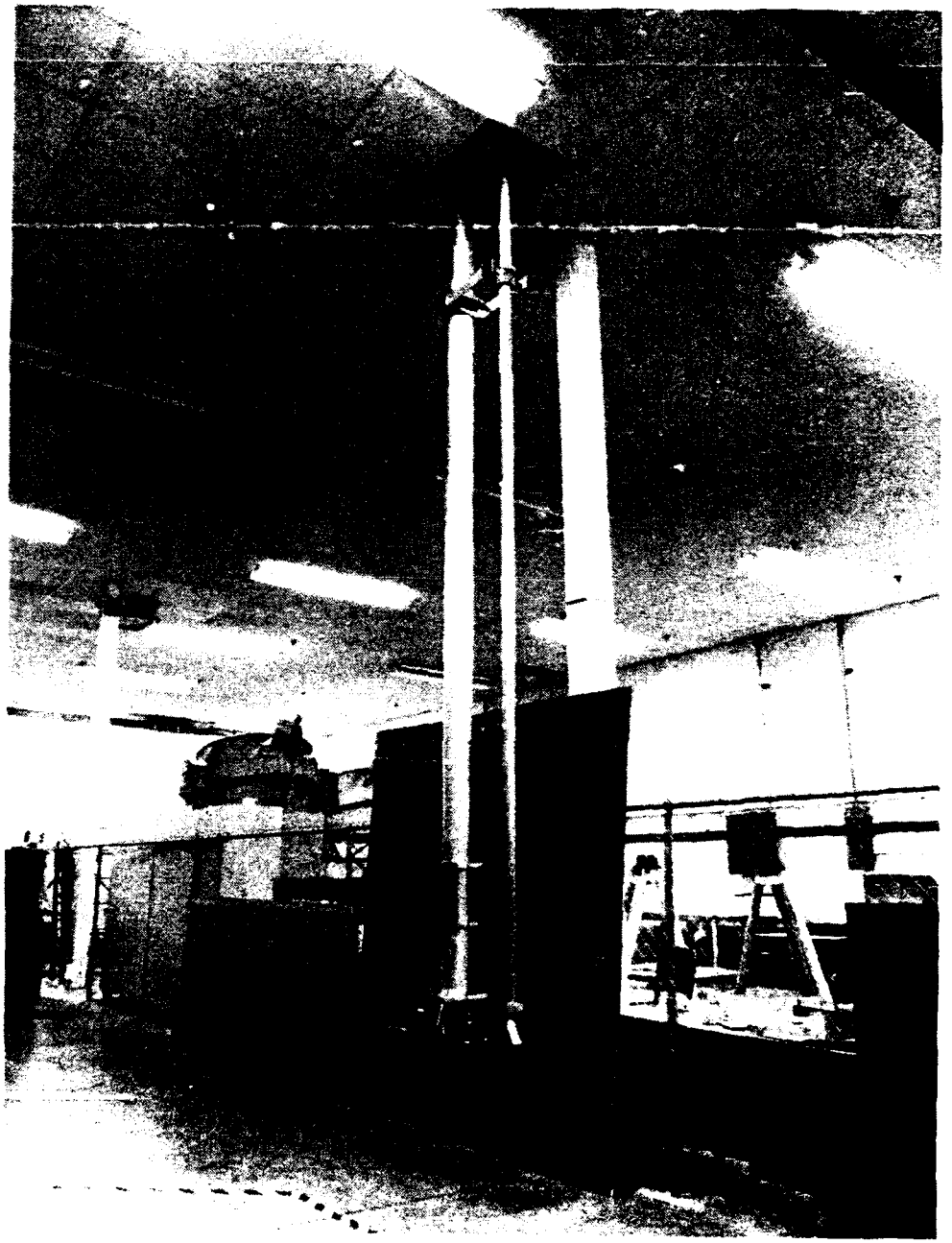

Figure 1.1. The Double Pendulum Experiment was developed to investigate control of low frequency structural modes. This experiment demonstrated the ability of the LDCM to provide high damping to modes below 2 Hz. The control law was designed using the optimal projection approach to fixed-order dynamic compensation and did not destabilize any of the higher frequency modes.

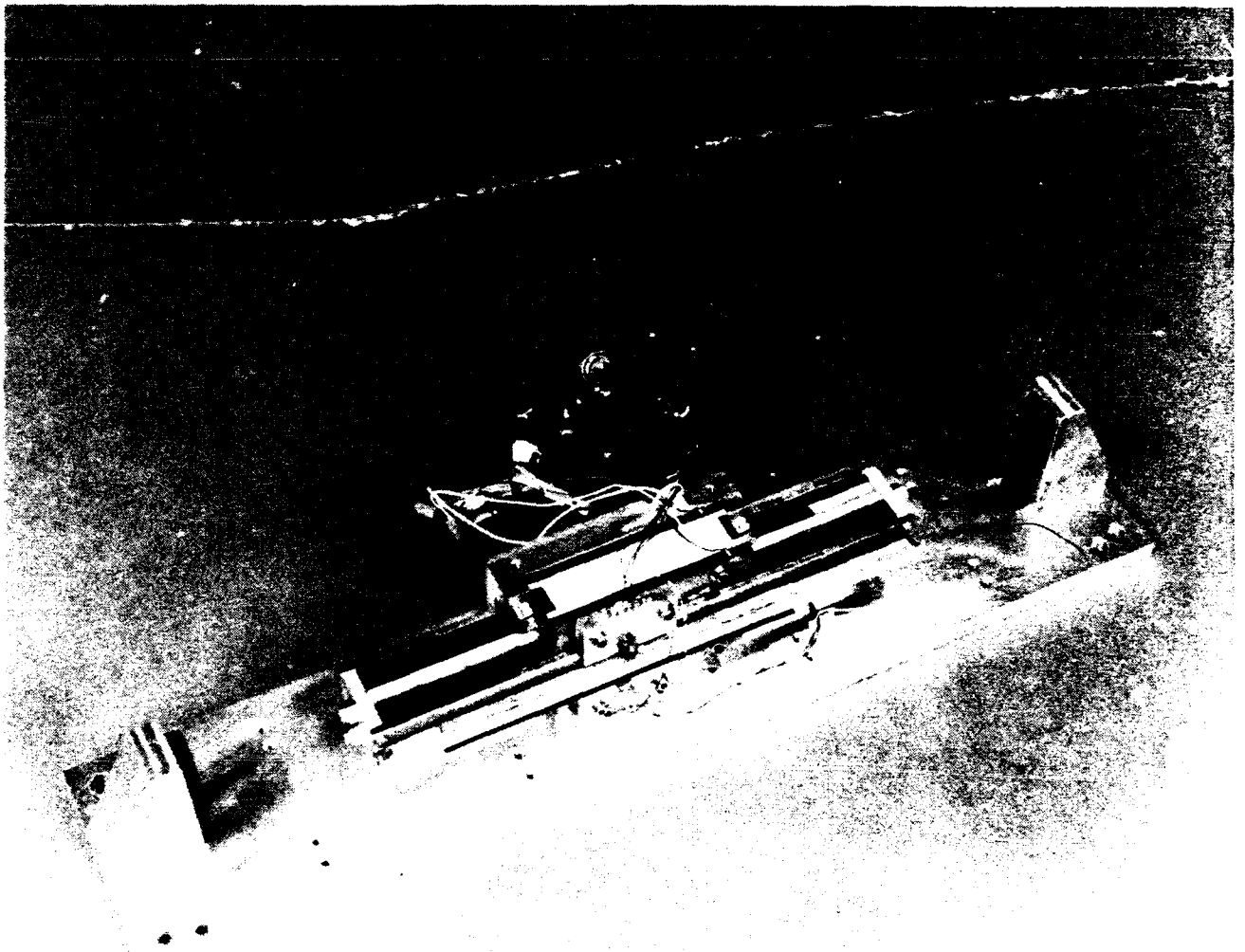

Figure 1.2. The Linear DC Motor (LDCM) was designed to enable high gain control of low frequency structural modes. The utility of this actuator was successfully demonstrated using the Double Pendulum Experiment.

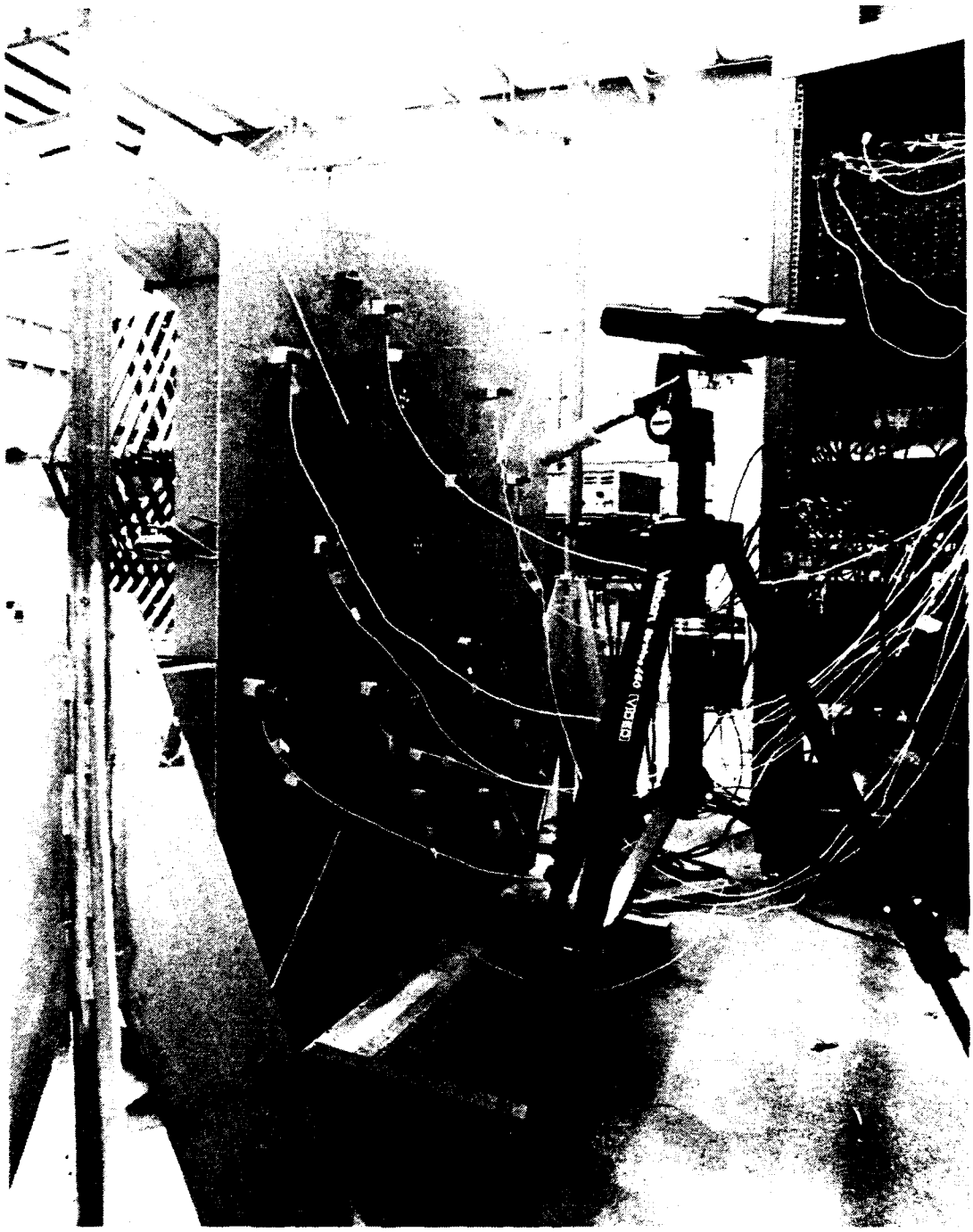

Figure 1.3. The Plate Experiment was used to investigate control design for a very lightly damped structure with a large number of closely spaced modes. The implemented controller used rate feedback to achieve significant closed-loop attenuation.

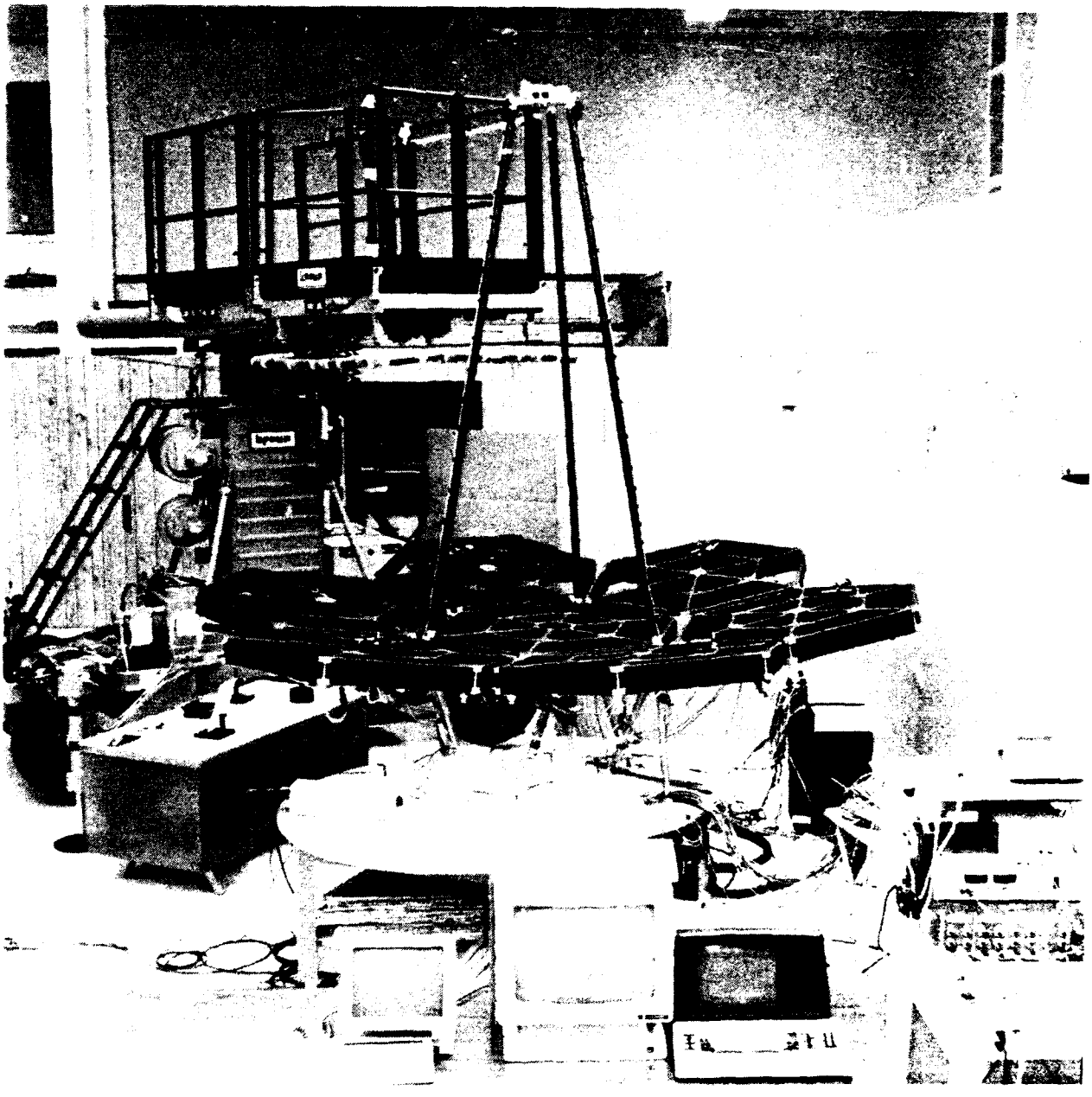

Figure 1.4. The Multi-hex Prototype Experiment is the third in a series of 3 experiments designed and implemented at Harris.

The MHPE was conceived in early 1988. The design incorporates many of the features and technology of the Harris Solar Dynamic Concentrator shown in Figure 2.2. The initial configuration of the MHPE was first built and instrumented in the spring of 1988. Figure 2.3 shows an early configuration of the MHPE. Figure 2.4 shows an early configuration which included a reflector surface. These configurations and all subsequent configurations incorporated six Linear Precision Actuators (LPACTs) of Figure 2.5 in the center of the outer hexagonal panels.

The MHPE apparatus was reconfigured in early 1990 to provide curvature to the primary surface and to add a secondary support tower (see Figures 2.6 thru 2.8). The latest configuration, shown in Figures 2.8 and 2.9, includes the addition of three LPACTs on the support tower in addition to six miniature mirrors on the six outer panels. The mirrors are part of a laser-based optical display which provides visual demonstration of the line-of-sight performance.

Figure 2.10 shows all of the major components of the present configuration and their interrelationships. The secondary tower is attached to the hex panel array at three non-adjacent vertices of the center hexagonal box truss. Figure 2.11 shows a close-up of one of these hexagonal box trusses. Graphite-epoxy was chosen for the structure because it is a space-qualified material and thus provides greater traceability of the structure to real flight systems. The seven panel array is attached to an aluminum circular base plate by a six-member aluminum support truss, shown in the close-up of Figure 2.12. The base plate is isolated from ground by three air-bag isolator supports and three electrodynamic shakers.

3. Actuators and Sensors

To enable high performance structural control it is imperative that a structure be equipped with appropriate actuators and sensors. Suitable actuators and sensors have bandwidths greater than the desired bandwidth of the controller and also have smooth transfer characteristics within the desired controller bandwidth. In this section we discuss the features of the LPACT and Hybrid Accelerometers used for control. We also discuss

Subsystem	Primary Functions	Described In
Secondary Tower	Emulates the optics associated with a secondary mirror.	Section 2
Seven Hexagonal-Panel Structure	Represents a primary mirror support structure.	Section 2
Vibration Platform	Provides physical support for the MHPE.	Section 2
Actuators and Sensors	Provide actuation and sensing for control law implementation and also provide disturbances and sensing for performance evaluation.	Section 3
Support Electronics	Enables analog compensation.	Section 4
Support Computer	Enables digital control law implementation and performance evaluation.	Section 4

Table 2.1. The MHPE hardware consists of 6 major subsystems.

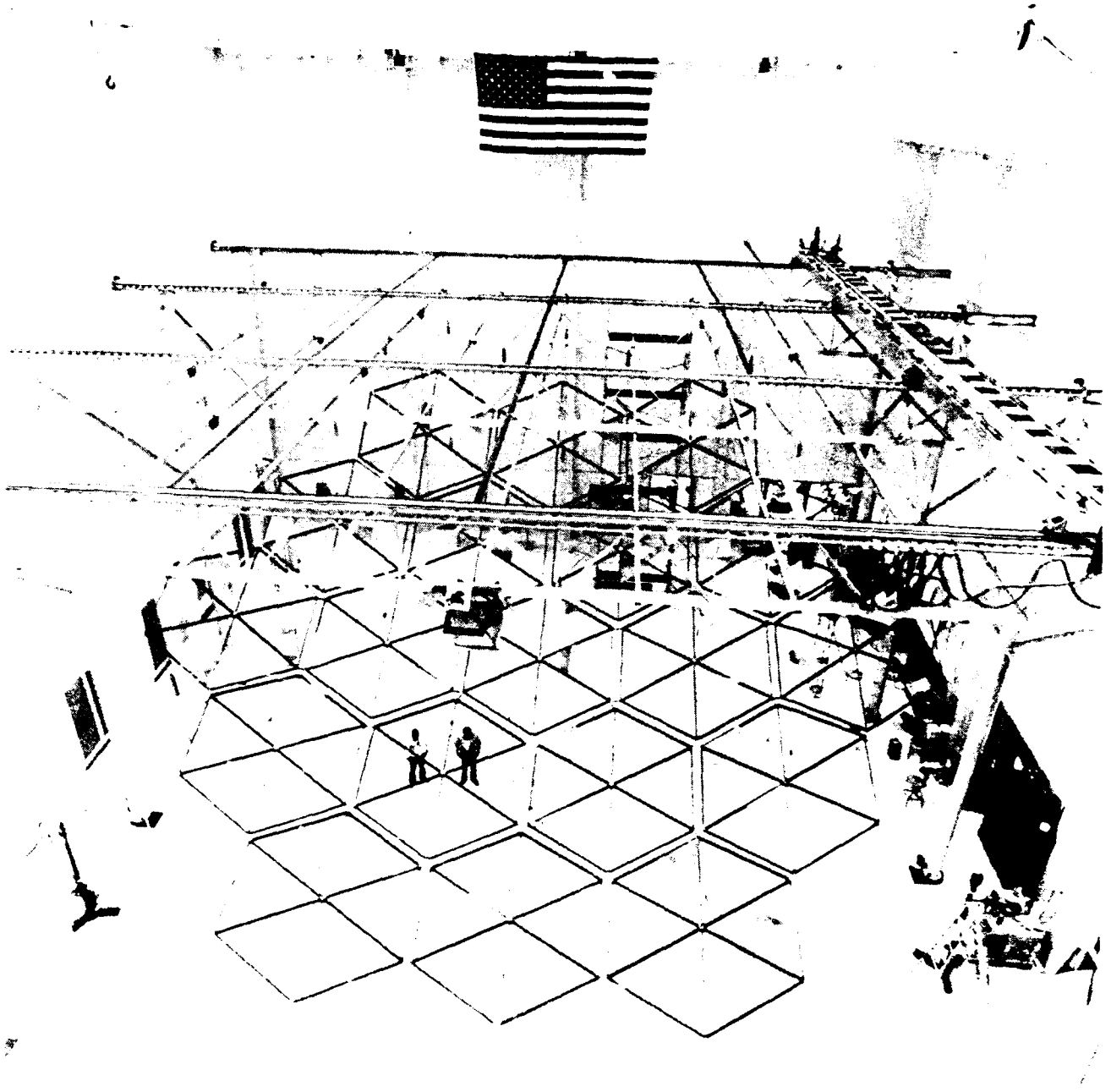

Figure 2.2. Experience in designing and building the Solar Dynamic Concentrator shown here was used to develop the Multi-Hex Prototype Testbed.

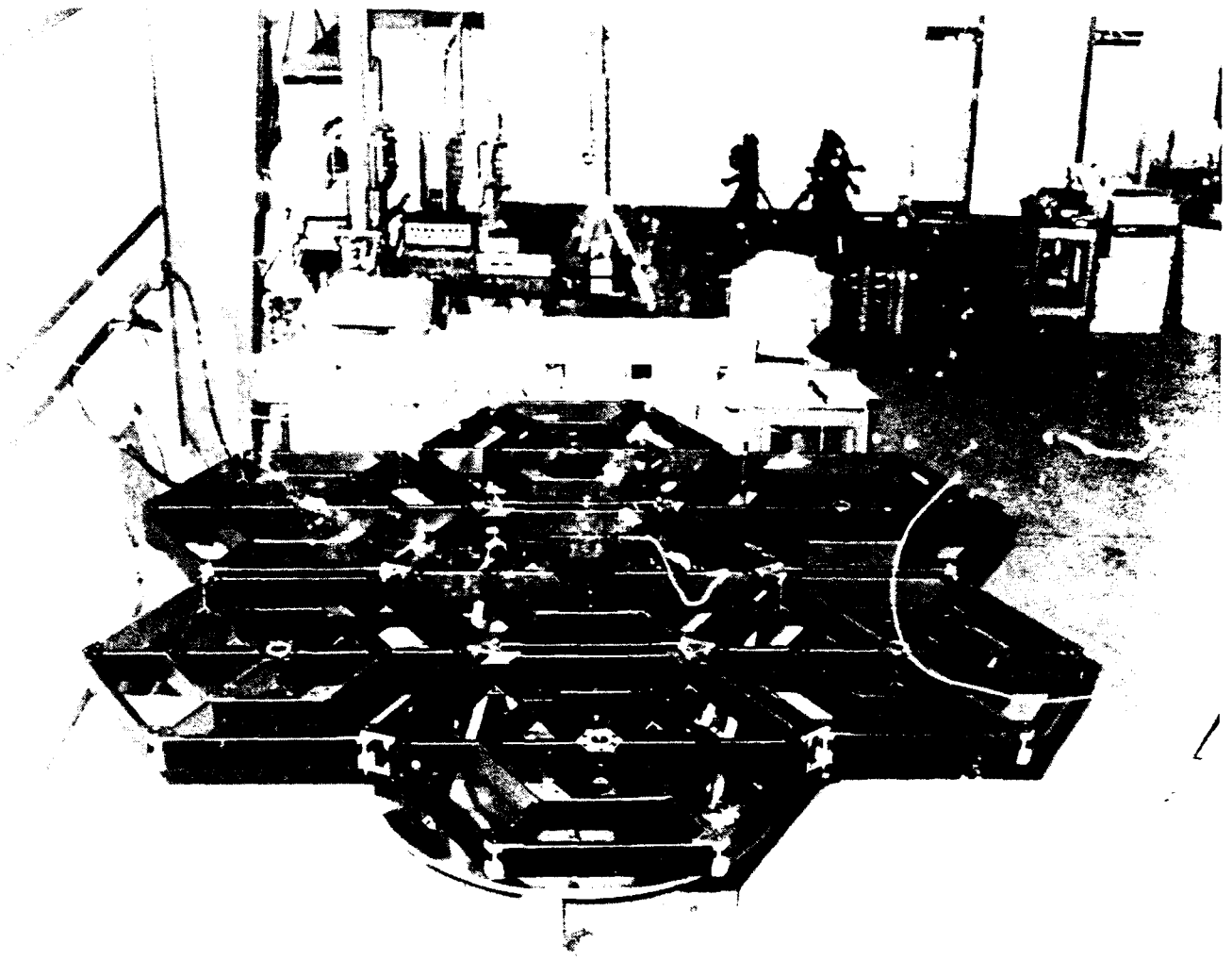

Figure 2.3. This picture shows the initial configuration of the MHPE testbed. Notice that the surface is flat

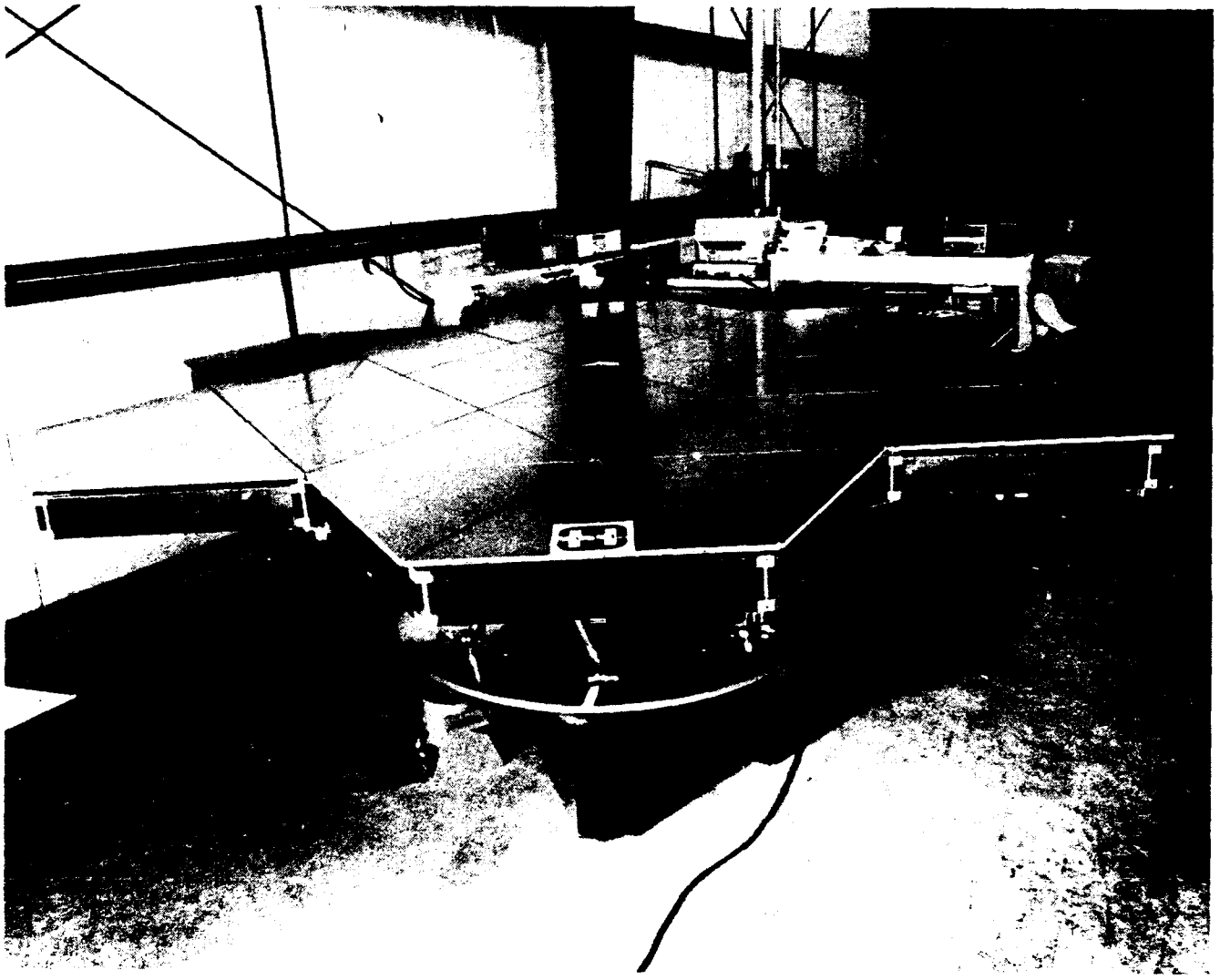

Figure 2.4. This picture shows an early configuration of the MHPE testbed with a reflector surface. The surface consisted of trianglular aluminum honeycomb plates which emulated the dynamic characteristics of a carbon-carbon mirror.

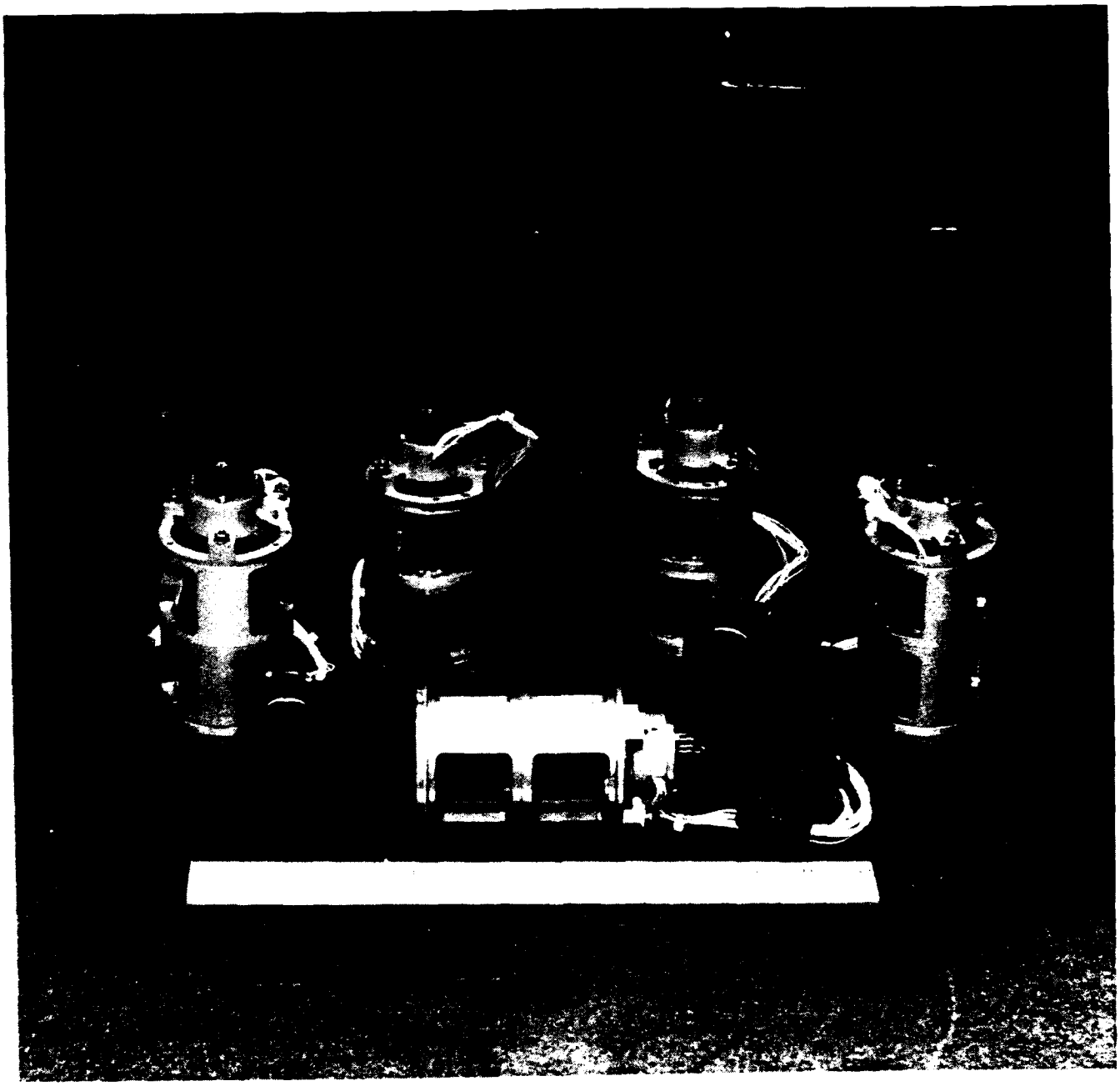

Figure 2.5. The Harris Linear Precision Actuator (LPACT) is a proof mass actuator developed for vibration suppression of flexible structures. The internal control loops of the LPACT yield a device transfer function which has high bandwidth and flat response over a large frequency range.

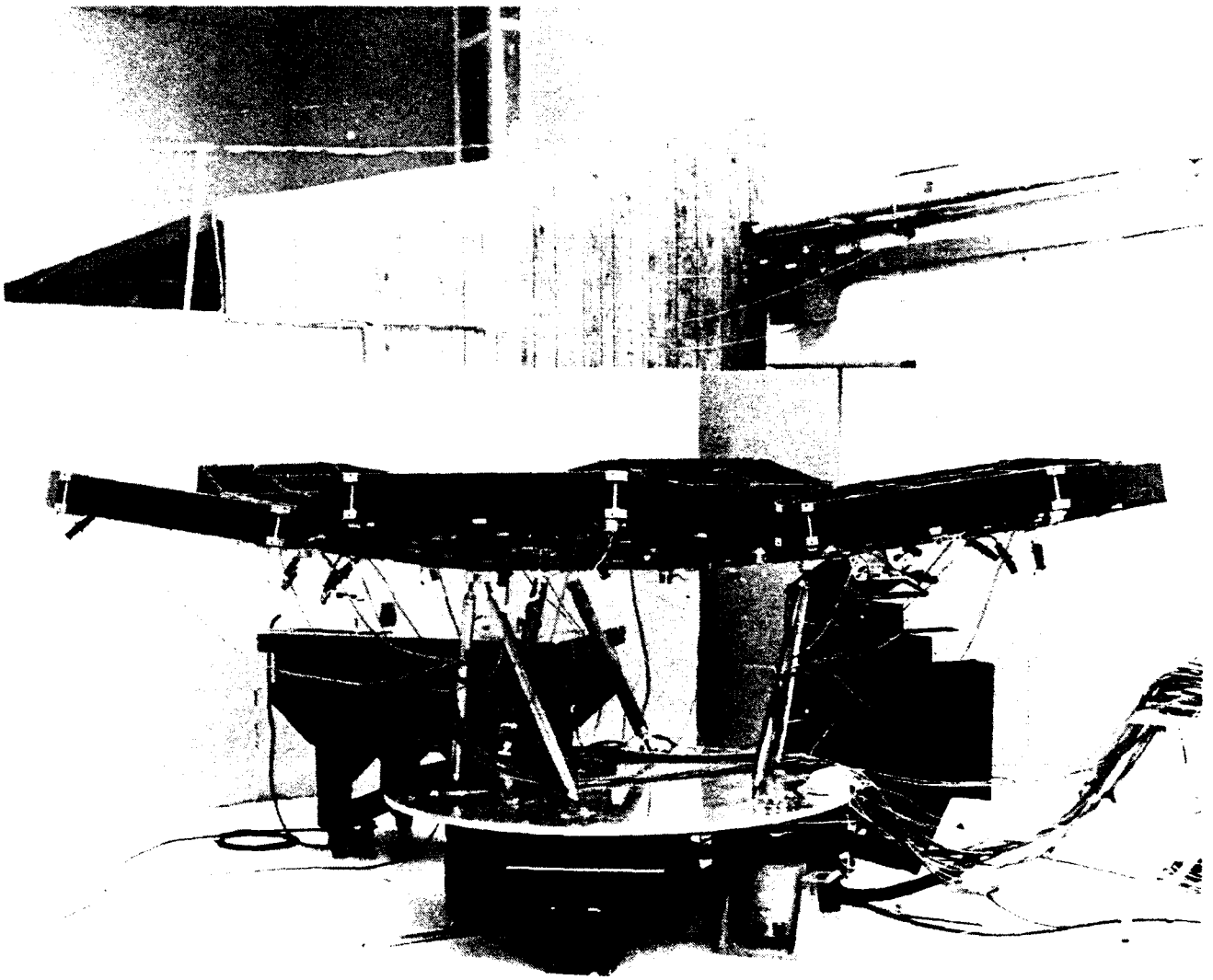

Figure 2.6. This picture shows a picture of the MHPE testbed reconfigured to give the primary surface a parabolic shape.

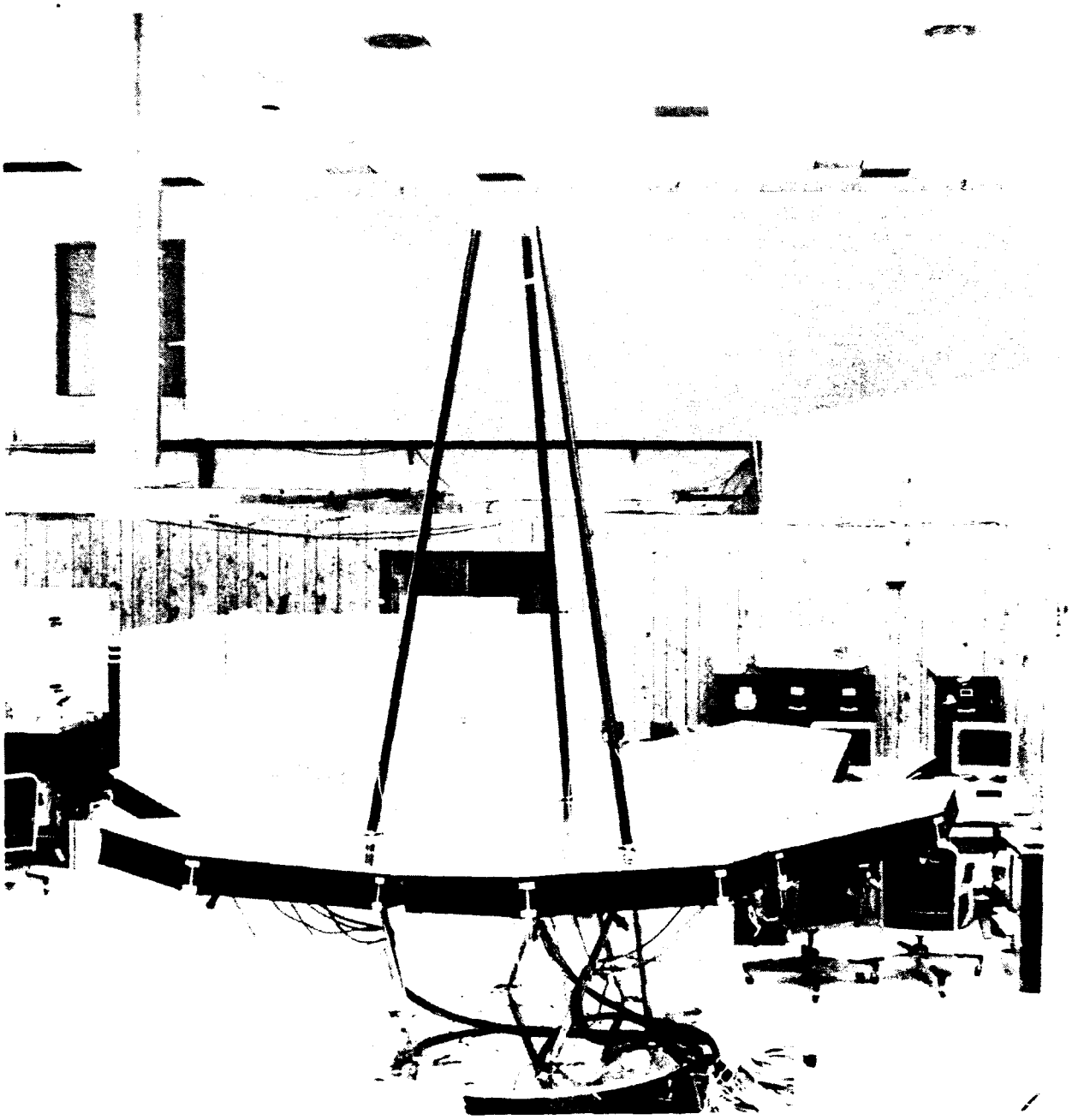

Figure 2.7. This configuration of the MI'PE testbed included a secondary tower in addtion to the aluminum honeycomb reflector surface.

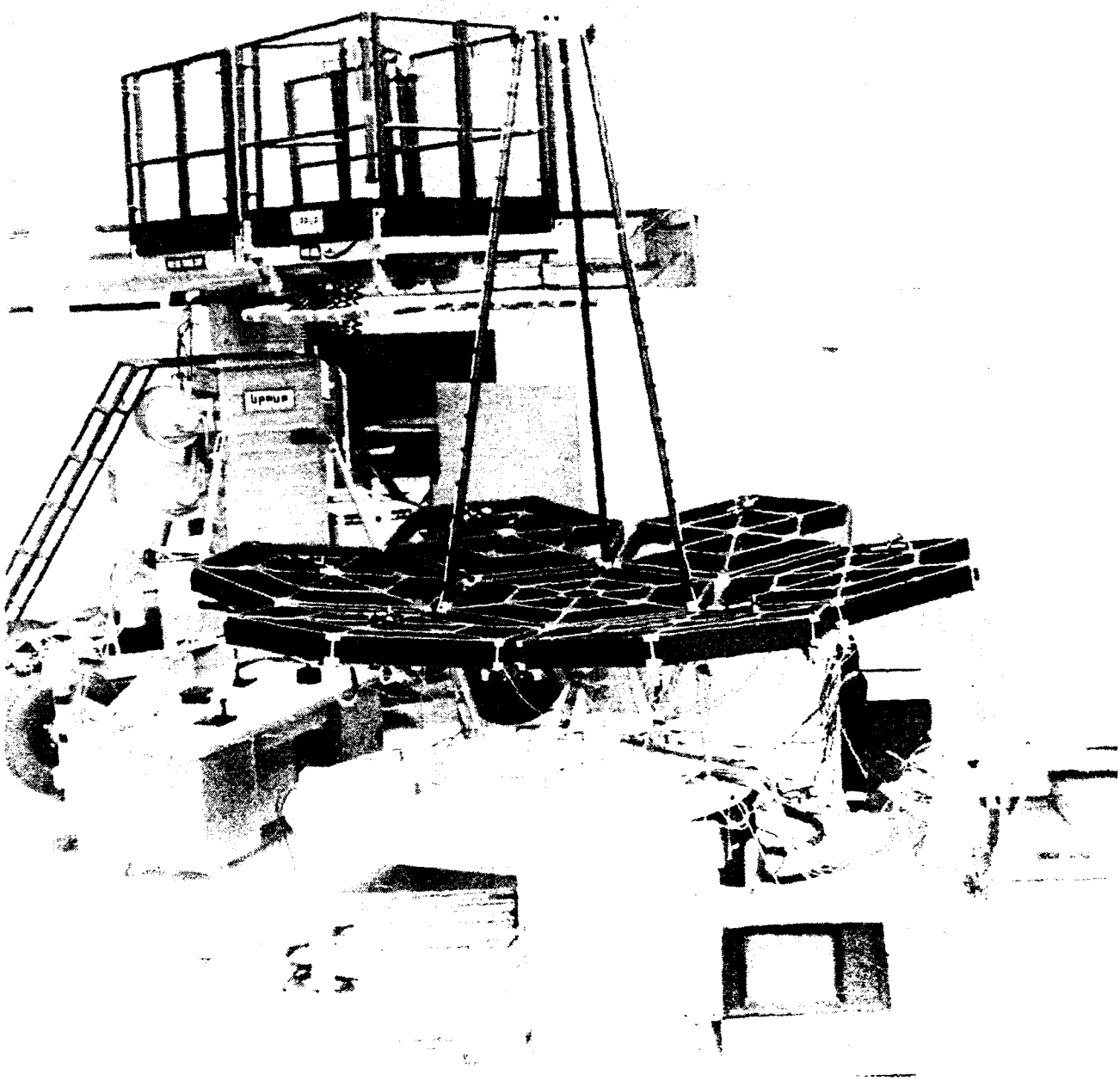

Figure 2.8. The present configuration of the MHPE testbed includes 3 LPACTs on the triangular plate at the top of the secondary tower and a small mirrors between the center and outer edge of each of 6 outer hexagonal panels. The mirrors are used in a laser-based optical system for visual representation of the line-of-sight performance. The Optical Precision Measurement System (OPMS) is located on the circular table underneath the hexagonal panels.

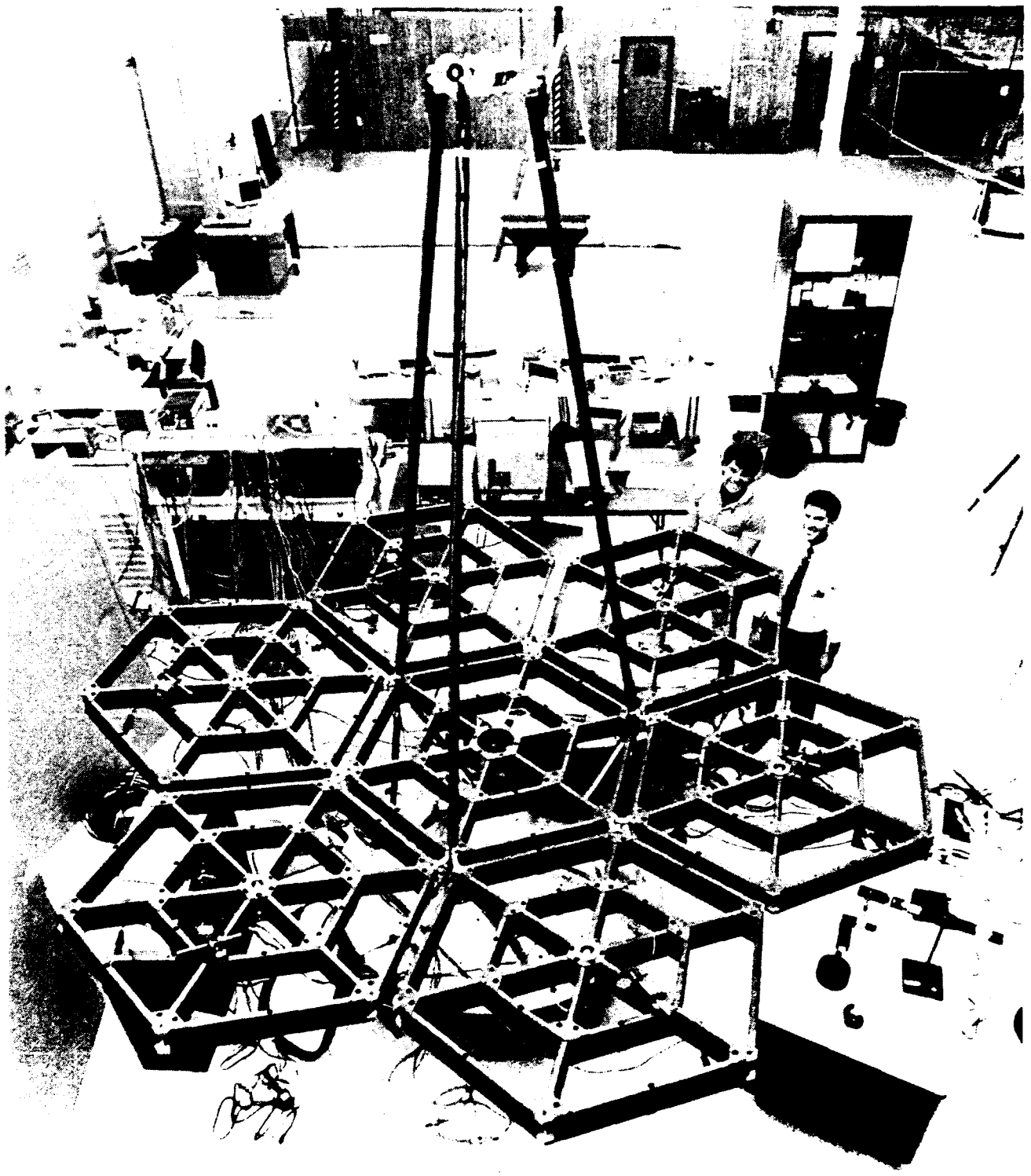

Figure 2.9. This figure shows an overhead view of the present configuration of the MHPE testbed.

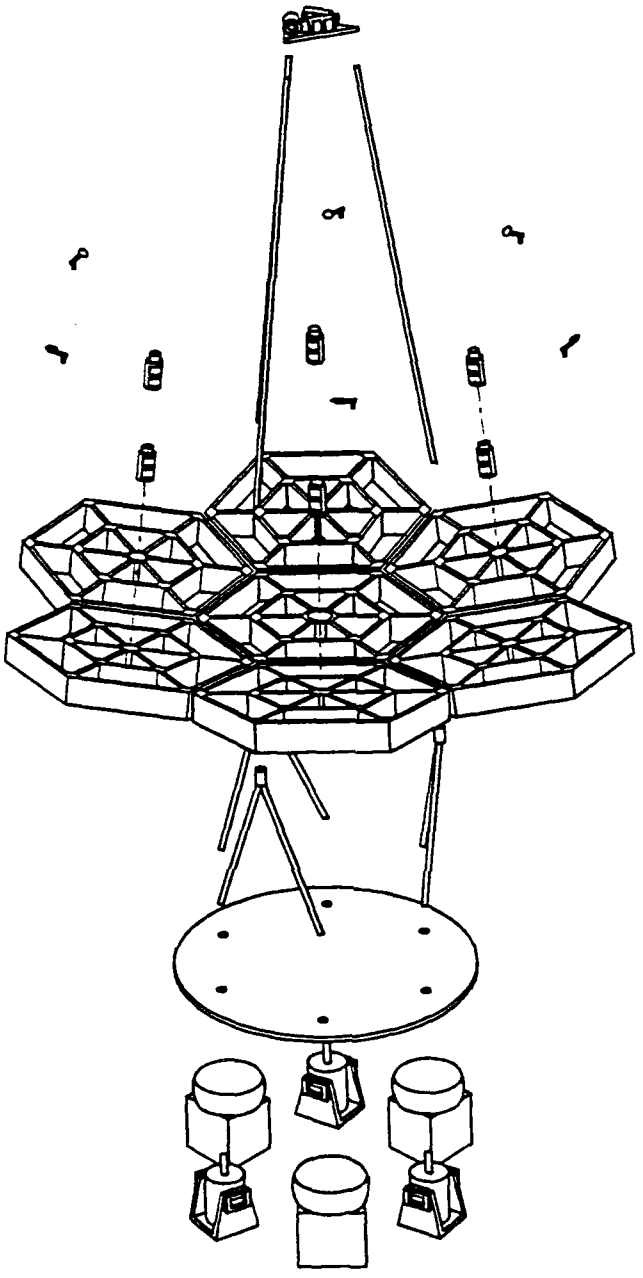

Figure 2.10. The major components of the latest configuration of the MHPE testbed are a secondary tower, a 6 hexagonal panel array, 6 small mirrors, 9 LPACTs, a 6 member aluminum support truss, a circular aluminum base, a disturbance isolation system and the electrodynamic shakers.

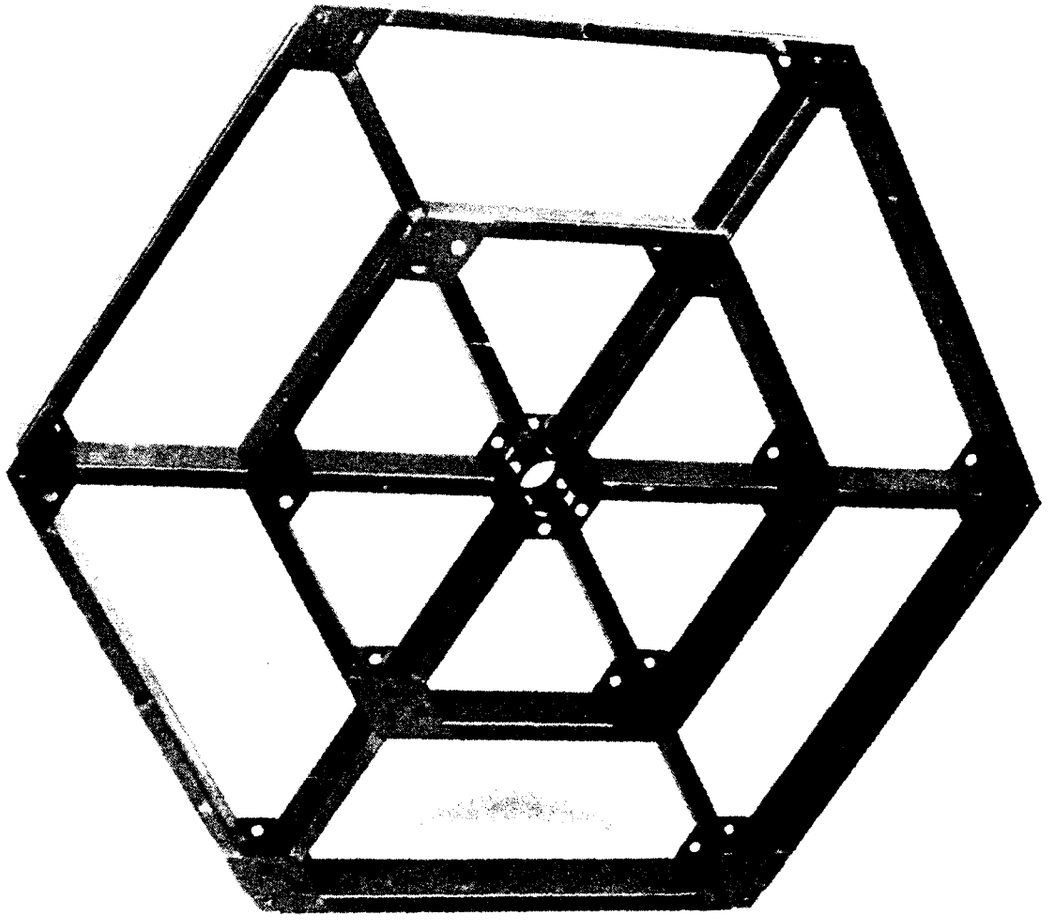

Figure 2.11. This picture shows a close-up of a graphite-epoxy hexagonal box truss used to form the primary support structure of the MHPE testbed.

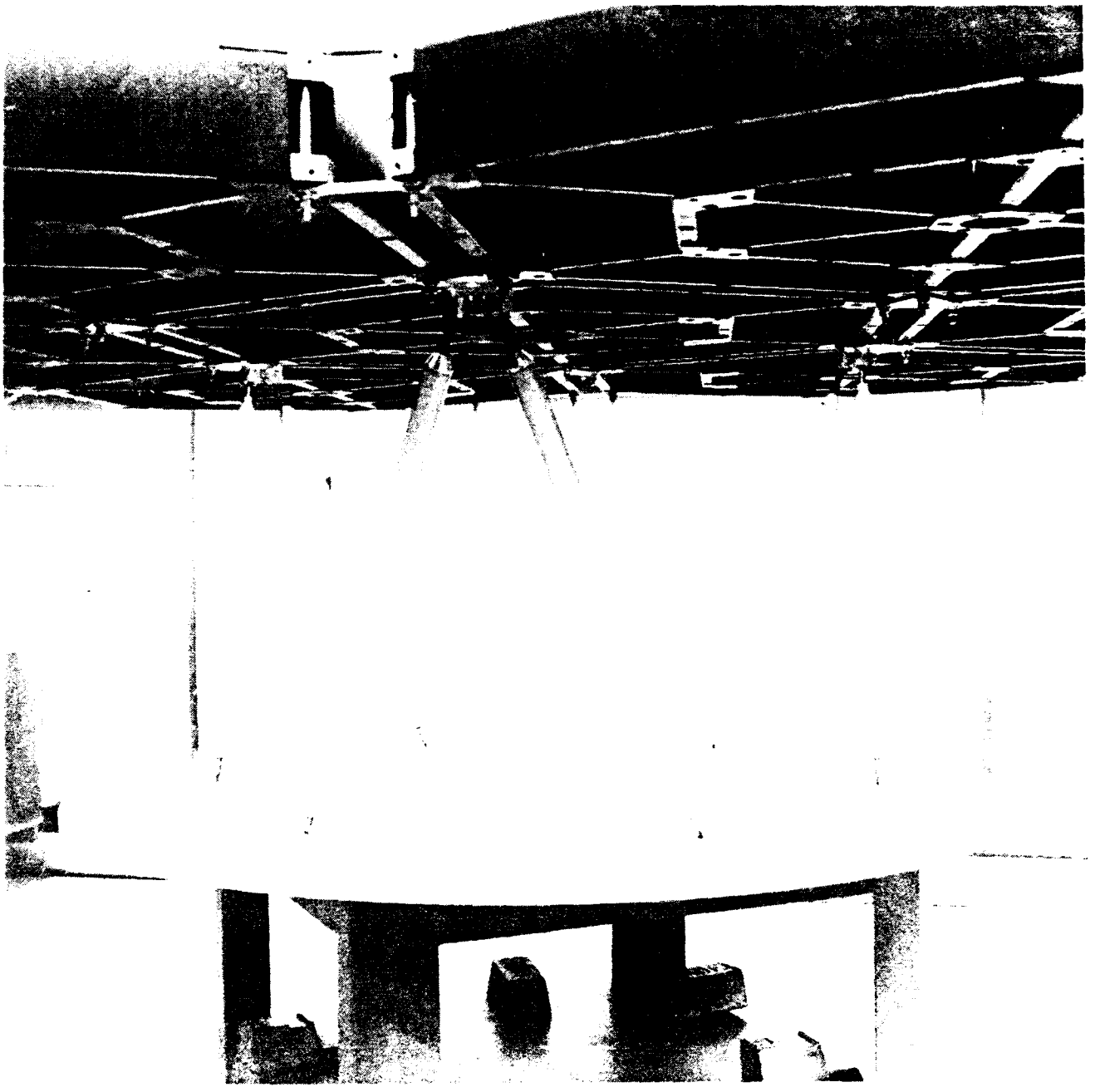

Figure 2.12. This picture shows a close-up of the 6 member aluminum support structure.

the Unholtz-Dickie shaker used to disturb the MHPE testbed and the Zygo Optical Precision Measurement System (OPMS) used to measure relative vertical displacements of the hexagonal panels as a means of monitoring performance.

The Linear Precision Actuator (LPACT)

The LPACT device, shown in Figure 2.5, is a bearingless, linear voice coil actuator. This device was designed, tested and fabricated at Harris and has been patented. The proof mass of the LPACT is restrained by two graphite-epoxy flexures. The flexures have a resonance that appears in the response of the actuator to input commands. (Here we are viewing the actuator as a plant with a reference input, the desired force profile, and an output, the actual force applied by the actuator.) The flexure chosen for an LPACT located on the secondary tower is less compliant than the flexure chosen for an LPACT located in the center of a hexagonal panel because the tower actuators are required to control modes which are lower in frequency than the modes controlled by the panel actuators. The more compliant flexure of the tower LPACT lowers the resonant frequency in the device transter function, enabling the LPACT to be used to control the tower modes.

Each LPACT utilizes a proof mass mounted accelerometer to close a force control loop which greatly reduces the effects of the resonance of the restraint flexures and also serves to reduce the influence of nonlinearities on the response of the actuator. As seen in Figure 3.1, without the force compensation a panel LPACT diplays a second order, very lightly damped resonance at 9 Hz in the transfer function from voltage input to force output while with the force compensation this actuator has a flat response from 5 Hz to 500 Hz. An LPACT can provide a maximum force of five pounds and has a twenty micro-pound force resolution.

The transfer function of a panel LPACT is adequately modeled by

$$\frac{\text{force}}{\text{command}} = \frac{2s^2}{s^2 + 2(.707)(13 \cdot 2\pi)s + (13 \cdot 2\pi)^2}.$$

The tranfer function of a tower LPACT is given by

$$\frac{\text{force}}{\text{command}} = \frac{2s^2}{s^2 + 2(.707)(9 \cdot 2\pi)s + (9 \cdot 2\pi)^2}.$$

The Hybrid Accelerometer

Each LPACT device also includes a colocated Hybrid Accelerometer. The Hybrid Accelerometer electronically combines the signals of two different accelerometers, the Sundstrand QA-700 and the Piezotronics PCB-303A to yield an acceleration measurement which is superior to that obtained by either of the individual accelerometers. The QA-700 is a servo accelerometer which has high accuracy but low bandwidth while the PCB-303A is a piezo electric accelerometer with lower accuracy than the QA-700 but much higher bandwidth. Hence, the Hybrid Accelerometer has a high bandwidth (the response is flat from DC to 5 kHz) and is very accurate at low frequencies.

The Unholtz-Dickie Shaker

The Umholtz-Dickie Shaker is used to disturb the MHPE structure. This device has a 50 pound maximum force capability and can reliably excite the structure at frequencies up to at least 100 Hz. Both random and deterministic signals may be used to command the shakers by using a variety of analog sources or the support computer described in the next section.

The Zygo Optical Precision Measurement System (OPMS)

To aid in performance analysis the Zygo OPMS, shown in Figure 2.8, has been included as part of the MHPE. The OPMS is a laser-based interferometric device which allows very accurate measurement of relative displacements. The OPMS is has a resolution of 6 nanometers.

As shown in Figure 3.2, this measurement system can allow the measurement of the relative vertical diplacements of up to 12 points on the array of seven hexagonal panels.

4. Support Electronics and Computer

The Structural Interface Electronics (SIE) and the MCX-5 Data Acquisition and Control Computer (DACC) are essential to the implementation of control laws. This section discusses these two components in turn.

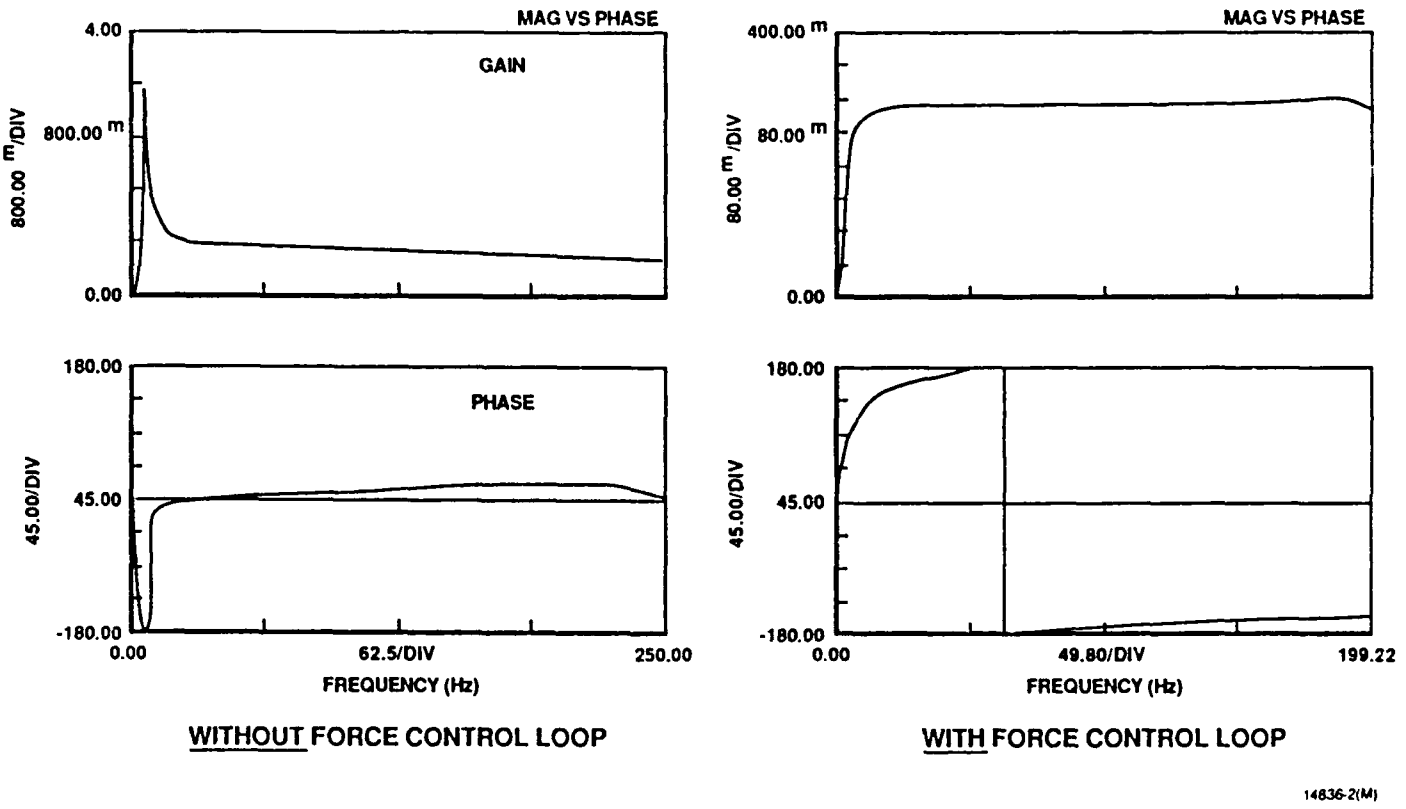

Figure 3.1. Each of the LPACTs has an internal force loop which reduces the influence of the mechanical flexure resonance on the LPACT transfer function. Shown here are the frequency responses of a panel LPACT with and without force loop compensation.

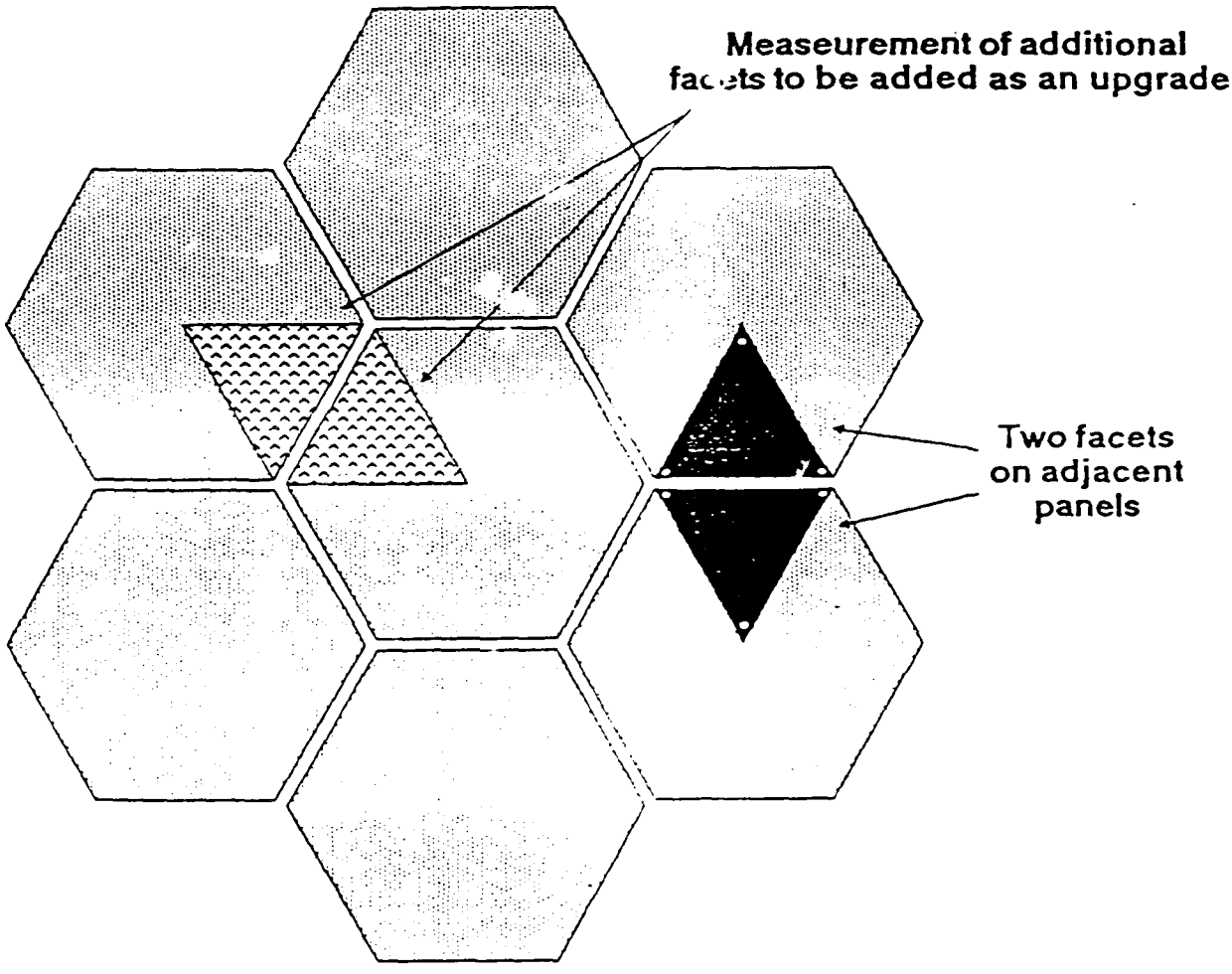

Figure 3.2. As illustrated here, the OPMS can be used to measure the displacements at up to 12 points on the 7 panel array of the MHPE testbed.

Structural Interface Electronics (SIE)

The Structural Interface Electronics performs the 6 major functions listed below.

(i) It implements internal force compensation for each of the LPACTs.

(ii) It uses roof-top integration to produce velocity estimates for each of the acceleration measurements. The transfer function $G_{RT}(s)$ of each of the current roof-top integrators is

$$G_{RT}(s) = \frac{s}{(s + .5 \cdot 2\pi)^2}.$$

However, these dynamics may be changed.

(iii) It implements decentralized analog controllers (based on the velocity estimates.)

(iv) It sends commands to the LPACTs to offset any biases in the postions of the proof masses.

(v) It is used to command the LPACTs when they are used as disturbance sources.

The MCX-5 Data Acquisition and Control Computer (DACC)

The MCX-5 DACC is used for real-time floating point digital control law implementation. This computer is also used for performance analysis and is capable of sending disturbance commands to the shakers. The software package that enables these functions is the Data Acquisition and Control and Processing Software (DACAPS). The DACC also hosts the A/D and D/A signal processing boards. These boards process or output analog signals between ± 5 volts and digital signals of 12 bits.

The DACC can sample up to 256 sensor outputs and can currently command as many as 8 actuator inputs. There are plans to expand the capability of the DACC to command up to 16 actuators. The DACC is currently capable of implementing at 330 Hz a 12th order digital control law that uses 6 inputs and 6 outputs. There are plans to expand this capability so that the DACC can implement at 330 Hz a 50th order digital control law that uses 9 inputs and 9 outputs.

The DACC can receive and process any of the acceleration or velocity estimate signals and generate the appropriate plots. Its processing capabilities include the ability to generate power spectral densities and frequency response functions.

5. Finite Element Model of the MHPE Structure

A finite element model of the MHPE structure was developed using the Harris software program Non-Linear Structural Analysis (NLSA). The finite element model was generated using 48 plate elements, 1041 beam elements and 3 spring elements (for the 3 tower LPACTs). These elements correspond to 775 nodes and yielded an initial finite element with 4401 degrees of freedom. This initial model has been modified to better correlate with actual test data. The first 28 modes were retained in the latest finite element model.

Table 5.1 lists the frequencies, damping ratios and gives a brief mode shape description of the 34 modes retained in the finite element model. The mode shapes are each classified as being in one of the following 6 categories: (i) Quasi Rigid Body Modes, (ii) Panel Modes, (iii) Tower Modes, (iv) LPACT Modes, (v) Strut Modes and (vi) Complex Modes. Each of these mode classifications is defined as follows.

i) Quasi Rigid Body Modes are the modes in which the structure moves almost rigidly about the three support points.

ii) Panel Modes are modes in which the primary motion is one or more of the seven panels. The Panel Modes include the "cup mode" in which all the outer panels move up and down in phase and the "alternating mode" in which adjacent panels have the opposite motion.

iii) Tower Modes are the modes in which the primary motion of the structure is the tower. For these modes either the tower moves as if it were attached to a fixed rigid base or the rest of the structure moves in reaction to the tower motion.

iv) LPACT Modes are modes which are induced by the motion of the proof masses of the tower LPACTs. These modes are a consequence of the LPACT flexures (or springs). The tower LPACTs were originally modeled as point masses but by comparing the

Mode No.	Frequency Hz	Damping Ratio	Mode Shape Description
1	1.945	.035	Quasi Rigid Body - rocking
2	1.955	.035	Quasi Rigid Body - rocking
3	4.129	.035	Quasi Rigid Body - vertical displacement
4	6.761	.035	LPACT - in X-Y plane
5	6.889	.035	LPACT - in X-Y plane
6	6.892	.035	LPACT - in X-Y plane
7	9.870	.075	Quasi Rigid Body - Z rotation
8	11.90	.075	Tower - bending
9	11.91	.031	Tower - bending
10	15.43	.075	Quasi Rigid Body
11	15.44	.075	Quasi Rigid Body
12	18.37	.055	Tower - torsion
13	26.60	.055	Panel - induces LPACT Z motion
14	26.67	.020	Panel - induces LPACT Z motion
15	30.67	.031	Complex
16	30.70	.031	Complex
17	32.90	.035	Panel - cup
18	33.71	.035	Panel - alternating
19	41.46	.035	Strut
20	44.70	.031	Complex
21	44.83	.033	Complex
22	49.27	.030	Tower - bending
23	49.27	.030	Tower - bending
24	49.39	.030	Tower - torsion
25	55.05	.010	Tower
26	55.08	.010	Tower
27	60.62	.010	Tower
28	82.19	.010	Panel

Table 5.1. This table describes the 28 modes of the MHPE finite element model.

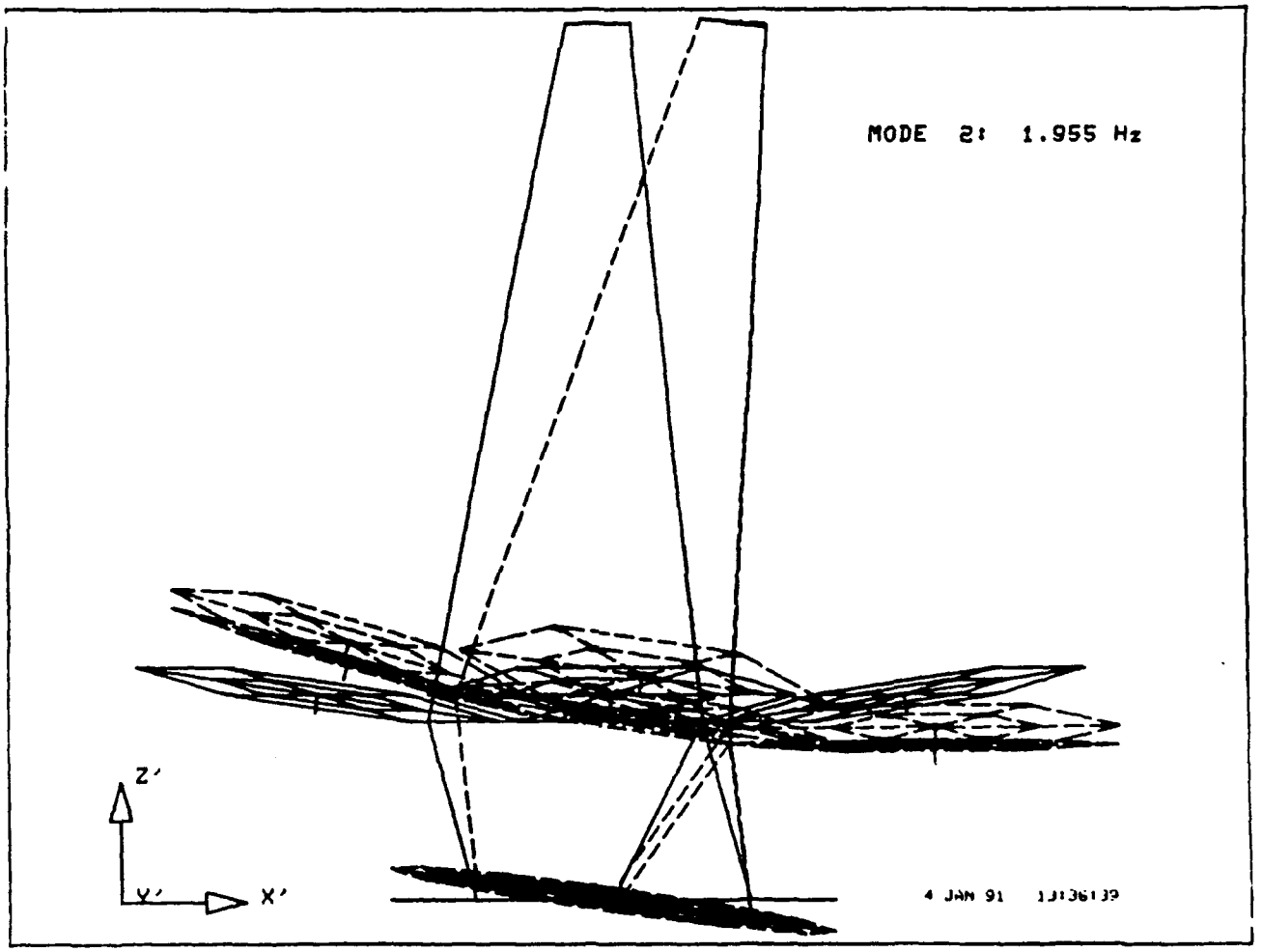

Figure 5.2. This figure shows the mode shape corresponding to a quasi rigid body mode.

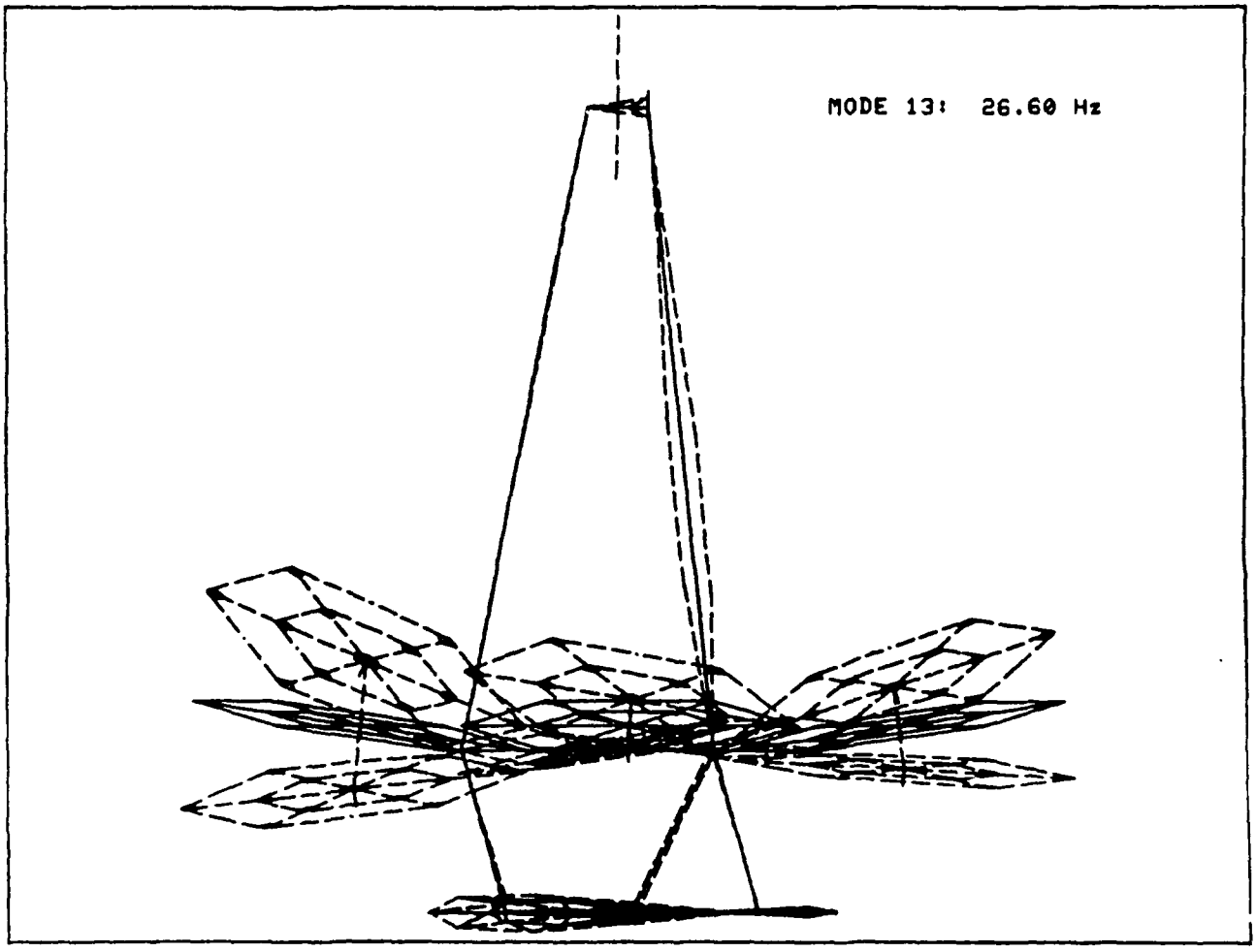

Figure 5.3. This figure shows the mode shape corresponding to a panel mode.

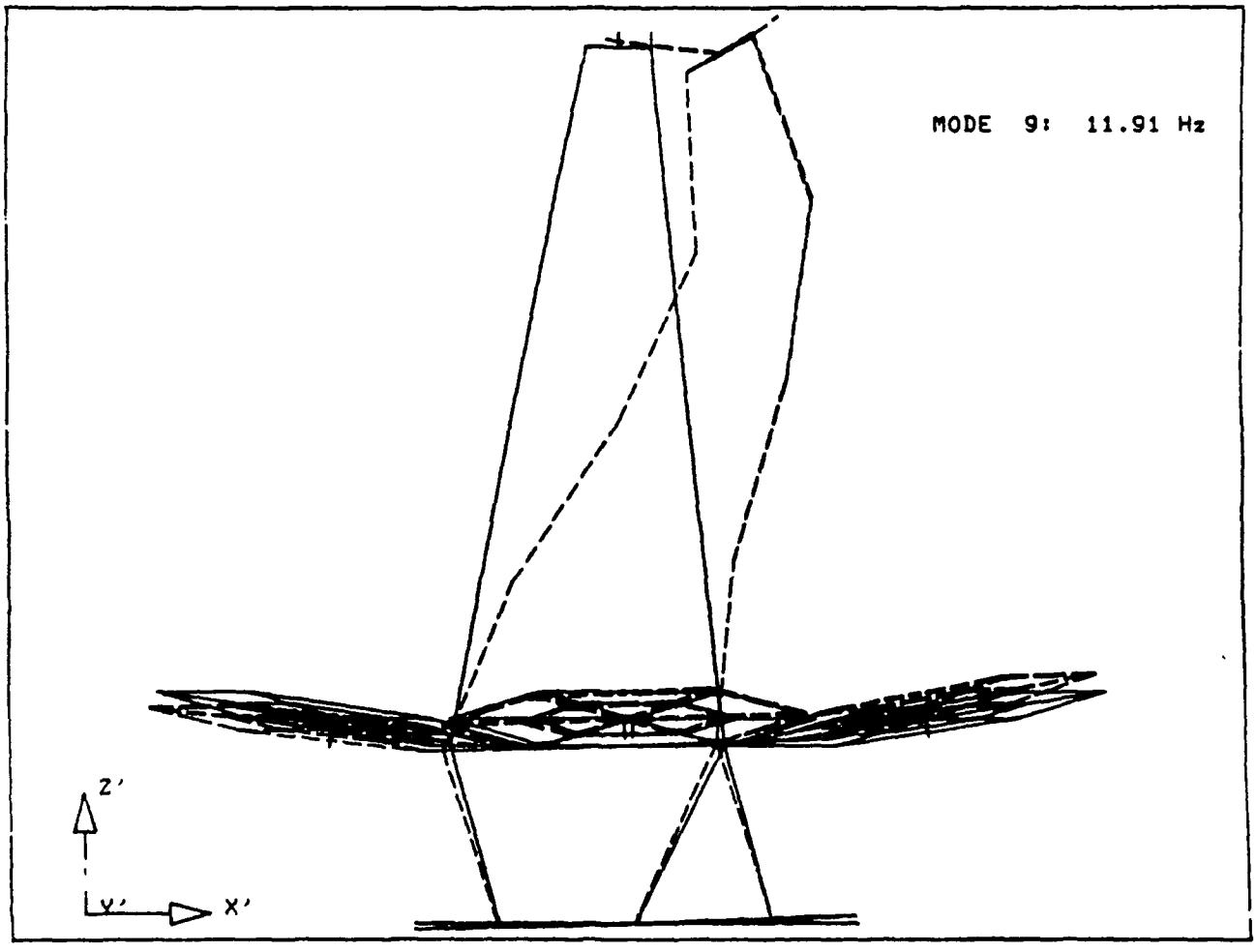

Figure 5.4. This figure shows the mode shape corresponding to a tower mode.

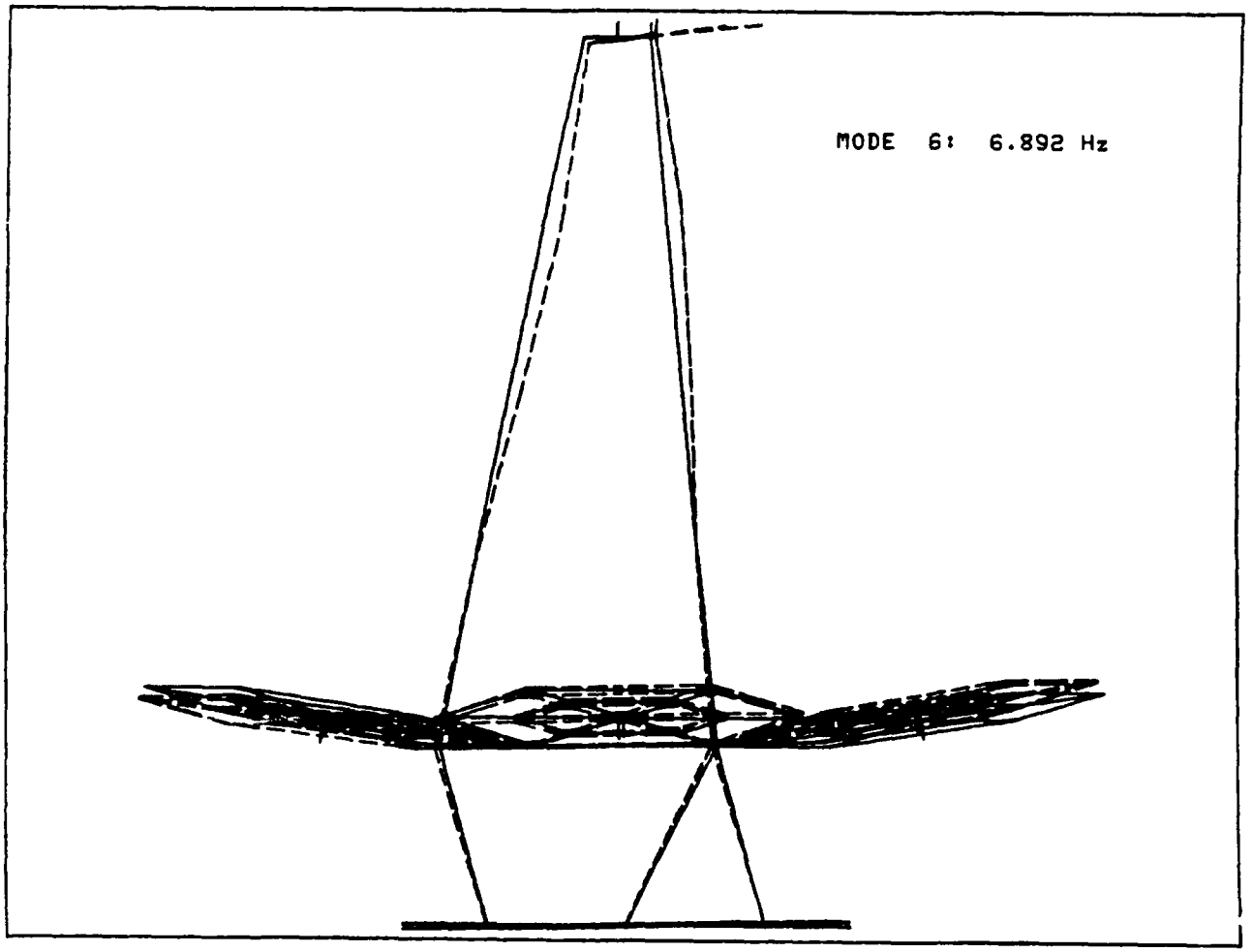

Figure 5.5. This figure shows the mode shape corresponding to a LPACT mode.

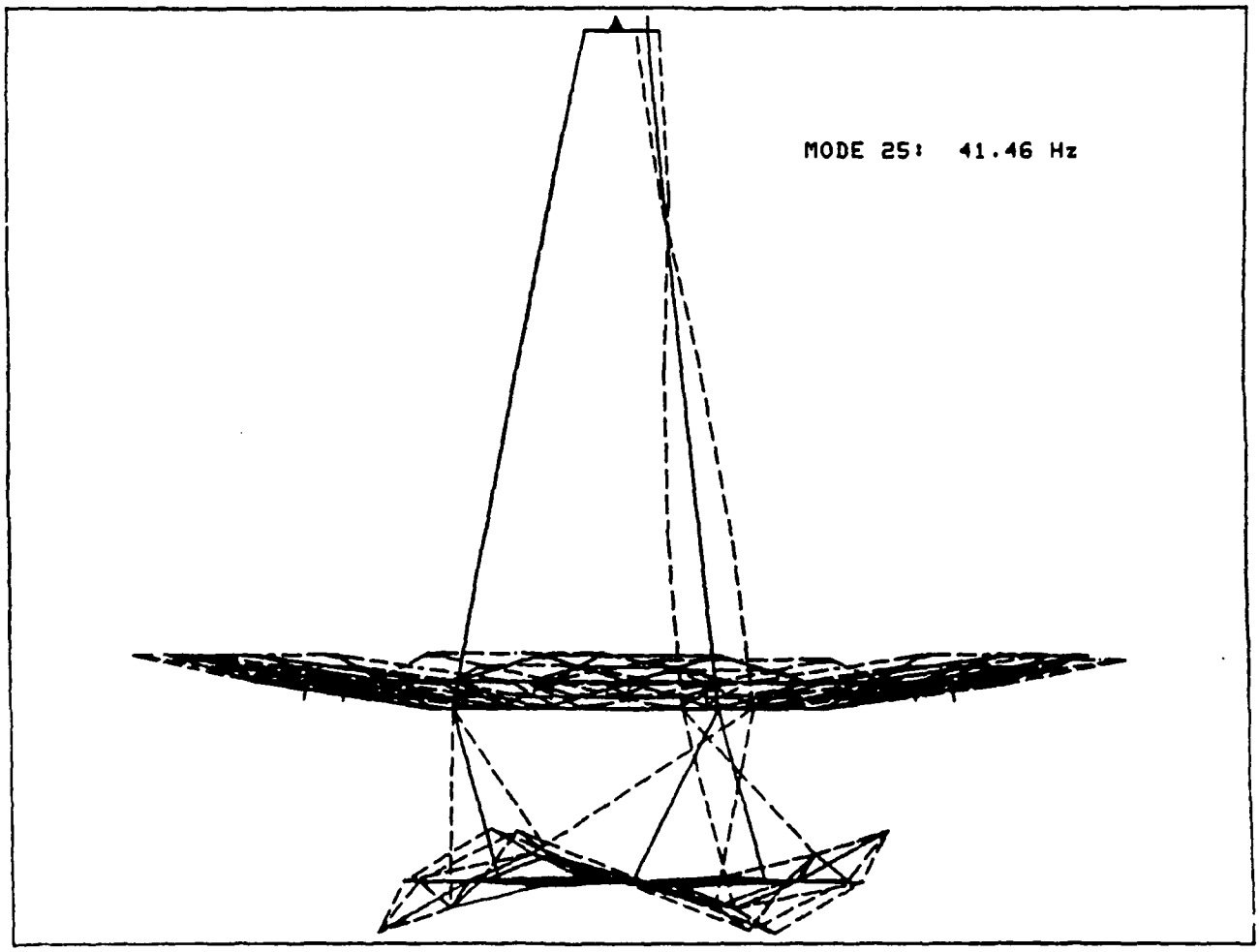

Figure 5.6. This figure shows the mode shape corresponding to the strut mode.

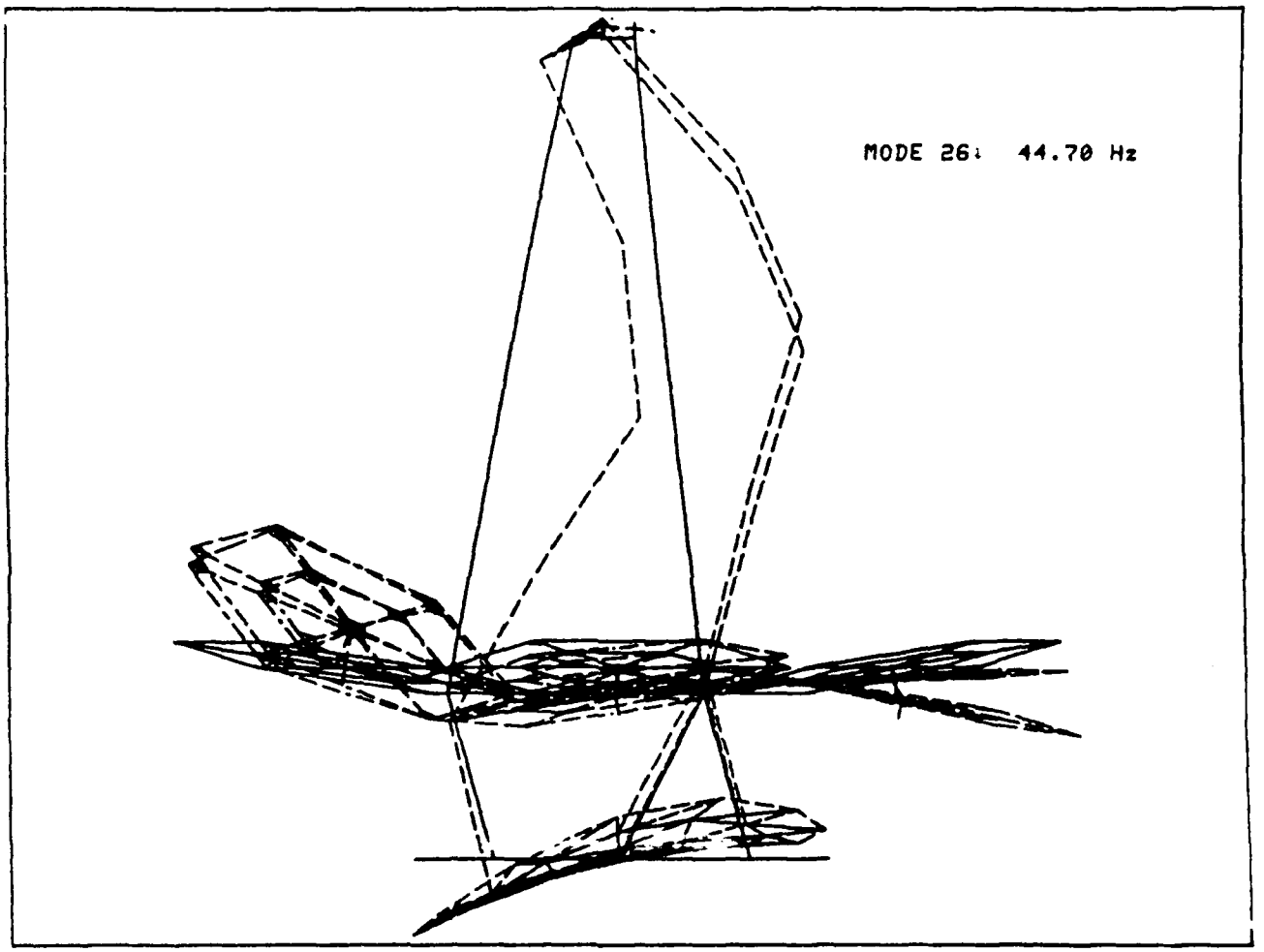

Figure 5.7. This figure shows the mode shape corresponding to a complex mode.

resultant finite element model with experimental data it became evident that it is necessary to include the flexure dynamics of these LPACTs in the finite element modeling process.

v) Strut Modes are modes in which the primary motion is due to the motion of the support struts. Only one of the 28 retained modes is a Strut Mode.

vi) Complex Modes are modes which involve significant motion of various parts of the structure. These are the modes which dynamically couple the primary structural components.

Figures 5.2 thrcugh 5.7 show representative mode shapes for the six types of modes. Diagrams of each of the 28 mode shapes are given in the Appendix.

6. Control Design Models

Although the finite element model described above has been modified to better correlate with experimental data, inaccuracies which remain in this model may make it difficult to use for high performance control design. Thus, in addition to making the finite element model available, Harris will also provide models obtained from experimental data using the Eigensystem Realization Algorithm (ERA) developed by NASA.

It is important to note that nine analog feedback controllers are available. Each of these controllers uses one of the nine LPACTs and its associated colocated accelerometer and is implemented by using the Structural Interface Electronics. These controllers are particularly useful for attenuating high frequency modes which cannot be controlled by a digital controller due to sample rate limitations. At least one of the ERA models will correspond to the system with the nine analog feedback controllers on.

Two models are currently available. The first is a 99 state ERA model that corresponds to the system with the analog feedback controllers off. The second is a 55 state reduced-order ERA model which corresponds to the system with the analog feedback controllers on. Both models were developed using data collected at a 330 Hz sample rate and are closely correlated with experimental data as illustrated by Figure 6.1 which compares

frequency responses from the 55 state ERA model with frequency responses obtained directly from experimental data. This latter model has been used by Harris to design a multi-input/multi-output Maximum Entropy/Optimal Projection controller that was successfully implemented and was experimentally seen to improve performance. It is apparent that the 99 state model can be significantly reduced and still maintain its accuracy but this step has not yet been taken.

Future plans include further development of ERA models. We also plan to better correlate the finite element model with experimental data using more advanced finite element model refinement techniques. The new finite element model should be even better for high performance control system design. Of course, guest investigators are welcome to develop their own models of the MHPE structure.

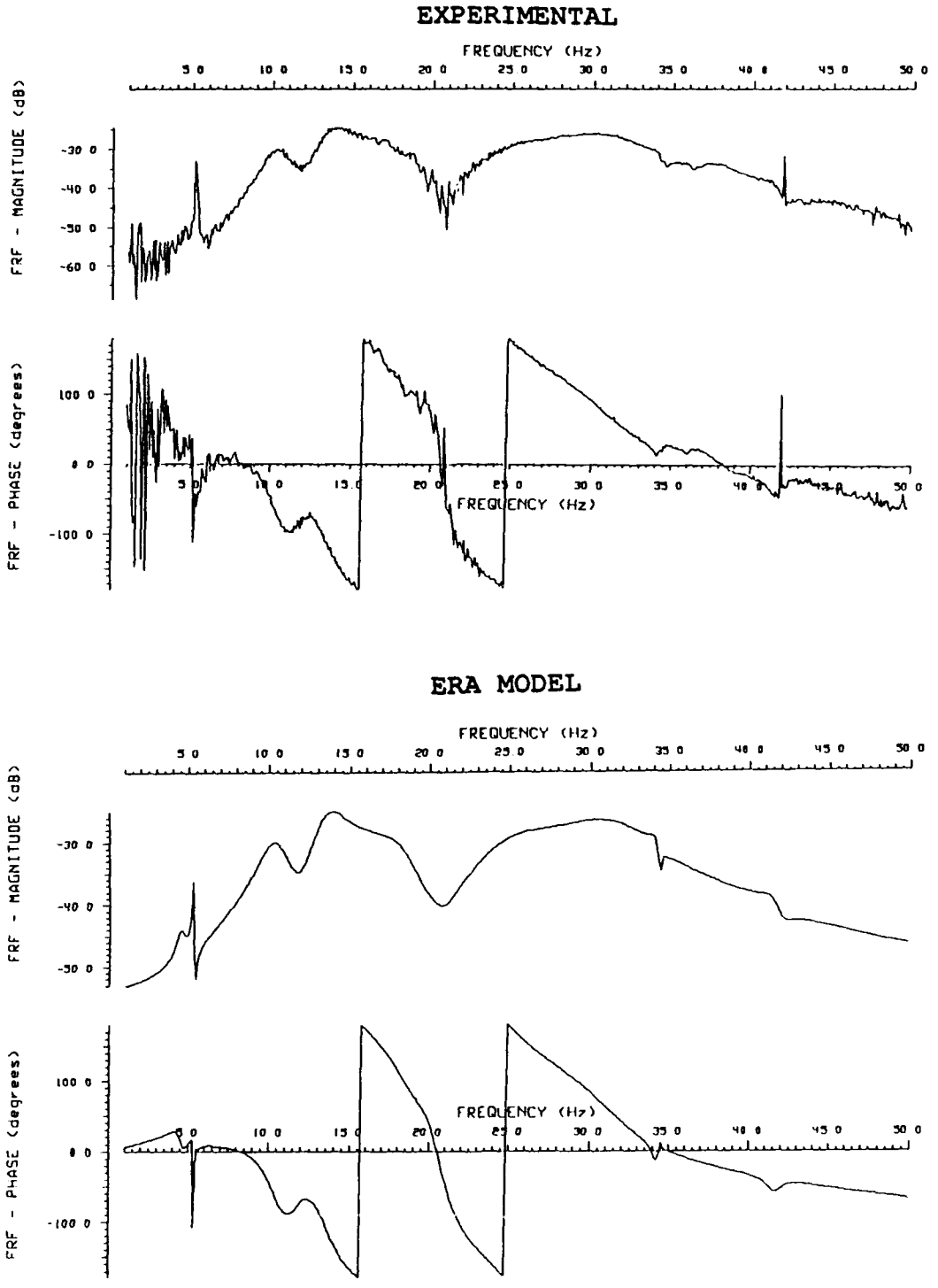

Figure 6.1. The ERA models correlate well with experimental data as illustrated by the close correspondence between the (top) frequency response developed from experimental data and the corresponding frequency response derived from an ERA model.

7. Control Law Implementation

Notation

T	sample period
$y(\cdot)$	measurement vector
$u(\cdot)$	input vector
$x_c(\cdot)$	compensator state vector
(A_c, B_c, C_c, D_c)	compensator matrices

Digital control laws can be implemented in either of the two following forms.

Form 1

$$x_c(kT+T) = A_c x_c(kT) + B_c y(kT)$$
$$u(kT) = C_c x_c(kT) + D_c y(kT-T)$$

Form 2

$$x_c(kT+T) = A_c x_c(kT) + B_c y(kT)$$
$$u(kT+\varepsilon) = C_c x_c(kT) + D_c y(kT)$$

where

$$0 < \varepsilon < T.$$

For 2 allows a closer approximation to direct feedthrough but put more restrictions on the compensator order than does Form 1. These restrictions have not yet been quantified.

Currently, if Form 1 is used, a 30th order, 6 input - 6 output control law can be implemented at 220 Hz. There are plans to improve the system so that a 50th order, 9 input - 9 output controller can be implemented at 330 Hz.

Guest investigators are able to choose the sample period at which their controllers are to be implemented. They must also inform Harris as to which actuators the elements of the input vector correspond and to which sensors the elements of the measurement vector correspond.

8. Performance Evaluation

There are currently 2 types of measurements available for performance analysis: the displacement measurements from the OPMS and the acceleration measurements. Velocity estimates can be derived from the acceleration measurements using the roof-top integration of the SIE. The displacement measurements of the OPMS can be used to determine primary mirror dephasing or rms roughness.

The OPMS is capable of measuring displacements at 12 pts on the primary as shown in Figure 3.2. The acceleration measurements and velocity estimates can be used to determine the amount of damping evident in other parts of the structure.

The MHPE currently includes a laser-based optical system which is used for visual representation of the LOS performance. Future plans include the addition of an optical detector as part of this laser system.

9. Final Remarks

This document has described the Multi-Hex Prototype Experiment which was designed and implemented at Harris Corporation. This testbed was developed to contribute to the development and validation of structural control technology. The information provided here will aid guest investigators in developing and implementing controllers for the MHPE.

APPENDIX
Mode Shape Diagrams

Notes:

(i) The orientation of the coordinate axes for each of the mode shapes are the same as the orientation given for Mode 1 unless axes that list an alternative orientation are included in the diagram.

(ii) Also notice that two diagrams (showing two views) are included for Modes 8 and 23.

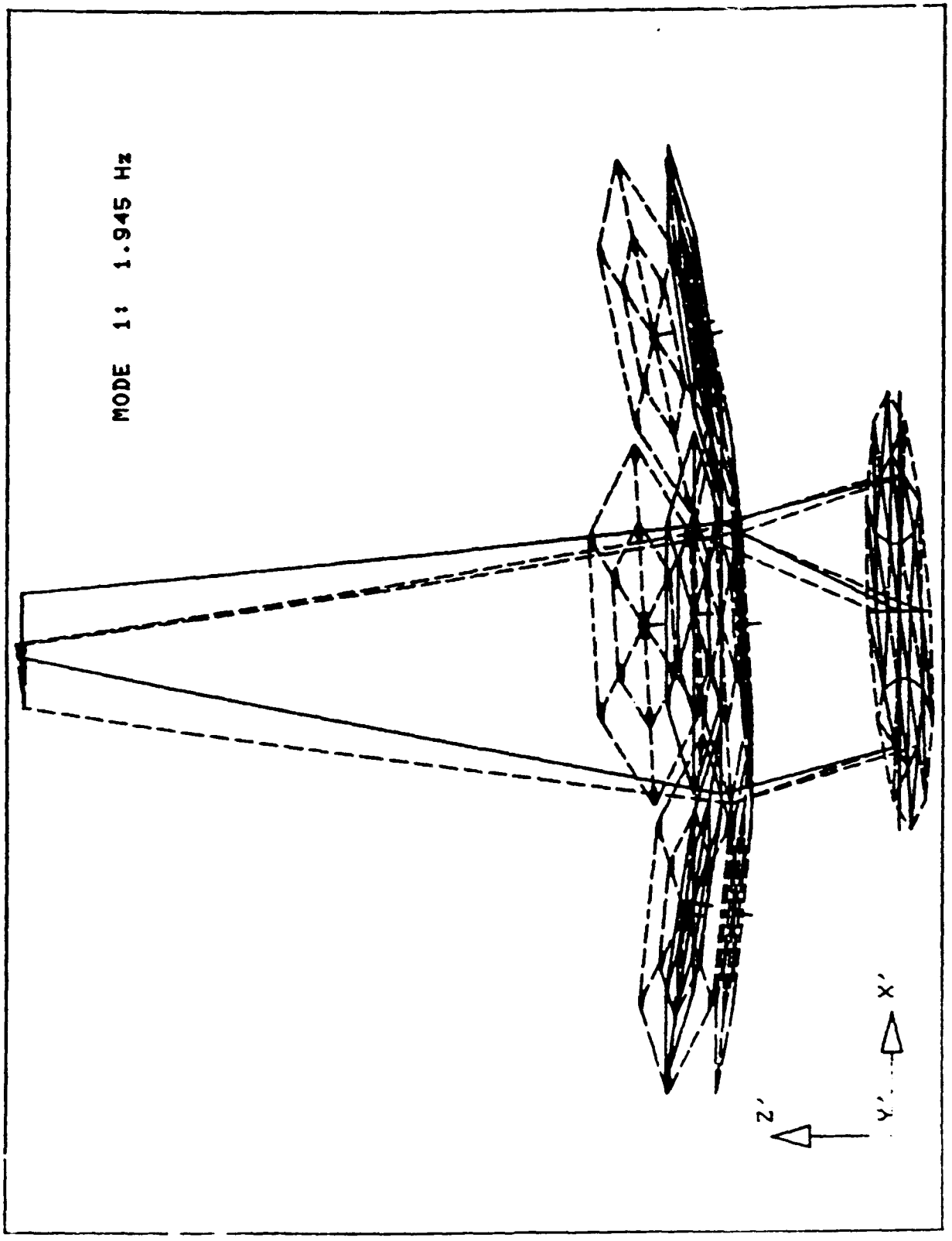
MODE 1: 1.945 Hz
Z'
Y'
X'

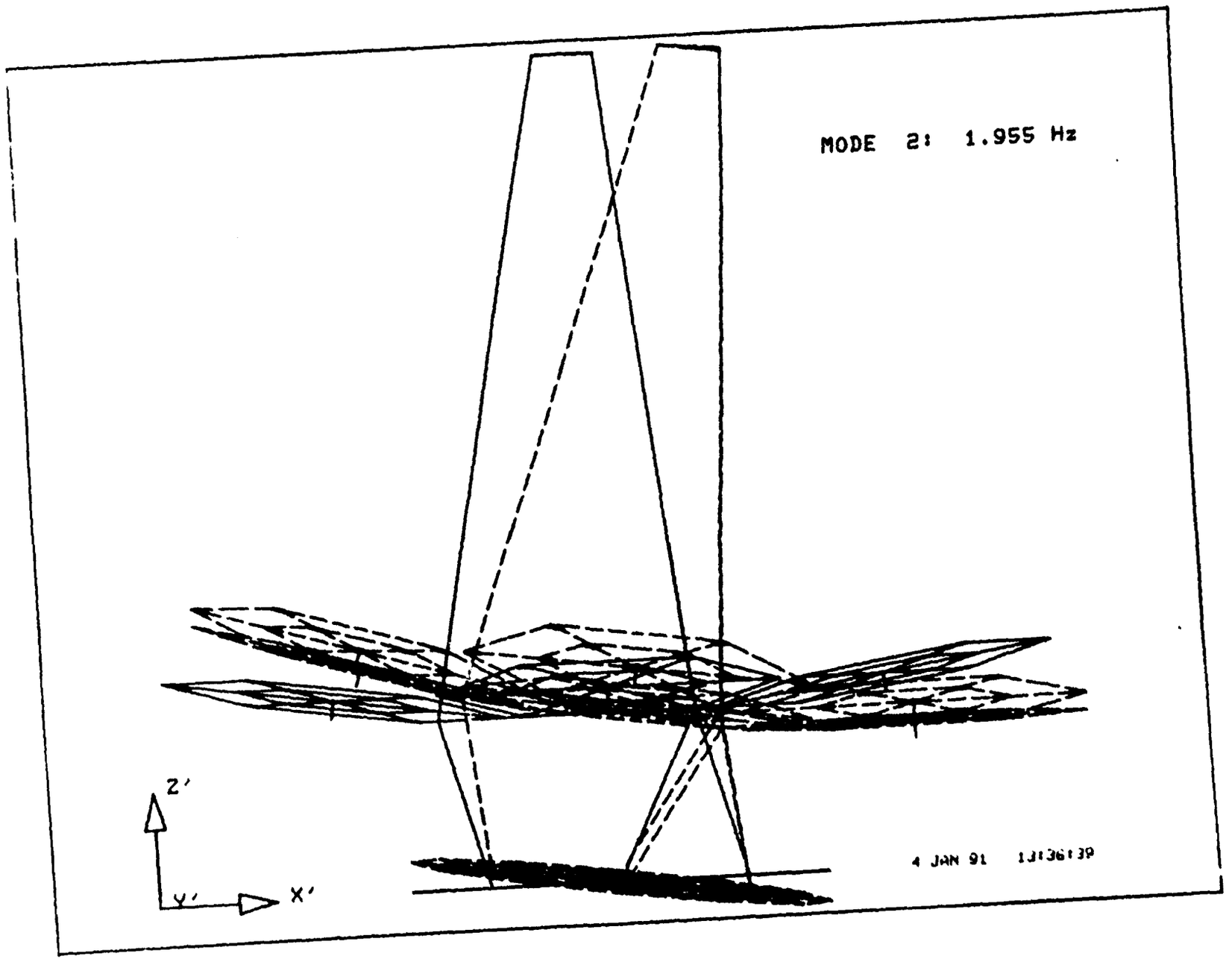
MODE 2: 1.955 Hz
Z'
Y'
X'
4 JAN 91 13:36:39

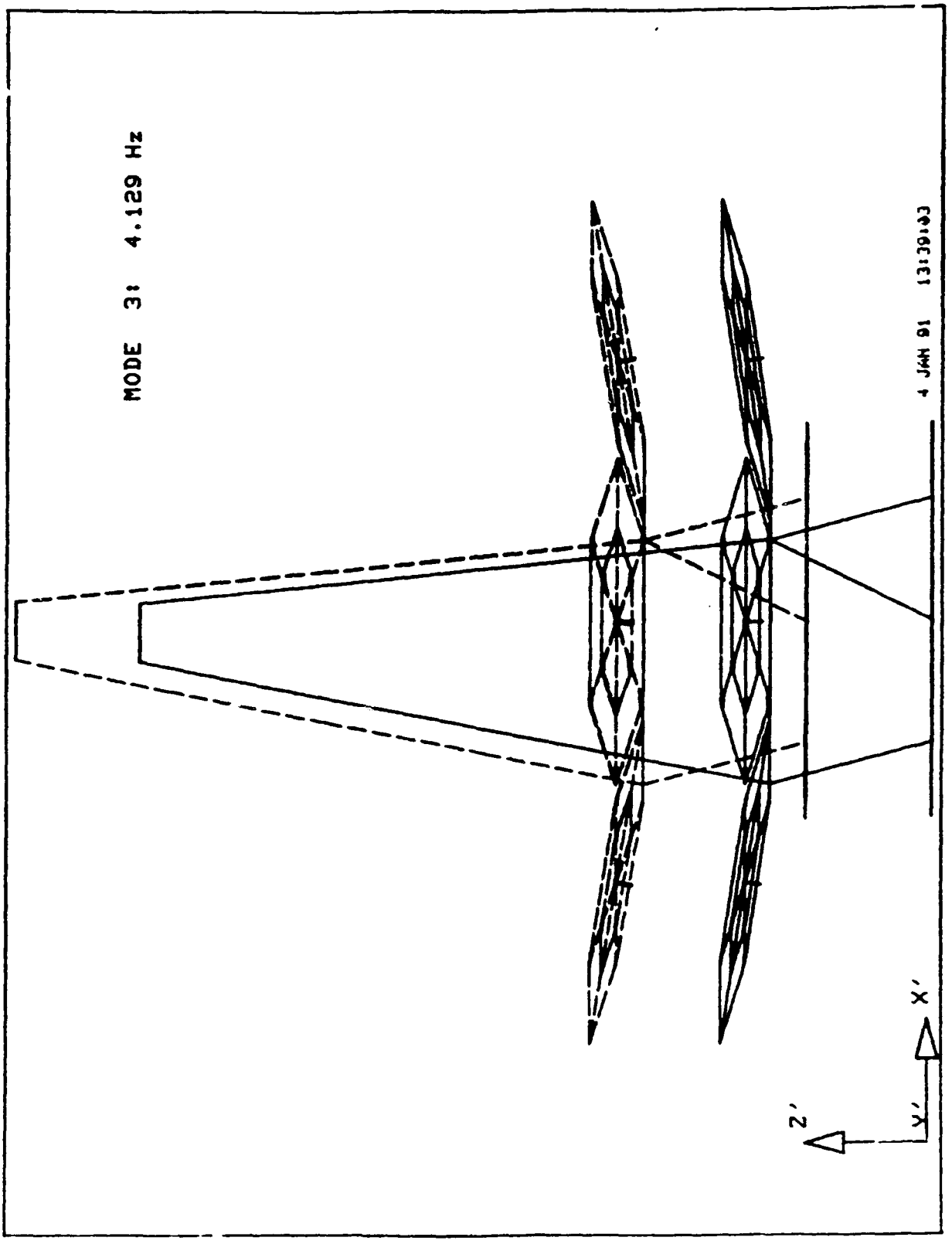
MODE 3: 4.129 Hz
4 JAN 91 13:39:03
X'
Y'
Z'

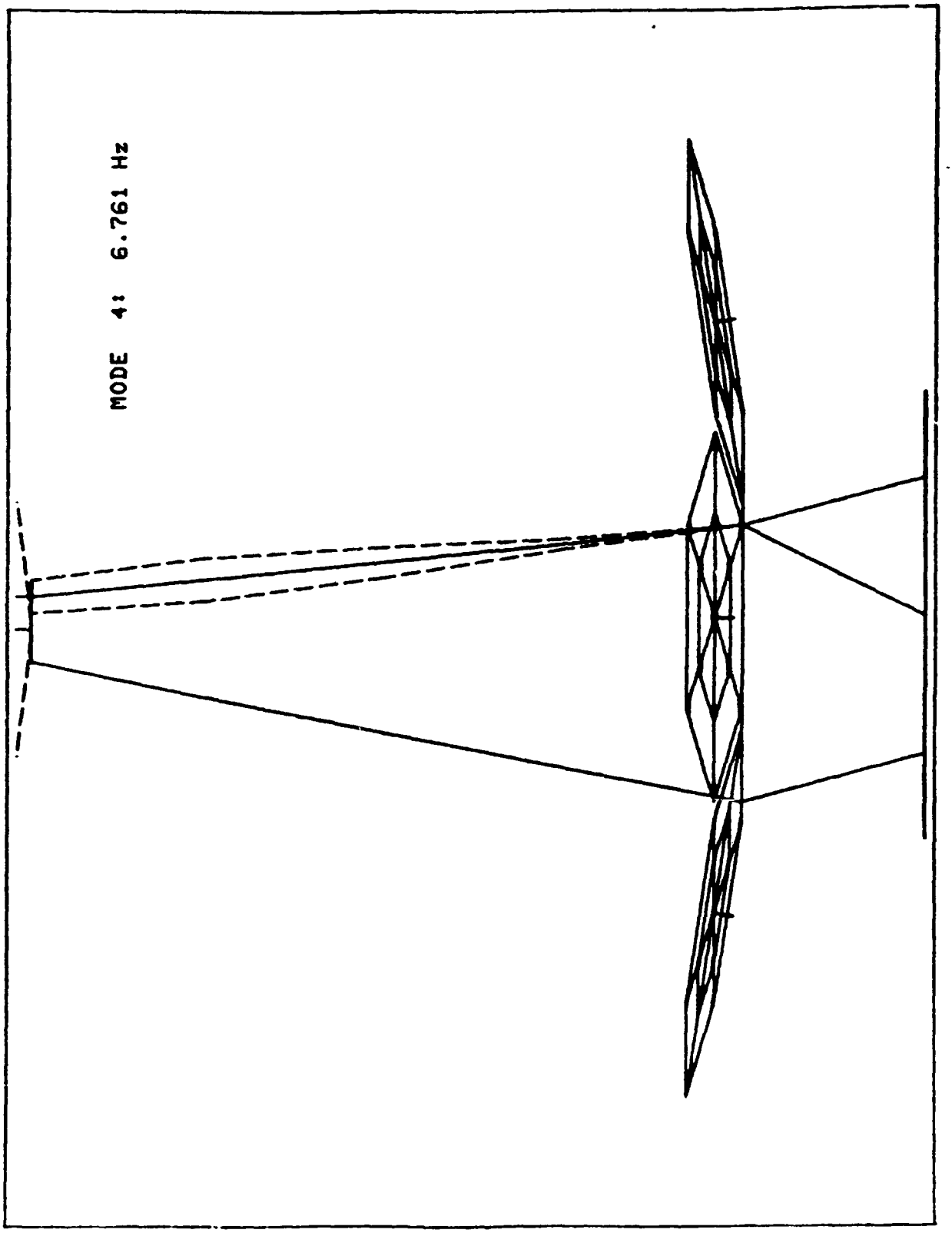
MODE 4: 6.761 Hz

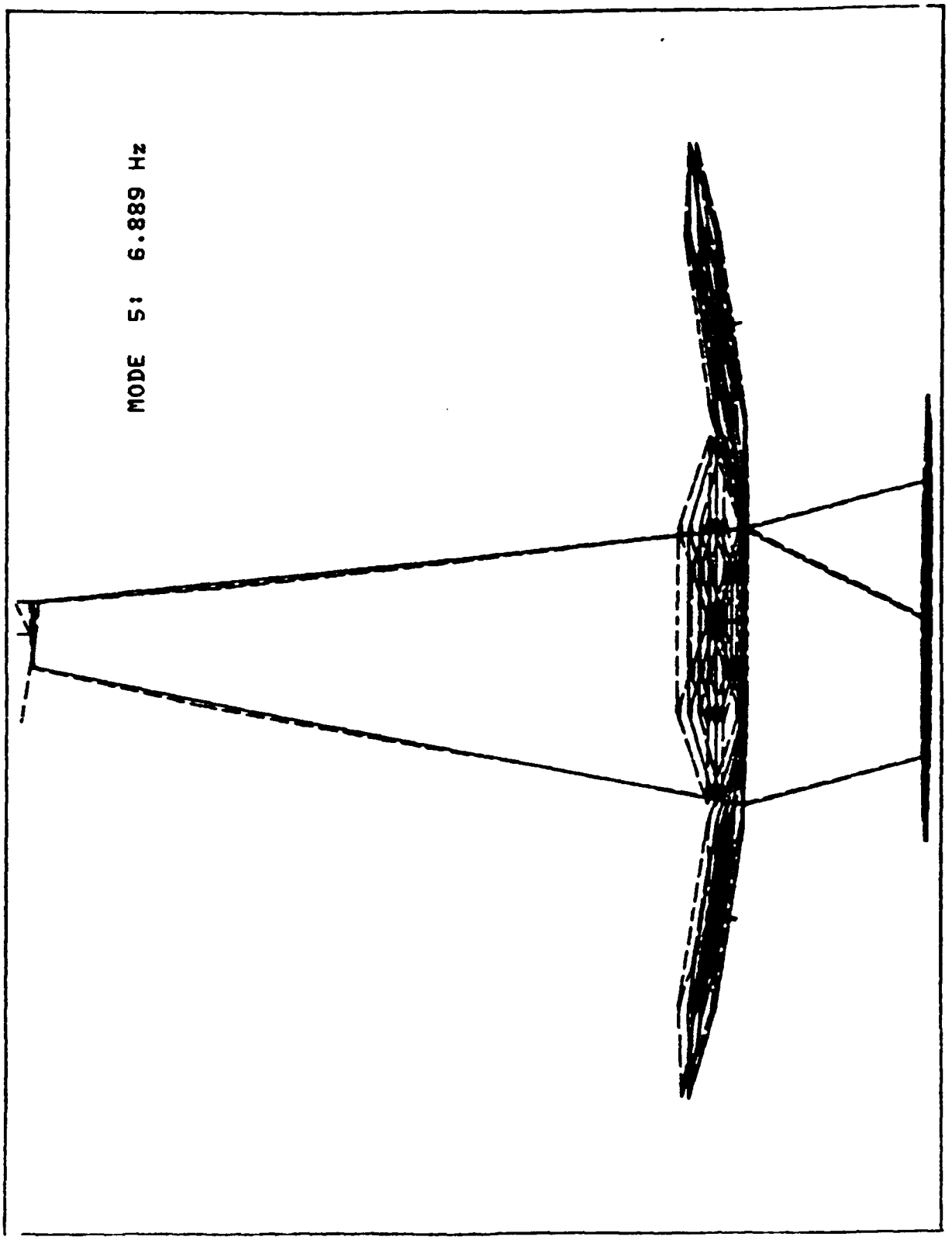
MODE 5: 6.889 Hz

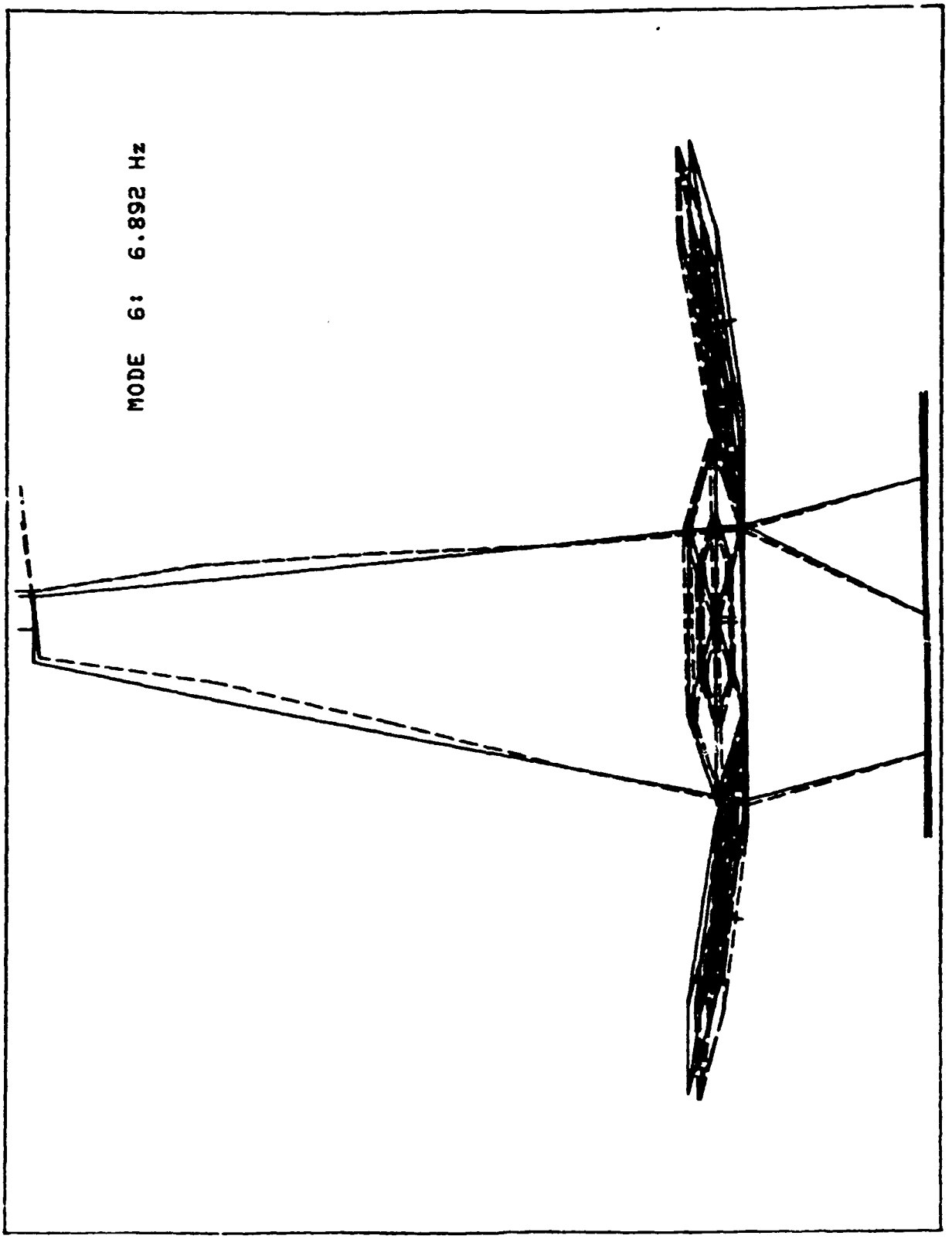
MODE 6: 6.892 Hz

MODE 7: 9.870 Hz
727

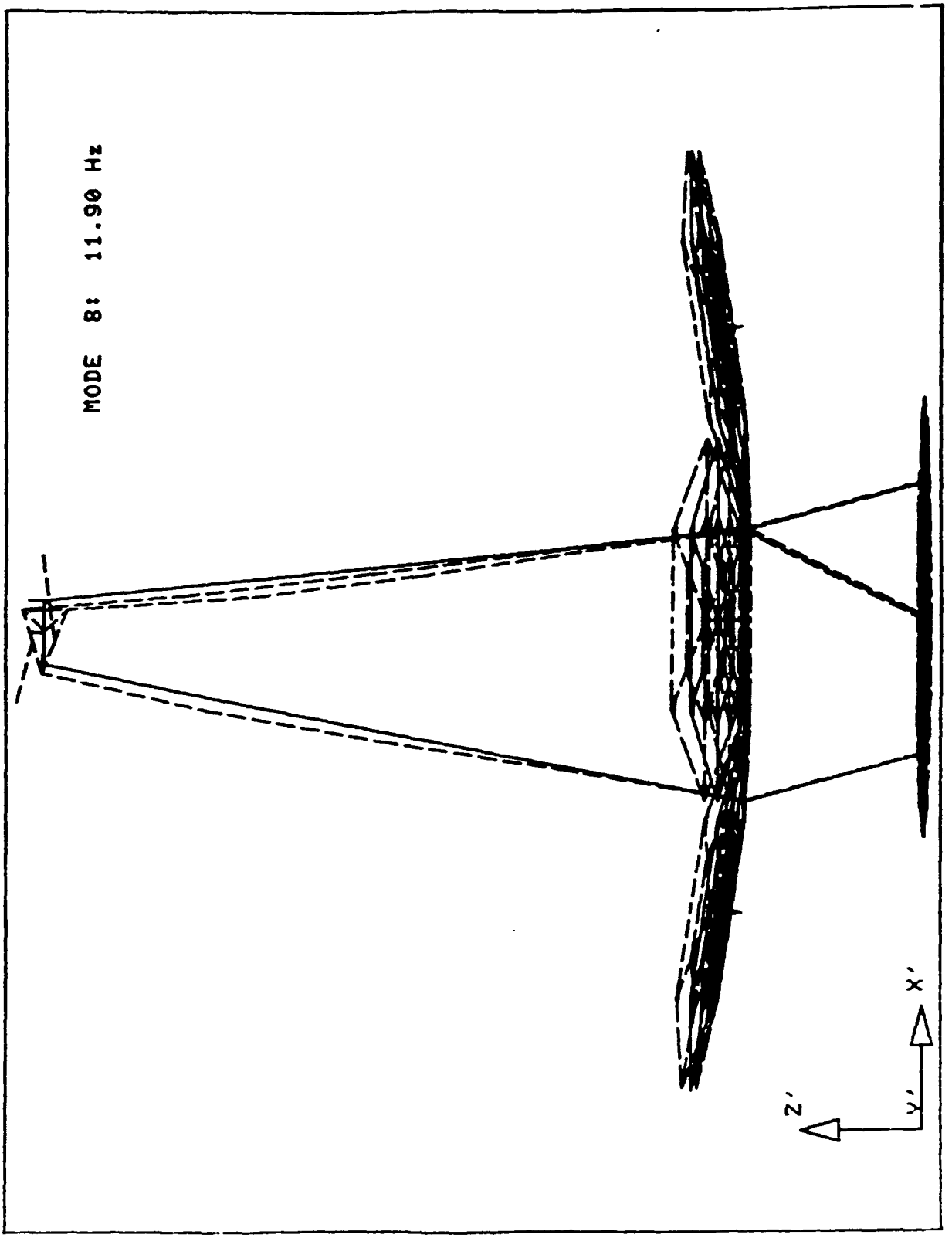
MODE 8: 11.90 Hz
X'
Y'
Z'

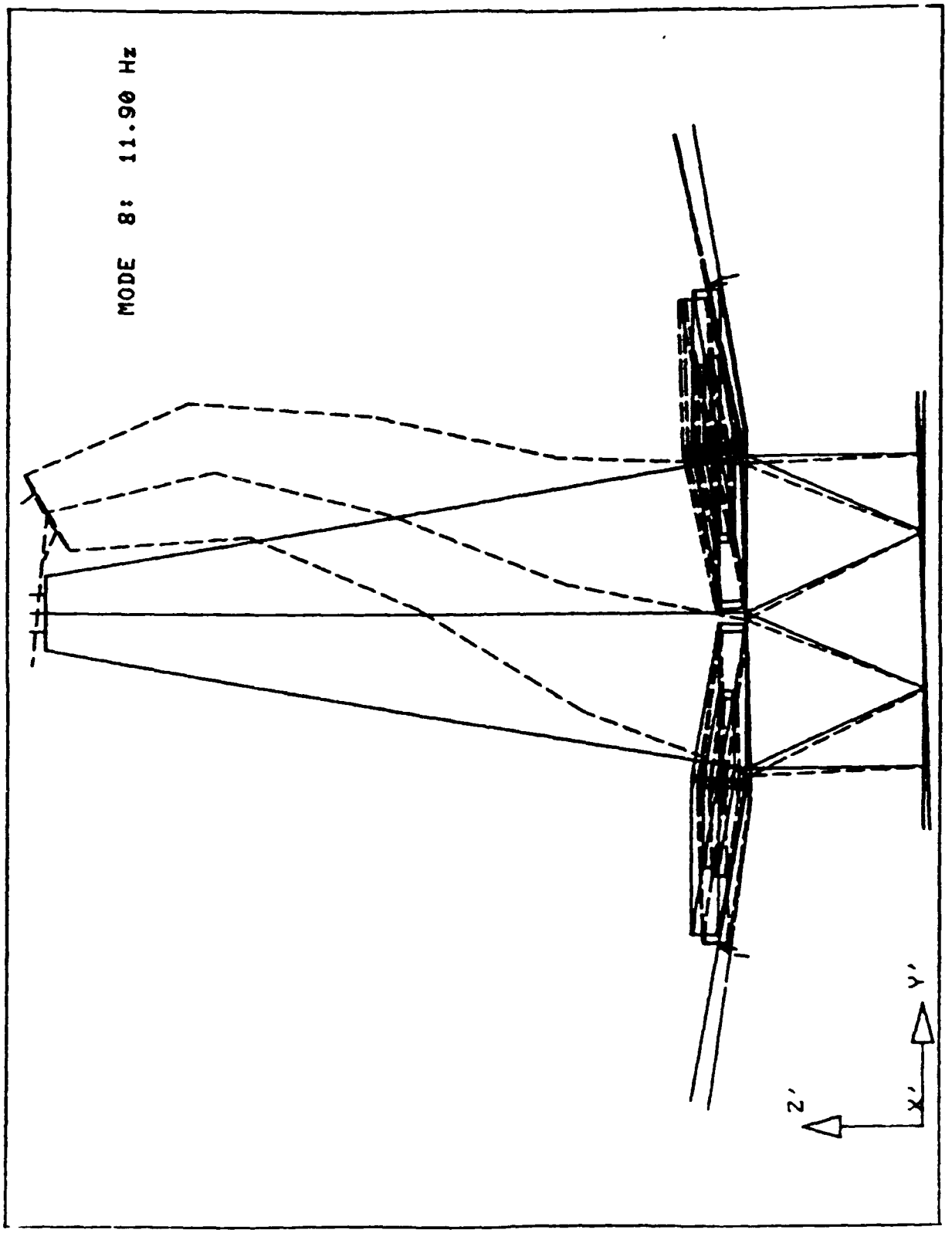
MODE 8: 11.90 Hz
Y'
Z'
X'

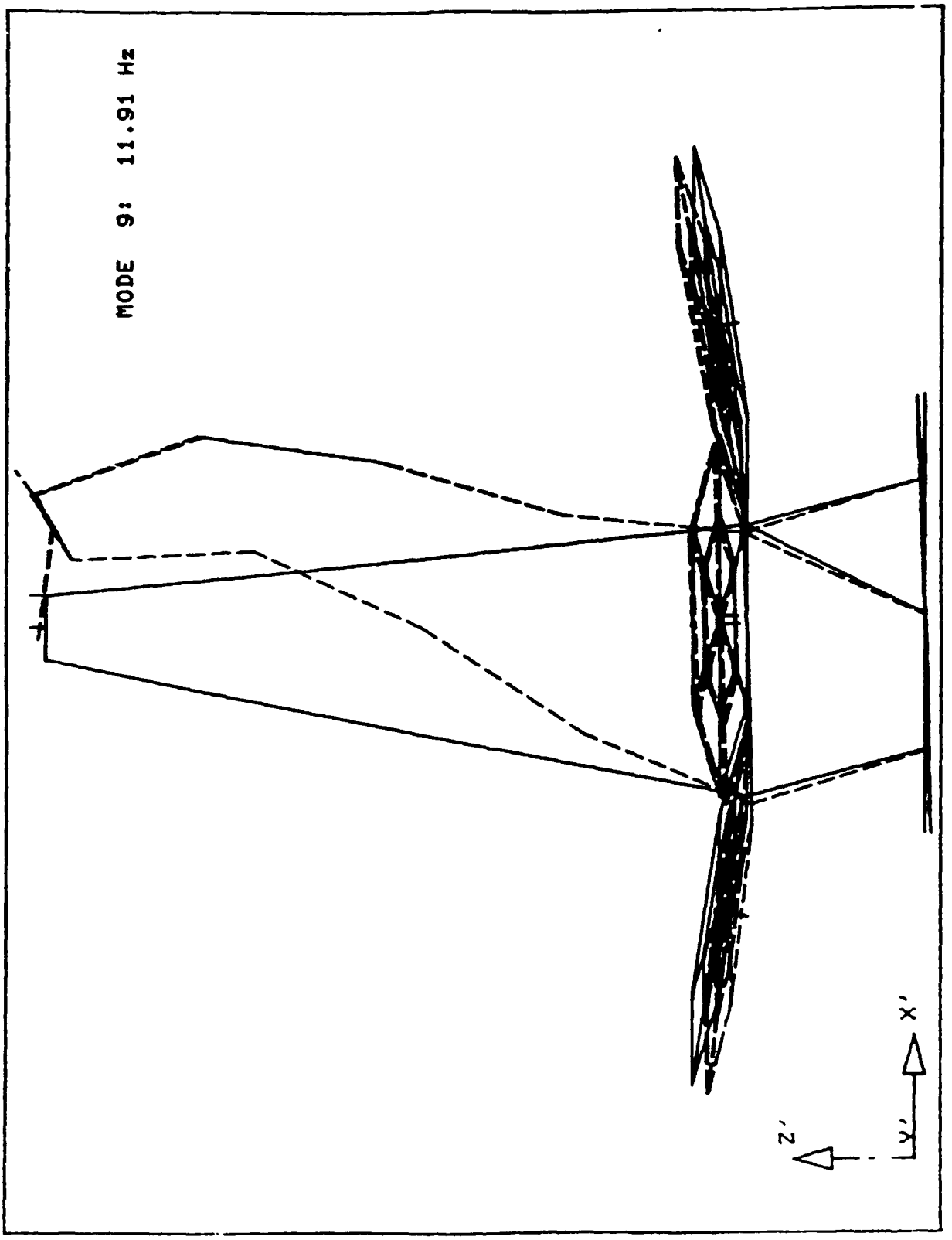
MODE 9: 11.91 Hz
Z'
Y'
X'

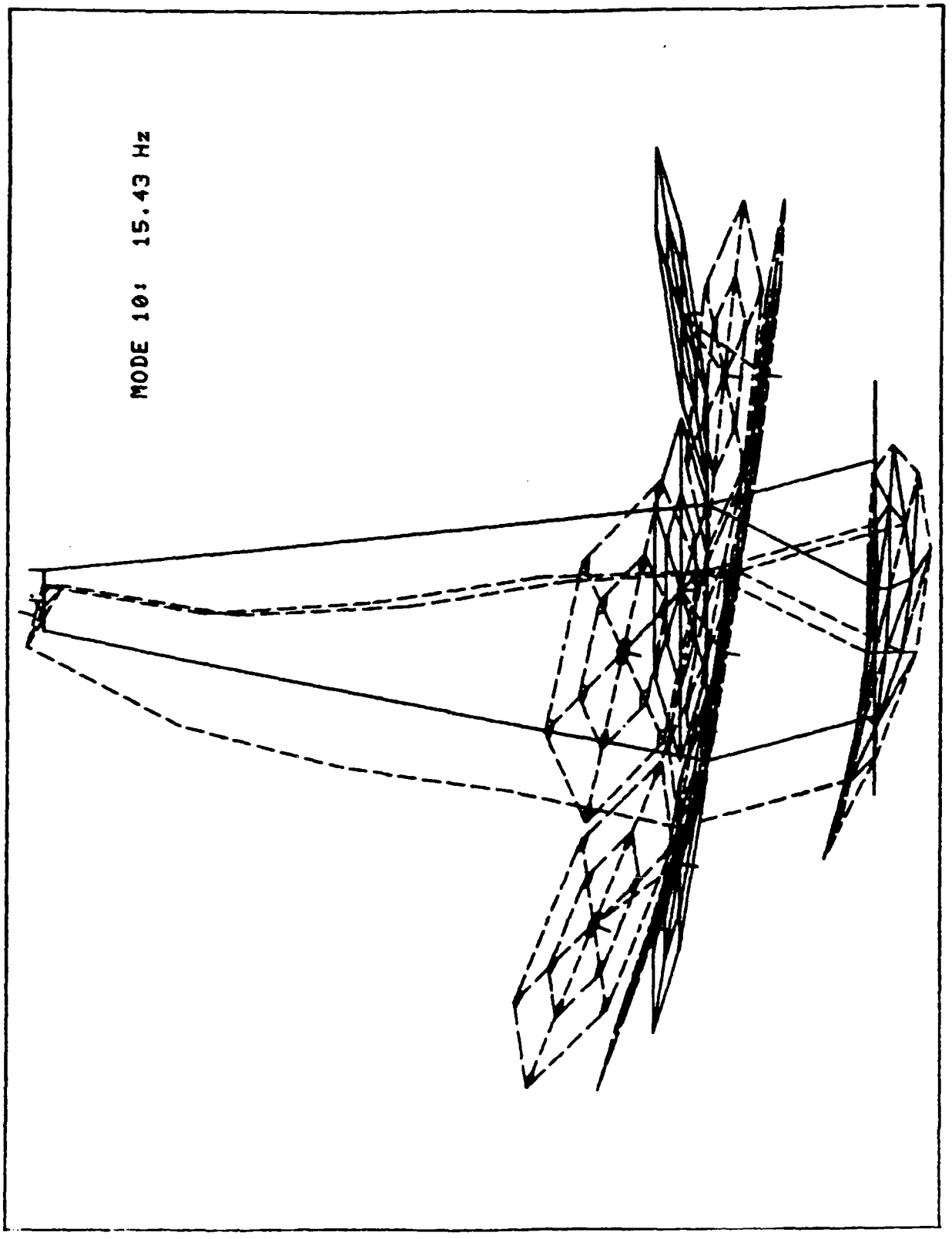
MODE 10: 15.43 Hz

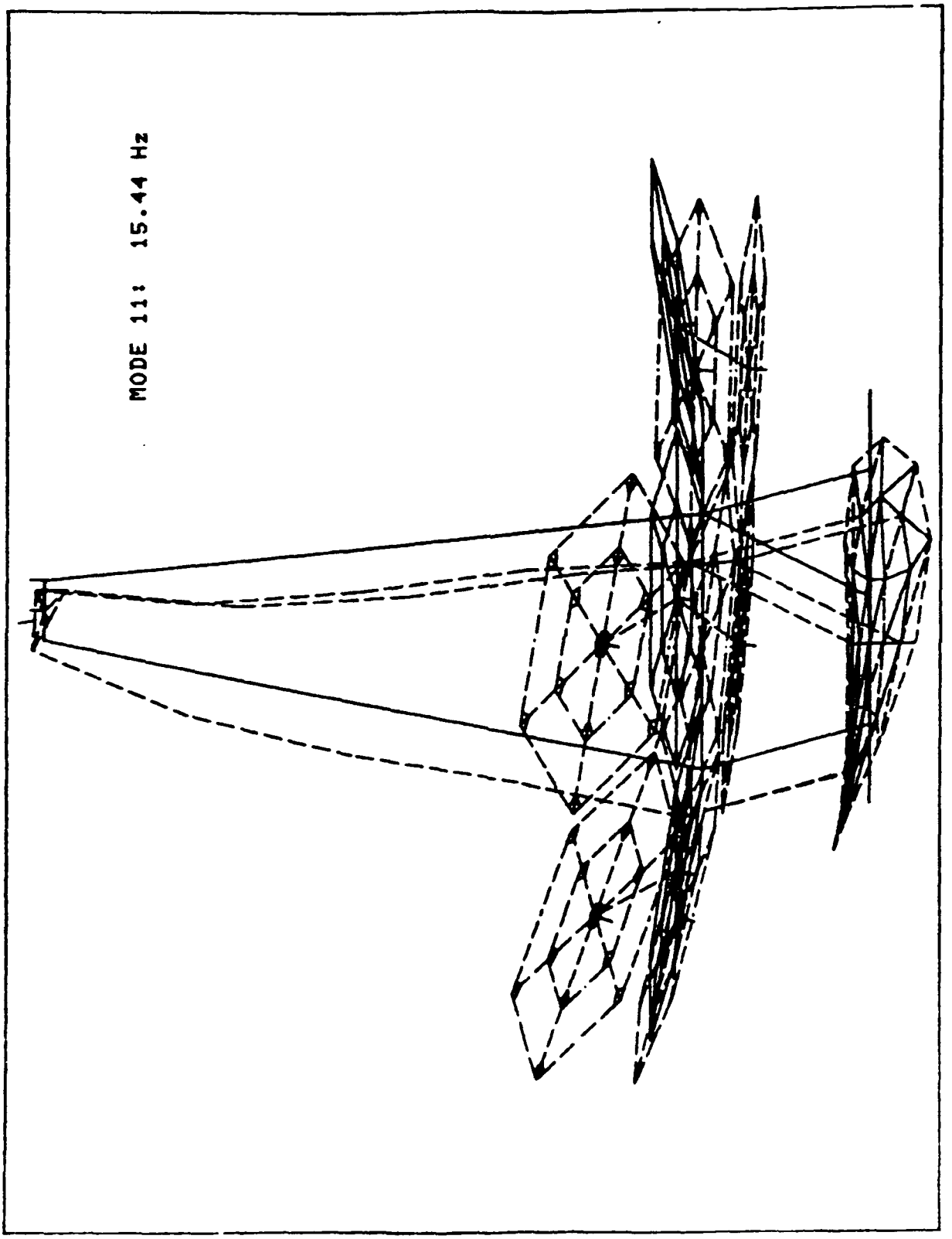
MODE 11: 15.44 Hz

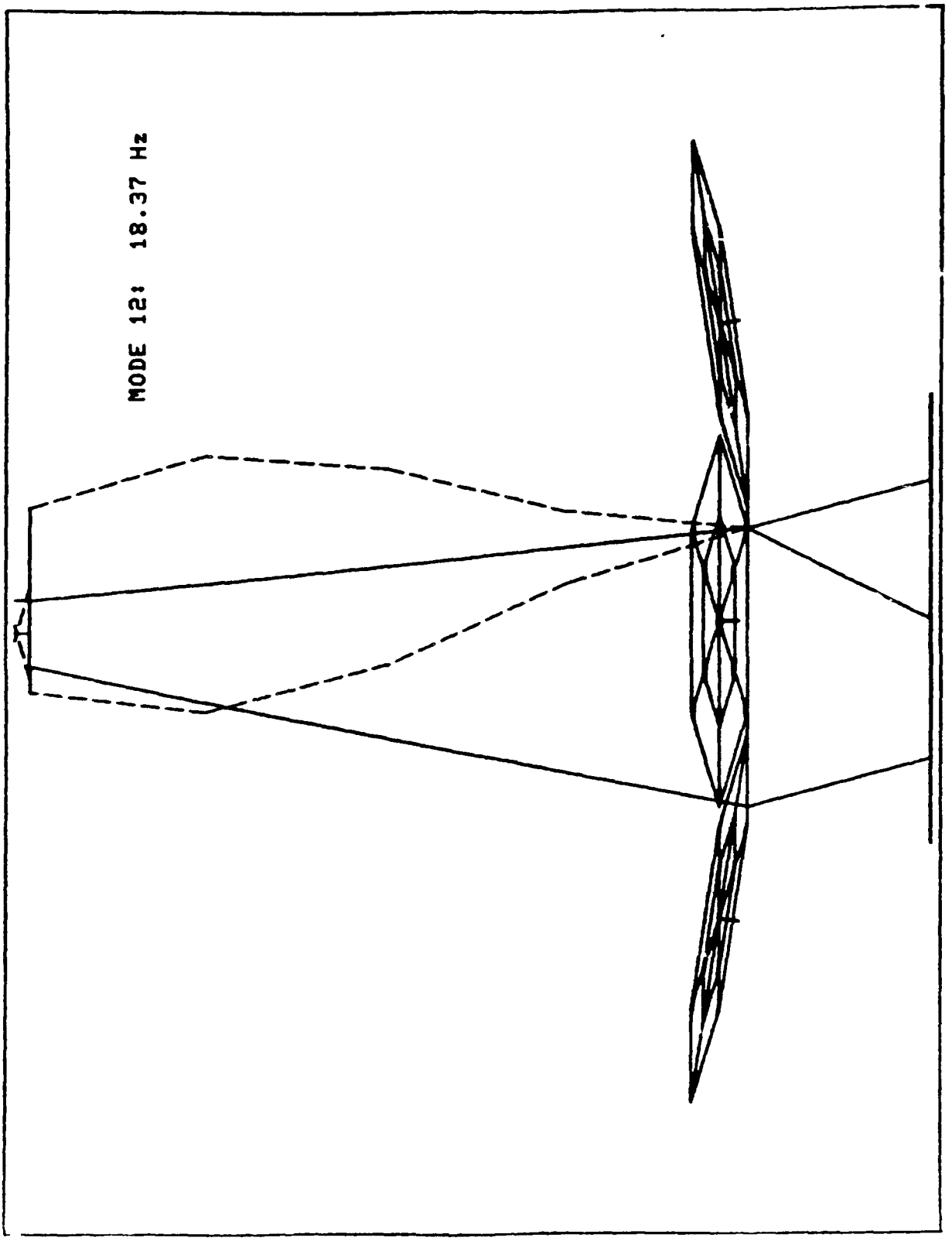
MODE 12: 18.37 Hz

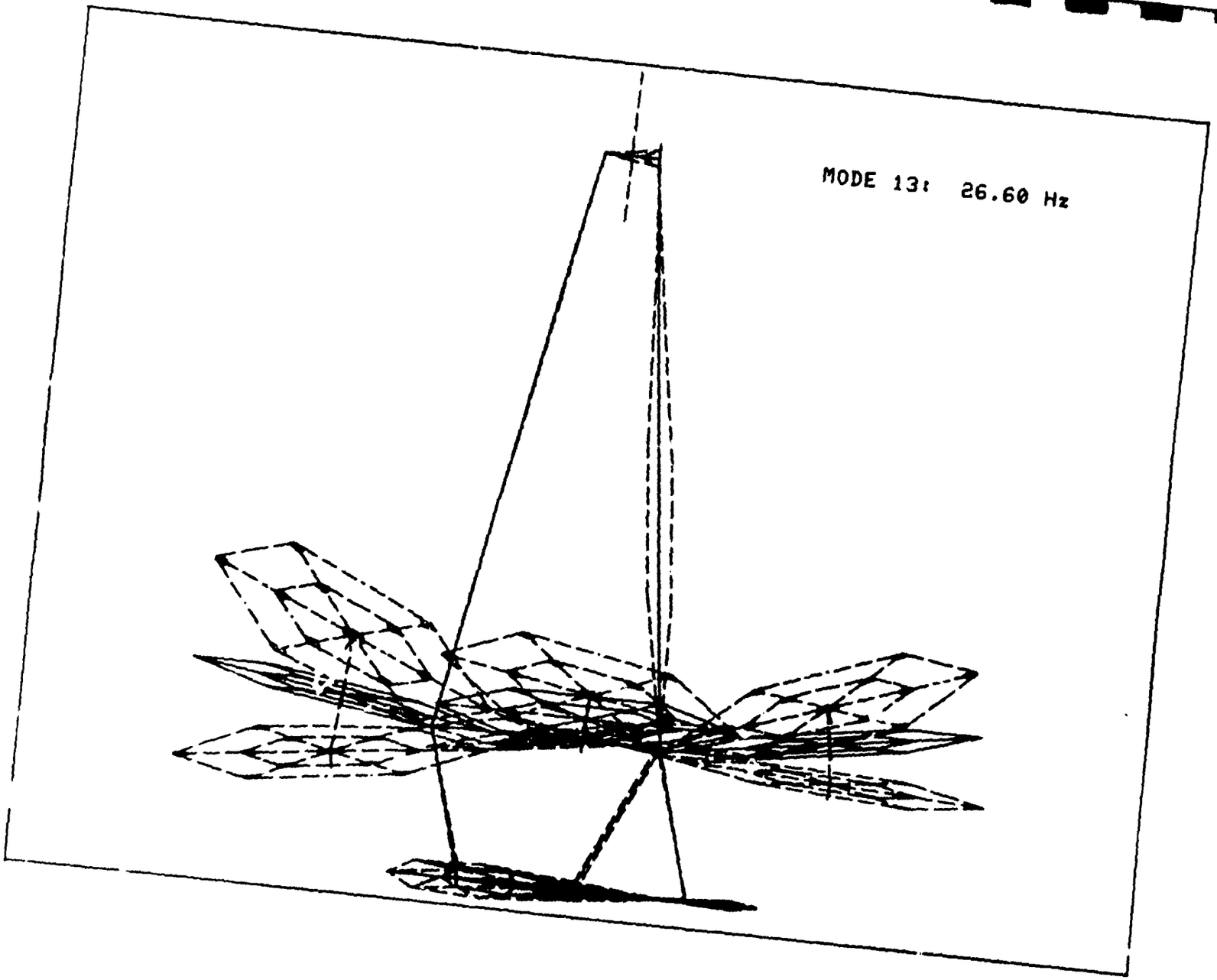
MODE 13: 26.60 Hz

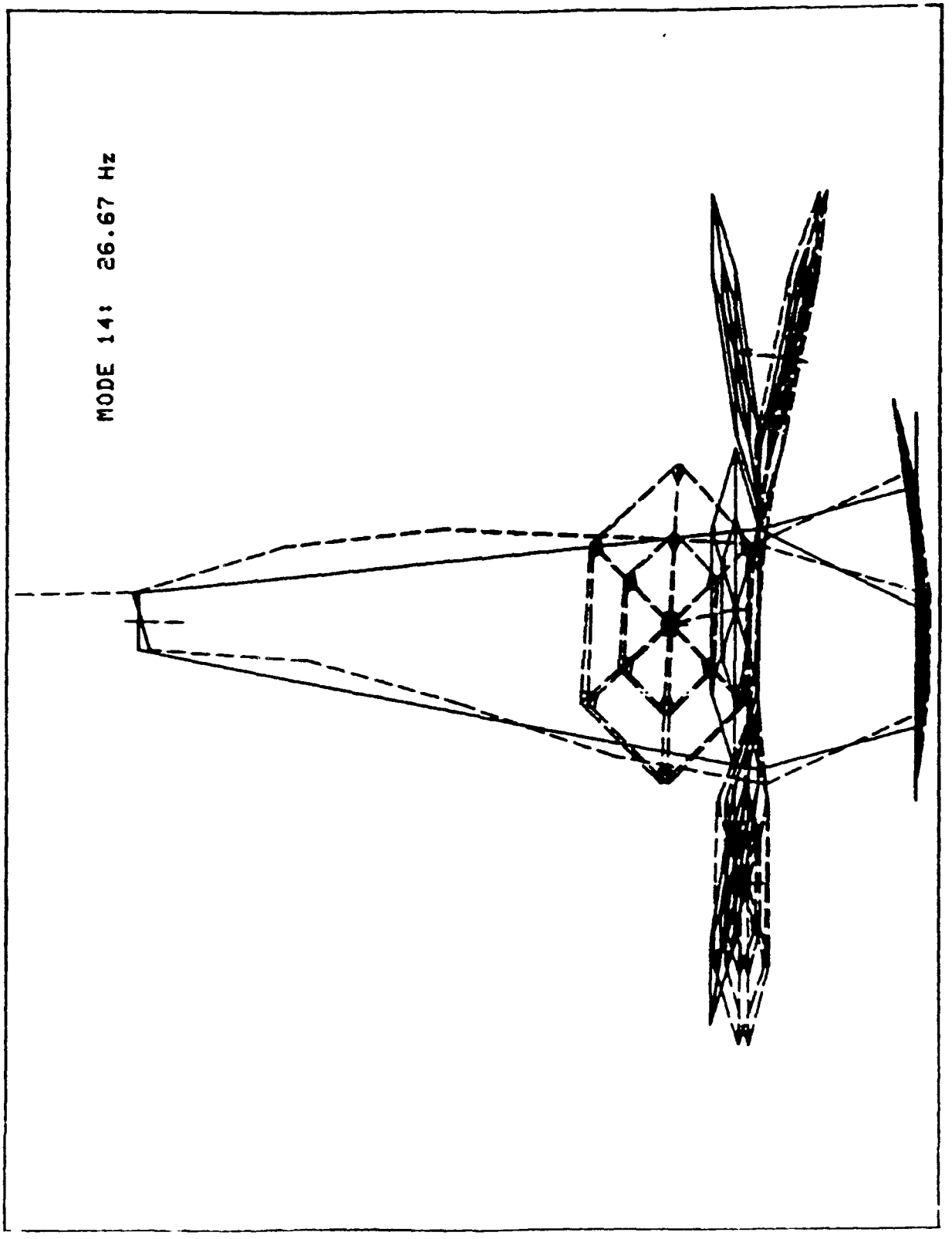
MODE 14: 26.67 Hz

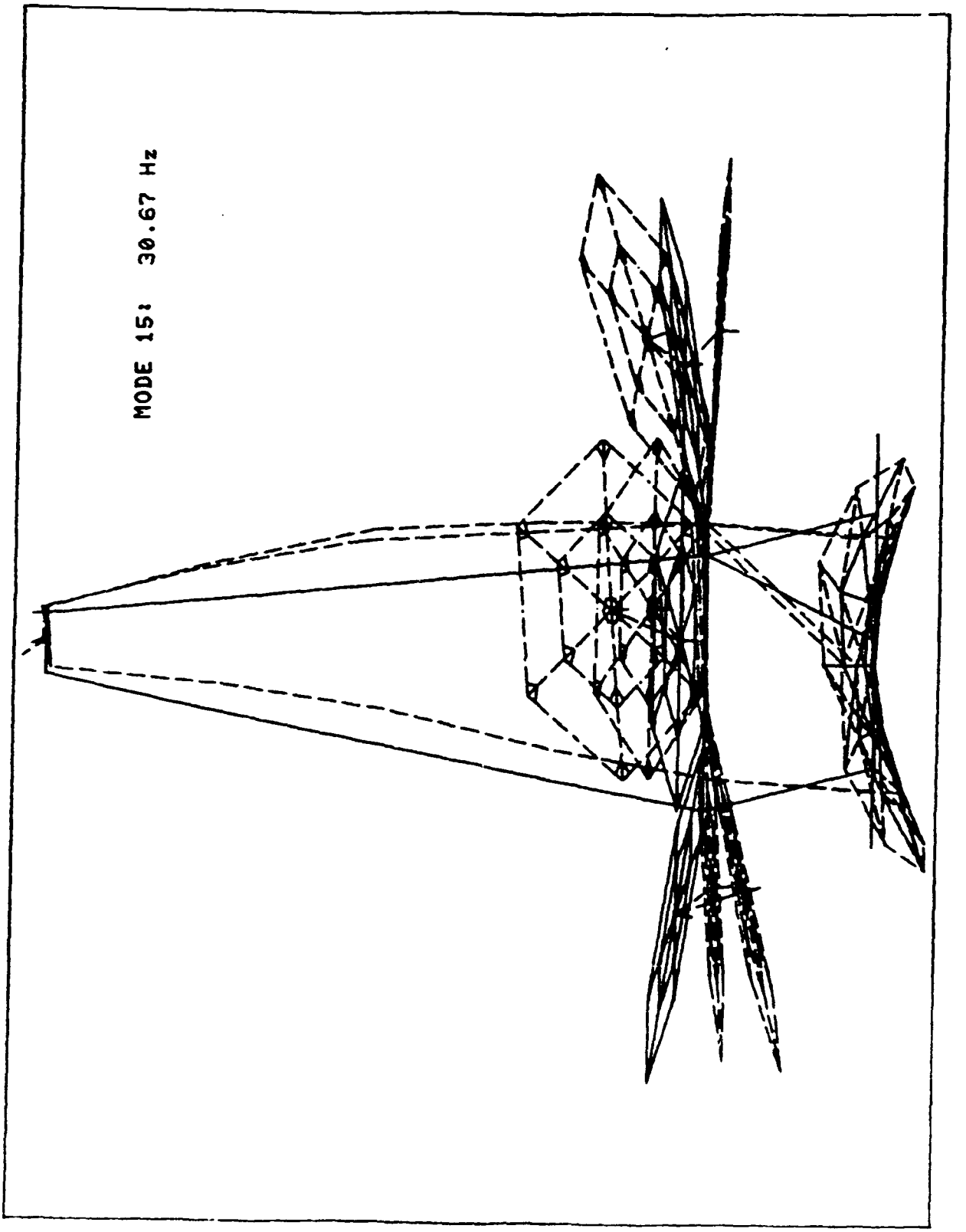
MODE 15: 30.67 Hz

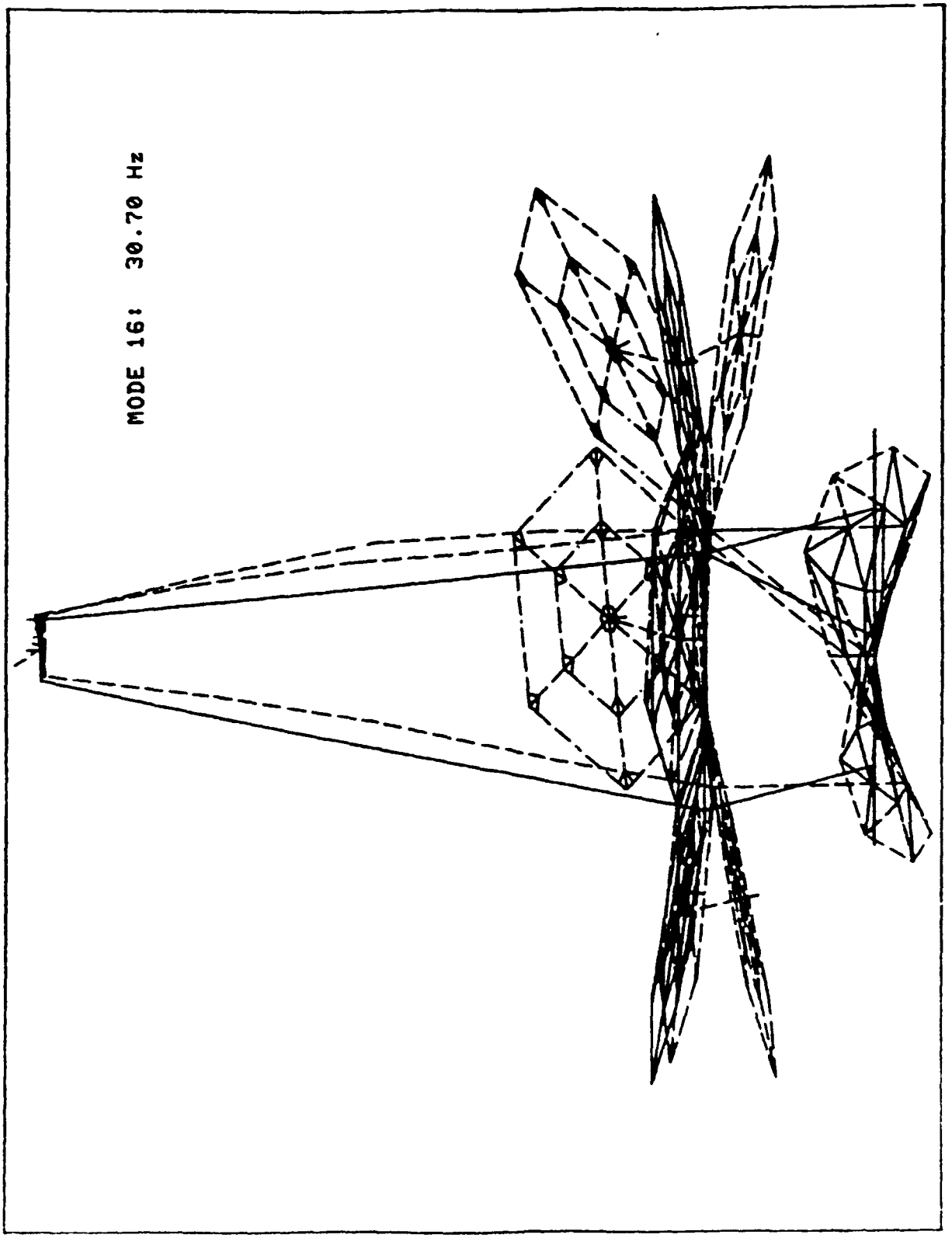
MODE 16: 30.70 Hz

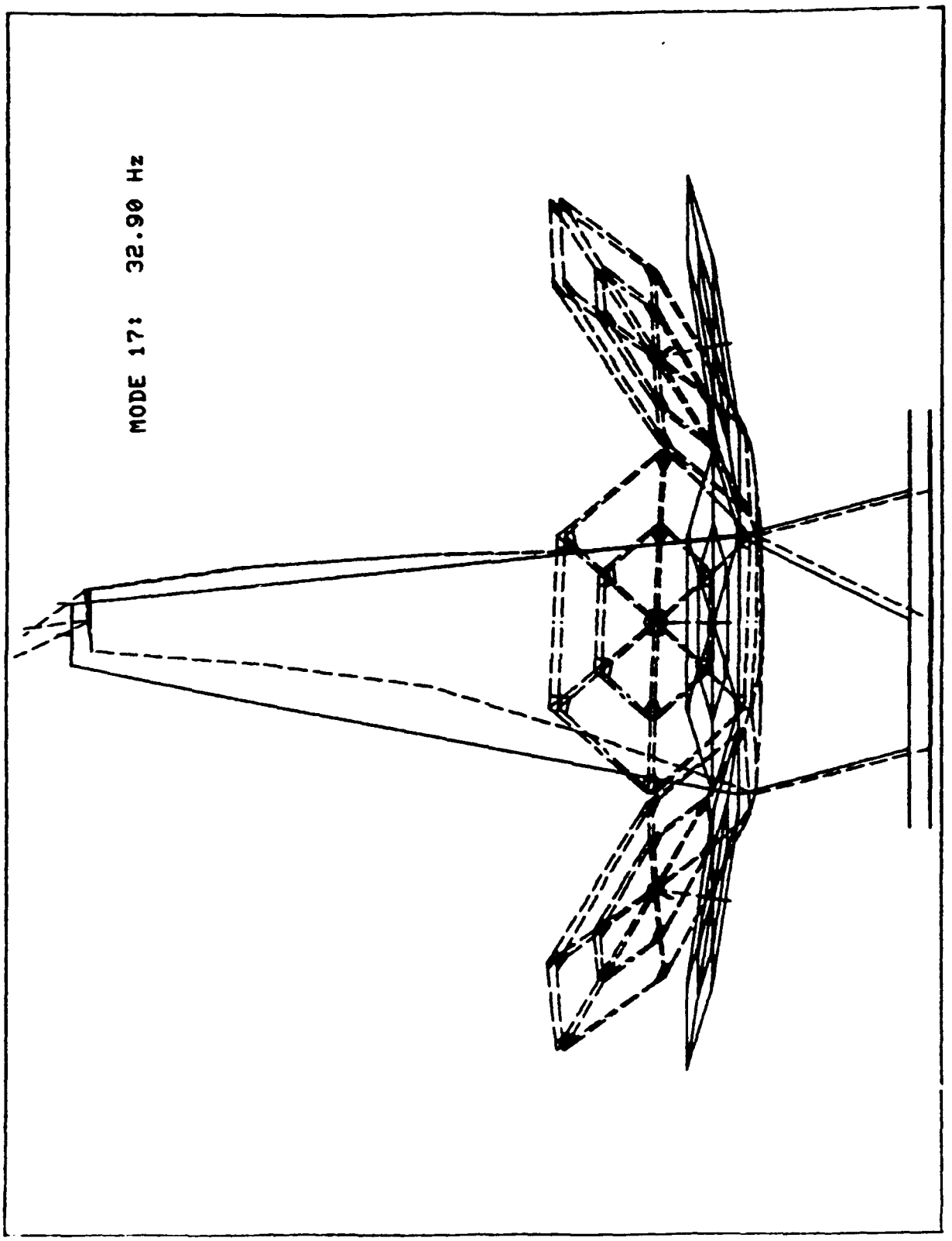
MODE 17: 32.90 Hz

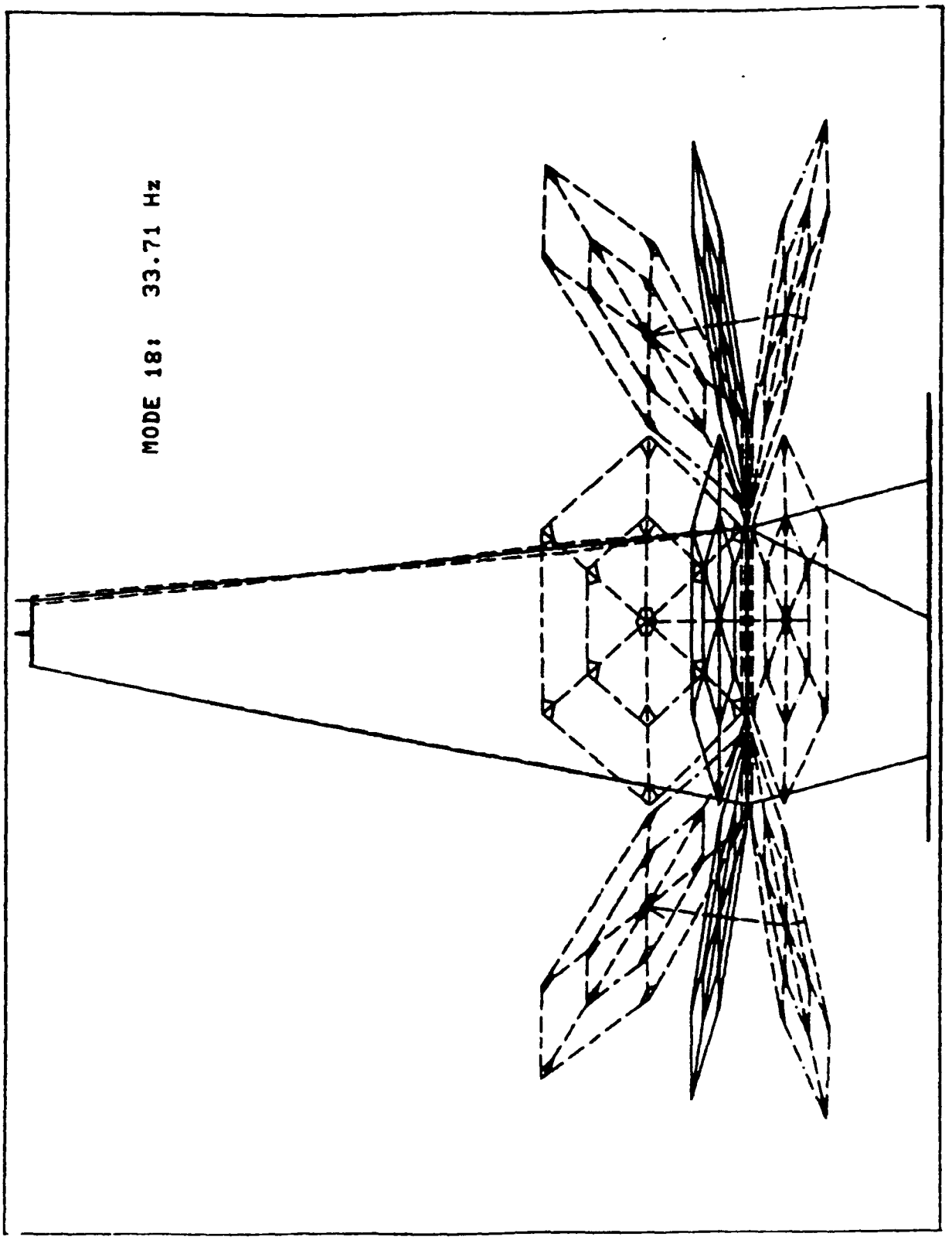
MODE 18: 33.71 Hz

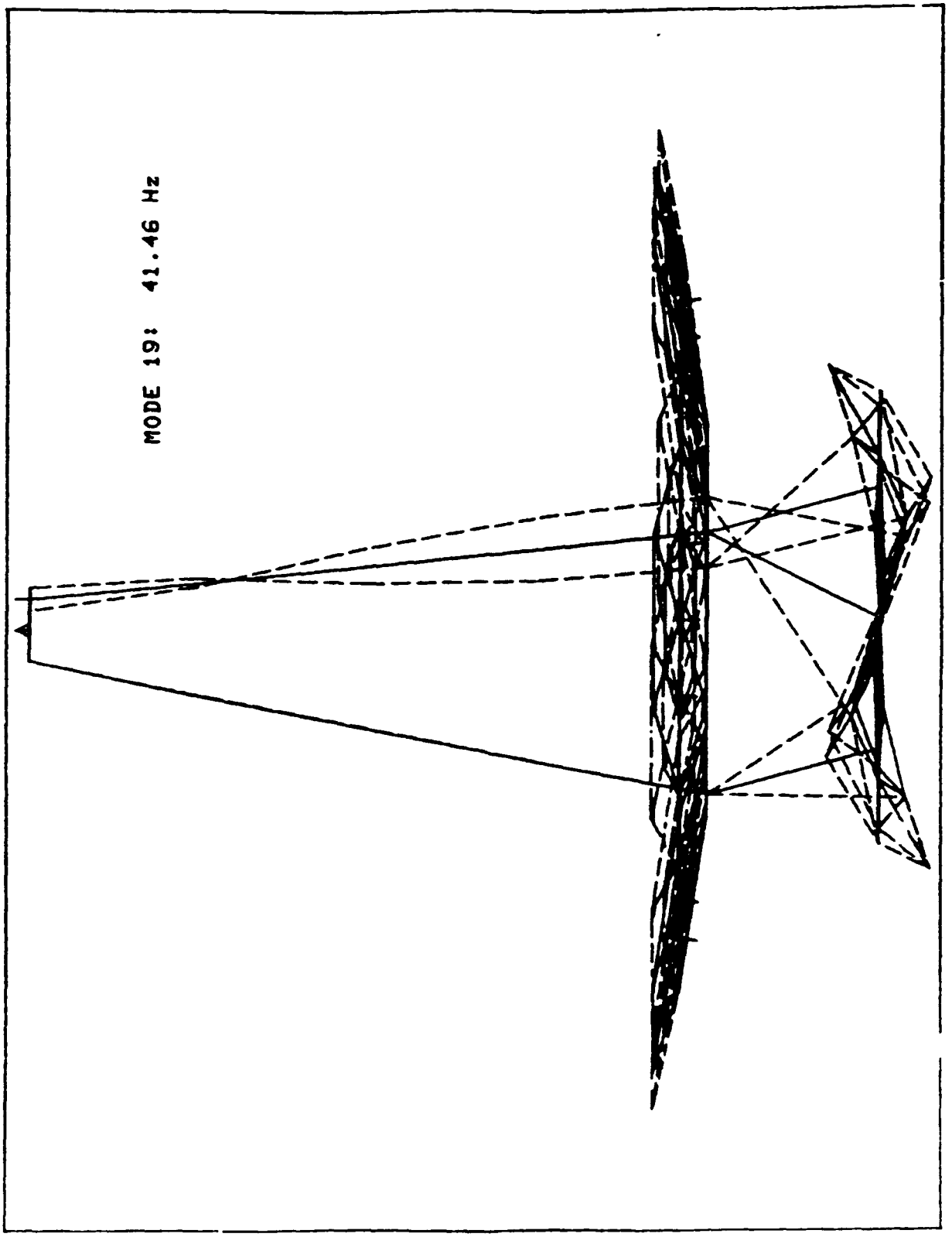
MODE 19: 41.46 Hz

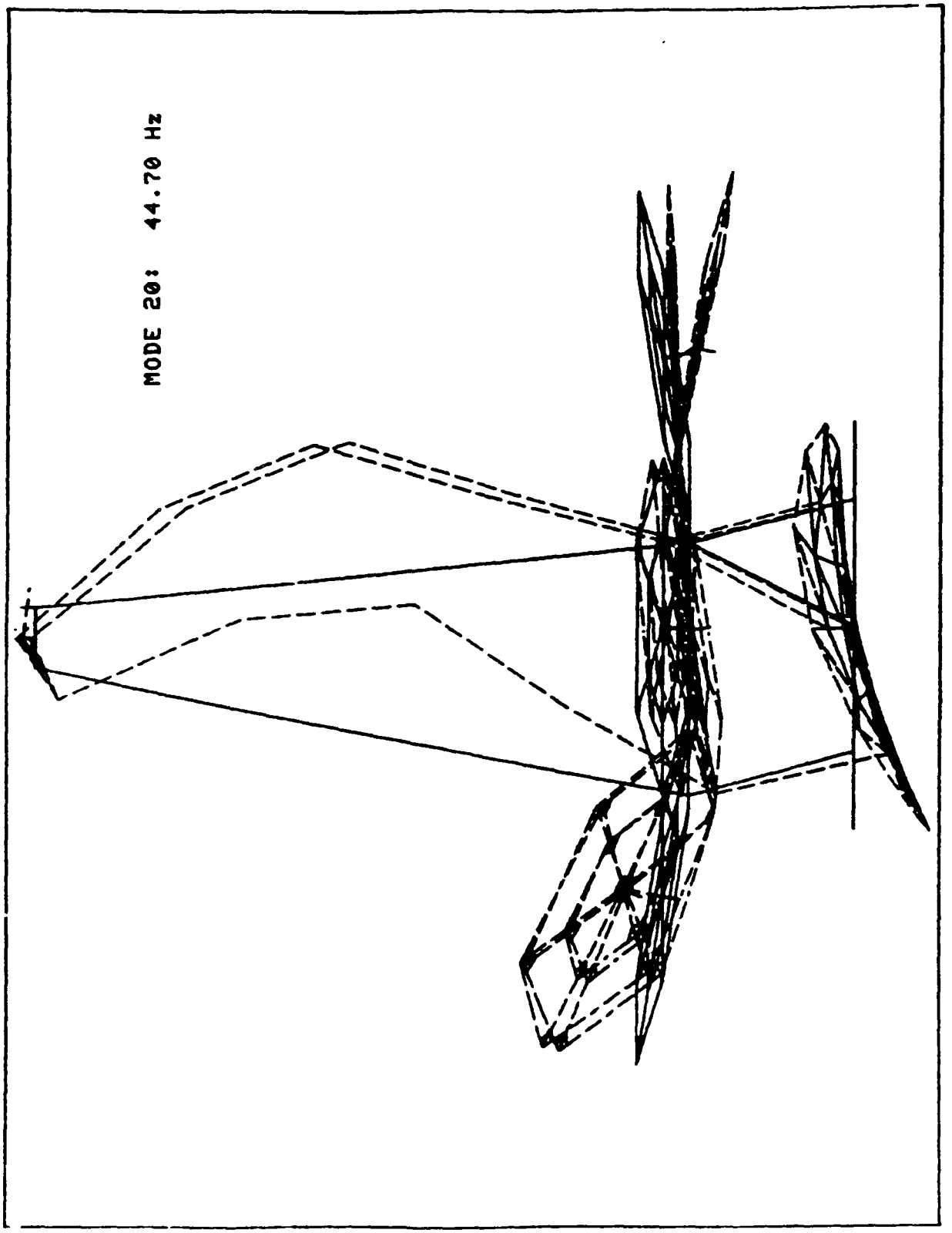
MODE 20: 44.70 Hz

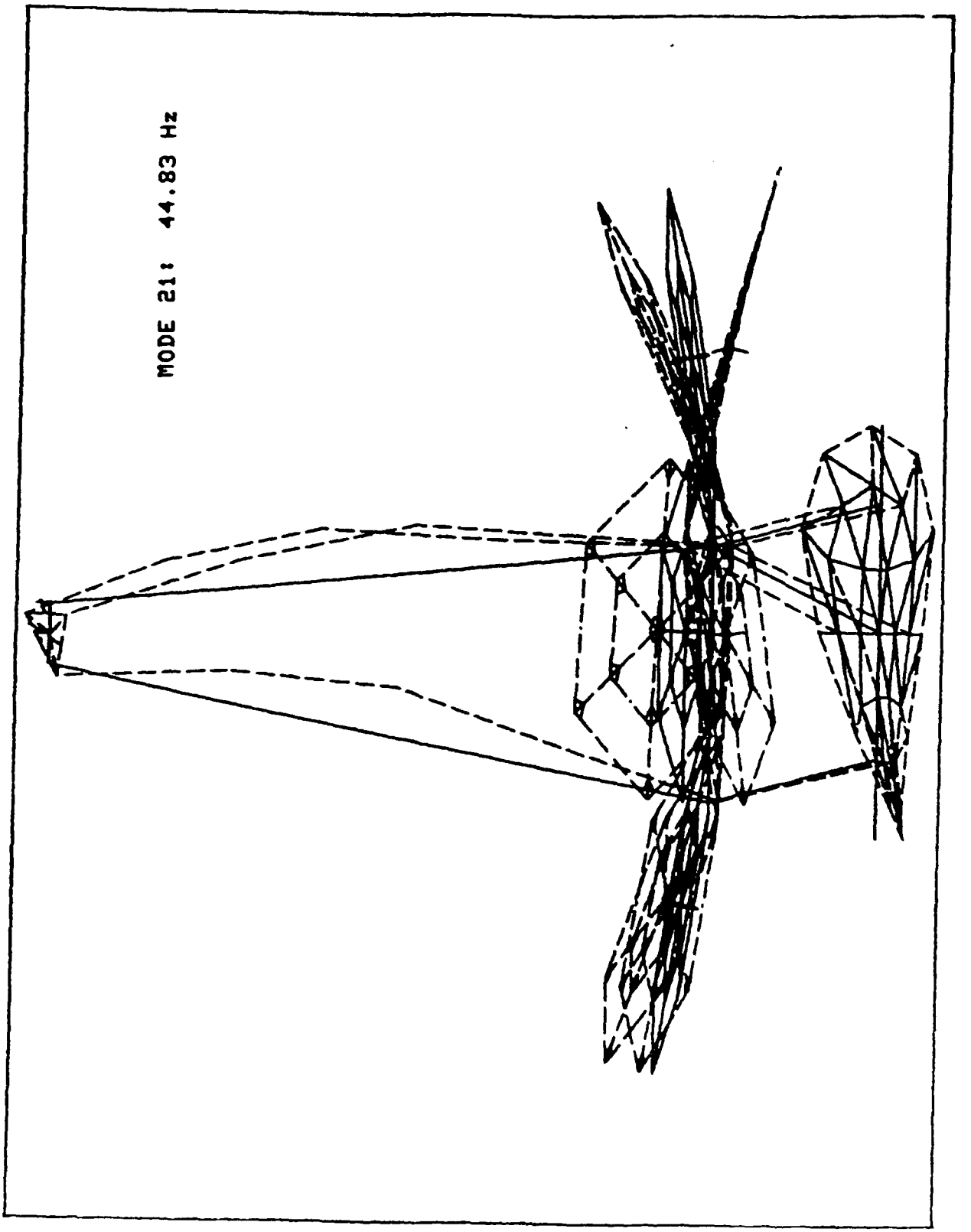
MODE 21: 44.83 Hz

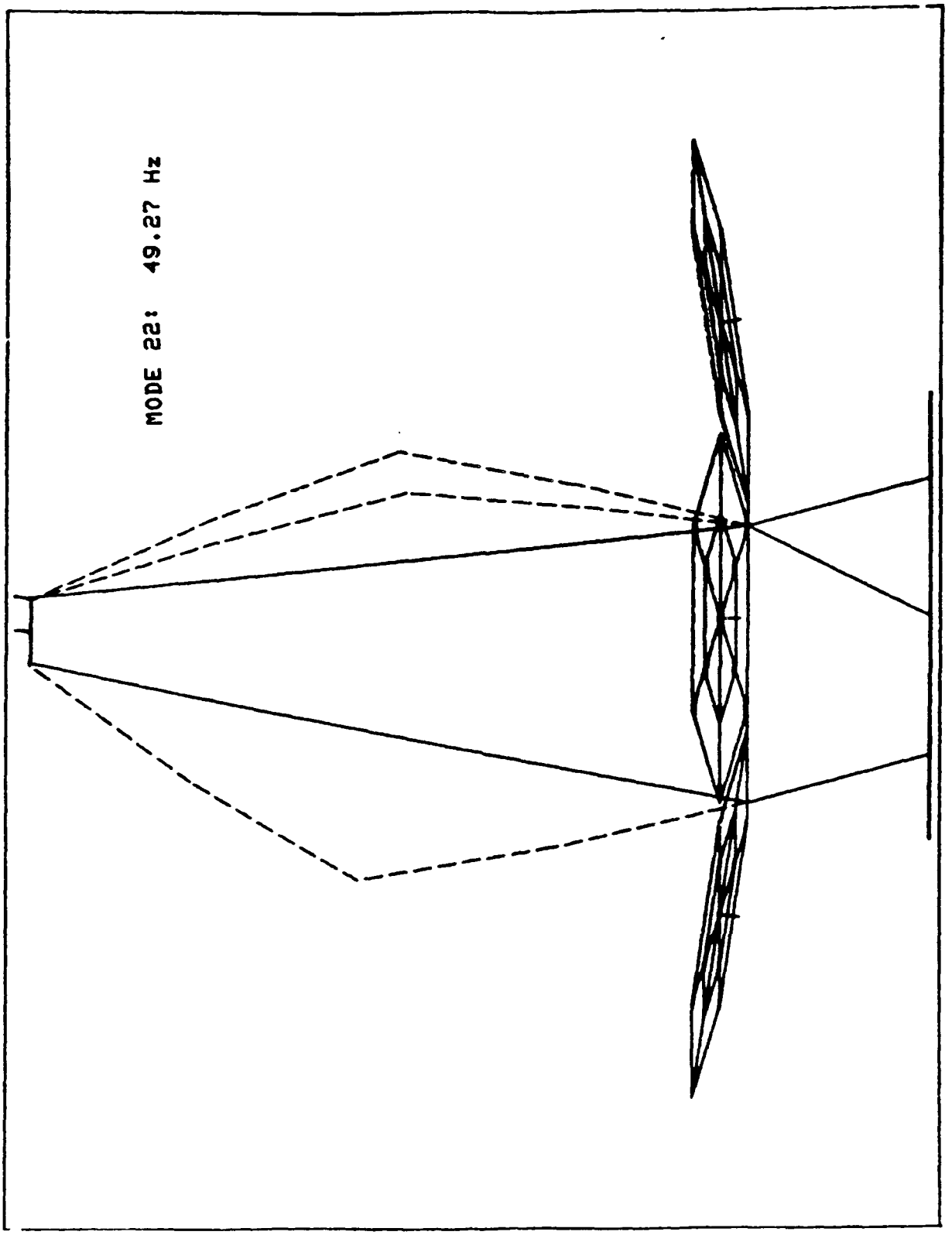
MODE 22: 49.27 Hz

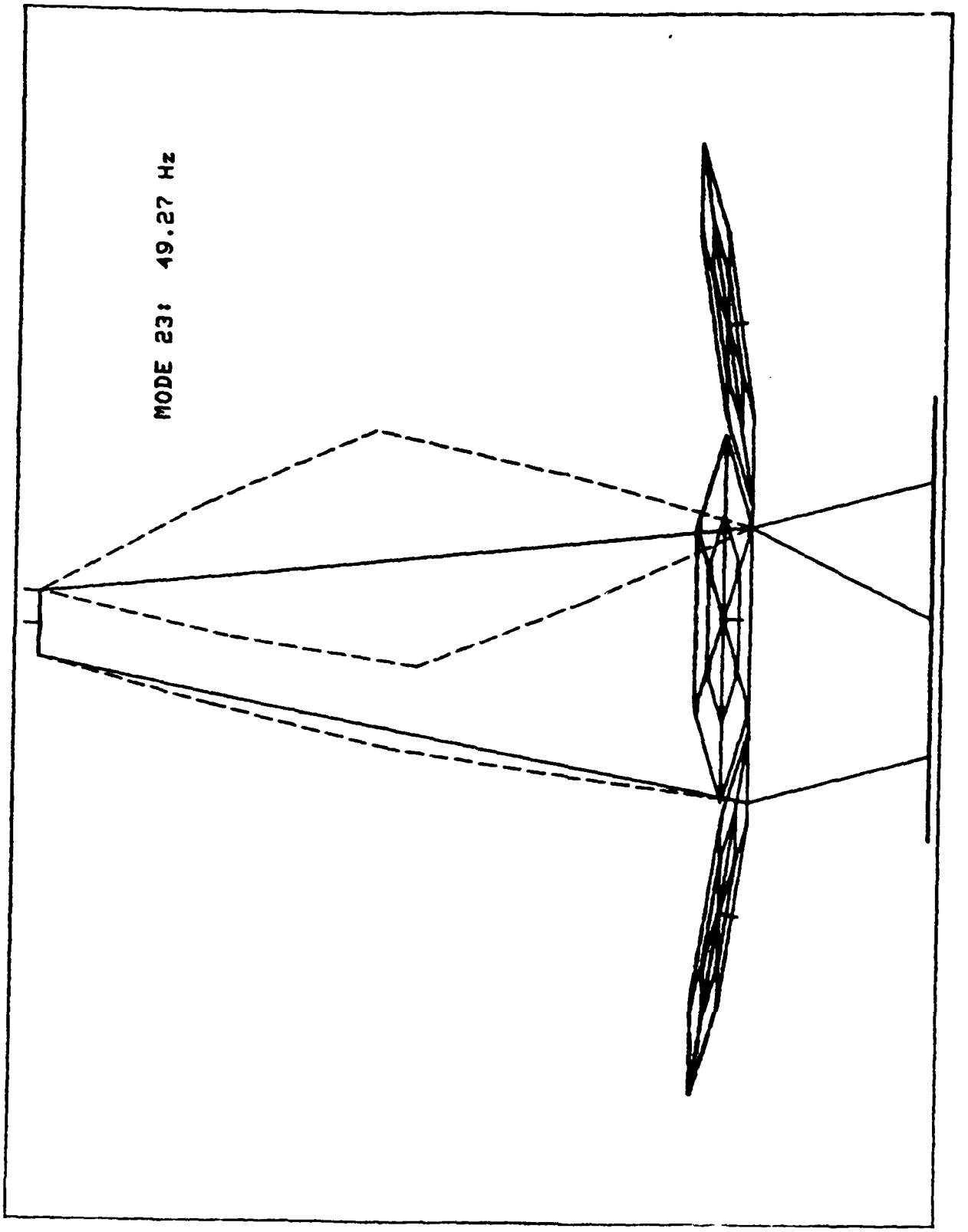
MODE 23: 49.27 Hz

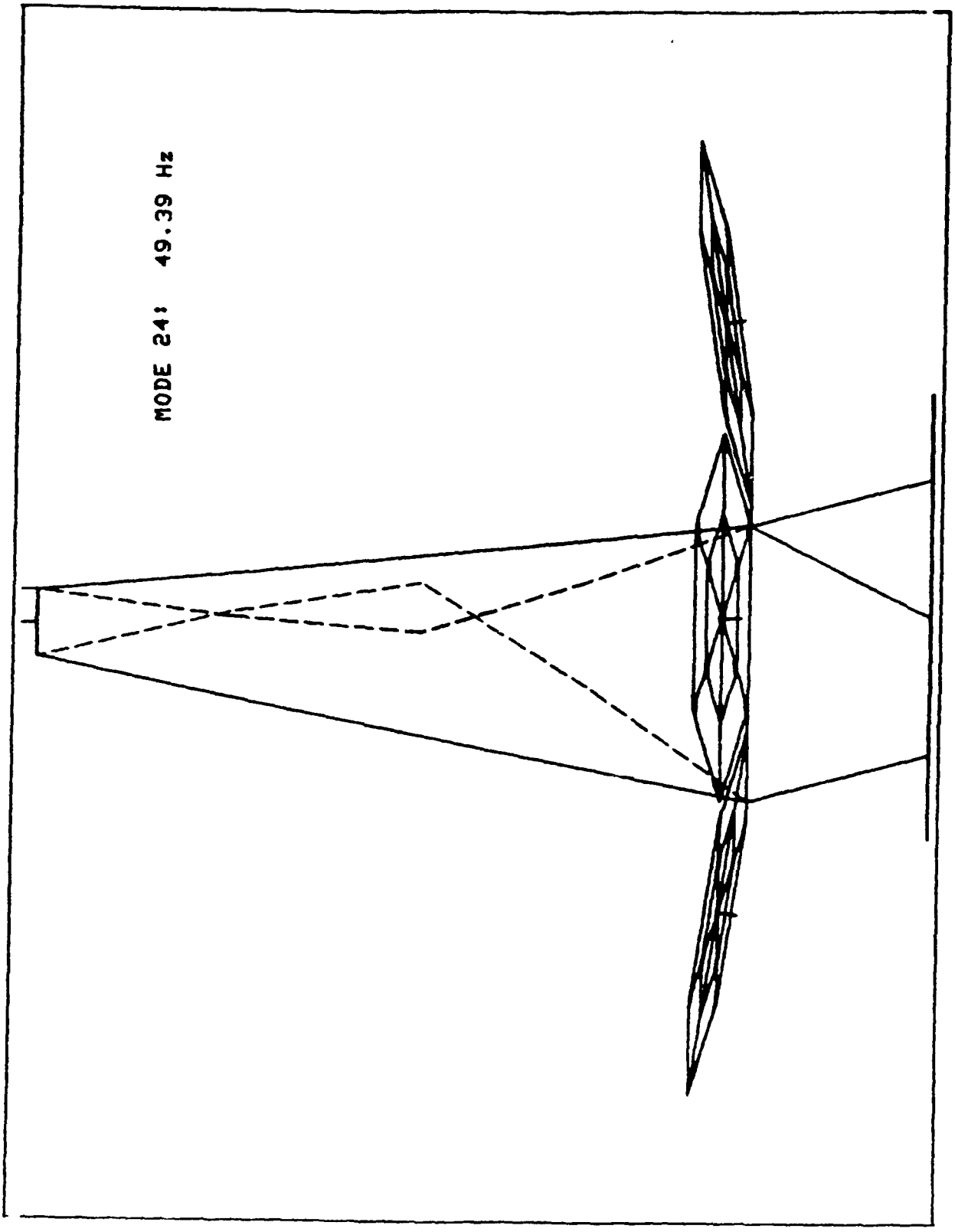
MODE 24: 49.39 Hz

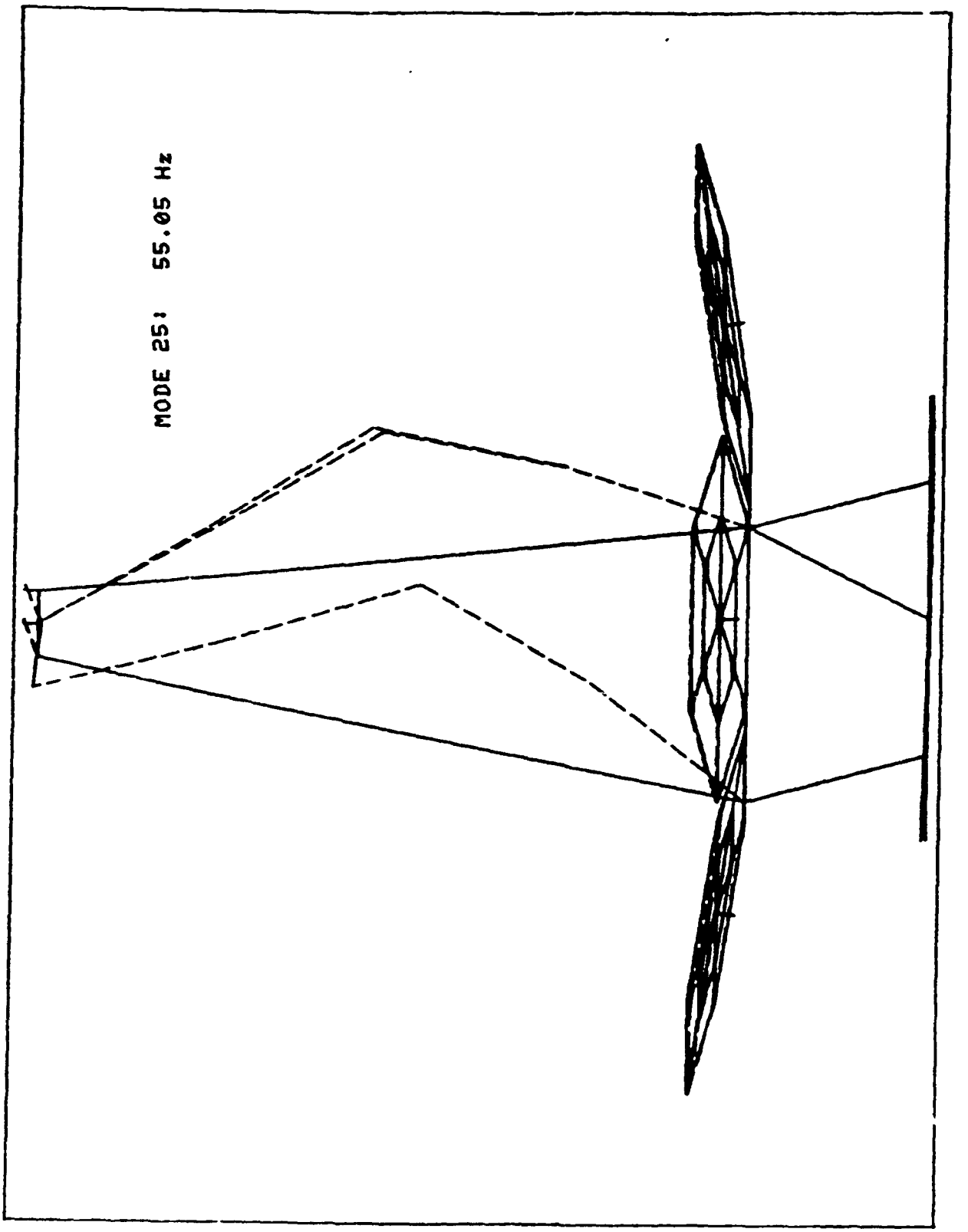
MODE 25: 55.05 Hz

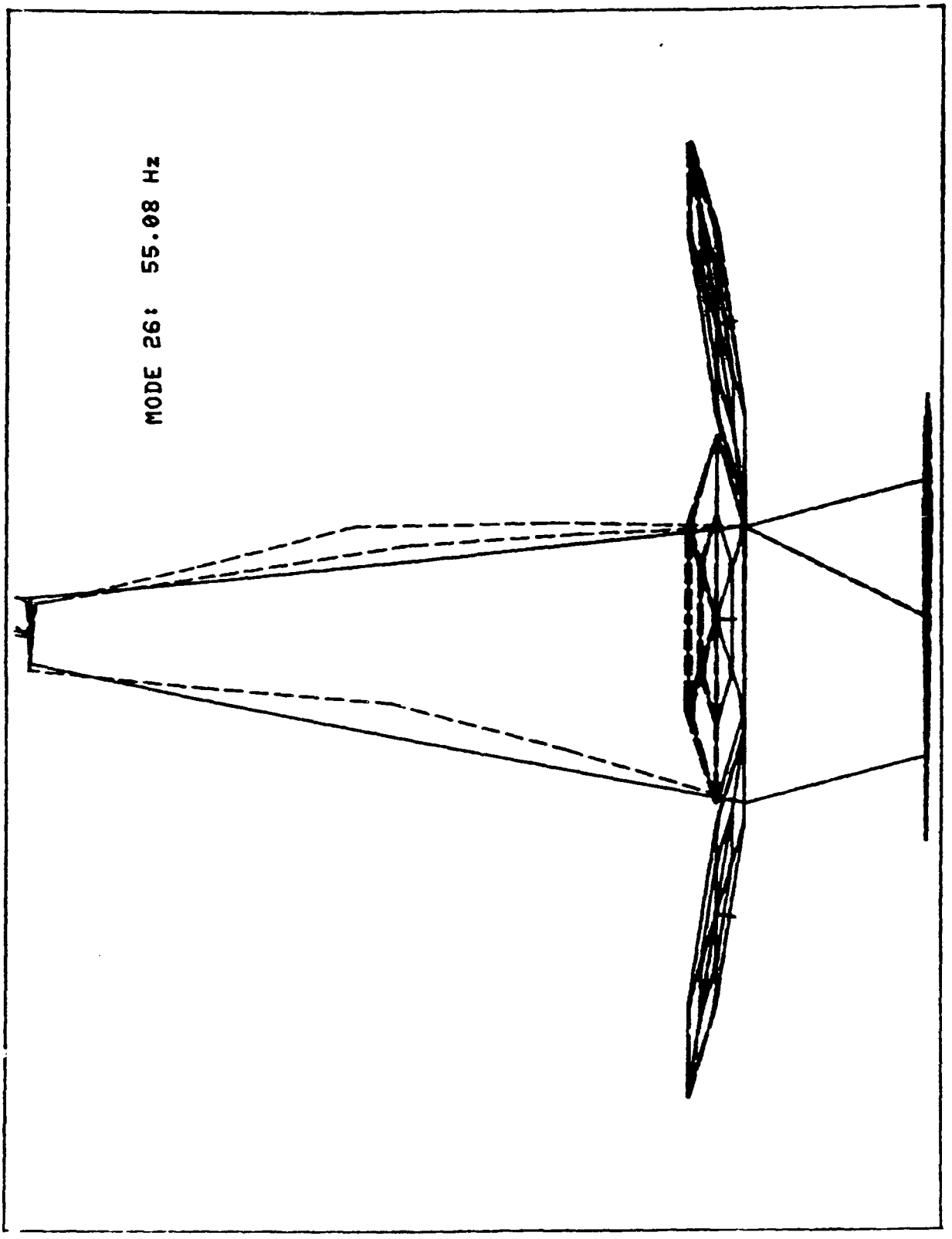
MODE 26: 55.08 Hz

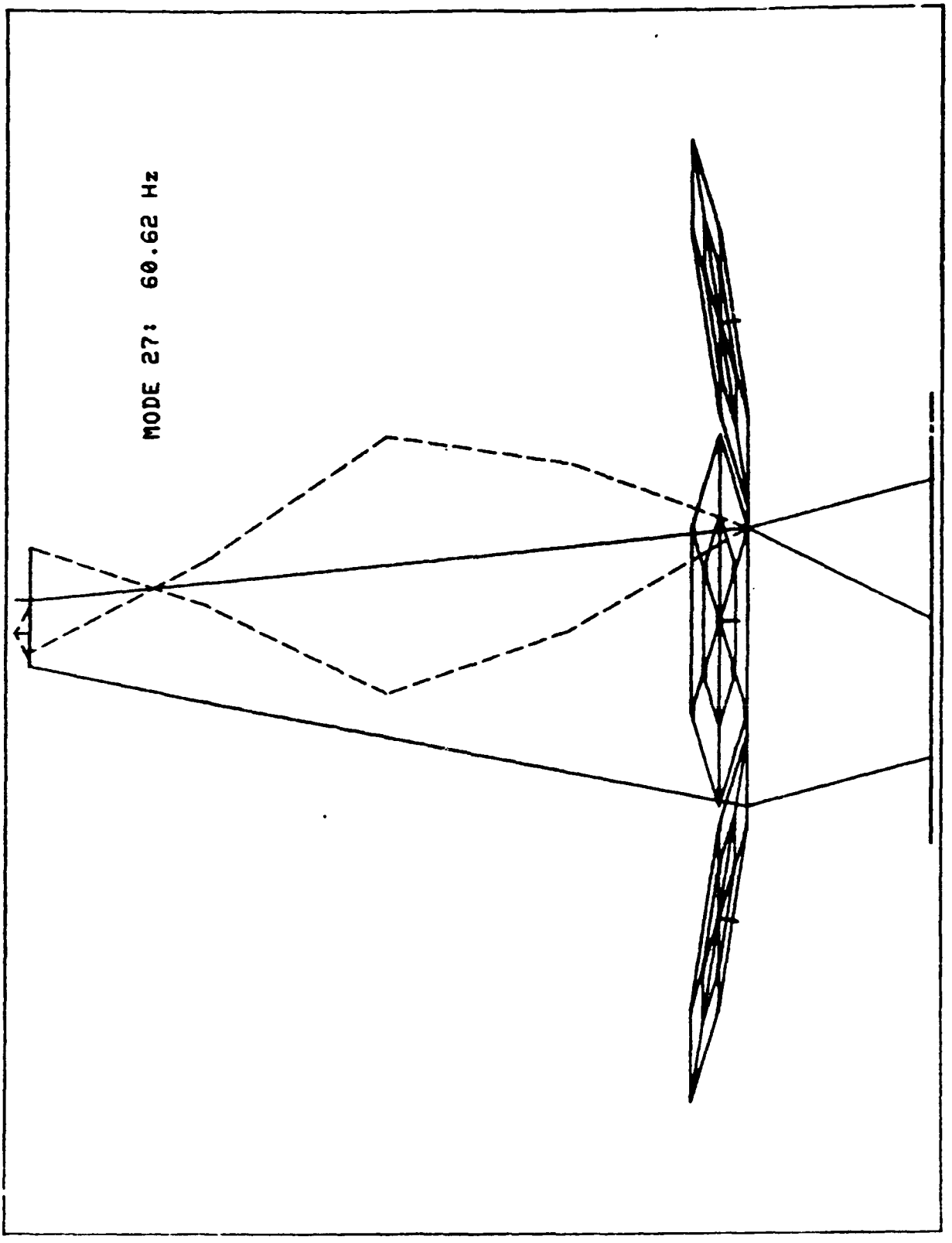
MODE 27: 60.62 Hz

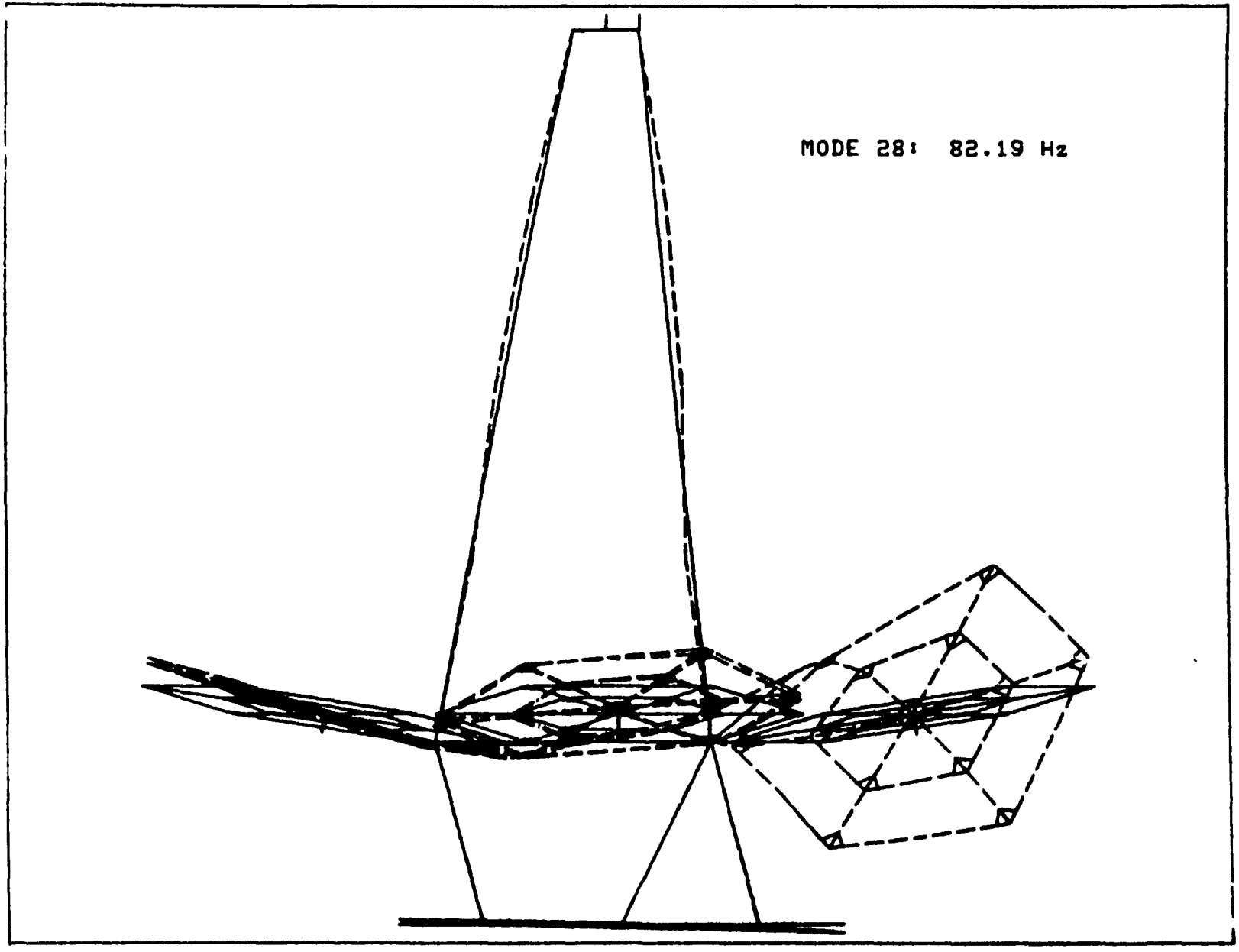
MODE 28: 82.19 Hz

Appendix B

MHPE/Majorant Reference List

D. C. Hyland and D. S. Bernstein, "The Majorant Lyapunov Equation: A Nonnegative Matrix Equation for Robust Stability and Performance of Large Scale Systems," *IEEE Trans. Autom. Contr.*, Vol. AC–32, pp. 1005–1013, 1987.

B. J. Boan and D. C. Hyland, "The Role of Metal Matrix Composites for Vibration Suppression in Large Space Structures," *Proc. MMC Spacecraft Survivability Tech. Conf.*, MMCIAC Kaman Tempo Publ., Stanford Research Institute, Palo Alto, CA, October 1986.

S. W. Greeley, D. J. Phillips and D. C. Hyland, "Experimental Demonstration of Maximum Entropy, Optimal Projection Design Theory for Active Vibration Control," *Proc. Amer. Contr. Conf.*, pp. 1462-1467, Atlanta CA, June 1988.

D. C. Hyland, "An Experimental Testbed for Validation of Control Methodologies in Large Space Optical Structures," *Structural Mechanics of Optical Systems II*, pp. 146–155, A. E. Hatheway, Ed., Proceedings of SPIE, Vol. 748, Optoelectronics and Laser Applications Conference, Los Angeles, CA, January 1987.

D. C. Hyland, "Experimental Investigations in Active Vibration Control for Application to Large Space Optical Structures," *Space Structures, Power, and Power Conditioning*, R. F. Askew, Ed., Proc. SPIE, Vol. 871, pp. 242– 253, 1988.

D. C. Hyland and D. J. Phillips, "Development of the Linear Precision Actuator," 11th Annual AAS Guid. Contr. Conf., Keystone, CO, January 1988.

S. W. Greeley, D. J. Phillips, and D. C. Hyland, "Experimental Demonstration of Maximum Entropy, Optimal Projection Design Theory for Active Vibration Control," *Proc. Amer. Contr. Conf.*, pp. 1462–1467, Atlanta, GA, June 1988.

D. C. Hyland and E. G. Collins, Jr., "A Robust Control Experiment Using an Optical Structure Prototype," *Proc. Amer. Contr. Conf.*, pp. 2046-2049, Atlanta, GA, June 1988.

E. G. Collins, Jr., and D. C. Hyland, "Improved Robust Performance Bounds in Covariance Majorant Analysis," *Int. J. Contr.*, Vol. 50, pp. 495–509, 1989.

D. C. Hyland and E. G. Collins, Jr., "A Majorant Approach to Robust Stability and Time-Domain Performance for Discrete-Time Systems," *Proc. Amer. Contr. Conf.*, pp. 1604–1609, Pittsburgh, PA, June 1989.

D. C. Hyland and E. G. Collins, Jr., "An M-Matrix and Majorant Approach to Robust Stability and Performance Analysis for Systems with Structured Uncertainty," *IEEE Trans. Autom. Contr.*, Vol. 34, pp. 631–710, 1989.

D. C. Hyland and D. S. Bernstein, "Hardware Realities in the Active Control of Large Space Structures," *Third Annual Conference on Aerospace Computational Control*, Oxnard, CA, August 1989.

D. J. Phillips and E. G. Collins, Jr., "Four Experimental Demonstrations of Active Vibration Control for Flexible Structures," *Proc. AIAA Guid. Nav. Contr. Conf.*, pp. 1625–1633,

Portland, OR, August 1990.

D. J. Phillips, E. G. Collins, Jr., and D. C. Hyland, "Experimental Demonstrations of Active Vibration Control for Flexible Structures," *Proc. IEEE Conf. Dec. Contr.*, Honolulu, HI, December 1990.

D. C. Hyland, D. J. Phillips, and E. G. Collins, Jr., "Active Control Experiments for Large Optics Vibration Alleviation," SPIE Optoelectronics Conf., Orlando, FL, April 1990.

A. W. Daubendiek, D. C. Hyland, and D. J. Phillips, "Systems Identification and Control Experiments on the Multi-Hex Prototype Test Bed," *2nd USAF/NASA Workshop on System Identification and Health Monitoring of Precision Space Structures*, Pasadena, CA, march 1990.

Appendix C

Selected MHPE/Experimental Results Papers

2nd USAF/NASA Workshop on
System Identification and Health Monitoring
of Precision Space Structures

System Identification and Control Experiments on the Multi-Hex Prototype Test Bed

by

Allen W. Daubendiek, David C. Hyland and Douglas J. Phillips

Abstract

The Harris Multi-Hex Prototype Experiment is a four meter diameter, seven panel reflector which has been built by the Harris Corporation as a test bed for development and validation of control design and testing methodology for large high precision space structures. This paper reports on system identification and control activities. It particularly addresses the systems identification design task and test results. An assessment of data quality necessary to support controller design of a system with large numbers of actuators and sensors (typical of precision structures) is made. Also, constraints on controller architecture design which result from the systems I/O test limitations are discussed.

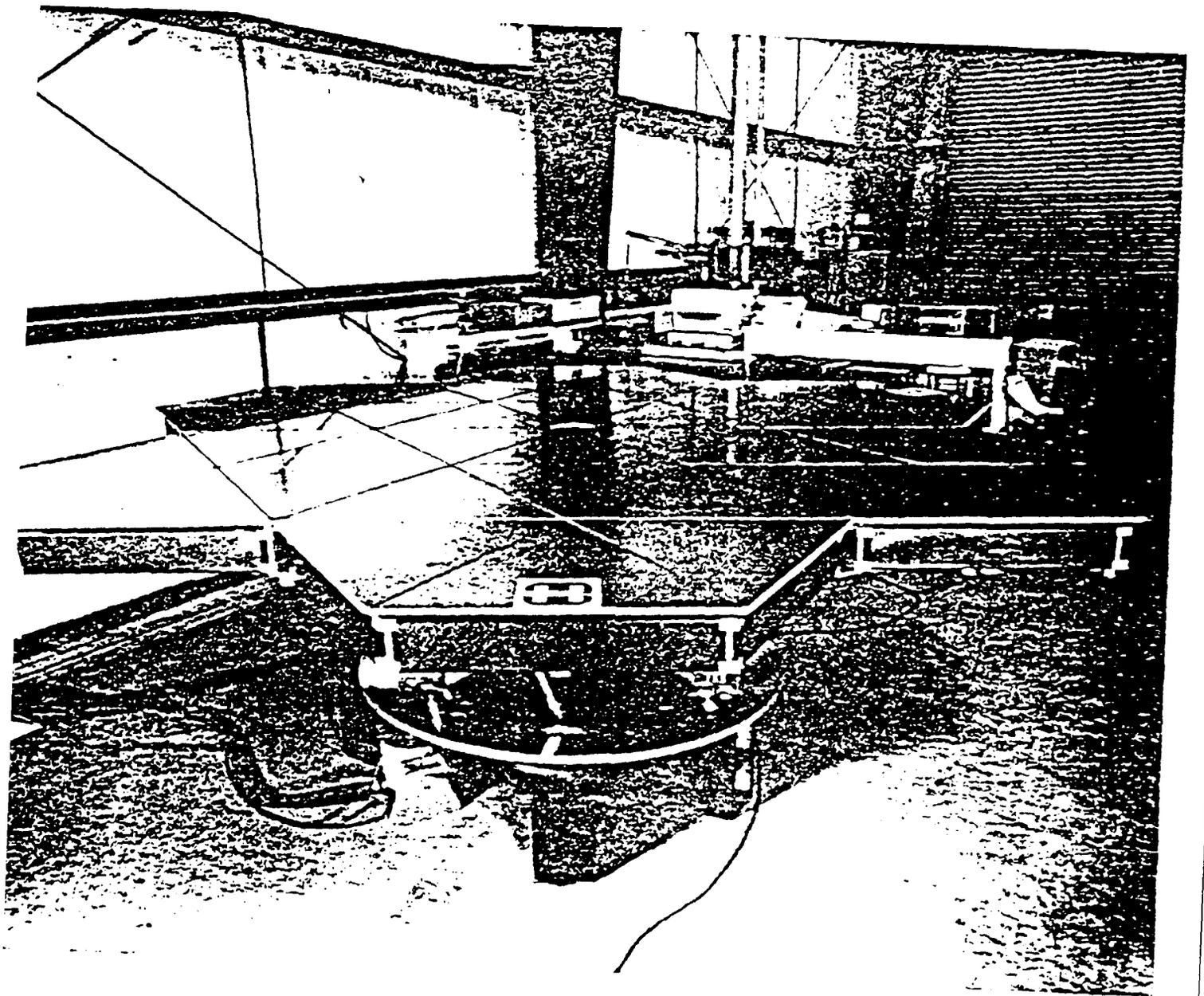

Figure 1. MHPE struct[illegible]

INTRODUCTION

Large space based RF and optical systems are driven by two opposing requirements: high performance versus the payload size and weight constraints of available boosters. The latter requires that a large system be deployable, or in some cases erectable. These restrictions greatly limit the strength and stiffness of the RF/optical surface components and supporting structures.

The RF/optical system is only one portion of an overall spacecraft; it must perform in concert with other mission-critical operations such as maneuvering and power generation. These disturbances can induce structural vibrations which compromise or limit performance.

Numerous analytical studies indicate that RF/optical shape and pointing performance can be improved by incorporating active vibration control into large spacebourne systems. It is widely agreed that the first important step is to thoroughly test vibration suppression methods prior their deployment in space.

Because of the inability to test large lightweight structures in an ambient (weightless) environment, there exists a technology gap in verifying performance of large space systems. A systematic methodology for planning a combined analysis and testing qualification program that will result in accurate performance predictions at minimal cost is needed to fill that gap.

The Multi-Hex Prototype Experiment (MHPE) testbed was developed and fabricated on the Harris Precision Structures and Controls IR&D Program to work toward this goal. Since its completion in the summer of 1988, test activities have been underway to refine and develop system identification techniques in support of vibration control studies.

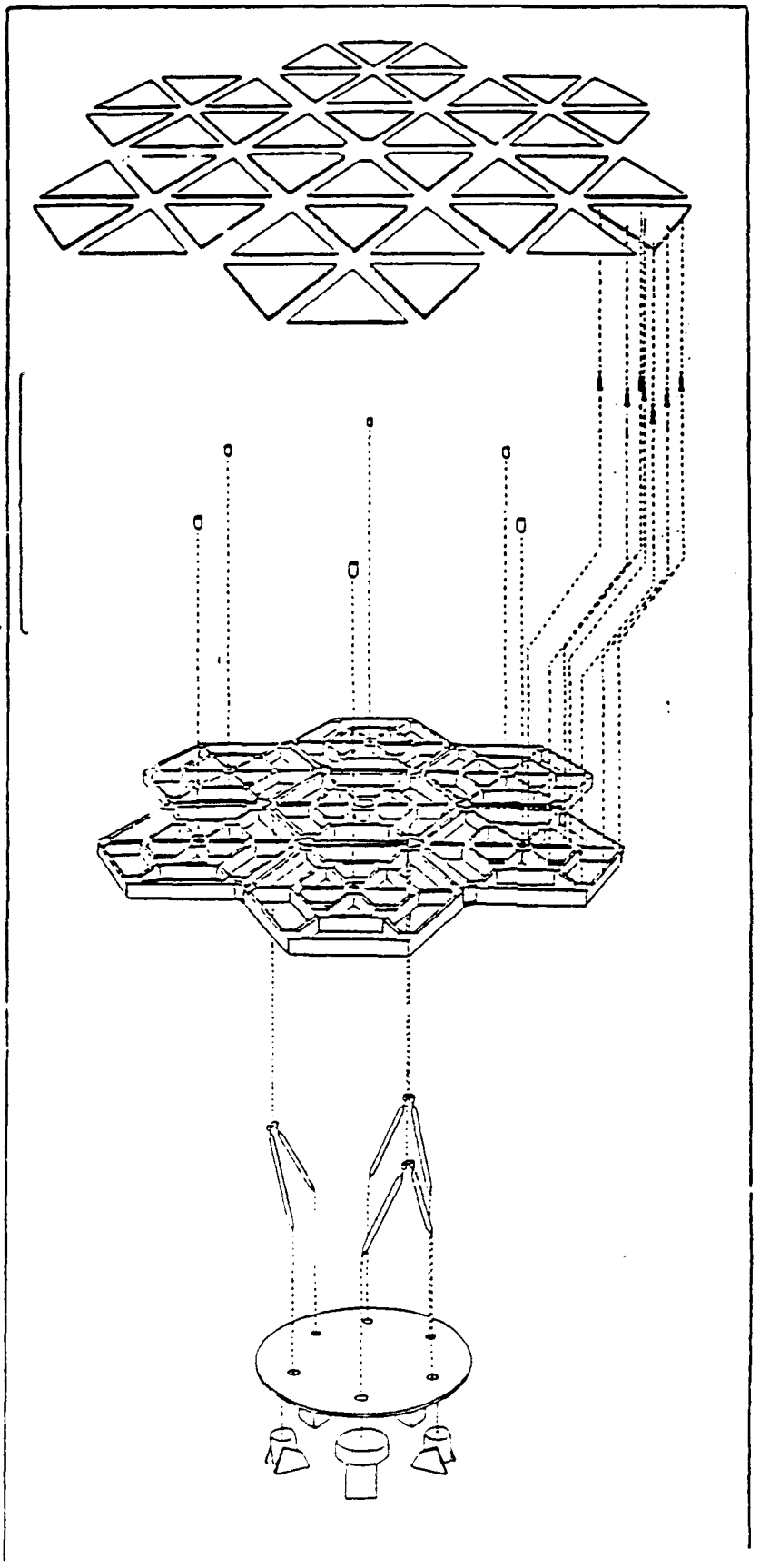

Figure 2. Multi-Hex Prototype Experiment (MHPE) Structural Configuration

DESCRIPTION

Figure 1 shows a photograph of the MHPE as of May 1988 and Figure 2 shows a blow-up drawing indicating the separate components. The basic structure consists of 42 surrogate mirror facets mounted on a seven panel graphite-epoxy box truss array. The seven panel array is mounted on a circular aluminum base plate via six tubular aluminum struts. Air bag isolators support the static weight, and electrodynamic shakers are used to provide base plate vibrations emulating aft-spacecraft disturbances.

Each hexagonal cell measures 4.3 feet across. The whole array weighs 117 pounds (including the 42 surrogate mirror facets) and is 12.8 feet across. The aluminum base plate is five feet in diameter and one inch thick.

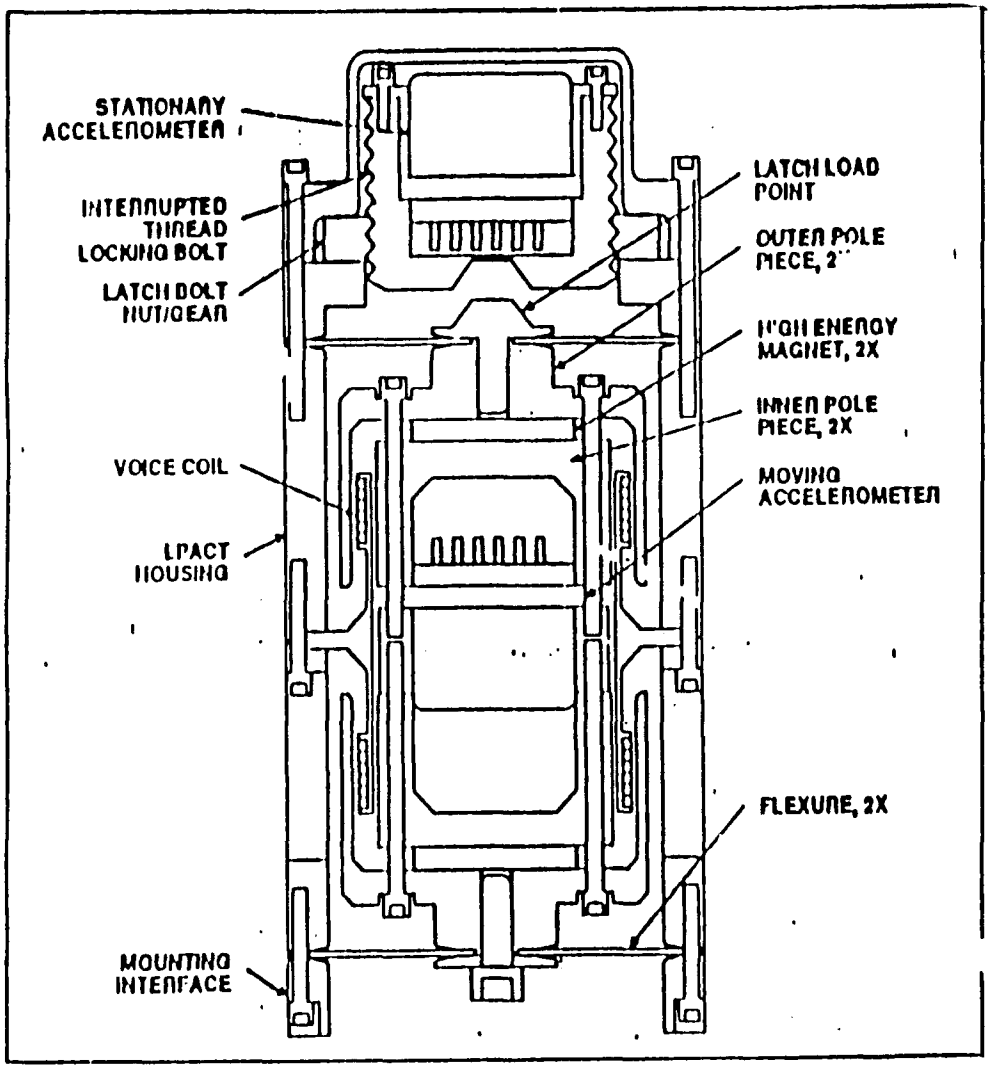

- PROOF MASS / VOICE COIL DESIGN
- GRAPHITE-EPOXY FLEXURES OBVIATE BEARING STICTION PROBLEMS
- ULTRA-HIGH-BANDWIDTH CASING-MOUNTED ACCELEROMETER MEASURES STRUCTURAL MOTION
- PROOF-MASS MOUNTED ACCELEROMETER CLOSES INTERNAL CONTROL LOOP RESULTING IN RELIABLY SHAPED FREQUENCY RESPONSE

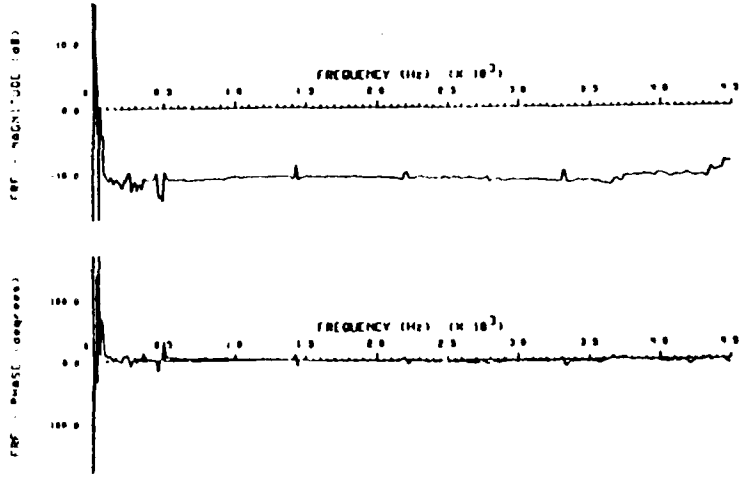

Figure 3. LPACT Damping Unit Provides Reliable, High-Bandwidth Sensor/Actuator in a Single Package.

Six voice-coil driven proof-mass actuators placed at the center of each of the six outer hex panels constitute the actuators for active vibration control. These devices are the patented Harris Linear Precision Actuators (LPACT). Each LPACT utilizes a proof-mass mounted accelerometer used in an internal feedback configuration which serves to override non-linearities and to reduce the effect of the restraint flexure-mass resonance. Figure 3 shows a diagram of the LPACT and lists its significant properties.

Developed in 1987 on Harris IR&D, the LPACT has exceptionally flat frequency response from 5 Hz to 5 KHz. The stroke is limited to +/- 0.25 inches, and the peak force of the device is 2.5 pounds. The moving mass is 0.68 kg, including the proof-mass accelerometer, and the (uncompensated) motor force constant is 3.10 Newton/Ampere.

Piezo-electric actuators are currently under evaluation for use in the struts which connect the hex panel array to the base plate. Similar devices are contemplated for position control of individual mirror facets.

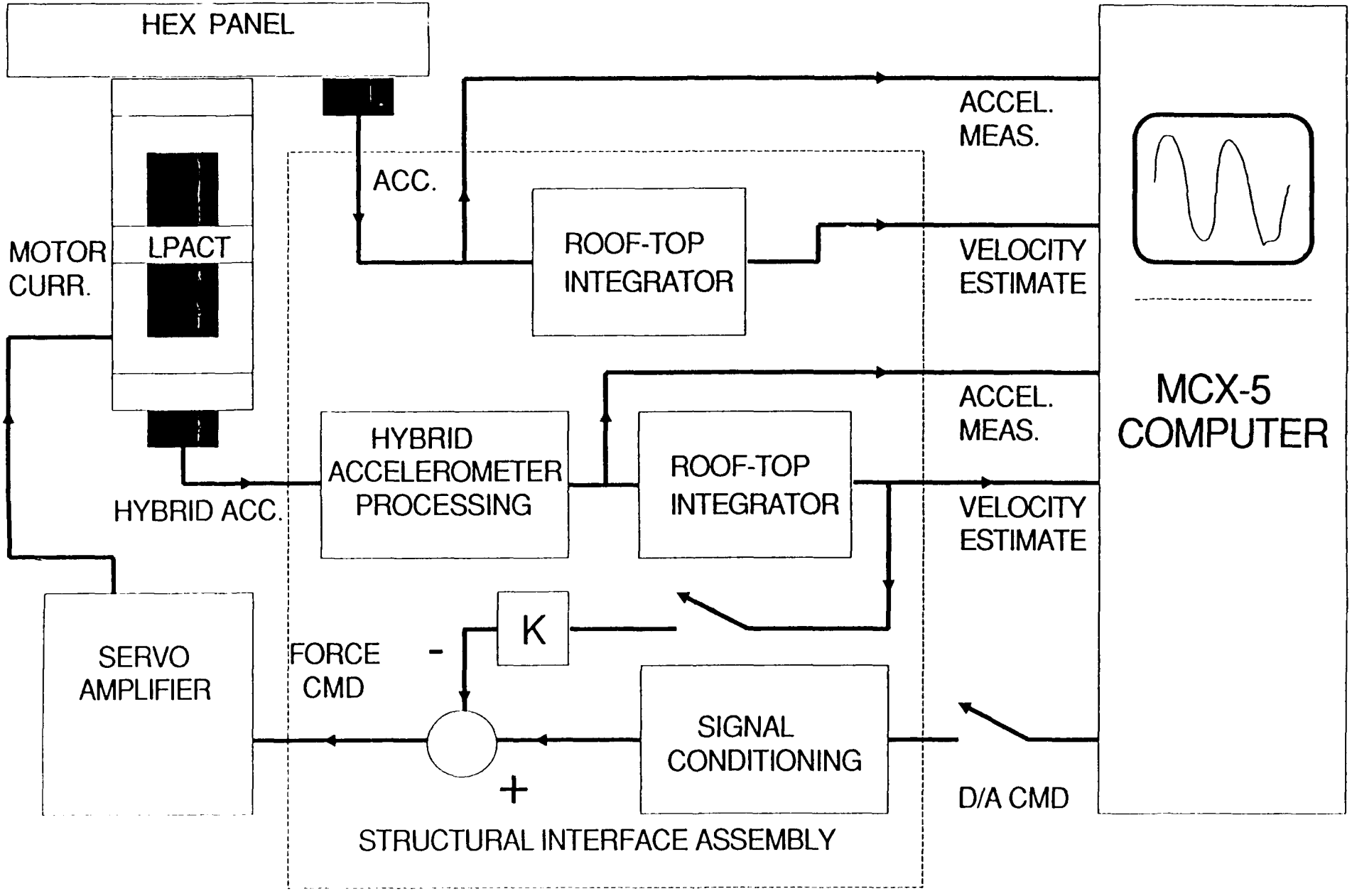

Figure 4. MHPE Control System Signal-Flow Diagram

System identification and control computations are performed on a Masscomp (Concurrent) MCX-5 mini computer. Up to eight D/A channels and 256 A/D channels are available. Typically 48 A/D channels and 6 D/A channels are used in an identification or control test. Sample rates in excess of 500 hertz have been attained while executing a 12-state control law and simultaneously recording over 50 data channels.

Figure 4 outlines the controller/processor architecture implemented on the MHPE. As indicated, there are two types of control loops. The first is a set of purely decentralized loops implemented with analog electronics components. Operating in parallel with the "analog loops" is a centralized discrete time controller implemented with the MCX-5 computer.

The analog electronics (excluding the servo amplifier) are contained in the Structural Interface Assembly (SIA), shown in the figure. This unit has several distinct subsystems: hybrid accelerometer processing, rooftop-integrator velocity estimators, feedback gain summers, and D/A signal conditioning circuits. The LPACT moving mass (secondary) accelerometer feedback loop is also closed through the SIA, though not shown in the figure. The SIA permits access to all test signals for hardware debugging.

Every accelerometer on the MHPE structure is integrated to provide a velocity estimate. Additionally, each LPACT primary accelerometer has been augmented with a piezo-electric accelerometer to enhance its useable bandwidth. Thus the high bandwidth of the LPACT as an actuator is complemented by the availabilty of wide bandwidth acceleration and velocity measurements.

DISTURBANCE PSD

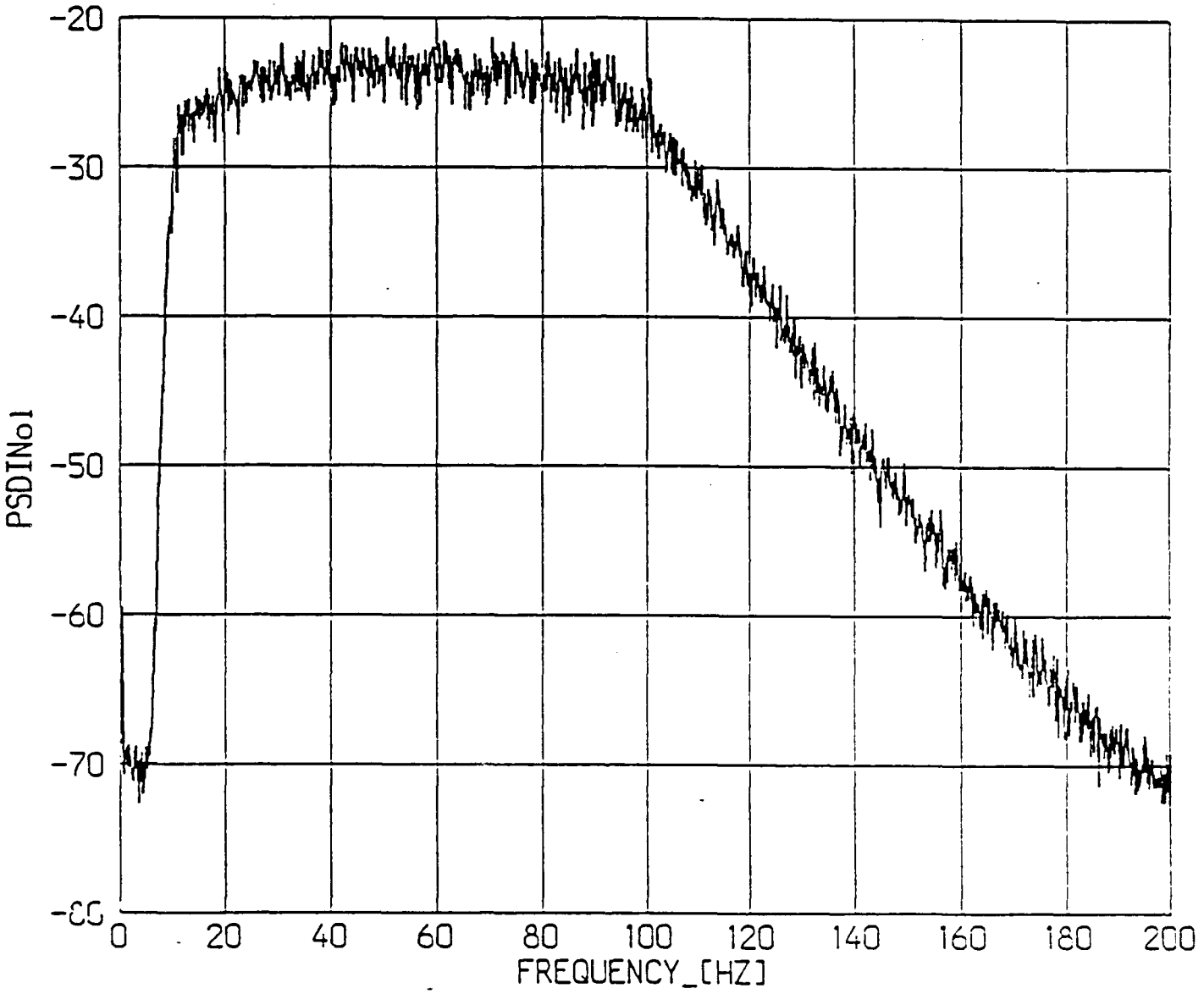

RMS = 5.3 lbf - each shaker

Figure 5. Power Spectral Density function as measured by Force Gauge at Shaker-Baseplate interface.

Shaker excitation signals can be supplied by an analog signal generator, bandlimited random noise generator, or one channel of the MCX-5 D/A converter. Figure 5 shows a random disturbance power spectral density having a 5.3 lbf total RMS output, measured at the baseplate interface.

For structural identification, similar test signals can be applied via the LPACTs. Since each LPACT has a dedicated D/A channel, multiple pseudorandom signals as well as deterministic test patterns can be utilized.

Data analysis software on the MCX-5 supports off-line analysis of test results. Fundamental tools, such as frequency response functions, coherence, power spectral density, and correlation functions are all supported. More advanced tools, including realization and control design programs, have also been implemented.

Design studies indicate that PM dephasing error cannot be readily compensated by alignment elements in the system optical train and that structural control of the PM assembly is needed.

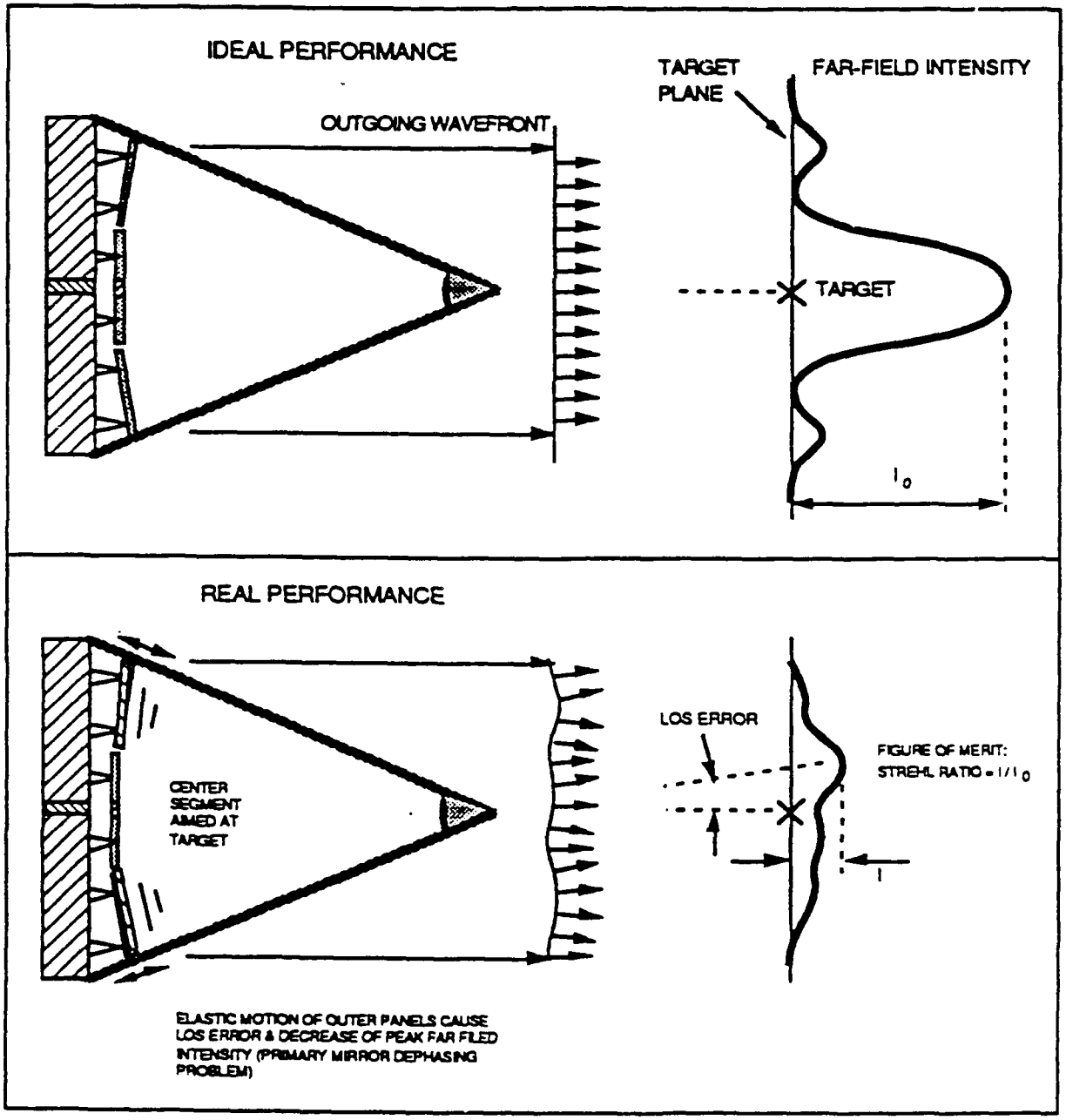

Development of structural control technology needed to solve mirror dephasing and related vibration problems is a thrust of Harris IR&D. To support our technology validation efforts,

Figure 6. Vibration Control of Primary Mirror surfaces improves Strehl Ratio, a measure of Optical Performance

PERFORMANCE MEASURES

The MHPE was designed to emulate generic pathologies of Large Space Structures for high frequency RF and optical applications. With respect to critical technologies, such as structural identification and control, the experimental configuration is intended to be as challenging as an actual space structure.

Of paramount importance to optical systems is Primary Mirror (PM) dephasing. The Strehl Ratio, a measure of relative intensity illustrated in Figure 6, is a good figure of merit for mirror performance. Simulation results show the potential benefits of active vibration control in improving Strehl Ratio.

In order to address the dephasing problem, the control objective for the MHPE apparatus is to suppress the relative motion of the hexagonal panels due to vibration induced by broadband disturbances. At present, the mirror surface error is not measured directly by optical means, but is computed by post-processing time histories from the 18 accelerometers mounted at various points on the MHPE structure. Future experiments will employ direct optical measurements using the Optical Position Measurement System (OPMS) upgrade, presently being implemented.

MODELING FOR CONTROL DESIGN

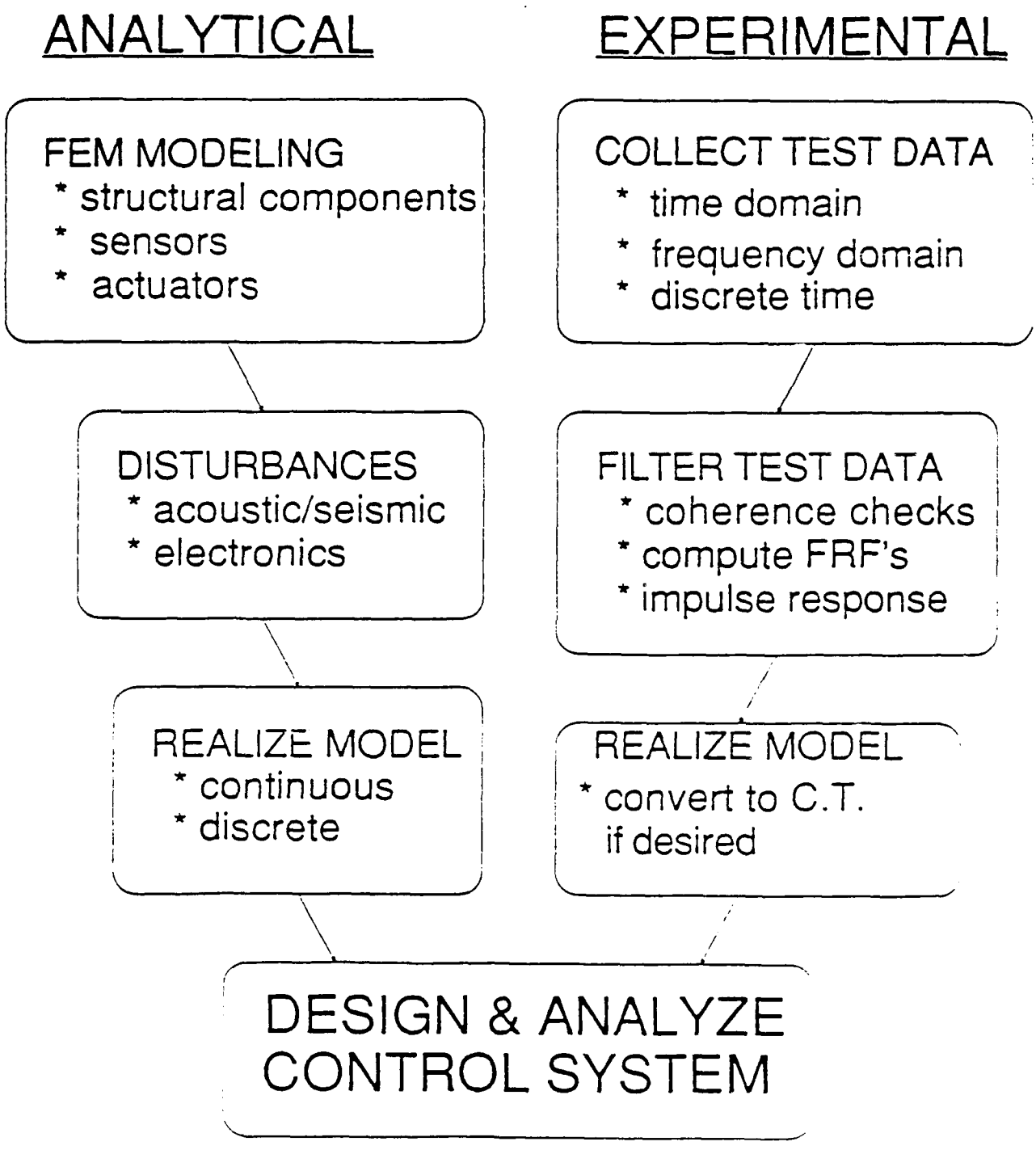

Figure 7. There are two fundamental paths to obtaining models for control system design

SYSTEM IDENTIFICATION

Since the MHPE became operational, activities have alternated between system identification, hardware upgrades and vibration control testing. The first stage of our study involved a priori modeling and initial control design studies. This was followed, after fabrication was completed, by initial structural testing.

In this section, we describe these activities in order to shed light on a basic dichotomy in system identification for control; namely the use of analytical, physically motivated modeling versus directly acquired, input/output representations. Figure 7 illustrates these two approaches.

The analytical, physically motivated modeling approach is the path most often followed in the preliminary phases of an engineering project. Many studies never progress beyond this phase. It provides order-of-magnitude estimates of system parameters such as frequencies and mode shapes, which are adequate for sizing sensor and actuator requirements.

The other path can be broadly labeled the "experimental" approach. Assuming the system exists, we can collect test data and construct an external representation of the system dynamics (input/output model) which explains the input/output relationships observed. The correctness of the model for control purposes can be tested incrementally, by implementing simple controllers of increasing authority.

MHPE MODAL SUMMARY

[MODAL FREQUENCIES IN HERTZ]

FRF	FEM	ERA	comments
1.3	1.68		isolation system mode
1.8	1.69		isolation system mode
3.1	3.04		isolation system mode
3.5	3.04		isolation system mode
4.3	3.89		isolation system mode
		8.08	damping ratio = .06, isolation system?
		9.59	damping ratio = .03
		16.02	damping ratio = .06, isolation system?
		17.05	damping ratio = .03
26.5	23.56	25.41	damping ratio = .14, asymmetric dble mode
27.5	23.56	25.96	damping ratio = .16
32.0	29.16	22.97	damping ratio = .05, cupping mode
39.0	38.83	36.47	damping ratio = .03, bending mode pair
39.0	38.84	36.91	damping ratio = .03
45.0	44.21	43.51	damping ratio = .05, torsion mode?
64.0	73.6	61.61	damping ratio = .005, bending mode pair
69.0	73.6		
83.0	82.6	80.58	damping ratio = .04, bending mode pair
85.0	82.6		
95.0	96.0	98.16	damping ratio > .5, hex array / baseplate?
131.5	131.87		bending mode pair
	131.89		
138.0		139.0	same bending mode pair?
		140.3	damping ratio = .015 and .024
167.0	161.44	155.4	hex array / baseplate or strut mode?
		158.9	damping ratio = .015 and .01
	170.18	175.7	damping ratio = .016, bending pair mode
	170.19	177.9	damping ratio = .016
189.0		189.8	damping ratio = .02, bending pair mode
191.0		199.0	damping ratio = .08

Figure 8. Good agreement between FRF data, Finite-Element Models and ERA generated models was obtained on the MHPE structure.

The purposes of the initial MHPE tests were to establish open-loop dynamics data and provide end-to-end checkout of the system electronics. The initial test data also showed substantial disparities with the predictions of the pre-test model.

To refine the model, a sensitivity analysis was first performed to determine the most likely sources of error. Ranked in order of importance, they were determined to be

1) Stiffness of the aluminum strips which connect each of the outer panels to adjacent outer panels.

2) Stiffness of the small triangular aluminum plates which connect the outer panels to the inner panels.

3) Base plate modulus of elasticity.

4) Aluminum support strut stiffness

5) The extent of moment transmitted by joints connecting struts with the center hex panel.

6) Hex panel graphite-epoxy elastic modulus.

Candidate subsystem components were then subjected to simple static and dynamic tests to determine more accurate physical parameters. The refined parameter values were used to construct a finite element model which produced significantly better agreement with the original test data. The end result of this process is summarized in Figure 8, which compares modal frequencies from the test data with the refined model eigenvalues.

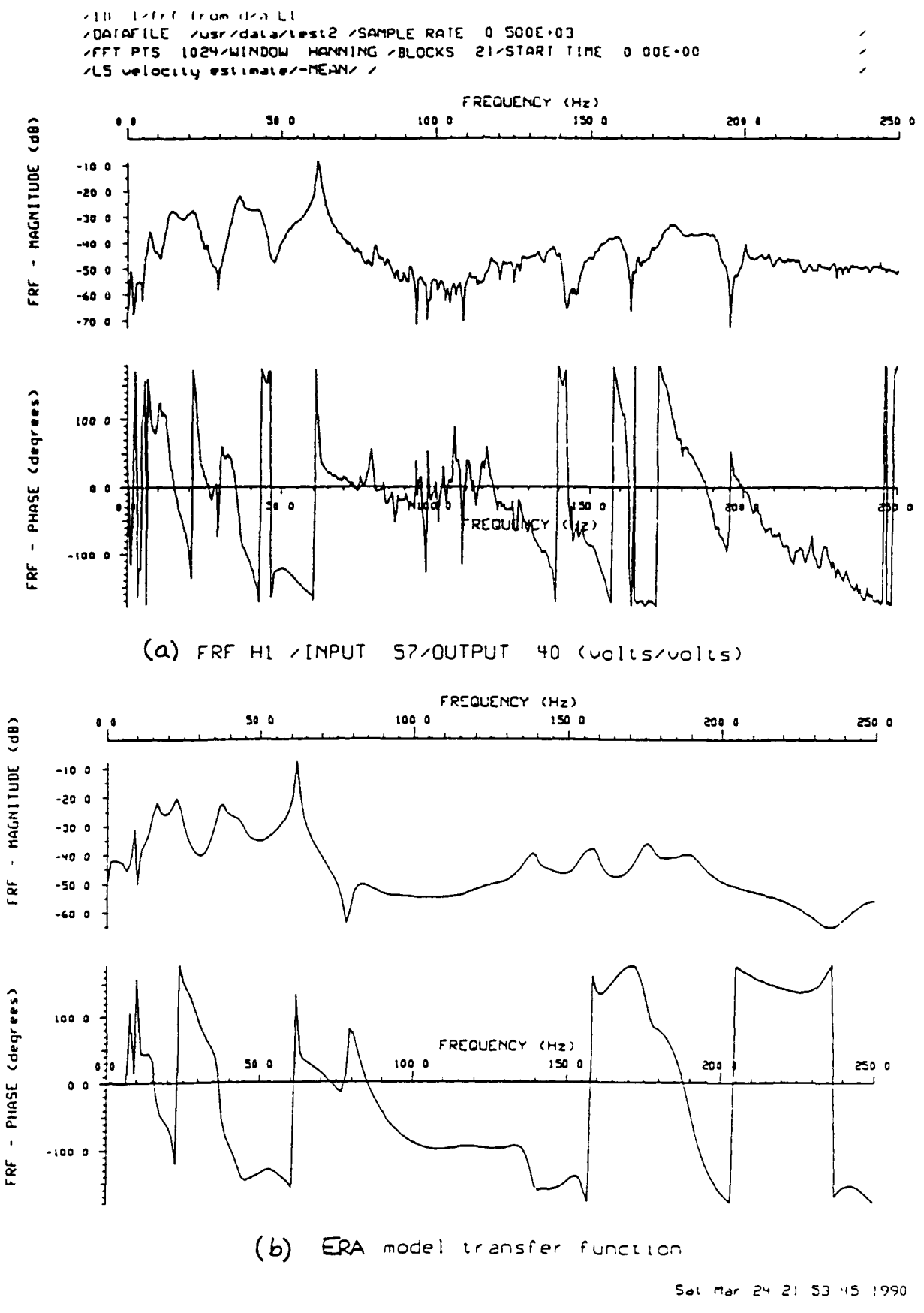

Figure 9. Comparison between FRF data and ERA transfer function shows importance of data integrity.

In late 1988 and early 1989 Harris developed realization software based on the popular Eigensystem Realization Algorithm (ERA) of J.-N. Juang and R.S. Pappa. A comparison between the FRF computed from time data and the transfer function of an ERA state space model is shown in Figure 9. The transfer function is from LPACT number 1 force command to LPACT number 5 velocity estimate.

The interface for the realization software is the Markov block (implulse response) file. The ERA itself is quite resilient, and can produce a model which matches the original impulse response with an arbitrary degree of fidelity, given enough states. As would be expected, one of the secrets to obtaining good state space models with the ERA is to first extract a clean impulse response from the test data, if possible. In the figure it is clear that the best match is obtained in that part of the spectrum which has the best signal to noise ratio.

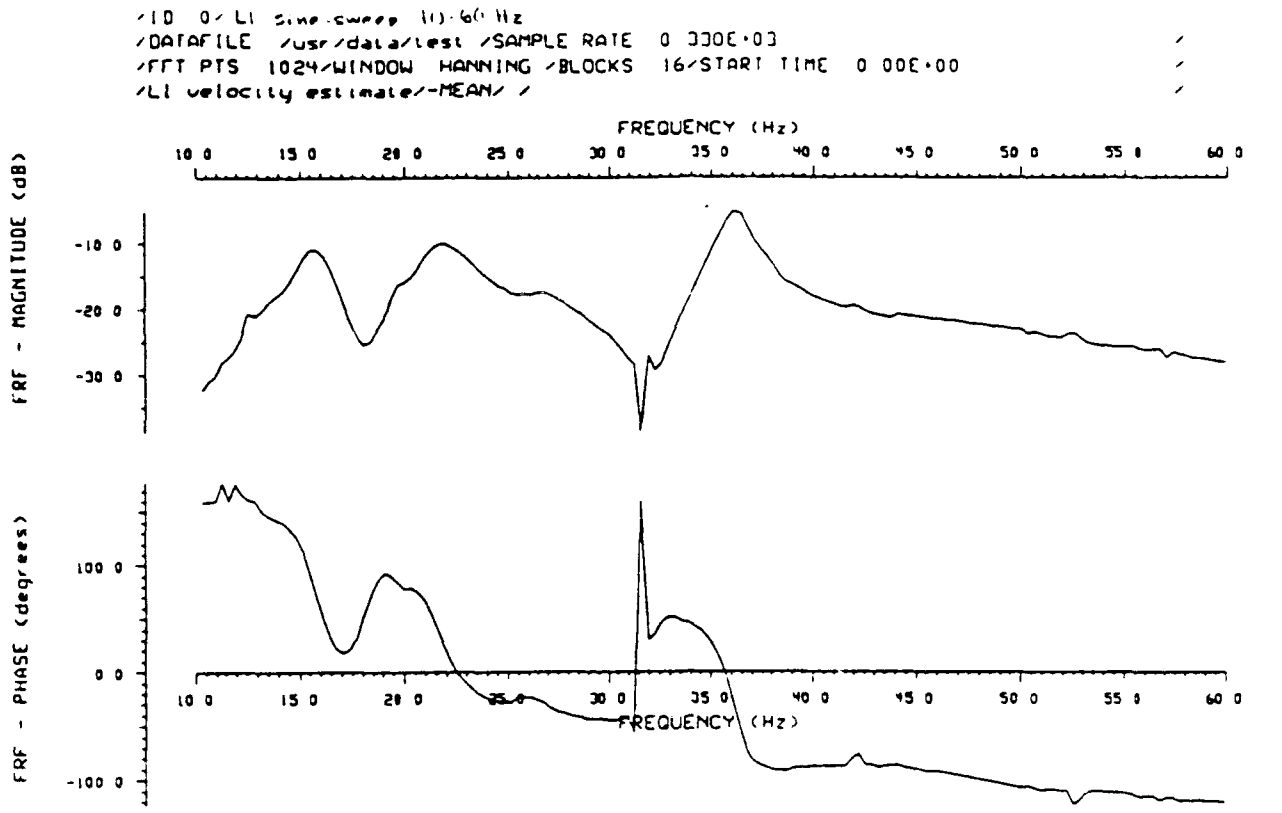

(a) FRF Hi /INPUT 49/OUTPUT 8 (volts/volts)

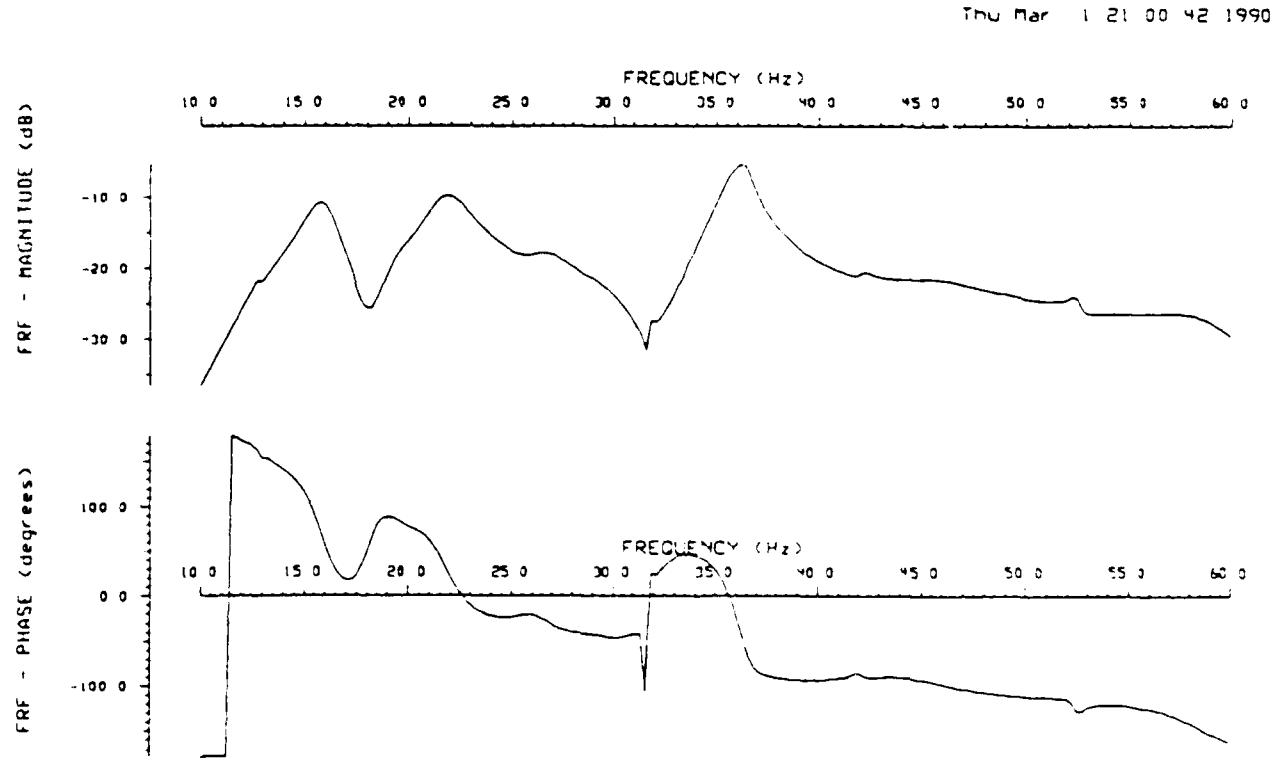

(b) ERA model transfer function

Figure 10. Structural Changes make FEM obsolete. ERA model can be developed quickly for design studies.

In late 1989 two significant structural changes were made to the MHPE. The outer panels were canted slightly to more closely resemble a curved reflector surface. Canting the panels required the replacement of the triangular aluminum plates connecting the inner and outer panels with solid fixtures. The aluminum strips connecting the outer panels to each other were also removed to more realistically emulate a deployabe structure.

In early 1990 the structure and all support equipment was relocated to another building. All of these changes dictated a new round of testing to re-identify the system.

One nagging problem of earlier identification and control experiments was the sample rate; 500 Hertz was near a significant box-beam mode, which was a common cause of instability in high authority discrete time controller testing. 330 Hertz was determined to be a much better sample rate because no higher-frequency modes were excited by square waves at this frequency.

Preliminary wide band tests showed that the structure was now active primarily in the 10 to 60 Hertz band. A sine-sweep test strategy was used to probe this band for detailed identification. A representative FRF, taken with the analog control loops turned off is shown in Figure 10a. Analysis of this and other FRF data concluded that the 61 Hertz mode shape of the old structure had migrated to 36 Hertz. An apparent glitch in the data at approximately 32 Hertz is a frequency modulation artifact of the sine-sweep method. Close inspection shows other glitches spaced at intervals of 10 Hertz which have the same cause.

An inverse FFT program was used on this data to produce an impulse response for the ERA modeling program. Frequency windowing was used to filter the data in the 10 to 60 Hertz band. The transfer function of the resulting model is shown in Figure 10b. Note that the ERA model faithfully reproduces the frequency modulation glitches.

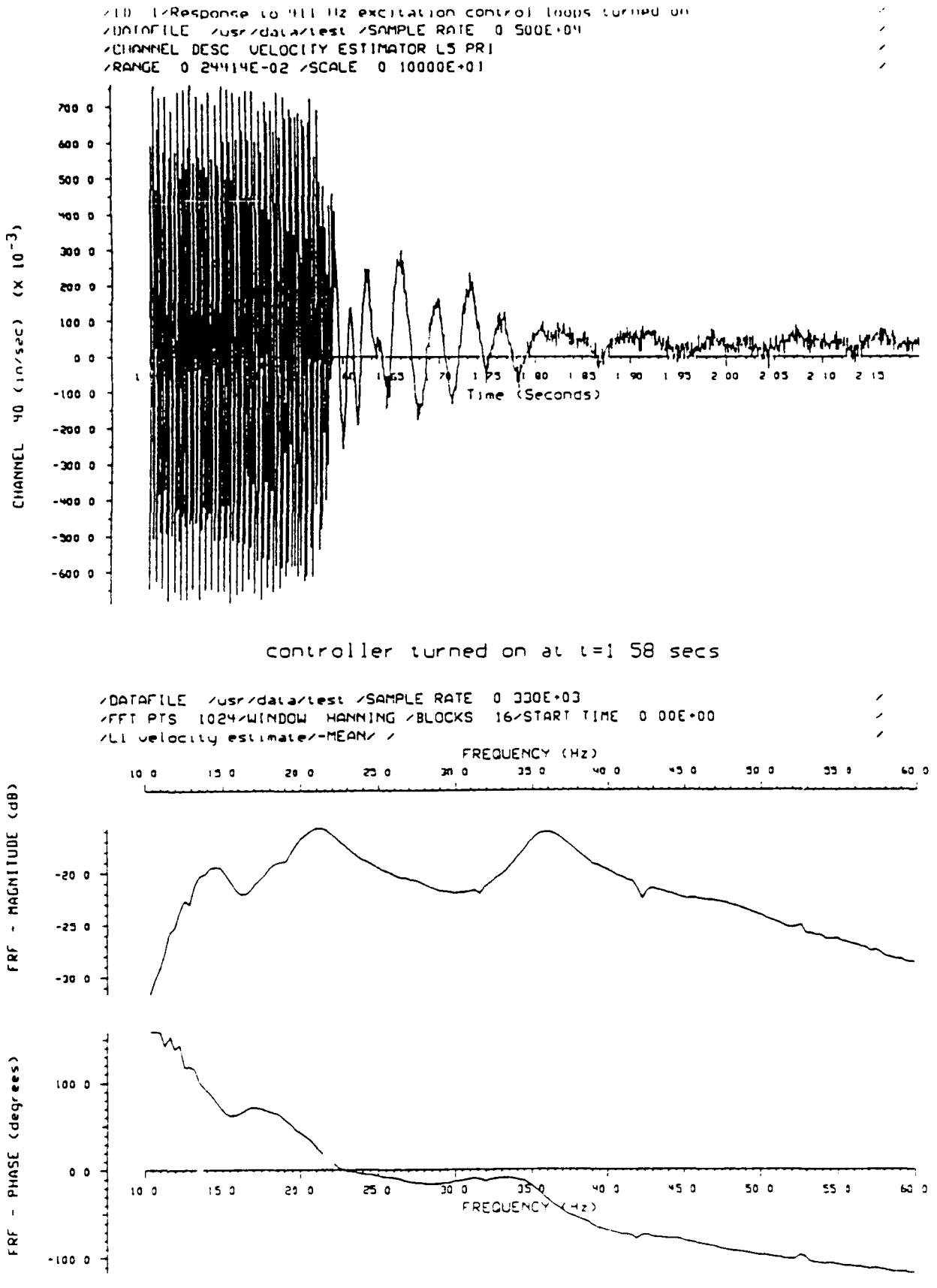

Figure 11. Colocated analog control loops performance illustrated in both time and frequency domain.

CONTROL EXPERIMENTS

Initial test data on the MHPE structure was more than adequate for designing and testing the colocated analog rate feedback loops. Visitors to the MHPE facility are often treated to a "hands on" demonstration of the effectiveness of these control loops. The structure is excited sinusoidally at a modal frequency through one LPACT with the rate feedback loops disabled. One or more LPACT loops are then closed, causing a noticeable reduction in the vibrational level.

The MHPE structure contains many modes above the bandwidth of any discrete time control law implementable on the MCX-5 computer, however the MCX-5 can be used to collect data at very high rates when no discrete time control law is being computed. Figure 11a is a time history of a test such as the one described above. Excitation was supplied to the structure through the LPACT located on hex panel 3 at a frequency of 411 Hertz, and all of the other LPACT analog loops were closed at approximately 1.58 seconds. This particular figure is a plot of the velocity estimate at the LPACT on panel 5. All other LPACT responses are similar.

Plots showing the effect of the analog control loops on the colocated frequency response between 10 and 60 Hertz are shown in Figure 11b. This band is within the realm of discrete time controllers. (Compare this with the open loop FRF in Figure 10a.)

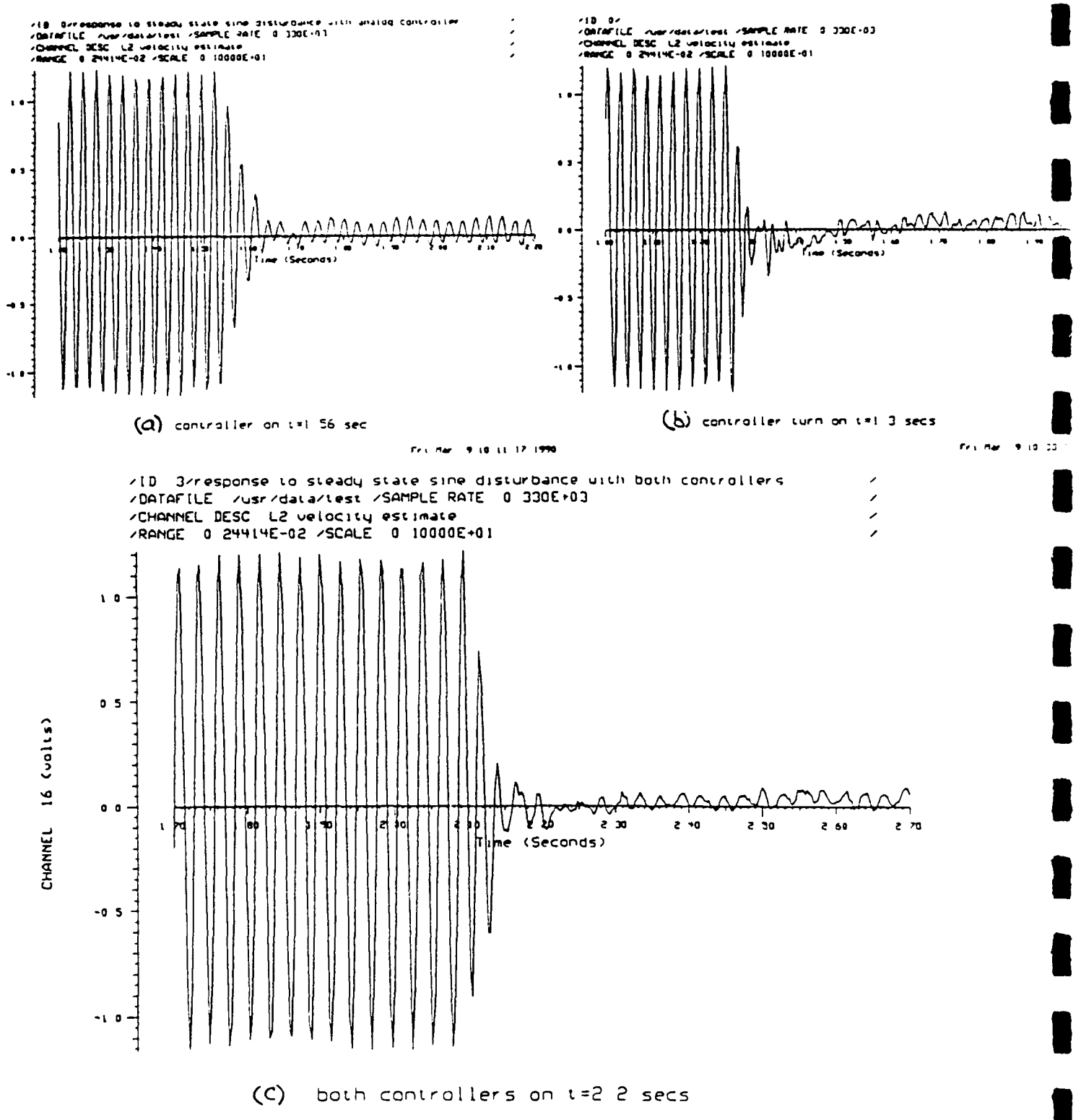

Figure 12. The MHPE hybrid control heirarchy features both performance and fault tolerance.

A simple second order discrete time decentralized controller was designed specifically to suppress the 36 Hertz mode. The goal of this task was to demonstrate that the hybrid controller architecture of the MHPE was stable, cooperative and fault tolerant.

Figure 12a shows the performance of the analog loops operating alone when the structure is excited sinusoidally through LPACT 3. The response of the discrete time loops is demonstrated in Figure 12b. Note that the discrete time controller seems to have slightly more authority than the analog loops. Finally, Figure 12c shows that both the discrete and analog controllers working together have better performance than either operating alone.

COMPARISON OF THE TWO PATHS

	ADVANTAGES	DISADVANTAGES
ANALYTIC APPROACH	• subsystem analysis relates frequencies and modeshapes to physical parameters • structure does not need to exist • simple state space realization	• FEM process is tedious, expensive and error-prone • required modeling fidelity difficult to assess a-priori • real material parameters may differ from handbook values
EXPERIMENTAL APPROACH	• efficient data collection and analysis techniques • mature realization technology (ERA) gives state space model of entire system • guidelines exist for appropriate model order selection	• structure must exist and be instrumented adequately • interaction/relation between subsystems not always clear w/o reference to FEM or substructure tests

THE TWO APPROACHES ARE NOT MUTUALLY EXCLUSIVE. THEY ARE OFTEN COMPLEMENTARY!

Figure 13. Advantages and Disadvantages of each approach to the Modeling Challenge.

Each path (analytical/experimental) to meeting the modeling challenge has advantages and disadvantages, as outlined in Figure 13. Often the control designer must take the analytical approach because the structure does not exist. However when it does exist, the designer is obligated to consider the test data. Certainly, when the structure exists, the two paths are not exclusive. In many respects, they are complementary.

Occasionally a control system must be retro-fit to an existing structure for which a FEM does not exist, or is inadequate. In these cases it can be economical to utilize a direct realization technology, such as the Eigensystem Realization Algorithm (ERA), or other commercial system identification "toolbox".

When using a realization tool, the engineer must still pay attention to the fundamentals of good experimental science. Coherence testing (in the frequency domain) and sanity testing (in the reality domain) have often proven invaluable in distinguishing good data from bad on the MHPE project. When drawing conclusions about continuous time properties of a system, the continuous time properties of the test signals used to generate data must be considered.

THE ACES CONFIGURATION

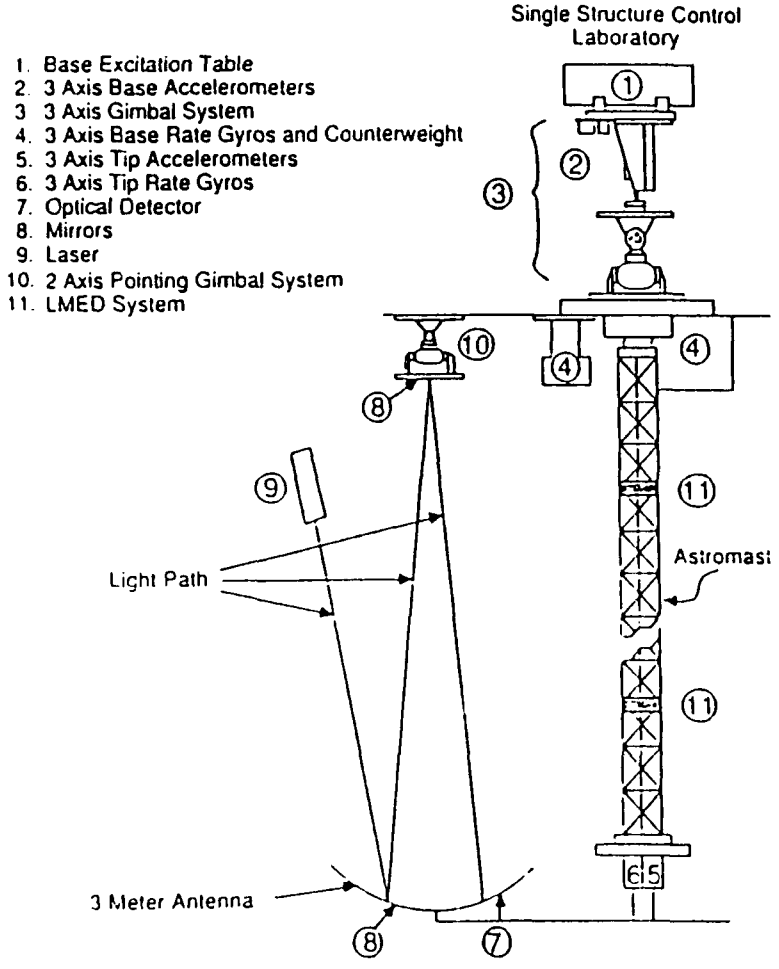

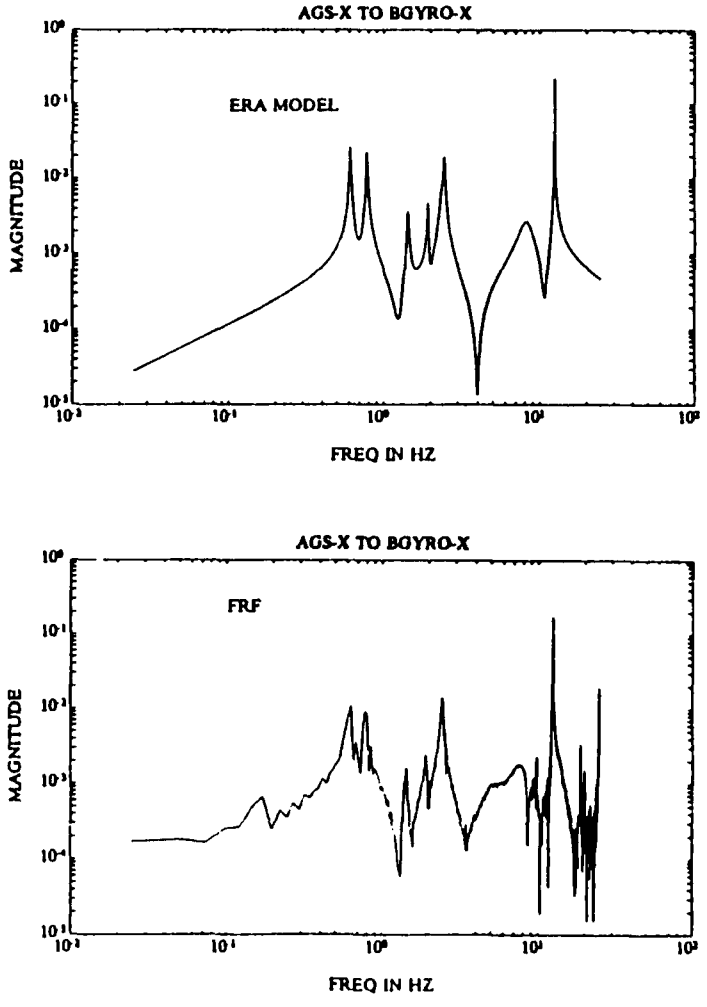

Figure 14. The NASA/MSFC ACES structure provides a case study for modeling in support of control design.

A CASE STUDY IN MODELING FOR CONTROL

Modeling lessons learned on the MHPE were put to good use when Harris controls group members designed controllers for the ACES test structure at Marshall Spaceflight Center as part of NASA's Guest Investigator Program. The physical layout of the ACES structure, shown on the left in Figure 14, is dominated by the 45 foot Astromast, which is suspended from the Base Excitation Table.

A variety of sensors and actuators are available for use in a pointing control system design. One important path is the Automatic Gimbal System X-torque input (AGS-X) to Base Rate Gyro, X-axis (BGYRO-X). Our success in modeling the structure for control design is illustrated on the right in Figure 14, which compares one transfer function of the ERA state space model with the FRF computed from the same history.

As discovered earlier on the MHPE, clean data is essential to generating good realizations. Reference to the FEM supplied by the facility, as well as knowledge of the signal processing, was also very useful in selecting an appropriate model order for the ERA realization.

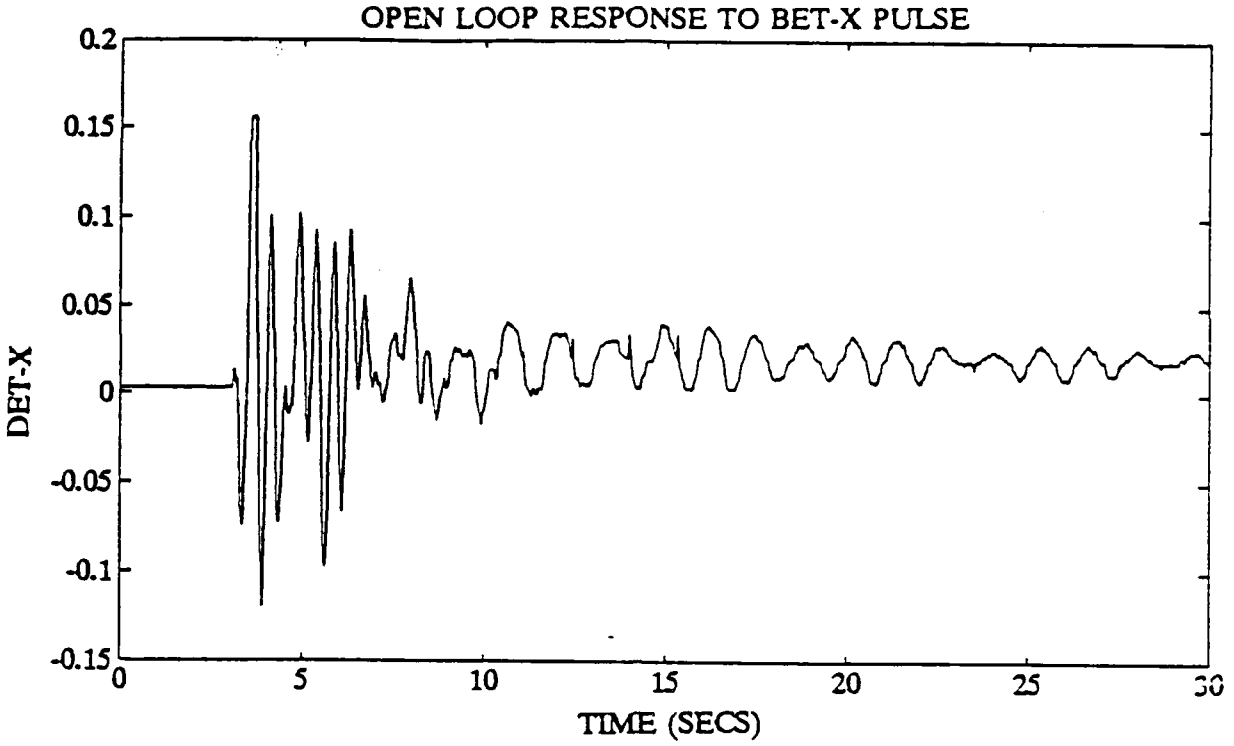

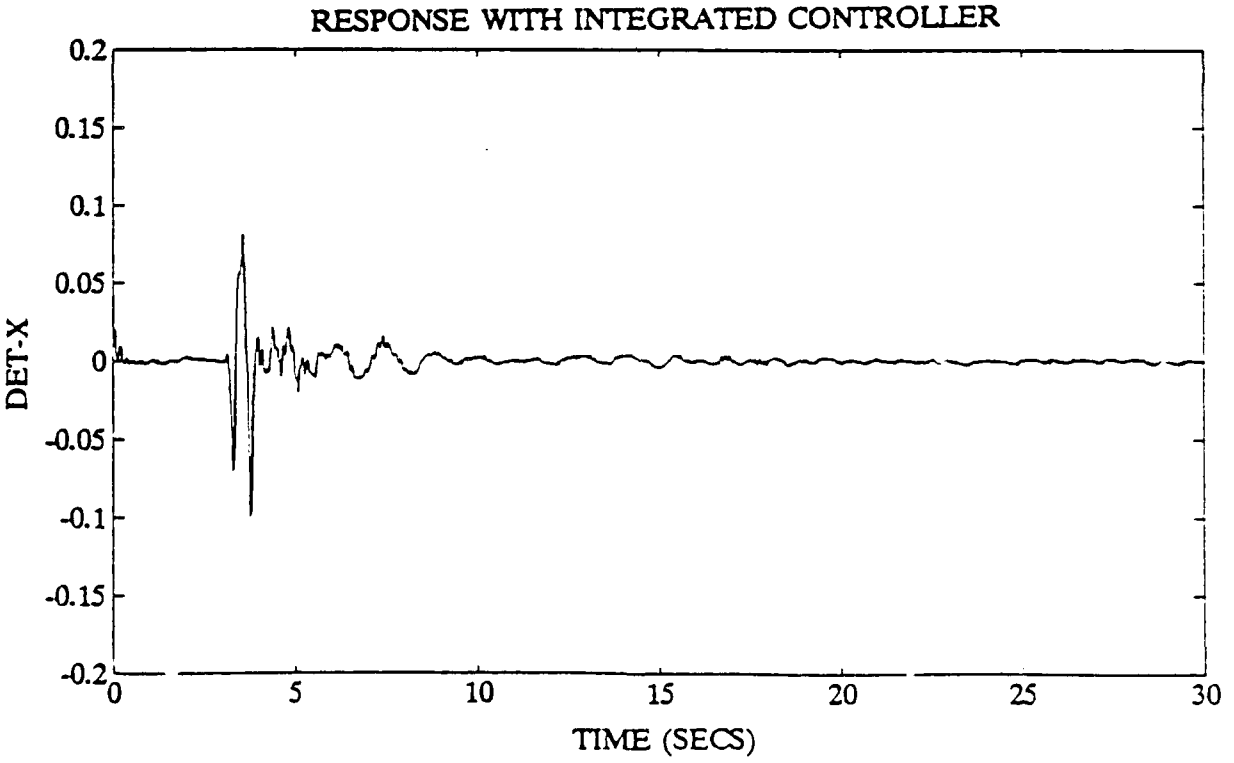

Figure 15. Pulse response of the Harris integrated controller reduces ACES LOS pointing errors.

Thorough knowledge of the model, including its limitations, guided the Harris design team in applying their methodology to obtain a successful integrated control system design. Time histories demonstrating the open and closed-loop response of the system Y-LOS Error are shown in Figure 15. The Harris-designed controller provides greater than 50 dB reduction in LOS bias (mean) error and greater than 9 dB improvement in RMS LOS error about the mean.

The NASA/MFSC Guest investigator experience demonstrates the advantages of the direct, experimental approach to system identification for control design and verification. Analytic methods are greatly enhanced by this approach when actual structural data are available.

Jan. 1990

Four Experimental Demonstrations Of Active Vibration Control For Flexible Structures

Doug Phillips and Emmanuel G. Collins, Jr.

Harris Corporation
Government Aerospace Systems Division
MS 22/4842
Melbourne, FL 32902

Abstract

Many future space missions involving flexible structures may require active vibration control to satisfy mission objectives. Thus, it is important for active control of flexible structures to be practically demonstrated in ground based experiments. These experiments can validate (or invalidate) existing theories and technology and provide directions for future research. This paper discusses four experiments conducted by Harris which successfully demonstrate control of flexible structures. Three of the experiments were conducted in-house at Harris while the fourth experiment involved control design and implementation for the ACES structure at NASA Marshall Space Flight Center. The paper concludes with some remarks on the lessons learned from conducting these experiments.

1. Introduction

Many large space system concepts will require active vibration control systems to satisfy critical performance requirements such as line-of-sight (LOS) accuracy and constraints on rms surface roughness. In order for these concepts to become operational it is imperative that active vibration control be practically demonstrated in ground based experiments.

In regard to theoretical developments these experiments serve a two-fold purpose. First of all, they can validate (or even invalidate) existing theories proposed for the control of flexible structures. Secondly, the insights gained from actual hardware experiments elucidate important issues in practical control design and thus provide needed direction for future theoretical research. For example, based on our experience, it is clear that sampled-data control design and analysis are important (though somewhat neglected) areas of research. In the past, the integration of theory and experimentation has perhaps been lacking in the modern controls community. However, recent trends seem to show that this integration is increasing.

In addition to validating and guiding theory, experimentation also highlights the primary technology issues involved in implementing active control for flexible structures. For example, experiments tend to reveal the importance of sensor and actuator development tailored for flexible structures. Also, the number of design iterations required in the control design portions of these same experiments and the large amounts of data manipulation reveal the need for the continual evolution of efficient and ergonomically sound design environments such as MATLAB and MATRIX$_x$.

This paper discusses four experiments conducted by Harris which successfully demonstrate active vibration control for flexible structures. The first three experiments were conducted in-house at Harris while the forth experiment involved control design and implementation for the ACES structure at NASA Marshal Space Flight Center. The experiments cover a variety of structural configurations, ranging from simple one and two dimensional structures to a complex, multi-paneled optical system.

The primary control synthesis method chosen for the experiments is the Maximum Entropy/ Optimal Projection (MEOP) method. The MEOP method allows for the simultaneous optimal trade-off of four fundamental issues in control design: actuator sizing, sensor accuracy, controller order and robustness versus system performance. The MEOP design equations comprise four coupled matrix equation, which when solved will yield optimal, reduced order controllers that are

robust to parametric plant uncertainties. When the plant is known perfectly and a full order controller is desired, the MEOP design equations reduce to the standard LQG Riccati equations. Further information about the MEOP methodology, such as theoretical development, numerical algorithms and numerical illustrations, are contained in [2–6].

The paper is organized as follows. Section 2 discusses the Pendulum Experiment. The structure is of the form of a 5 meter compound pendulum and was designed as an end-to-end testbed for a linear proof mass actuator and its supporting electronics. Experimental results are shown for two controllers designed to achieve 5% damping in the first two pendulum modes.

The second experiment, the Plate Experiment, discussed in Section 3, exhibits significantly greater dynamic complexity. Here, the structure is a thin, 4 ft. square aluminum plate. The plate is cut at the corners along the diagonals to produce a configuration which yields high modal density and many closely-spaced modes. We discuss the application of MEOP theory to the control design and demonstrate the design capabilities for broad-band vibration suppression via experimental results.

The third test, discussed in Section 4, is based upon the Harris Multi-Hex Prototype Experiment (MHPE) apparatus. This is a large optical reflector structure comprising a seven panel array and supporting truss which typifies a number of generic characteristics of large space systems.

Section 5 discusses control design and implementation for the ACES structure at NASA Marshall Space Flight Center. The ACES structure is a three dimensional beam-like structure to which optics are attached. This structure illustrates many characteristics which are directly traceable to future space flight systems.

The paper concludes in Section 6 with some remarks on the lessons learned from conducting these experiments.

2. The Pendulum Experiment

The Pendulum Experiment testbed [11] was designed to emulate the characteristics of large space structures that exhibit large amplitude, low frequency dynamics. The vibration control aims of the experiment were to deal successfully with significant actuator dynamics and realistic actuator force and stroke limitations while providing specified closed-loop damping of the lower frequency modes. Figure 1 shows a photograph of the testbed and descriptions of its geometry.

The structure is a compound pendulum with parallelogram arrangement designed to constrain the bottom platform to horizontal motion. Table 1 lists the modal characteristics of the structure. The control instrumentation, mounted on the bottom platform, consists of a linear proof mass actuator and a collocated accelerometer. The proof mass actuator was designed to provide large stroke and good low frequency force response. The actuator, as shown in Figure 2.a, employs a magnetically driven reaction mass to provide the control force and incorporates an internal motor compensator to exploit the full capabilities of the device while ensuring that it operated within its force and stroke limits. The motor compensator is designed such that the relative position between the reaction mass and the actuator base tracks input commands to approximately 1 Hz, and the output force of the actuator tracks inputs above 1 Hz. The transfer function for force/command and relative position/command are shown in Figures 2.b and 2.c. The device has a peak force capability of 30 Newtons and maximum stroke of 0.3 meters. Limiters in the motor compensation electronics prevent the reaction mass from impacting the mechanical stops.

The vibration suppression controllers were implemented on a MCX-5 computer operating at a sampling and actuator update rate of 150 Hz. The computer was interfaced to the analog actuator input and conditioned accelerometer output via 12 bit D/A and A/D, respectively. Before sampling, the accelerometer signal was signal conditioned by a single-pole, 1 Hz, low pass filter. This filter was chosen because it provides both anti-aliasing and velocity estimation. A block diagram of the Pendulum Experiment is shown in Figure 3.

The experimental goals were to utilize the actuator to achieve at least 5% damping in the first two pendulum modes while not destabilizing the very lightly damped tube bending modes (particularly the 27 Hz mode). The design model of the plant is a 19th order model that included the modes of Table 1, a fourth order actuator model and a third order accelerometer/signal conditioner model. Here we summarize the experimental results for open loop dynamics and for closed loop performance using a positive real control design and a MEOP design.

For comparison, Figure 4.a shows open-loop excitation and free decay. The excitation consists of five periods of sinusoid at the first mode frequency. For the same excitation, Figure 4.b shows closed-loop damping with a positive-real controller design. The positive real design achieved 5% damping for the first mode and just under 5% damping for the second pendulum mode. However, the positivity design constraint proved to be difficult to impose at the low frequencies while ensuring stabilization of the higher frequency bending modes; this necessitated a relatively high order

controller.

To see if the difficulties could be alleviated, Maximum Entropy/Optimal Projection (MEOP) design theory was used to obtain a sixth order controller. The design attained 15% damping in the first pendulum mode, over 5% damping in the second pendulum mode, and experienced no difficulty in stabilizing the higher bending modes. These test results correlated very well with the analytically predicted values. Figure 5 shows the test results using the MEOP controller with an input excitation consisting of two superimposed sinusoids having frequencies equal to those of the first and second pendulum modes.

The above test successfully demonstrated selective suppression of low frequency modes in the presence of simultaneous stabilization of higher frequency modes in the presence of significant actuator dynamics and digital computer sampling effects. Neither of the designs stressed the actuator beyond its force and stroke limits, nor resulted in saturation of the controller states due to the finite word length of the computer.

3. The Plate Experiment

In contrast to the pendulum apparatus, the plate experiment [11] was designed to explore broad-band vibration suppression of an inherently two dimensional structure exhibiting numerous, high frequency, closely space modes. Figure 6.a shows the overall apparatus. The structure is a four foot square, one eighth inch thick, vertically suspended aluminum plate having seventeen inch diagonal cuts from the corners toward the center. Figure 6.b indicates the finite element mesh, where locations on the plate are referred to by finite element model node numbers. From both test and analysis there are approximately thirty vibrational modes below 100 Hz, many of them occurring in closely spaced groups due to the symmetry of the structure.

There are four control actuators and one disturbance actuator mounted on the plate surface. Each actuator is a microshaker especially developed for this experiment to achieve the precise force resolution over a bandwidth of 1000 Hz. The microshaker consists of an independently suspended solenoid coil and an iron stud which is attached to a rare earth magnet mounted to the plate. The iron stud is suspended inside that solenoid coil which maintains a constant flux density inside the solenoid thus eliminating the output force vibration due to the plate (magnet) vibrations. This device has a maximum force output of 0.2 pounds, one inch stroke and a flat frequency response from D.C. to 100 Hz. Vibration sensors consist of eleven piezoelectric accelerometers (four that

are collocated with microshakers) with a flat frequency response form 1 to 2000 Hz. The locations of the actuators and sensors, which have been selected according to observability/controllability considerations, are shown in Figure 6.b.

On-line digital control is exercised via the MCX-5 Data Acquisition and Control Computer (DACC) which was also utilized for the Pendulum Experiment. The MCX-5 has the capability to sample up to 128 channels at a 1 MHz sampling rate, store the sampled data on disk, implement the control algorithm, load and strobe the eight D/A converters (expandable to 40 without software changes) and compute the performance while providing real time graphic displays.

The main experimental objective is to suppress total rms deviation from flatness (over the plate's surface) over a frequency range of 10 to 120 Hz while the disturbance actuator imposes a broad-band random input that has nearly constant power spectral density from 10 to 100 Hz.

When designing a discrete time closed loop controller for the plate we observed a large number of high frequency, high energy modes that would cause an instability when the controller was turned on. The instability of these modes was due to the sample delay time of the computer (the time period from when measurements are sampled to when the D/A's are strobed). These modes were excited by the transients introduces by the controller turn-on and the quantization of the D/A outputs. Several tests were run by rolling-off the controller authority at different frequencies, and predictably the frequencies of the instabilities were proportional to the controller bandwidth and the sample delay time.

To provide the required control authority in the 10 to 120 Hz band with a sampled delay time of 0.5 mSec and not destabilize the high frequency modes, a continuous-time decentralized controller was implemented. The decentralized loops provided enough damping in the high frequency modes to allow for a higher authority, discrete-time, centralized control algorithm. Both positive real and MEOP centralized control designs were tested, but only the MEOP results are described here. The MEOP theory essentially computes the optimal fixed form controller consisting of a dynamic compensator of fixed order in parallel with direct output feedback compensation. To obtain a simple implementable initial design, the MEOP design was constrained to be an output feedback system. Subsequent LQG designs studies showed only a marginal 20% performance improvement over MEOP design. Thus, in the class of all linear dynamic compensators, the MEOP direct output feedback design is near optimal for this problem.

Figure 7 shows test data for open-loop and closed-loop response PSD's at the disturbance location (Figure 7.a) and at a collocated actuator location (Figure 7.b). These results illustrate that at both collocated and noncolocated accelerometer positions, one has more than an order of magnitude reduction in peak amplitudes for most modes. Evidently the controller imposes a broad-band damping augmentation. Computing overall rms surface distortion using all eleven accelerometers, one obtains 15 dB reduction in the closed-loop response relative to the open-loop response.

4. The Multi-Hex Prototype Experiment

The Multi-Hex Prototype Experiment [1,11,12] combines features of both the Pendulum and Plate Experiments by exhibiting the joint dominated characteristics of the Pendulum along with the modal complexity of a two dimensional structure such as the Plate. The complexity of the Multi-Hex Prototype Experiment (MHPE) emulates the generic properties of large space structure concepts pertaining to high frequency RF or optical applications. The MHPE contains five major subsystems: the structure, vibration platform, actuators and sensors, the interface electronics, and the MCX-5 Data Acquisition and Control Computer.

The structure is composed of a Multi-Hex panel array mounted on top of a six-member truss which in turn is mounted on top of a vibration platform. As shown in Figure 8, the Multi-Hex panel array is a seven panel graphite/epoxy array wherein each panel is a hexagonal box truss measuring 4.3 feet across. The whole array weighs 177 pounds and is 12.8 feet across. On top of the Multi-Hex panel array a tripod tower supports the secondary reflector structure. The six-member truss consists of six aluminum tubes which attach to the array at three locations (every other corner of the center panel) and to the vibration platform. The structure also contains forty-two aluminum honeycomb facets which emulate a carbon-carbon mirror surface in weight and stiffness. A finite element model has been created for this MHPE structure. From this model fifty modal frequencies and modeshapes have been extracted. Typical modeshapes may be categorized into several groups. One group of modeshapes involves bending of the outer panels with little motion of the center panel. These modes depend on the stiffness of the joints that connect the outside panels to the center panel. Another group of modes involves significant bending of both the array panels and the six-member support truss. Finally there are numerous highly localized modes wherein a subset of the panels vibrate while the remaining panels are nearly quiescent.

The vibration platform consists of a five foot diameter, one inch thick aluminum table to which

three vertically directed disturbances can be applied (to simulate aft body disturbances from the spacecraft) by electrodynamic shakers. Mounted in tandem with each shaker is an air bag isolator with associated bracketry to support the weight of the entire structure and to isolate it from ground vibration.

The actuators and sensors consist of six Linear Precision Actuator (LPACT) units and twenty-four inertial grade accelerometers. The LPACT device, as shown in Figure 9, is a bearingless, linear voice coil actuator designed, fabricated, and tested at Harris Corporation [7]. Each LPACT utilizes a proof mass mounted accelerometer to close a force control loop which serves to override nonlinearities and to reduce the effect of the restraint flexure mass resonance. Without the force compensation, a second order, very lightly damped resonance at 9 Hz is present in the transfer function from voltage input to force output. With the force compensation this actuator has a flat response of 5 to 500 Hz (see Figure 10). This device can provide a maximum force of five pounds and has a twenty micro-pound force resolution. With each LPACT there is an externally mounted collocated accelerometer for the implementation of a decentralized (using collocated actuator/sensor only) structural control loop and/or a centralized (utilizing all of the actuators and sensors) control loop. Each accelerometer has one micro-g resolution with a flat response from 0 to 300 Hz. The locations of the actuators and sensors, shown in Figure 11, were determined by evaluating the modeshapes determined from the finite element model and considering only practical mounting locations.

The interface electronics consist of the signal conditioning electronics, force loop compensation electronics, decentralized control electronics, LPACT interface electronics, and the servo amplifiers. The signal conditioning, force loop compensation and decentralized control electronics, and the LPACT interface electronics reside in the Structural Interface Assembly (SIA) and the servo amplifiers reside in the Servo Amp Assembly (SAA). The signal conditioning electronics scale the sensor outputs so that they are in the measurement range of the A/D converter of the DACC; they also filter the signals to reduce aliasing effects. The force loop electronics takes the proof mass mounted accelerometer measurement and provides the electronic compensation required to generate a current command to close the force loop. The decentralized control electronics use the collocated accelerometer measurement input and provide up to eighth order compensation, which generates a command to close the decentralized control loop. The LPACT interface electronics sum the current commands from the force loop, decentralized loop and the command from the centralized control loop. The current command from the LPACT interface goes to the servo amplifier

which drives the LPACT unit.

The MCX-5 computer described briefly in the sections on the Pendulum and Plate Experiments performs the data acquisition and control required to close the centralized vibration suppression control loop during a controls experiment. This computer is used to correlate the test data with the modeling, analysis and simulation results.

The design goals of this experiment are to reduce the mirror panel dephasing and line of sight (LOS) error by 30 dB. The preliminary state space plant model contains the first twenty modes of the structure.

The first controllers successfully implemented were a set of decentralized collocated continuous-time controllers. To implement these controllers the Hybrid Accelerometer, a special type of sensor, was designed and fabricated. The Hybrid accelerometer was designed to take advantage of the high accuracy of the servo accelerometer (QA-700) and the high bandwidth of a piezo electric accelerometer (PCB 303A). These two accelerometer measurements are electronically combined to provide an acceleration measurement which has a flat frequency response from DC to 5 KHz. With LPACT dynamics flat from 5 to 500 Hz and hybrid accelerometer dynamics which are flat from DC to 5KHz a relatively simple controller can be designed that is positive-real up to 1000 Hz. These loops add damping to the unmodeled high frequency modes that can potentially destabilize sample-data controllers. Figures 12 and 13 show the open and closed loop transfer functions. One should observe the high degree of attenuation of the high frequency modes (modes above 120 Hz).

This decentralized control system architecture provides a high degree of fault tolerance. That is, if any of the actuators and sensors fail, the remaining actuator/sensor pairs will provide reduced but stable vibration attenuation performance. Also, since the loops are independent of each other synchronization during turn on is not required.

Since the addition of the tower, work has begun on designing 6 input-6 output dynamic compensators. These compensators will provide a high degree of vibration attenuation for modes whose frequencies are less than 120 Hz. The initial compensator design will concentrate particularly on attenuating the mode at ∪5.7 Hz, a wave number 3 mode in which each panel vibrates out of phase with its nearest neighbor.

5. The ACES Experiment*

* The description of the ACES Testbed is taken primarily from [8].

The ACES experimental testbed is located at NASA MSFC. The basic test article is a deployable, lightweight beam, approximately 45 feet in length. The test article is a spare Voyager Astromast built by ASTRO Research, Inc. It was supplied to MSFC by the Jet Propulsion Laboratory (JPL). The astromast is extremely lightweight (about 5 pounds) and is very lightly damped. It is constructed almost entirely of S-GLASS. It is the flight backup Voyager magnetometer boom.

The Astromast is a symmetric beam which is triangular in cross section. Three longerons form the corners of the beam and extend along its full length unbroken. The cross members, which give the beam its shape, divide the beam into 91 sections each having equal length and mass and similar elastic properties. When fully deployed, the Astromast exhibits a longitudinal twist of approximately 260 degrees.

The test article can be reconfigured from this basic form to any of several different configurations. The ACES configuration (Figure 14) consist of the antenna and counterweight legs appended to the Astromast tip and the pointing gimbal arms at the Astromast base. The addition of structural appendages creates the "nested" modal frequencies characteristics of LSS. Overall, the structure is very flexible and lightly damped. It contains many closely spaced, low frequency modes (more than 40 modes under 10 Hz).

The precise motion of the BET is obtained by supplying a commanded voltage input to the BET servo control system. The BET movements are monitored by the directional feedback electronic deflection indicators which are fed back to the servo controllers. The servo controllers compare the commanded input voltage to the electronic deflection indicators and automatically adjust the position of the BET. The closed loop controller allows any type of BET movement within the frequency limitations of the hydraulic system. In this experiment the disturbances are chosen to be position commands to the BET.

The Image Motion Compensation (IMC) System consists of a 5-mW laser, two 12-inch mirrors, two pointing gimbals, an analog servo controller a four quadrant detector and associated electronics, and two power supplies. Figure 14 shows the location of each of the components of the IMC system. The goal of the control d_sign is to position the laser beam in the center of the detector. The detector and pointing gimbals are each positioned on the end of a flexible appendage for the purpose of increasing the difficulty of the control problem. The lack of information about the appendage motion also adds complexity to the controller design (i.e., there is no accelerometer or gyro at the location of the gimbals or the detector).

In addition to the two IMC gimbals the control actuators also include the Advanced Gimbal System (AGS), a precision, two-axis gimbal system designed for high accuracy pointing applications, which has been augmented with a third gimbal in the azimuth. The gimbal system provides torque actuation at the base of the Astromast. The AGS receives commands from the control algorithm (implemented on an HP 9000 via the COSMEC data acquisition system) in the form of analog inputs over the range of -10 to +10 volts. This saturation represents a current limit of 27 amps which is built into the AGS servo amplifier as a protective measure. Because the AGS servo amplifier outputs a current which causes an applied torque proportional to the current, the control algorithms used in the COSMEC 1 must be designed to produce torque command signals.

The AGS gimbal torquers, with the power supply and servo amplifiers used in the SSC laboratory, can generate 37.5 ft-lbs of torque over an angular range of approximately $\pm$ 30 degrees. The azimuth torquer is capable of generating 13.8 ft-lbs over an angular range of $\pm$ 5 degrees. It can, however, be set manually to allow the $\pm$ 5 degrees of rotation at any position about the 360 degrees of azimuth freedom. This allows the test article to be rotated to any position desired without remounting.

Linear Momentum Exchange Devices (LMEDs) provide a collocated sensor/actuator pairs which apply forces and measure the resulting accelerations. Each LMED package contains two LMEDs having orthogonal axes, two accelerometers, and two LVDTs (Linear Variable Displacement Transducers). The two LMED packages are positioned at intermediate points along the ASTROMAST, where these points were selected to maximize the actuation capability. Each LMED package is aligned with the X and Y axes of the laboratory reference frame.

The LMED applies a force to the structure in a linear manner and measures the resulting acceleration at the actuator location. Each LMED consists of a linear permanent magnet motor whose magnet functions as a proof mass. Force is applied to the structure as a reaction against this proof mass. The magnet assembly travels along a single shaft on a pair of linear bearings. The coils of the motor consist of a hollow voice coil which extends inside the magnet assembly from one end. The magnet assembly then moves along the shaft with respect to the fixed coils. The magnet is constrained on each end by a bracket which provides a small centering force to the proof mass. A linear accelerometer is mounted in line with the shaft. An LVDT is utilized to measure the position of the proof mass with respect to the LMED assembly.

In addition to the two-axis detector associated with the IMC System and the accelerometers

and LVDT's associated with the LMEDs, the measurement devices include three-axis rate gyros at the tip and base as well as three-axis accelerometers at the tip and base. However, since the three-axis rate gyros at the tip are not available for controller implementation we will describe only the remaining measurement devices.

The rate gyros at the base are Apollo Telescope Mount (ATM) Rate Gyros and are mounted on the faceplate of the engineering gyro packages. They are designed to measure small angular rates very precisely. The output signals of the ATM rate gyro packages are $\pm$ 45 volts analog and are handled by the analog to digital converter card of the COSMEC 1 systems where they are converted to 12-bit binary words. The ATM rate gyro packages require a warmup period of approximately 40 minutes. Each package requires 1.5 amps during warmup and then 1.25 amps after stabilization; both at 28 Vdc.

The accelerations at the base and tip of the ASTROMAST are measured by the two identical three-axis accelerometer packages. The accelerometer outputs are input to the computer system. The accelerometers provide resolution finer than 0.0001 g and a dynamic range of $\pm$ 3 g with a bandwidth of 25 to 30 Hz. They require approximately 20 minutes for warmup, during which time each package requires 1.2 amps at 28 Vdc. After warmup the power requirement reduces to about 0.9 amp per package. The accelerometer electronics are included on board the instrument package.

The signals from the accelerometers are different from the ATM rate gyros. Two channels are required for each of the degrees of freedom of the accelerometer package, i.e., six channels per accelerometer package. One channel of each pair carries a 2.4-kHz square wave synchronization signal, and the other channel carries the acceleration information. Zero acceleration is represented by a signal identical to that of the synchronization channel, positive acceleration by an increase in frequency, and negative acceleration by a decrease in frequency as compared to the synchronization channel. As in the cases of the other instruments, these signals are monitored by a hardware card in the COSMEC system.

As mentioned previously the computer system consists at an HP 9000 digital computer interfaced with the COSMEC Input/Output system. The computer system is responsible for imputing, scaling, processing, plotting, storing, and outputing all the LSS GTF data. The HP 9000, COSMEC, vector processor, and faster HP 9000 CPU (Central Processor Unit) should provide sufficient computing power to satisfy the SSC facility needs for the next few years.

The HP 9000 performs the control algorithm, data storage, real-time plotting and the strapdown algorithm (described in the next section). The HP 9000 is a 32-bit machine with an 18-MHz clock rate. It includes an HPIB interface card, two 16-bit parallel interface cards, 512 Kbytes of extra memory, and a floppy disc drive. The benchmark test times for processing the present control and strapdown algorithms, plotting, and storage are .010 to .013 milliseconds.

The COSMEC is a highly modified AIM-65 microcomputer system used for I/O processing. The primary purposes of the COSMEC are to process the sensor inputs, to provide force and torque commands for the actuators, and to off-load control and sensor data to the computer system. Currently, the COSMEC performs these tasks with 25 sensor inputs and nine actuator outputs, while maintaining a 50-Hz sampling rate. The cycle time for COSMEC operation is approximately 5 milliseconds. This provides a margin of 10 percent relative to the 20 millisecond sampling period. The margin will be substantially increased when the new HP CPU is incorporated into the computer system.

In our control design and implementation we used 4 control inputs and 4 measurement outputs. The inputs were the X and Y torques of the IMC gimbals and the X and Y torques of the AGS gimbals. The measurements consisted of the X and Y detector (DET) outputs and the X and Y base gyro (BGYRO) outputs.

A finite element (FE) model was supplied by NASA MSFC and was evaluated by comparing single-input single-output (SISO) bode plots generated from the FE model with frequency response functions (FRFs) generated from input-output data obtained in actual hardware testing. From this evaluation we determined that the FE model was sufficient for preliminary control system design and analysis but is inadequate for the design of implementable controllers. The FRFs also revealed weak interaction between many of the sensor-actuator pairs. In the final analysis, we concluded that near optimal performance could be achieved by designing decentralized controllers for the following four loops:

(*i*) IMC$-y$ to DET$-y$

(*ii*) IMC$-x$ to DET$-x$

(*iii*) AGS$-x$ to BGYRO$-x$

(*iv*) AGS$-y$ to BGYRO$-y$.

The Eigensystem Realization Algorithm [9,10] was used to generate control design models for the four loops and reduced-order controllers were designed to improve line-of-sight performance. A significant increase in performance was achieved as illustrated by Fig. 15.

6. Conclusions

These experiments have demonstrated successful control system design and implementation for flexible structures and have provided validation of the Maximum Entropy/Optimal Projection approach to controller design. Based on our experience with these experiments we make the following remarks and recommendations for future development in the theory and technology associated with active control for flexible structures.

(*i*) For complex structures finite element models will probably not be sufficiently accurate for designing implementable controllers. Thus identification tools (such as the Eigensystem Realization Algorithm) need to be further developed to increase their accuracy and efficiency in producing models of flexible structures.

(*ii*) Actuator and sensor dynamics can be a very influential factor in control design. It is very important to develop sensors and actuators with dynamic characteristics tailored to achieving high performance for a given structure (or class of structures).

(*iii*) Sampled-data issues can also be very influential factors in control design although these issues are somewhat neglected by modern control theories. Much more attention should be given to sampled-data issues by control theoreticians.

(*iv*) Design of implementable controllers requires numerous iterations and the manipulation of large amounts of data. This necessitates the continual evolution of efficient and ergonomically sound design environments such as MATLAB and MATRIX$_x$.

(*v*) Relatively simple controllers (i.e., low order and/or decentralized) controllers can provide significant performance improvement.

References

1. D. C. Hyland, "An Experimental Testbed for Validation of Control Methodologies in Large Optical Structures," in *Structural Mechanics of Optical Systems II*, pp. 146–155, A. E. Hatheway, ed., Proceedings of SPIE, Vol. 748, Optoelectronics and Laser Applications Conference, Los Angeles, CA, January 1987.

2. D. S. Bernstein and D. C. Hyland, "Optimal Projection for Uncertain System (OPUS): A Unified Theory of Reduced-Order, Robust Control Design," in *Large Space Structures: Dynamics and Control*, S. N. Atluri and A. K. Amos, eds. Springer-Verlag, New York, 1988.

3. D. C. Hyland and D. S. Bernstein, "The Optimal Projection Equations for Fixed-Order Dynamic Compensation," *IEEE Trans. Autom. Contr.*, Vol. AC–29, pp. 1034–1037, 1984.

4. D. S. Bernstein and S. W. Greeley, "Robust Controller Synthesis Using the Maximum Entropy Design Equations," *IEEE Trans. Autom. Contr.*, Vol. AC–31, pp. 362–364, 1986.

5. D. S. Bernstein, L. D. Davis and S. W. Greeley, "The Optimal Projection Equations for Fixed-Order, Sampled-Data Dynamic Compensation with Computation Delay," *IEEE Trans. Autom. Contr.*, Vol. AC–31, pp. 859–862, 1986.

6. S. Richter and E. G. Collins, Jr., "A Homotopy Algorithm for Reduced Order Compensator Design Using the Optimal Projection Equations," *Proc. 28th IEEE Conf. Decis. Contr.*, pp. 506–511, Tampa, FL, Dec. 1989.

7. D. C. Hyland and D. J. Phillips, "Development of the Linear Precision Actuator," *Proc. 11th Annual AAS Guid. Contr. Conf.*, Keystone, CO, January 1988.

8. R. D. Irwin, V. L. Jones, S. A. Rice, D. J. Tollison and S. M. Seltzer, *Active Control Technique Evaluation for Spacecraft (ACES)*, Final Report to Flight Dynamics Lab of AF Wright Aeronautical Labs, Report No. AFWAL–TR–88–3038, June 1988.

9. J. N. Juang and R. S. Pappa, "An Eigensystem Realization Algorithm for Modal Parameter Identification and Model Reduction," *J. Guid. Contr. Dyn.*, Vol. 8, pp. 620–627, 1985.

10. J. N. Juang and R. S. Pappa, "Effects of Noise on Modal Parameters Identified by the Eigensystem Realization Algorithm," *J. Guid. Contr. Dyn.*, Vol. 9, pp. 294–303, 1986.

11. S. W. Greeley, D. J. Phillips and D. C. Hyland, "Experimental Demonstrations of Maximum Entropy, Optimal Projection Design Theory for Active Vibration Control," *Proc. Amer. Contr. Conf.*, pp. 1462–1467, Atlanta, GA, June 1988.

12. D. C. Hyland and E. G. Collins, Jr., "A Robust Control Experiment Using an Optical Structure Prototype," *Proc. Amer. Contr. Conf.*, pp. 2046–2049, Atlanta, GA, June 1988.

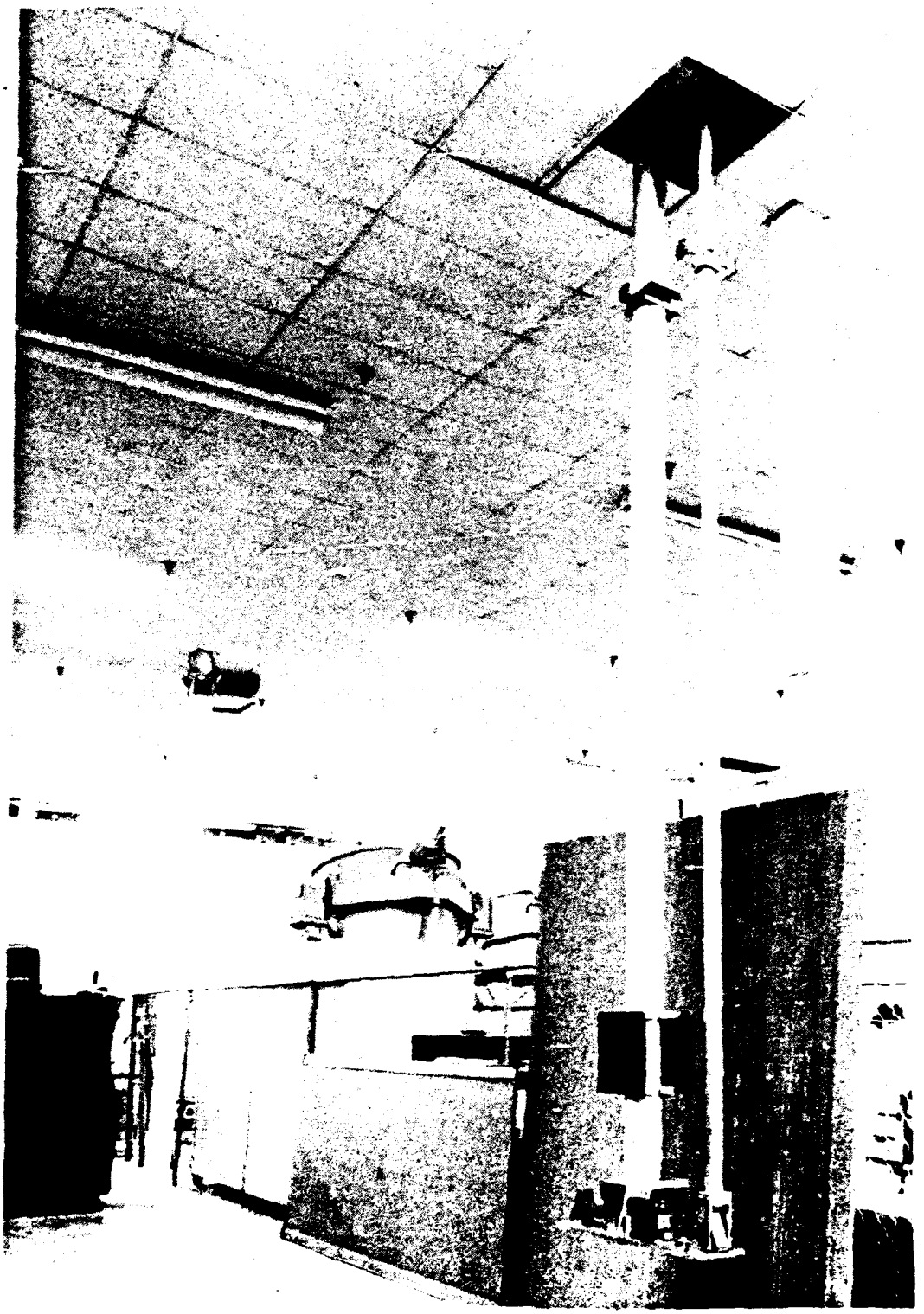

Figure 1. Pendulum Experiment Apparatus and Description.

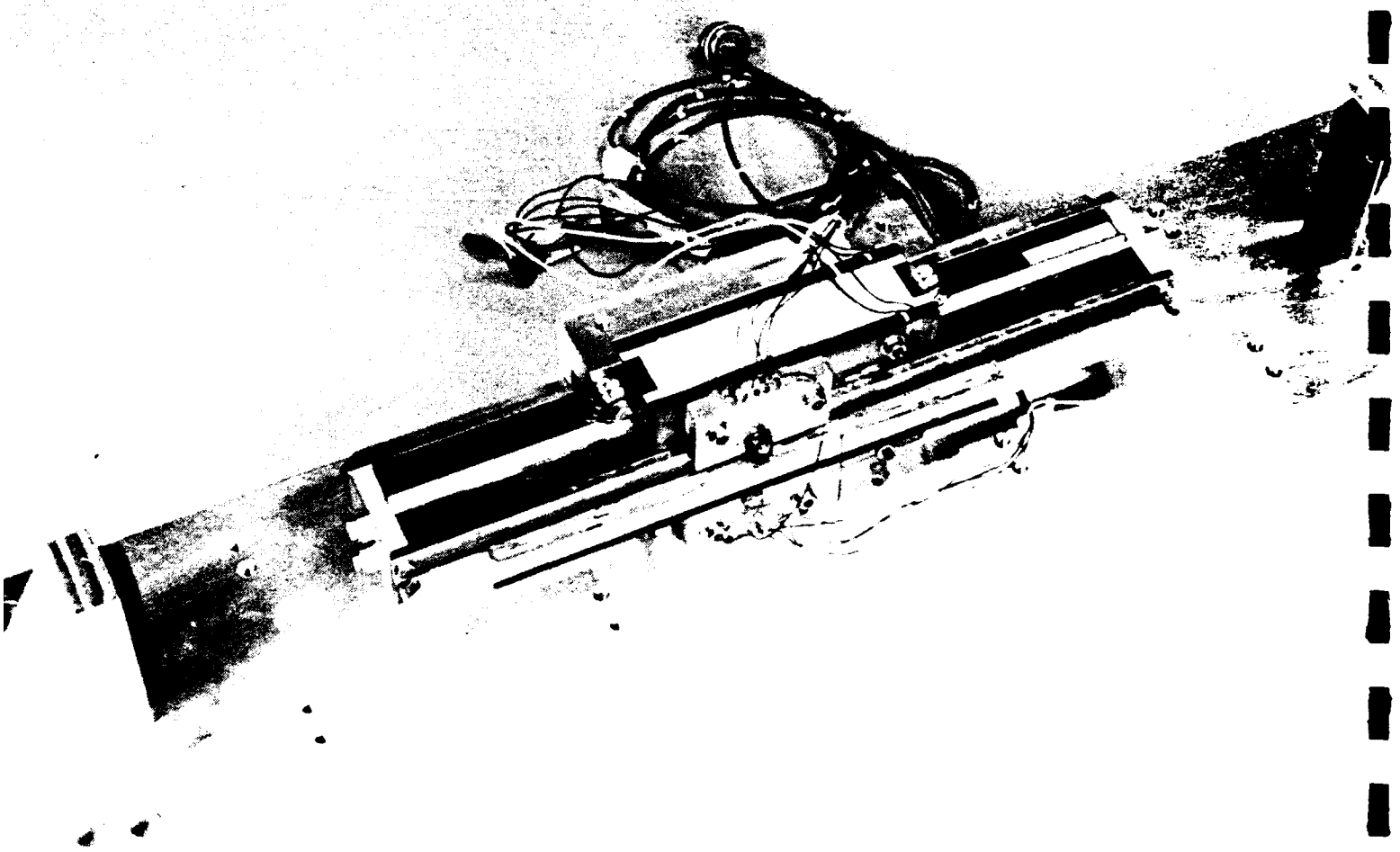

Figure 2a. Linear Proof Mass Actuator of Pendulum Experiment

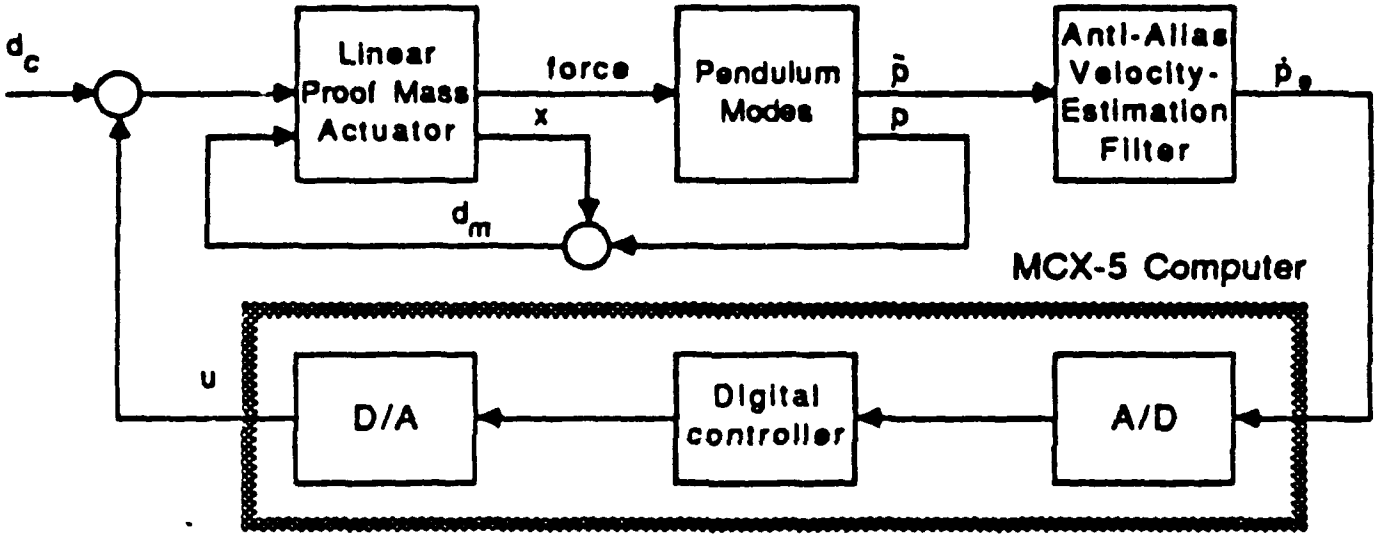

Figure 3. Block Diagram of the Pendulum Experiment.

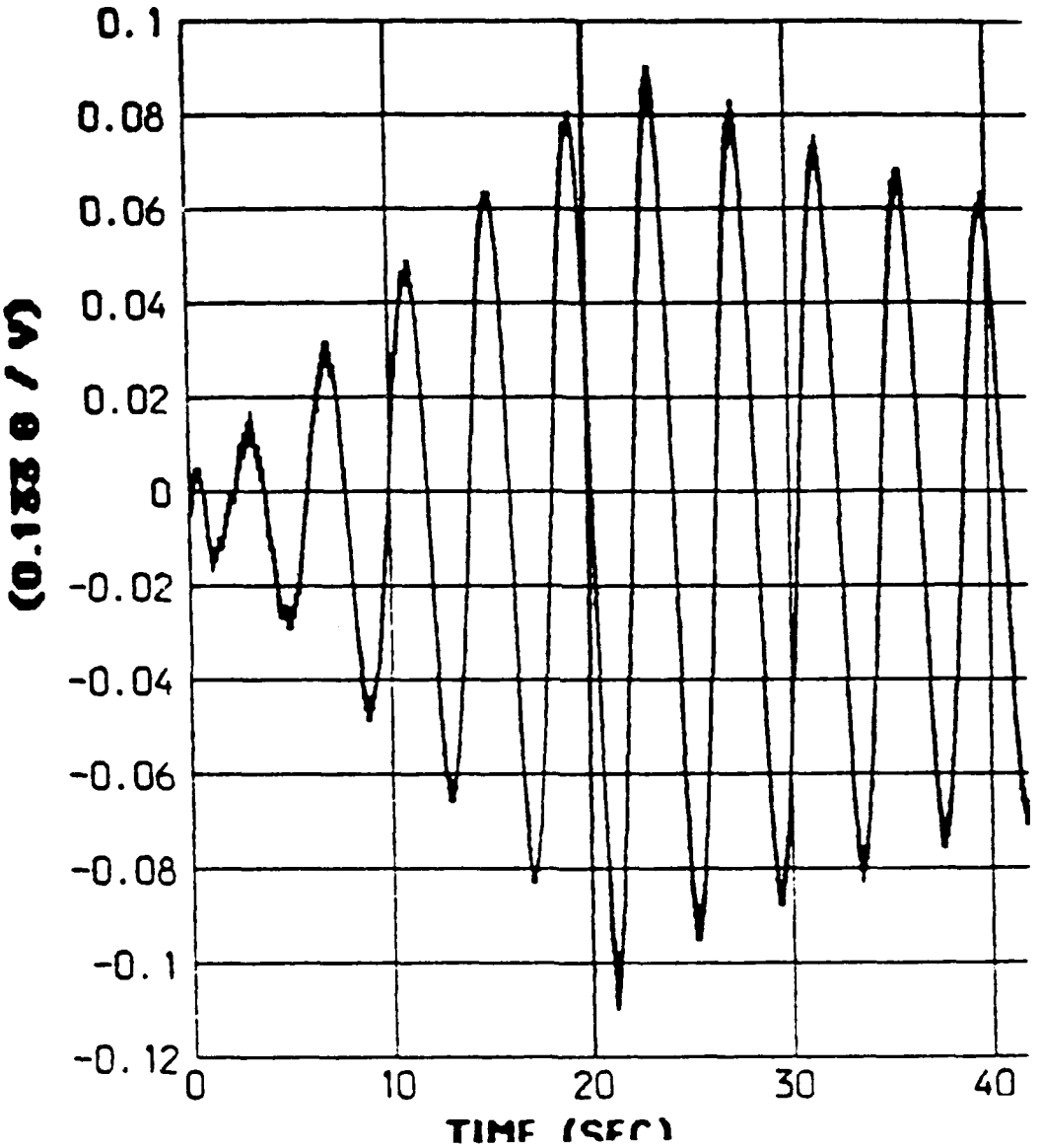

Figure 4a. Pendulum Test Results with First Mode Sine Excitation and Open Loop Decay.

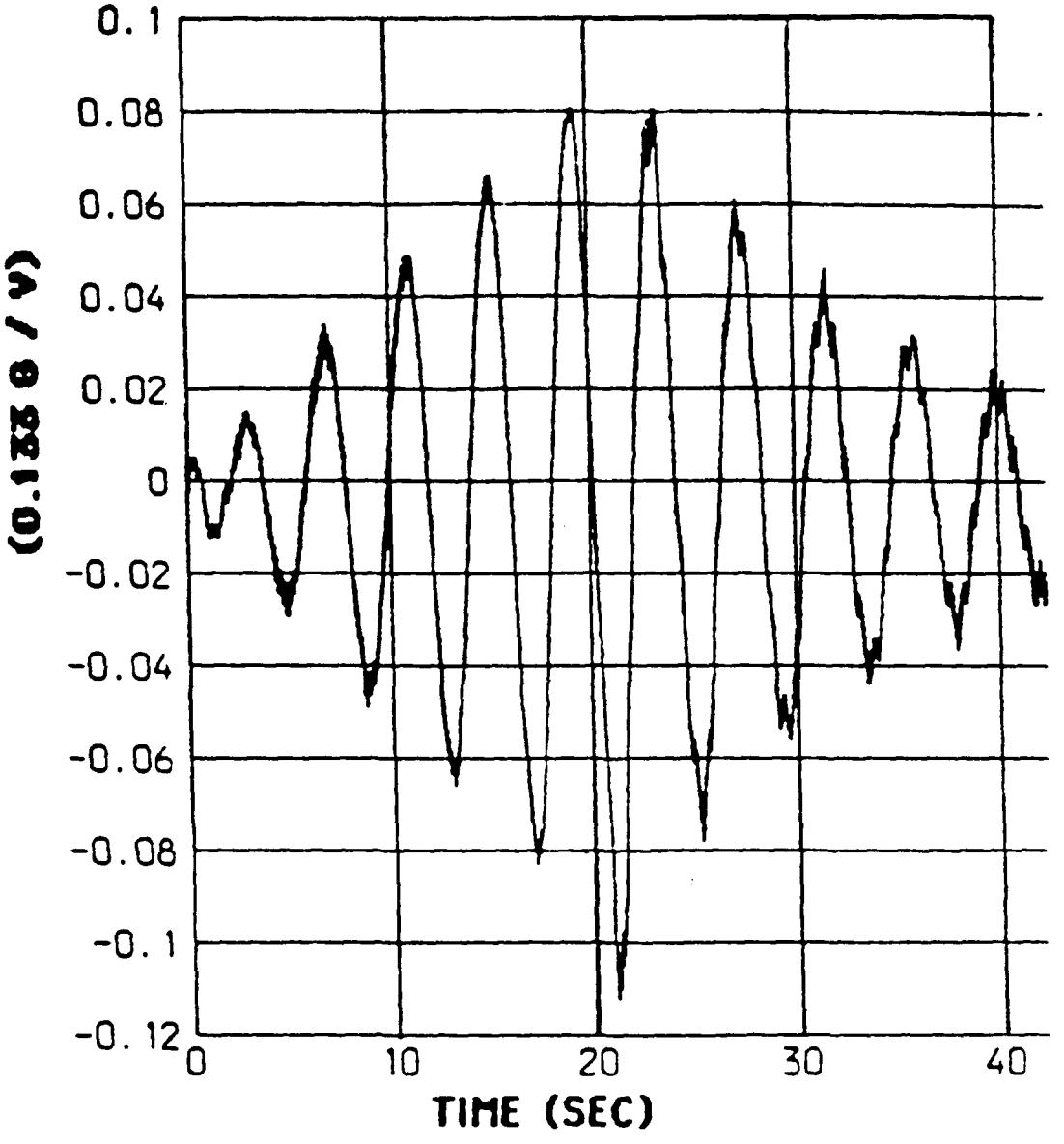

Figure 4b. Pendulum Test Results with Positive Real 5.0% Damping Controller.

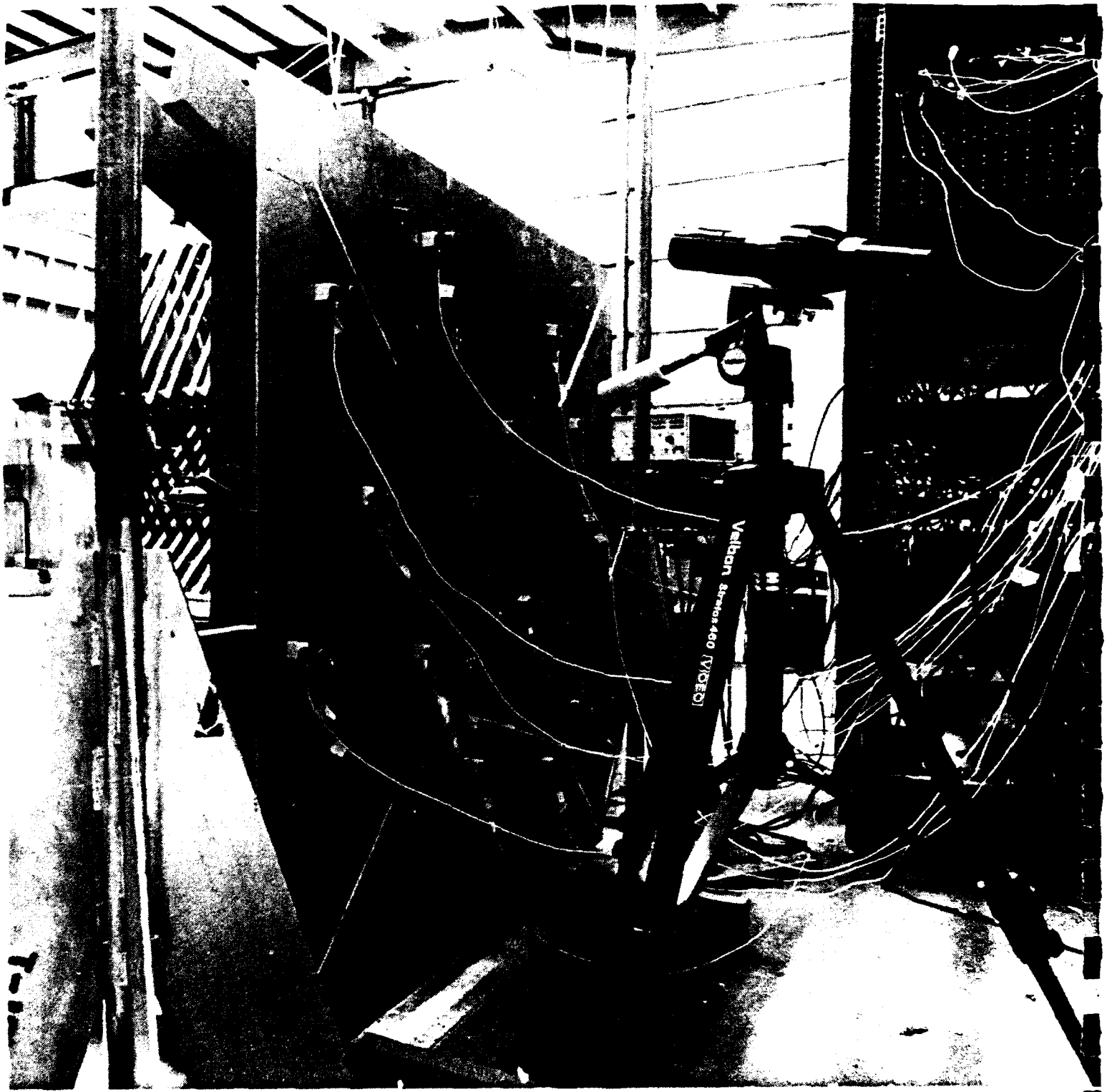

Figure 6a. Plate Experiment Apparatus.

PLATE EXPERIMENT: SENSOR/ACTUATOR CONFIGURATION

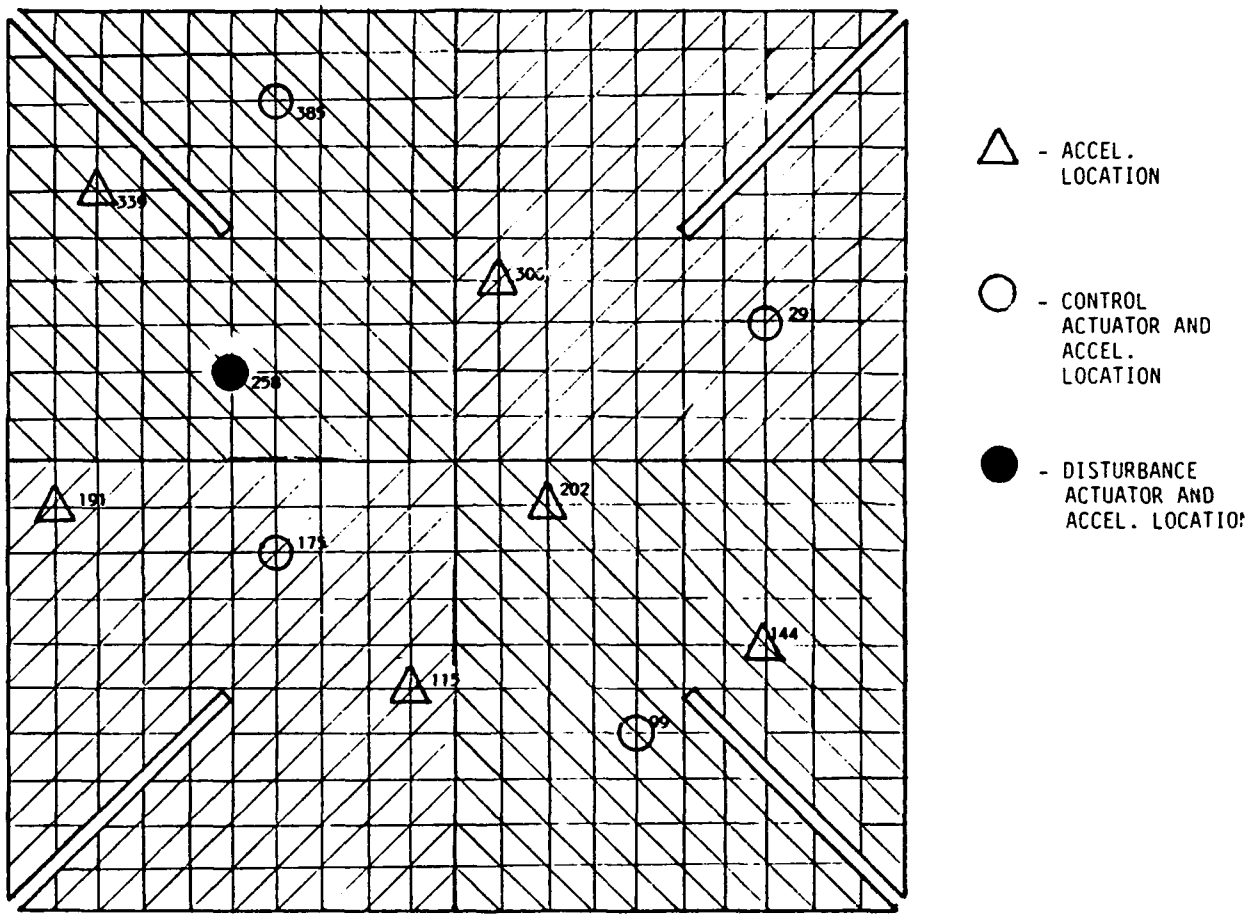

Figure 6b. Plate Experiment Actuators and Sensors Configuration.

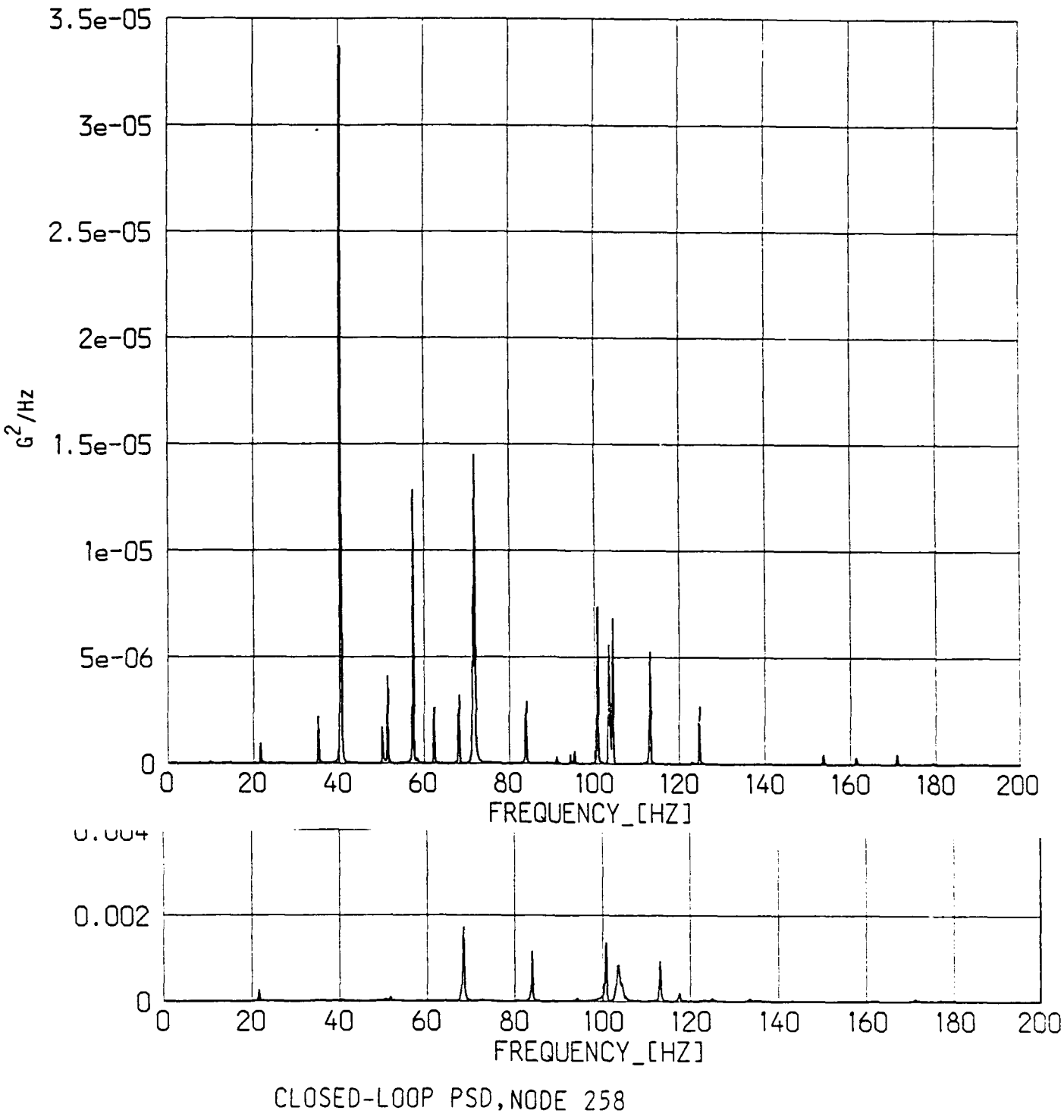

Figure 7a. Plate Experiment Open and Closed Loop Response PSD at disturbance location.

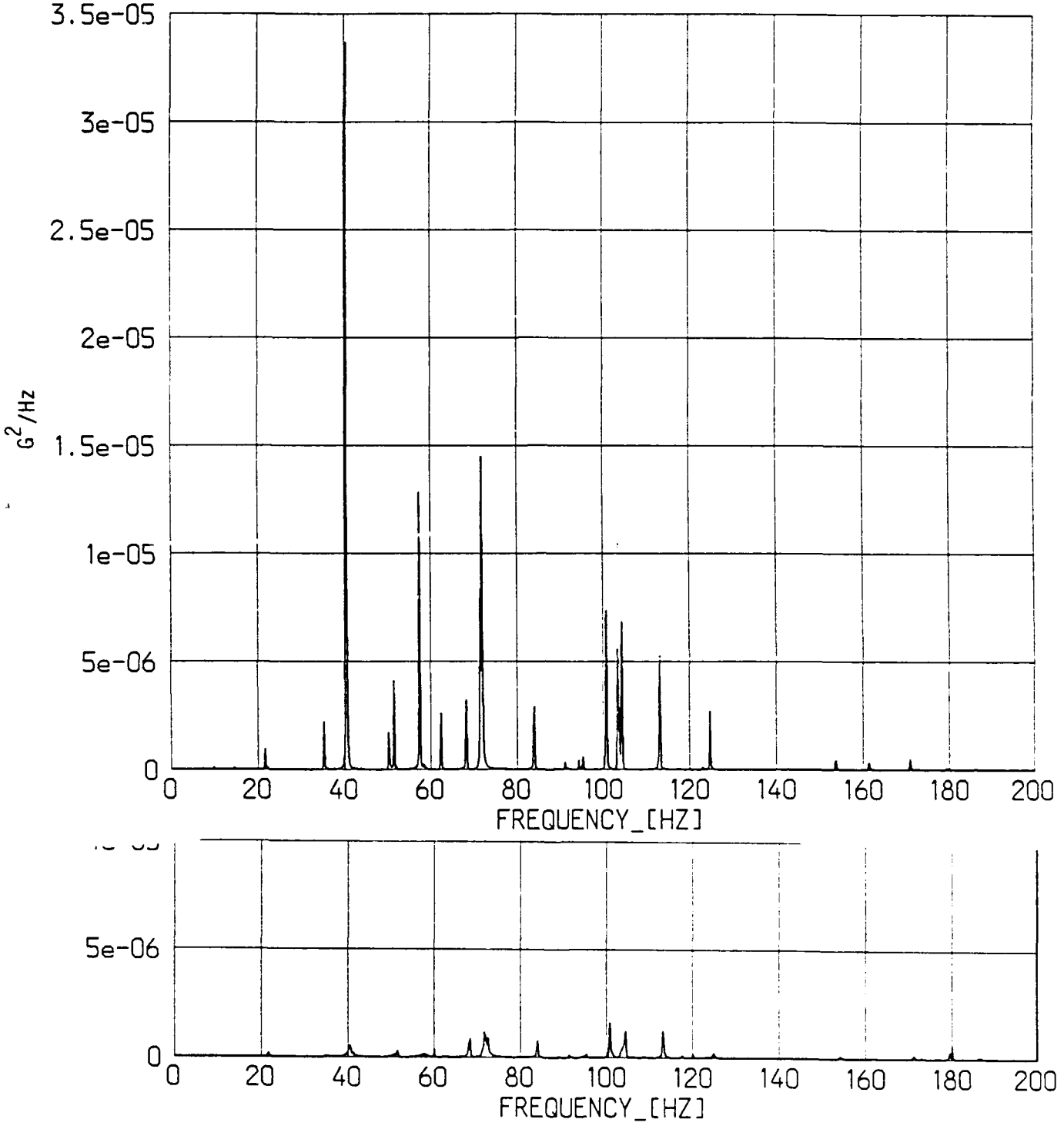

Figure 7b. Plate Experiment Open and Closed Loop Response at Collocated Actuator/Sensor Location.

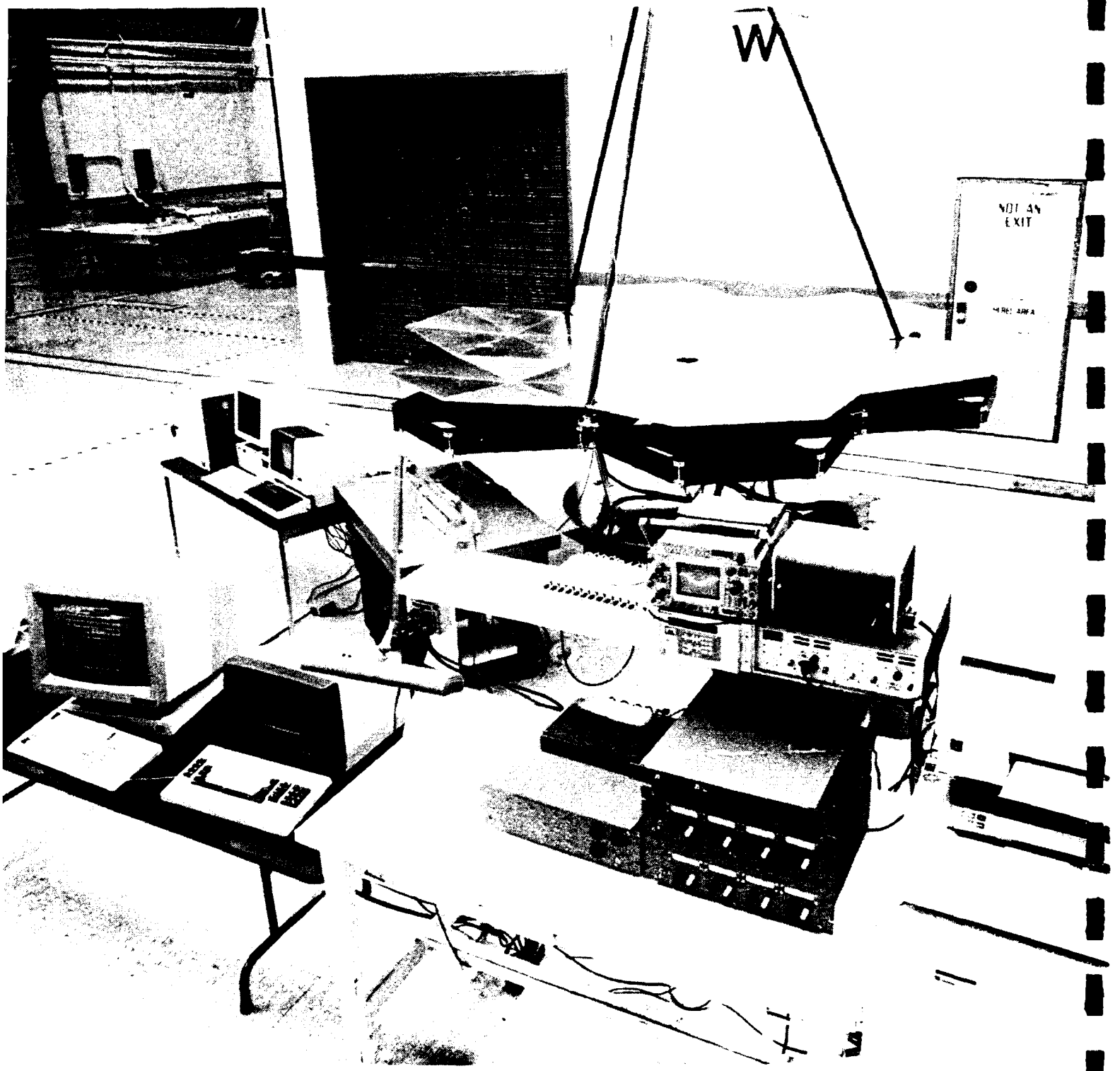

Figure 8. Multi-Hex Prototype Experiment Apparatus.

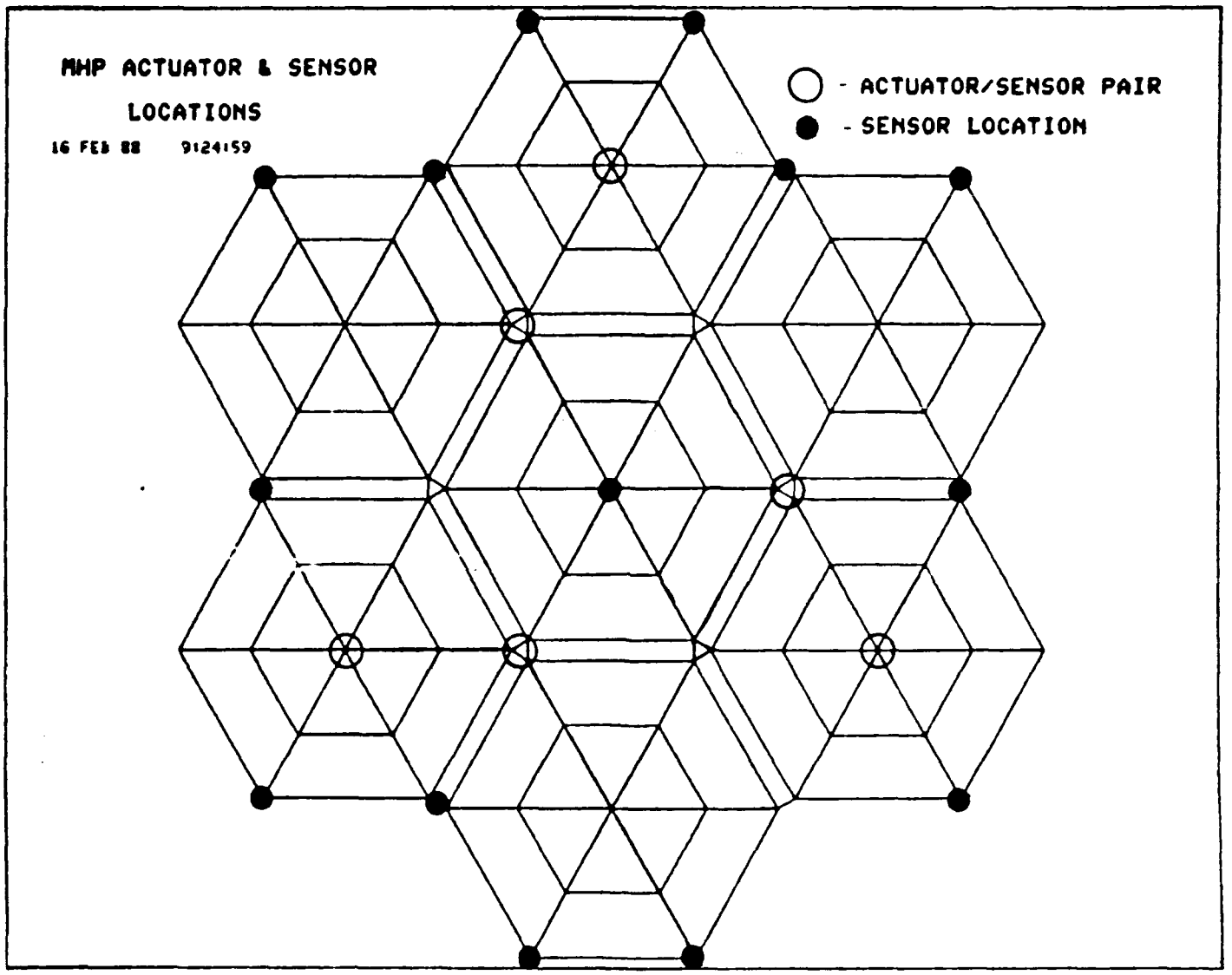

Figure 11. MHP Actuator and Sensor Locations.

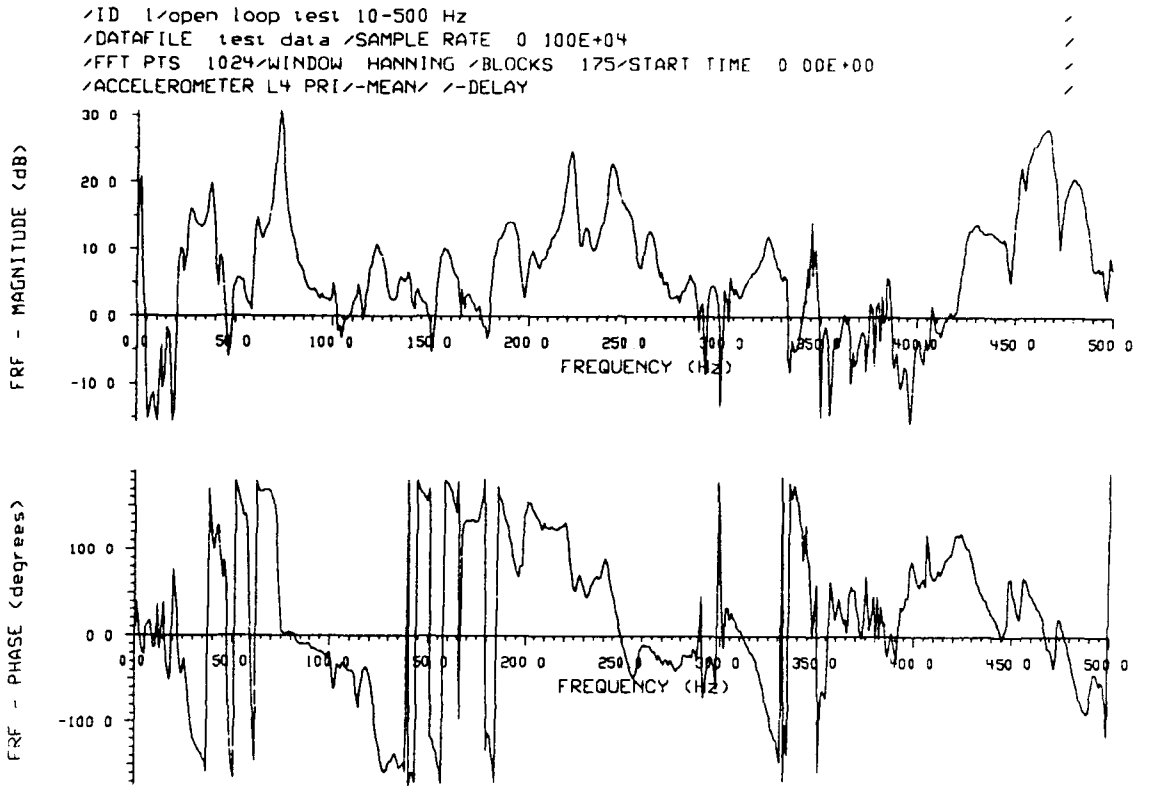

FRF H1 /INPUT 49/OUTPUT 31 (in/sec**/volts)

Tue Jan 9 15 05 35 1990

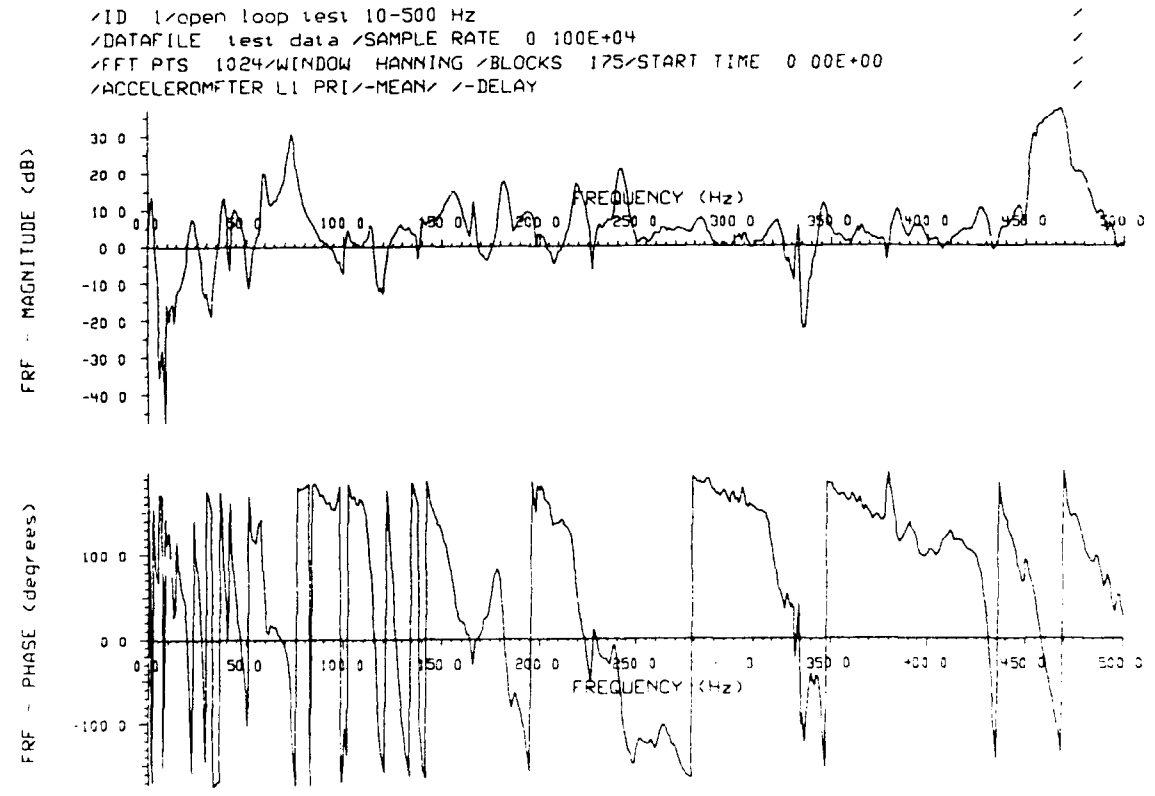

FRF H1 /INPUT 49/OUTPUT 7 (in/sec**/volts)

Figure 12

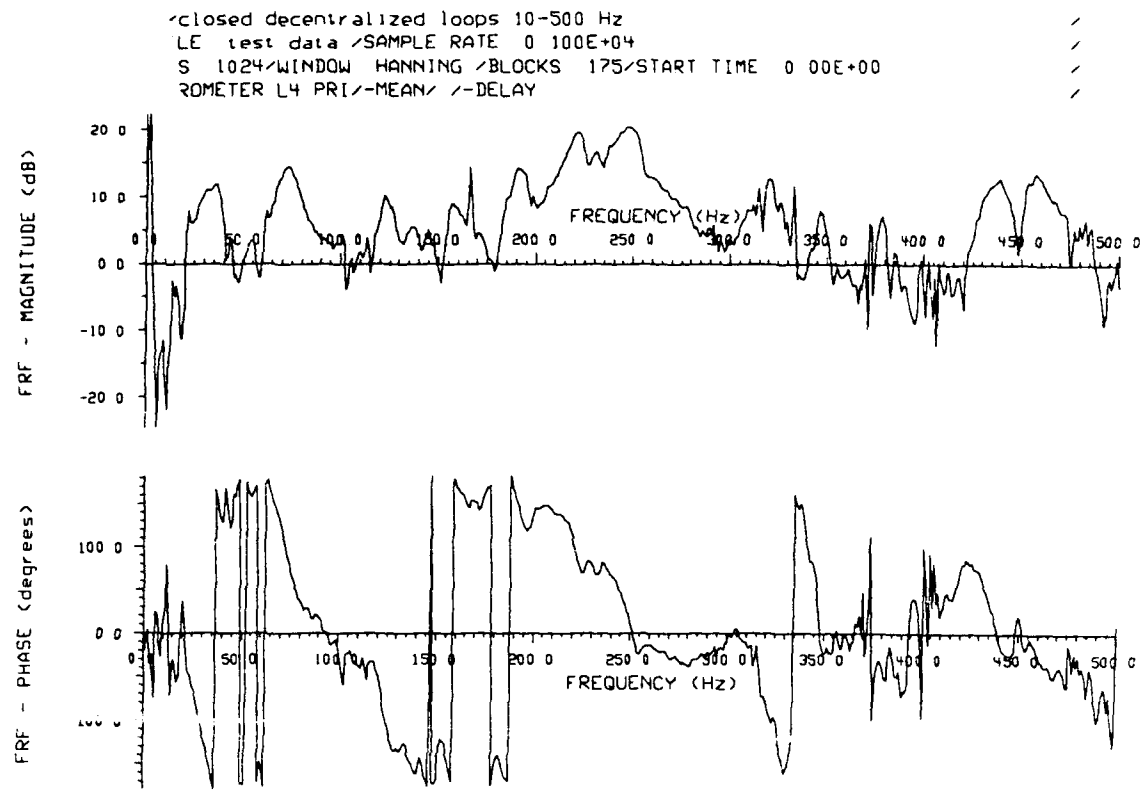

FRF H1 /INPUT 49/OUTPUT 31 (in/sec**/volts)

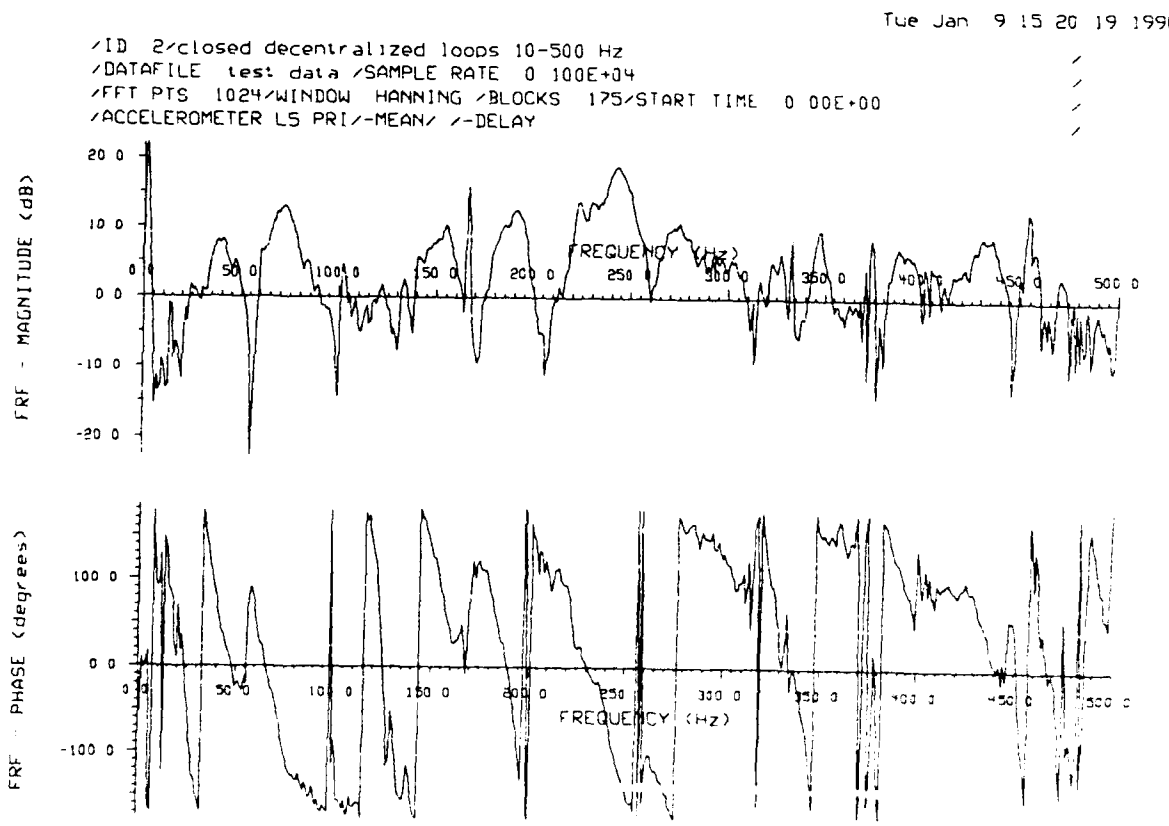

FRF H1 /INPUT 49/OUTPUT 39 (in/sec**/volts)

Figure 13

1. Base Excitation Table
2. 3 Axis Base Accelerometers
3. 3 Axis Gimbal System
4. 3 Axis Base Rate Gyros and Counterweight
5. 3 Axis Tip Accelerometers
6. 3 Axis Tip Rate Gyros
7. Optical Detector
8. Mirrors
9. Laser
10. 2 Axis Pointing Gimbal System
11. LMED System

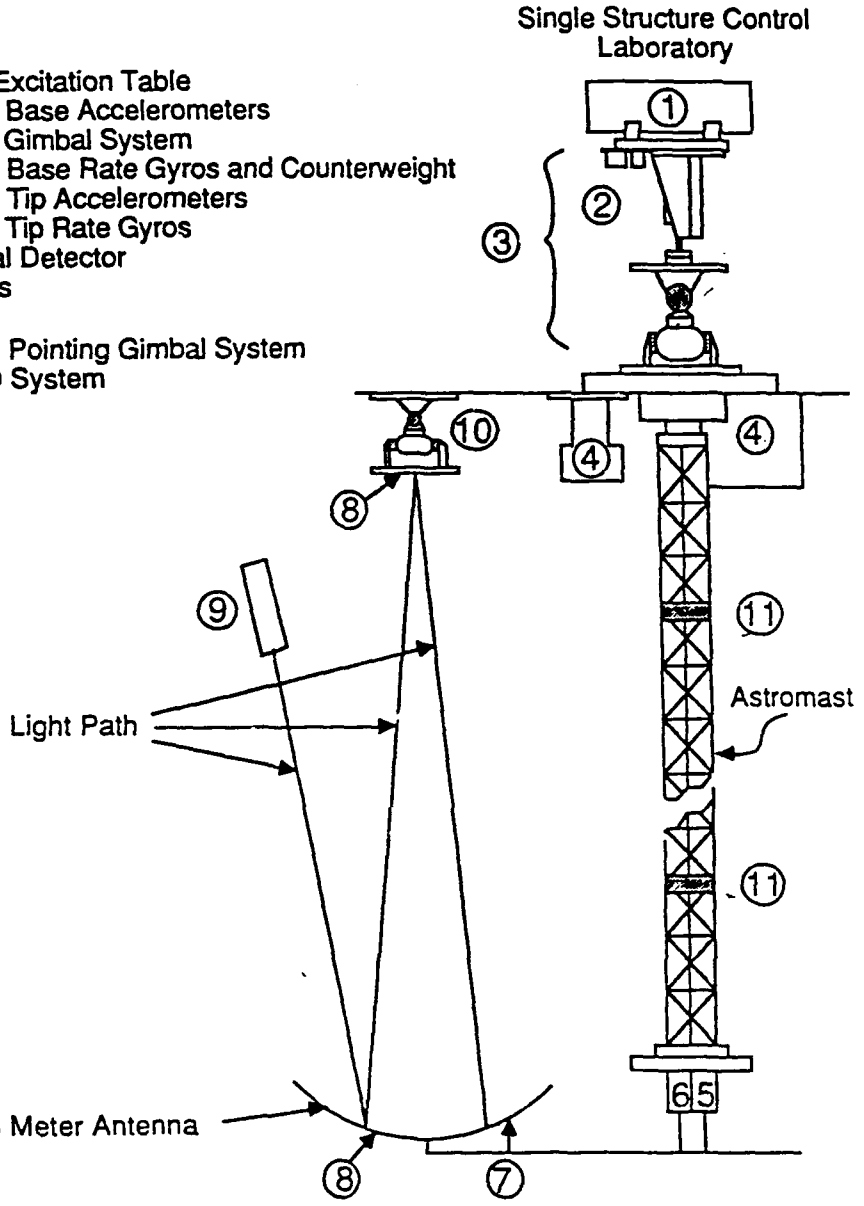

Figure 14 LSS GTF Experiment (ACES Configuration)

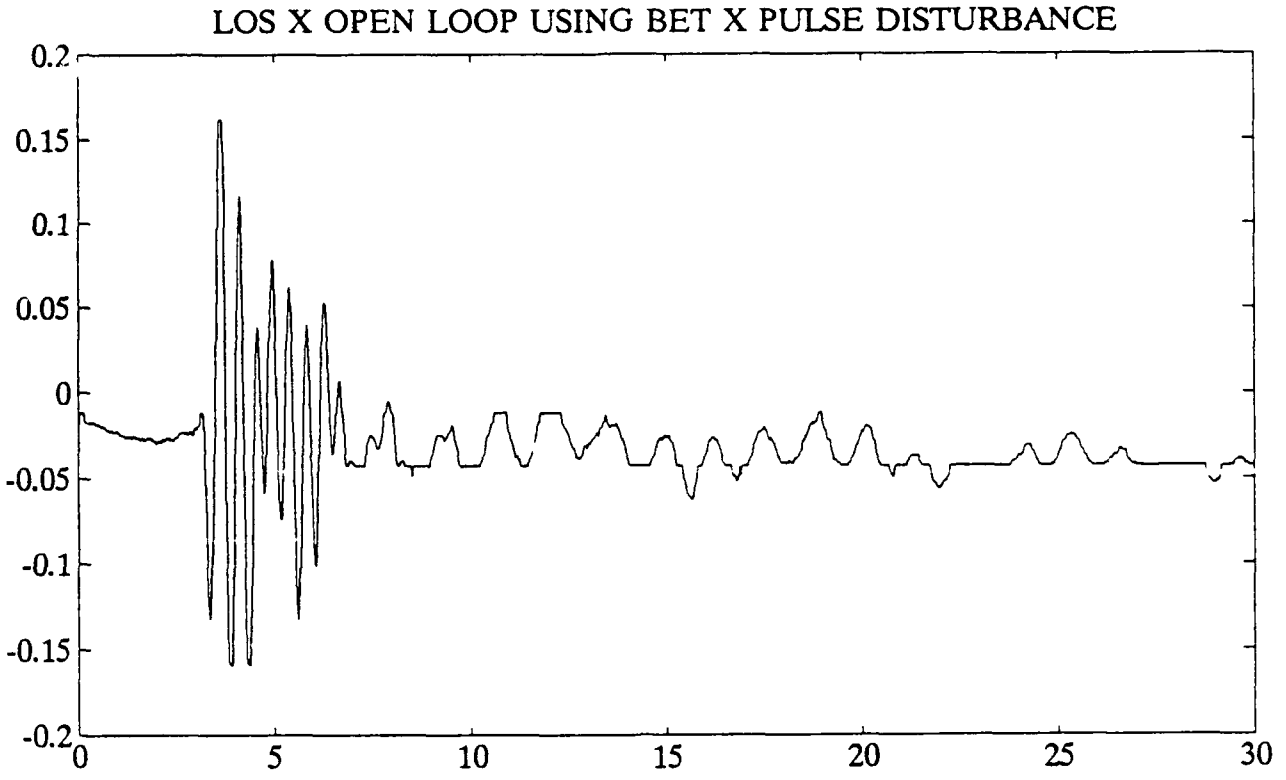
LOS X OPEN LOOP USING BET X PULSE DISTURBANCE
0.2
0.15
0.1
0.05
0
-0.05
-0.1
-0.15
-0.2
0
5
10
15
20
25
30

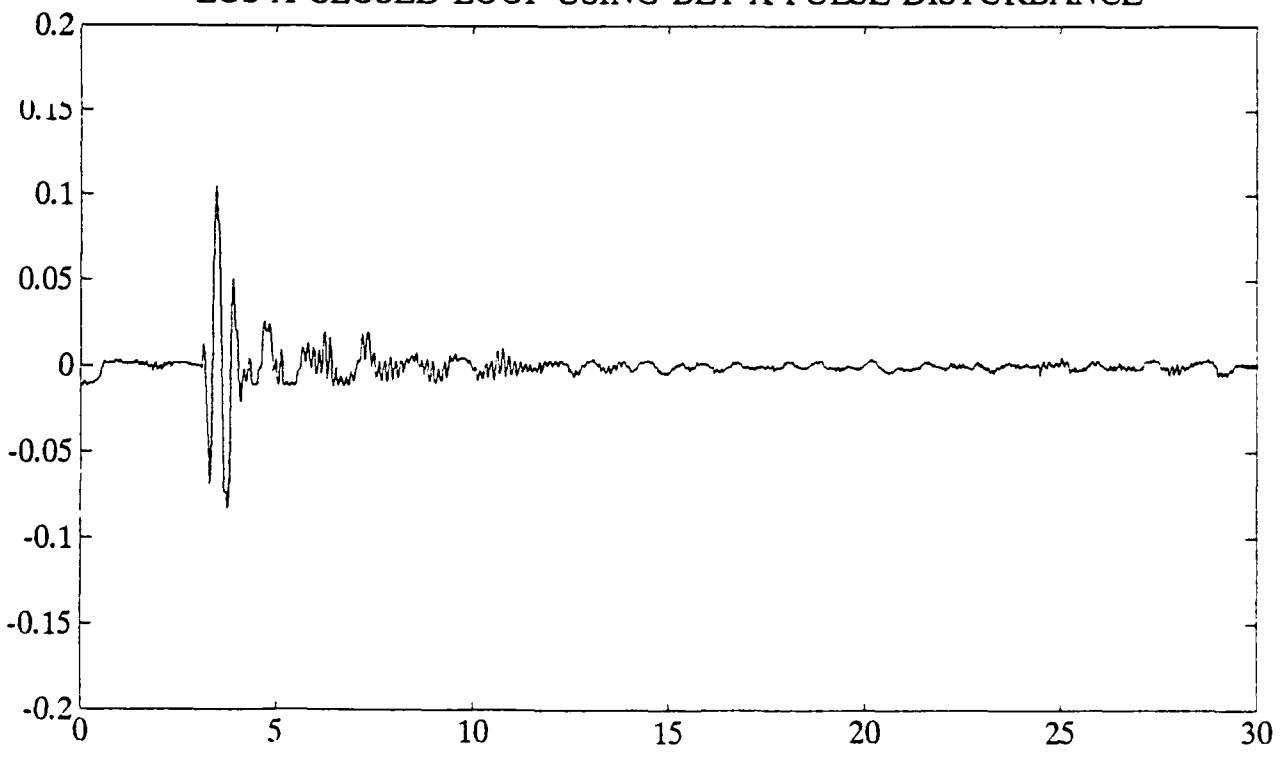
LOS X CLOSED LOOP USING BET X PULSE DISTURBANCE
0.2
0.1
0.05
0
-0.05
-0.1
-0.15
-0.2
0
5
10
15
20
25
30

Figure 15

Appendix D

Program Personnel

Dr. David C. Hyland

Principal Engineer

Dr. David C. Hyland received his education at the Massachusetts Institute of Technology. He completed his undergraduate work in June 1969 and received an S.B. degree in Aeronautics and Astronautics. Specializing in structural and dynamics with particular interest in probalistic methods, he was awarded the M.S. and Sc. D. degrees in Aeronautics and Astronautics in June 1971 and November 1973, respectively.

During the period September 1969 through August 1973, Dr. Hyland was employed as a Research Associate at the M.I.T. Lincoln Laboratory where he was assigned to the Mechanical Engineering and Electromechanical System Groups. Responsibilities encompassed preliminary design of attitude control systems for Lincoln Experimental Satellites (LES) 8 and 9, dynamic analysis of the separation and deployment of LES 8 and 9 and statistical analysis of spacecraft response to excitation due to the Titan III-C booster during acceleration phase.

After completing his Doctoral work in November 1973, Dr. Hyland served on the technical staff of Cambridge Collaborative, Inc. until October 1974. During this period, his major activities included vibration analysis of elevated guideway structures for a D.O.T. contract, analysis of the acoustic performance of multi-layered porous material under water acoustic absorbers for US Naval applications as well as independent consulting in the area of dynamics and control.

Beginning in November 1974 until July 1983, Dr. Hyland served a member of the technical staff at M.I.T. Lincoln Lab, assigned first to the Aerospace Engineering Groups (Nov 1974-May 1981) and subsequently to the Control Systems Engineering Group (May 1981-July 1983). During this period, Dr. Hyland's major technical activities were:

1. Dynamic and aerothermal analysis for the LL fixed-length RCS masker for the Continuously Dispensed Masker (CDM).

2. CDM Carrier vehicle re-entry dynamics analysis in coordination with ICBM flight test planning and execution.

3. Development of the RBSP Dynamics and Control Simulation Software package.

4. Re-entry analysis of the STAR decoy for SAMSO/ABRES.

5. Analysis of Unconventional Re-entry Vehicle Design for Foreign Technology Division.

6. Dynamic analysis and attitude control design for the Space Based Radar Program.

7. Inauguration and direction of the ACTUS program - a DARPA sponsored study for the development of innovative control design synthesis methods for Large Space Systems (LSS).

In addition, Dr. Hyland served as Government technical advisor in support of independent Government technical reviews/audits (sanctioned by DARPA, SDC and the GAO) of a variety of spacecraft and technology development programs, including the FLTSATCOM Review (organized by General F. McCartney in 1977), SMALL SAT Program, SLC-SAT Program and ACOSS Program.

Beginning in August 1983, Dr. Hyland initially organized and presently leads the Control Systems Research (CSR) Group within the Government Aerospace Systems Division of Harris Corporation. The CSR Group's role is the development of fundamentally new spacecraft control technology and the transitioning of this technology into applications. The scope of activities range from fundamental theoretical research in the area of robust, fixed-structure control design, to development of actuation and sensing hardware to overall control subsystem design and end-to-end system performance analysis and simulation. Ongoing basic research activities have resulted in the Optimal Projection for Uncertain Systems (OPUS) control design technology with supporting software. To date OPUS has been documented in approximately 130 publications and its recent extensions, uniting time and frequency domain approaches, have earned international recognition. Actuation hardware activities include the development of the LDCM actuator and the LPACT actuator. These new devices, as well as OPUS design have been and continue to be validated through several vibration control experimental facilities developed by the CSR group, including the Multi-Hex Prototype Experiment (MHPE). Activities in support of payload design and end-to-end performance analysis are typified by the group's past contributions and current role within the Zenith Star program.

In recognition for his accomplishments on behalf of Harris Corporation, Dr. Hyland received the Harris GASD patent Award (November 1987), the Harris GSS Executive Incentive Program Award (July 1987) and the Harris GASD Engineering Award for Outstanding Individual Contribution (November 1986).

Dr. Hyland is a member of AIAA and has authored or co-authored over 80 conference papers, archival journal articles and monographs in the areas of spacecraft dynamics and control and mathematical control theory.

Dr. John W. Shipley

Senior Scientist

Dr. Shipley is a Senior Scientist in the Mechanical Systems Department. Before being promoted to Senior Scientist he was section head of the Mechanical Systems Engineering section where he supervised more than 45 engineers.

He has over 14 years of experience in controls engineering, structural dynamics, design and testing as an individual contributor and technical supervisor. His background is in solid mechanics and his principal area of research at Georgia Institute of Technology was in the application of random noise theory to mechanical system problems. He is the author of a number of publications in the professional literature in the areas of controls and dynamics of large space structures, random vibration, fatigue and computer structural modeling.

At present, Dr. Shipley is engaged in precision space structures technology and is responsible for the controls section. Before joining Harris in 1979, he worked for the Martin Marietta Orlando Division for eight years. There he worked in dynamics and structural analysis for Air Defense Systems.

Dr. Shipley worked on the development of a digital control system for vibration testing while working as a summer employee at the Jet Propulsion Laboratory when he was completing his education.

Education: B.S.E.M., Georgia Institute of Technology
M.S.E.M., Georgia Institute of Technology
Ph.D. E.M., Georgia Institute of Technology

Dr. Emmanuel G. Collins

Associate Principal Engineer

Dr. Collins joined Harris Government Aerospace Systems Division in July 1987 as an Associate Principal Engineer in the Mechanical Systems Department. Since joining Harris, he has helped to develop analysis tools capable of evaluating control systems for robust stability and performance. He has also been an active participant in the development of novel numerical algorithms for robust fixed-order control synthesis. His current responsibilities include the development and implementation of a high precision position measurement system for the Multi-Hex Prototype Experiment. This measurement system used laser interferometry.

Prior to employment at GASD, Dr. Collins was a research assistant in the School of Aeronautics and Astronautics at Purdue University. His primary research areas were control design for multiple objectives, model reduction and reduced-order control design. The research centered around the active control of large flexible space structures. Dr. Collins has authored or coauthored several papers for archival journals and technical conferences.

EDUCATION:

Ph.D. May 1987 - Purdue University, School of Aeronautics and Astronautics
M.S.M.E. Aug. 1982 - Purdue University
B.S.M.E. June 1981 - Georgia Institute of Technology
B.S. May 1981 - Morehouse College, Interdisciplinary Science

Dr. Dennis S. Bernstein

Staff Engineer

Dr. Bernstein is presently assigned to the Harris Government Aerospace Systems Division in the Structural Control Group of the Mechanical Systems Department. As an undergraduate at Brown University, he majored in applied mathematics. Subsequently, he attended The University of Michigan where he obtained a Ph.D. from the Computer, Information and Control Engineering Program. His graduate research focused on optimization theory for dynamical systems and was supported by the Air Force Office of Scientific Research.

While at The University of Michigan, Dr. Bernstein was employed by Applied Dynamics International where he developed and implemented numerical integration algorithms for real-time digital simulation.

After receiving his Ph.D., Dr. Bernstein was with the Controls Systems Engineering Group of MIT Lincoln Laboratory. In the applications area of active control of large flexible space structures, he contributed to the development of the Maximum Entropy/Optimal Projection (MEOP) stochastic modeling and reduced-order design synthesis methodology.

At Harris Dr. Bernstein's research has concentrated on extending the MEOP methodology to a variety of modeling, estimation and control applications in distributed-parameter, discrete-time, sampled data and decentralized settings.

Dr. Bernstein's publications have appeared in IEEE Transactions on Automatic Control, SIAM Journal on Control and Optimization, and AIAA Journal on Guidance, Control and Dynamics.

EDUCATION: Brown University, Sc.B.
The University of Michigan, M.S., Ph.D.

Allen W. Daubendiek

Senior Engineer

Mr. Daubendiek joined the Structural Control Group in February 1987 as a Senior Engineer. He has worked on instrumentation and disturbance modeling for the Mast Flight System; performed satellite attitude estimation, pointing and slewing simulations for advanced studies, including Zenith Star; developed discrete-time signal processing, parameter estimation and experimental model realization software for the Multi-Hex Protype vibration control experiment. His work in these areas has resulted in the development of software to automate the design of static output feedback controllers. He has also developed software for designing dynamic output feedback controllers for systems of very high dimensionality.

While working on the Multi-Hex Prototype Experiment, Mr. Daubendiek was responsible for planning, implementing and testing modifications to the signal processing electronics. He has also made contributions in a number of key areas, including controller architecture, implementation and the associated precision optical measurement system.

Prior to employment at Harris, Mr. Daubendiek was a Graduate Assistant at Iowa State University for the Electrical Engineering Department. His work involved both research and teaching. His thesis topic applied a Maximum Entropy Method to the problem of designing robust continuous time state estimators (Kalman filters). A method for decoupling the matrix equations used in the design method was discovered and tested. The performance of several design examples was evaluated for both system and estimator parameter uncertainties. He is a member of the I.E.E.E.

Education: Bethel College, N. Newton,
B.A. Mathematics, B.S. Physics
Iowa State University, Ames, IA,
M.S. Electrical Engineering

Douglas J. Phillips

Lead Engineer

Mr. Phillips joined Harris Government Aerospace Systems Division in January 1985, as a Lead Engineer in the Controls Analysis Group of the Mechanical Systems Department. Since joining GASD, he has worked on the development of software to automate the design of Discrete Time Active Control Systems for large space structures. He has contributed in the formulation of space structure into a discrete time continuous time description. He designed and developed the Harris Dynamic Data Acquisition System which has been extensively used for testing both electrical and mechanical systems. He also specified and procured the MCX-5 computer and wrote the real-time data acquisition and control software which has enabled the implementation of multi-input, multi-output sampled-data controllers for Harris' IR&D programs. He has led the system integration efforts and developed a variety of controller architectures for Harris' IR&D Plate and Multi-Hex Panel Program. He has assisted in the development of Harris Intelligent Linear Precision Actuator specifically the computer architecture, for loop design and testing of the device.

Presently he is studying the feasibility of the use of Digital Signal Processors for the Active Vibration Control of Large Space Structures.

Prior to employment at GASD, Mr. Phillips was a Lead Engineer at Harris Government Satellite Communications Division in the Controls and Digital Processing Section from October 1984 - January 1985. At GSCD, he was involved in formulating models for the NESP antenna controls system. Both linear and nonlinear models were formulated. He was responsible for the development of the antenna test fixtures for the NESP antenna.

Prior to employment at Harris Corporation, Mr. Phillips was employed by Westinghouse Electric Corporation in Systems Development Division in the Electromechanical Feedback and Controls Design group from October 1980-October 1984. He was involved in the simulation, design and testing of the improved F-16 antenna control system. He was in charge of the verification of the automated testing of the antenna electronics for the improved F-16 Radar System. Mr. Phillips was in charge of the proposal effort for the antenna control system for the Taiwanese GD-53 fighter program. He was the Lead Design Engineer for the fire control display systems.

EDUCATION:
M.S.E.E. August 1984 - John Hopkins University, Baltimore, MD
B.S.E.E. August 1980 - University of Florida, Gainsville, FL

Stephen Richter

Associate Principal Engineer

Mr. Richter joined Harris Government Aerospace Systems Division in November 1985 as an Associate Principal Engineer. While at Harris, Mr. Richter has successfully applied homotopic continuation methods to the solution of the MEOP equations for robust fixed-order dynamic compensation. This contribution has helped to significantly advance the state-of-the-art in practical control system design for high-order systems. Mr. Richter's other responsibilities at Harris have included the system simulation tasks of the Zenith Star program.

Prior to employment at Harris Mr. Richter worked for three years in Inertial Navigation Systems at ITT Avionics in Clifton, New Jersey. His primary responsibilities included the development of performance specifications, fundamental algorithm design and simulation for algorithm verification.

Mr. Richter holds Masters degrees from Purdue in Electrical Engineering, Physics and Mathematics. His research as a graduate research assistant in Electral Engineering led to the development of a novel homotopy algorithm to solve a fundamental problem in decentralized eigenvalue placement. In Physics he studied questions involving general relativity and solar physics. His research has led to publications in a variety of engineering and physics journals.

Education: Purdue University, B.S. and M.S. Mathematics, M.S.E.E., M.S. Physics